

UNIVERSITA' DEGLI STUDI DI TORINO

DEPARTMENT OF CLINICAL AND BIOLOGICAL SCIENCES

PhD PROGRAMME IN EXPERIMENTAL MEDICINE AND THERAPY

CYCLE XXXV

THESIS TITLE

**STRATEGIES TO IMPROVE PERIPHERAL NERVE REPAIR AND REGENERATION:
FROM PRIMARY REPAIR TO COMPLICATIONS' MANAGEMENT**

THESIS' AUTHOR: ALESSANDRO CROSIO

SUPERVISOR: PROF. STEFANIA RAIMONDO

PhD PROGRAMME CO-ORDINATOR: PROF. PASQUALE PAGLIARO

ACADEMIC YEARS OF ENROLMENT: 2019-2023

CODE OF SCIENTIFIC DISCIPLINE: BIO/16, MED/33

INDEX

1. INTRODUCTION

1.1 FOCUSING THE PROBLEM - PERIPHERAL NERVE DAMAGE

- 1.1.1 Type of nerve injuries and changes during nerve injury and regeneration
- 1.1.2 What happens outside the nerve: perineural scar formation

1.2 NERVE REPAIR TECHNIQUES

- 1.2.1 Direct suture
- 1.2.2 Nerve reconstruction
 - 1.2.2.1 Autograft reconstruction
 - 1.2.2.2 Nerve conduits
 - 1.2.2.3 Nerve transfer

1.3 COMPLICATIONS OF NERVE INJURIES AND REPAIRS

- 1.3.1 Traction neuropathies
- 1.3.2 Painful neuromas

1.4 TECHNIQUES FOR TREATMENT OF TRACTION NEUROPATHIES AND PAINFUL NEUROMAS

- 1.4.1 Neurolysis and associated procedures
- 1.4.2 In continuity and terminal neuroma resection and associated procedures
- 1.4.3 Role of intraoperative ultrasound study in nerve reconstruction

1.5 ROLE OF TRANSLATIONAL RESEARCH IN NERVE REPAIR

- 1.5.1 Experimental models to simulate a peripheral nerve injury
 - 1.5.1.1 Somatic nerve injury: the median nerve injury
 - 1.5.1.2 Autosomic nerve injury: cavernous nerve injury model
- 1.5.2 Nerve conduits in peripheral nerve repair
- 1.5.3 Other devices for peripheral nerve repair
- 1.5.4 How to simulate a traction neuropathy

2 AIMS OF THE STUDIES

3 RESULTS

- 3.1 Fibroblasts Colonizing Nerve Conduits Express High Levels of Soluble Neuregulin1, a Factor Promoting Schwann Cell Dedifferentiation Fornasari BE, El Soury M, Nato G, Fucini A, Carta G, Ronchi G, Crosio A, Perroteau I, Geuna S, Raimondo S, Gambarotta G.. Cells. 2020 Jun 1;9(6):1366.**
- 3.2 Exploring an Innovative Decellularization Protocol for Porcine Nerve Grafts: A Translational Approach to Peripheral Nerve Repair. Muratori L, Crosio A, Ronchi G, Molinaro D, Tos P, Lovati A, Raimondo S. Under Submission**
- 3.3 Somatic to autonomic nerve transfer: review of the literature and future perspectives. Crosio A, Fregnan F, Muratori L, Falcone F, Tos P, Raimondo S, Ciclamini D. Under submission**
- 3.4 Prevention of symptomatic neuroma in traumatic digital amputation: A RAND/UCLA appropriateness method consensus study. Crosio A, Albo E, Marcoccio I, Adani R, Bertolini M, Colonna MR, Felici N, Guzzini M, Atzei A, Riccio M, Titolo P, Tos P. Injury. 2020 Dec;51 Suppl 4:S103-S107.**
- 3.5 Intraoperative ultrasound study of traumatic nerve injury: current applications and future perspectives. Crosio A, Verga L, Locatelli F, Magnani M, Clemente A, Odella S, Tos P. Under submission**
- 3.6 Preclinical Validation of SilkBridge™ for Peripheral Nerve Regeneration Fregnan F, Muratori L, Bassani GA, Crosio A, Biagiotti M, Vincoli V, Carta G, Pierimarchi P, Geuna S, Alessandrino A, Freddi G, Ronchi G.. Front Bioeng Biotechnol. 2020 Aug 7;8:835.**
- 3.7 Strategies for cavernous nerve repair in animal model: regeneration through chitosan membrane vs sciatic nerve to corpora cavernosa transfer. Crosio A, Fregnan, F, Muratori L, Ciclamini D, Tos P, Raimondo S. Under submission.**
- 3.8 Experimental Methods to Simulate and Evaluate Postsurgical Peripheral Nerve Scarring. Crosio A, Ronchi G, Fornasari BE, Odella S, Raimondo S, Tos P. J Clin Med. 2021 Apr 10;10(8):1613.**

4 DISCUSSION AND CONCLUSION

5 REFERENCES

1. INTRODUCTION

1.1. FOCUSING THE PROBLEM - PERIPHERAL NERVE DAMAGE

1.1.1. Type of nerve injuries and changes during nerve injury and regeneration

Peripheral nerve injuries belong to the most challenging and difficult surgical reconstructive problems, and often cause partial or total loss of motor, sensory and autonomic functions.

Every year, 20 million Americans suffer from peripheral nerve injuries that result in an average yearly cost of \$150 million (Taylor 2008)

In addition, nerve injuries have also a substantial economic impact on the society in terms of health care and long periods of sick-leave (de Putter 2012).

Peripheral nerve injuries occur in approximately 2.8% of trauma patients (Heulsenbeck 2012) and more than 73.5% of them occur in the upper extremities.

The injuries of peripheral nerves after a trauma could be classified as crush injuries when the nerve is in continuity and cut injuries when the integrity of the epineurium is interrupted. The cut injuries could also be with gap if a loss of substance exists or without gap if the two stumps are easily to approximate.

As well, a nerve injury could be secondary to a surgical procedure in which a nerve can be damaged involuntarily or the nerve should be resected for oncological reasons, for example when a prostatectomy is performed the neurovascular bundles are resected together with the organ, leading to erectly disfunction or a resection of colon or pelvic floor could induce bowel and bladder disfunction either.

Up to 33% of all peripheral nerve injuries (PNI) exhibit incomplete nerve recovery and poor functional outcomes, including the loss or partial recovery of motor and sensory function, chronic pain, and end target muscle atrophy and profound weakness (Atkins S 2006). As for somatic nerve reconstruction, also the reconstruction of autonomic fibers leads to contrasting results.

Nerve injuries (crush or cut injuries) can be divided in three categories according to Seddon's classification (1943): neuroprassia, axonotmesis and neurotmesis.

i) Neuroprassia, is an injury characterized by local damage of myelin and axon, without the interruption of endoneurium sheath. Surgery is unnecessary and the recovery occurs within hours, days, or up to few months.

ii) Axonotmesis is a lesion in which axons are damaged or destroyed and lose their continuity, but without any alteration of connective tissue. Axon damage is usually due to nerve crushing, pinching or prolonged pressure. All the axon portions located distal to the site of injury undergo Wallerian degeneration, while the proximal stump of nerve can re-grow inside the intact endoneurial tubes. The time of recovery depends on

the severity degree of the lesion as well as the distance of the injury site to the nerve target. Since connective tissue is intact, surgery could be unnecessary in some cases.

iii) Neurotmesis is a severe nerve injury where the nerve is transected. The proximal stump undergoes retrograde degeneration, while Wallerian degeneration occurs at the distal nerve stump. Due to the extended endoneurial tube disruption, spontaneous regeneration is slow and functional recovery does not easily occur; however, successful regeneration might be achieved by surgical intervention.

In 1951, Sunderland additionally divided axonotmesis in three categories with increasing level of severity (Figure 1).

The third grade of injury correspond to an axon and endoneurium damaged, with intact epi and perineurium. In the fourth grade of nerve injury, the internal structure of the nerve is completely destroyed, but its continuity is maintained by an undamaged epineurium. In the injury site, fibroblasts produce a fibrous scar that inhibits axonal regeneration, contributing to the formation of a mass of disorganized fibers, known as neuroma-in-continuity. This type of injury requires surgery in order to remove the fibrotic scar and to promote regeneration.

The fifth-degree of injury is the most severe type of nerve damage; it results in a complete transection of the nerve, the neurotmesis.

Since Sunderland's grades can be described only histologically, this classification has limited clinical utility. Moreover, since most nerve injuries are mixed, Mackinnon and Dellon included in Sunderland's classification another type of injury, which is a combination of all the degrees (grade 6) (Mackinnon 1989).

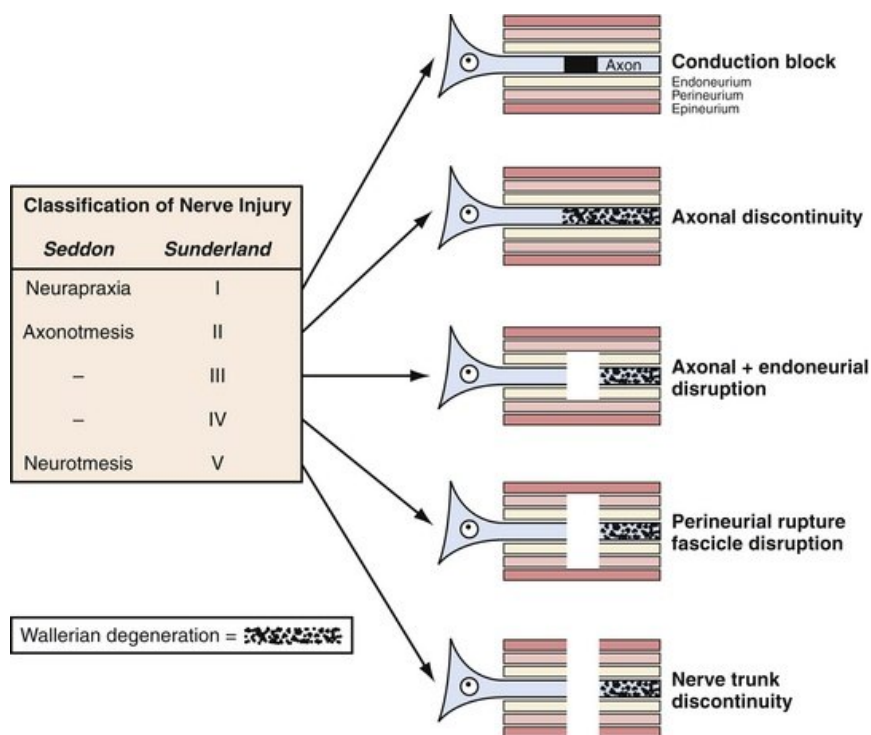


Fig. 1: Schematic representation of the five degrees of nerve injury in accordance with Sunderland's classification (Duemans 2010).

Peripheral nerve injury induces several morphological and molecular changes at multiple levels: at the injury site (proximal and distal nerve stumps), at the neuron cell body (dorsal root ganglion and ventral horns) and at the level of the target organs (Figure 2). These changes start immediately after injury and can be prolonged in time.

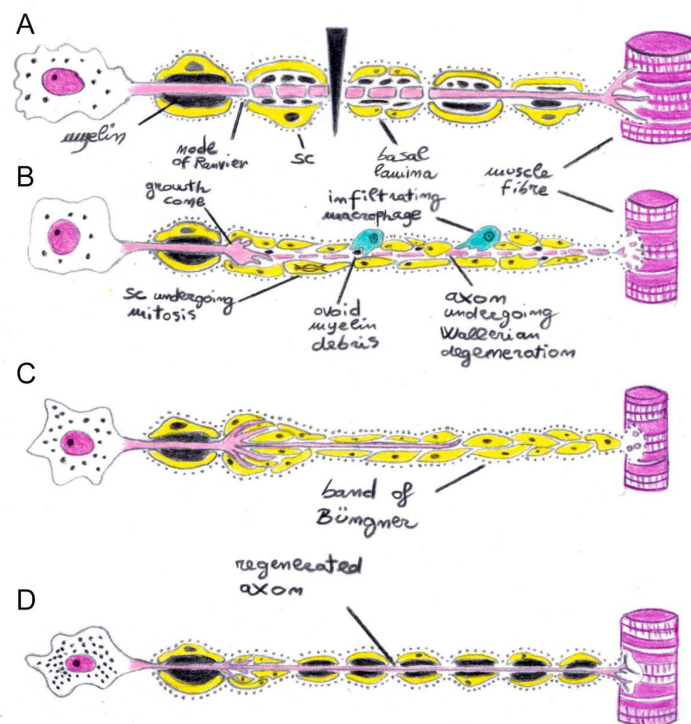


Fig. 2: Schematic representation of degenerative and regenerative events related to peripheral nerve injury (Fornasari 2016).

The first moments after a nerve injury (first few days), degenerative changes, including axon and myelin breakdown, started both proximally and distally to the injury site (Figure 2). The distal stump undergoes degeneration known as Wallerian degeneration (Figure 2A). It results in the axon and myelin fragmentation and, finally, in nerve debris elimination. Schwann Cells (SC) loose axon-contact, change their phenotype and start to degrade myelin (Figure 2B). Few days after the injury, activated SCs proliferate and later become aligned with the endoneurial tubes, forming the bands of Büngner, a supportive and guiding structure for regenerating axons (Figure 2C). This structure physically supports regrowing axons and guides the

regeneration through adhesion molecules and neurotrophic factors provided also by SCs (Hopker VH, 1999). Different types of neurotrophic factors have an important role in nerve regeneration. The SCs release nerve growth factor (NGF), brain-derived nerve growth factor (BDNF), neurotrophin 4 and 5 (NT-4 and 5), glial-cell-line derived neurotrophic factor (GDNF), ciliary neurotrophic factor (CNTF), insulin-like growth factor (IGF) and Neuregulin1 (NRG1) that attract the growing axons to distal targets (Geuna 2009).

A special consideration was directed to better characterize the role of NRG1. In this thesis a novel aspect regarding NRG1 release during nerve regeneration was investigated; our results demonstrated that fibroblasts are the major characters involved NRG1 release. The so called soluble NRG1 (sNRG1) induce SCs de-differentiation and consequently axons regrowth. Full results are presented in chapter 3.

Moreover, SCs of the distal nerve stump are the main source of cytokines that attract macrophages. Indeed, few days after nerve injury, the resident endoneurium macrophages become activated and move to the injury site (Chen P, 2015). Myelin clearance is one of the most important events for axon regrowth. In addition to the receptor-dependent phagocytosis of axon and myelin debris, macrophages release also some mitogenic factors active on SCs and fibroblasts (Klein D, 2016).

The Wallerian degeneration is therefore associated with a strong inflammatory response (Gaudet 2011). During this key stage a lot of chemokines, cytokines and interleukin (IL-1 and tumor necrosis factor (TNF)) are released. This fact leads to increase blood vessel permeability, facilitates macrophage migration to the injury site and, in addition, neutrophils are recruited from blood vessels, within the first week, and, together with lymphocytes, can lead to the development of neuropathic pain.

The nucleus modifies its morphology in a way resumed as "chromatolytic changes" (*Figure 2B*). Neurons modify their mRNA transcription profile with the up-regulation of proteins related to cell growth, like cytoskeletal components, transcription factors (c-Jun; c-Jun N-terminal kinase, JNK; activating transcription factor 3, ATF3) and growth factor receptors (Fornaro 2008).

The proximal nerve stump is involved in an initial retrograde degradation, consequently the axon retracts back to the first node of Ranvier, reduces its diameter, and then the neuronal regeneration process begins. Axon sprouting begins in different directions on basal lamina provided by SCs, guided by neurotrophic factors and adhesion molecules. Growth cones of attracted regrowing axons use these SC-made tubes as a growing substrate, extending at an average rate of 1-3 mm/day. At the end of the regeneration process, the interaction between maturing SCs and regrowing axons in the distal nerve stump, induces myelin formation with significantly shorter internodes (Luis 2007)(*Figure 2D*).

The recovery from such changes can last from few weeks to months, depending on the re-establishment of the appropriate connections with the target organs. Failure of axotomized neurons to re-establish the appropriate connections may result in chronic chromatolytic state or even in their degeneration. Such conditions lead to prolonged or permanent denervation of the target organs, with consequent atrophy (i.e. skeletal muscle fiber atrophy). Since severe peripheral nerve injuries involve connective tissue scarring, axon

regenerative attempts are often destined to fail and aberrant sprouting frequently occurs leading to neuroma development at the proximal nerve stump (Deumens 2010).

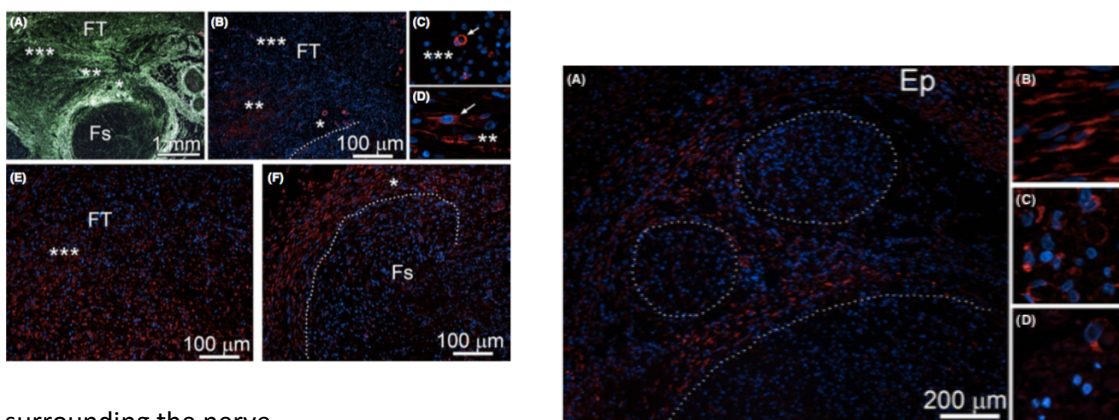
1.1.2. What happens outside the nerve: perineural scar formation

As other conventional wound-healing processes, peripheral nerve regeneration involves an early inflammatory phase, a granulation phase, and, finally, a remodeling phase and scar formation. Thus, it inevitably results in intraneural scarring that impedes axonal regeneration and is a mechanical barrier to sprouting axons (Mathur 1983).

During the first 24–96 hr, SCs recruit resident and hematogenous macrophages that also participate in the process. These cells are responsible for myelin removal by way of phagocytosis and may also contribute to collagen deposition during fibrosis (Burnett 2004).

Alpha smooth muscle actin (α SMA) and Heat Shock Protein 47 (HSP47) are involved in deposition and disposition of collagen fibers in all tissues, peripheral nerve included. The α SMA is expressed by pericytes surrounding blood vessels, whereas HSP47 is a chaperone protein upregulated during collagen production (Rivlin 2017).

The enrolment of α SMA and HSP47 is showed in *Figure 3* as presented by Rivlin. The authors demonstrated the key role of HSP47 in perineural scar formation, more than α SMA that appears to be rarely present in scar



tissue surrounding the nerve.

Fig 3: in right panels (A-F) with asterisks are represented α SMA positive cells in fibrotic tissue (FT). In left panels (A-D) HSP47 positive cells are highlighted. Note the high number of HSP47 cells Rivlin 2017.

In the pathophysiological process of wallerian degeneration and intra and perineural scar formation, also a specific form of autophagy, named myelinophagy, acts.

The autophagy on a healthy neuron is a physiological event that clears damaged and non-functional elements from the periphery of an axon to the cell body. In case of nerve damage, the retrograde flow of autophagic

vacuoles is impaired and the results is an increasing discomfort of cell body , called autophagous stress, that leads to autophagic cell death as reassumed in Figure 4. This process involves also SCs which remove myelin debris after a trauma.

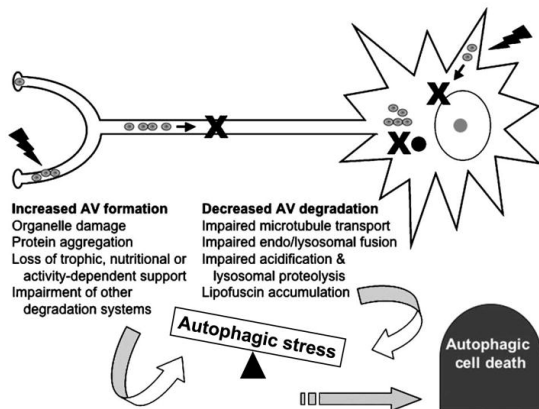


Fig. 4: autophagy process and autophagic stress from (Chu 2006). Autophagic vacuoles (AV) transport in impaired following a nerve injury; AV degradation is reduced and this increase autophagic stress and cell death.

This process, named myelinophagy, it has been understood for a long time that the first phase of myelin digestion in injured nerves is performed by Schwann cells.

Moreover, has been demonstrated that myelin debris are involved in scar tissue formation around the nerve (Ko 2018). These authors, in fact, demonstrated the reduction of scar tissue around a direct suture if autophagy process is increased giving rapamycin. Rapamycin inhibits the mammalian target of rapamycin complex 1 (mTORC1) (Chong 2012), which senses nutrients and negatively regulates autophagy. In figure 5 the different expressions of perineural scar after rapamycin somministration are shown.

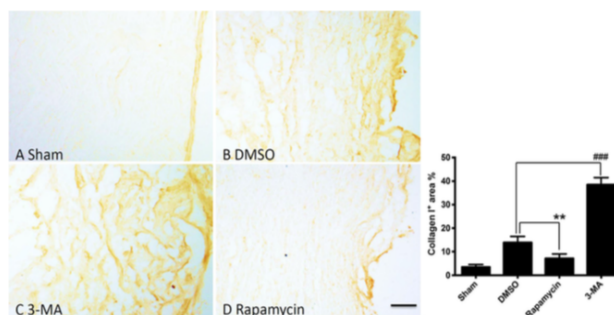


Fig. 5: effect of Rapamycin on reduction perineural scar enhancing the myelin autophagy process. From (Ko 2018)

As mentioned above the formation of scar tissue around peripheral nerve leads to the condition called by Hunter in 1991 traction neuropathy. The term indicates a condition related to impaired nerve gliding (Hunter 1991) with neurological symptoms due to the impaired movement of the affected nerve.

1.2. NERVE REPAIR TECHNIQUES

When a nerve is severed, different types of procedure are feasible nowadays to repair or reconstruct it according to the site of injury, the amount of the nerve to be reconstruct, the time between the insult and the procedure.

1.2.1. Direct suture

Over the years, different types of nerve suture have been described: epineural, perineural, epiperineural. The epineural suture represents the oldest of the neurorrhaphy techniques. The stitches pass through the epineurium. This method has the advantage of minimal manipulation of the nerve, leaving the possibility of neurotropic factors to guide the regeneration of axons to their respective target organs. When the suture is performed on large caliber nerves such as trunks, cords and nerves at the arm and forearm, the fascicles can be oriented approaching epineural vessels.

The perineurial or fascicular suture requires a meticulous dissection of the nerve stumps by performing the epineurectomy as described by Millesi in order to highlight each individual fascicles (Millesi 1982). The needle is passed through the perineurium. This type of technique guarantees considerable precision with fascicles orientation; however, the advantages may be undermined by the need for greater surgical manipulation and the risk of coaptating mismatched fascicles, with certain functional loss.

The epiperineural suture is a mixture of the previous ones and aims to summarize the advantages of both. Dissection is limited to the peripheral fascicles, which are isolated (limited manipulation). The needle is passed through the epineurium first and then the perineurium, thus merging groups of fascicles. This is a very durable type of suture, used for large nerve trunks and in incomplete lesions.

There is no clinical evidence that one technique is more effective than the other, and it is generally considered that simple epineural stump suturing is sufficient in proximal lesions where fibers admixture is greater. We believe that the epi-perineurial suture can, if one does not exceed in nerve manipulation, prepare for the best final result in term of functional recovery.

Usually a direct suture is performed under optical magnification and an 8-0/9-0 nylon suture is used. When the suture done with a 8-0 nylon breaks down spontaneously, a nerve gap appears and requires appropriate reconstruction. (Millesi 1982)

1.2.2. Nerve reconstruction

When tension between the transected nerve stumps is excessive or the gap between them is too wide to be repaired with direct neurorrhaphy, then the use of alternative technique is mandatory (Millesi 1976).

Millesi demonstrated, in the early seventies, that bridging a nerve defect with a segment of an autogenous nerve leads to better clinical results than suturing the two stumps under tension (Millesi 1976). Since that moment, the use of an autogenous nerve to treat a nerve gap, technique called nerve autograft, has seen a large clinical employment, especially in the field of hand surgery. However, this surgical procedure has several main disadvantages: it requires an extra surgical incision for the withdrawal of a healthy sensory nerve; the removal of the healthy nerve will result in sensory residual deficits; graft material is limited (in terms of length) especially in cases requiring the repair of extensive lesions, such as brachial plexus lesions. For these reasons, increasing efforts have been made over the last two decades to seek for effective alternatives to autogenous nerve grafts. Among the various strategies that have been attempted, the possibility of repairing nerve defects by bridging the gap by means of tubes made by non-nervous materials have been widely experienced, both experimentally and in clinical practice: this surgical approach is usually referred to as either tubulization or (en)tabulation (Schmidt 2003).

This technique is limited to gap no larger than 10 cm, for greater gaps no recovery can be expected through nerve grafting, so that others procedures have been developed as nerve transfer (Doi 2018). Since for skeletal muscle reinnervation well defined terminal nerves, trunks or cord can be reconstructed, for autonomic driven organs such bladder, rectus, penis, the innervation is provided through plexual terminal branches. When these branches are severed, classical reconstruction through nerve autograft failed (Davis 2009), thus alternative reconstructive techniques have to be investigated such as conduits and membranes promoting nerve recovery or novel nerve transfer.

1.2.2.1. Autograft reconstruction

The interfascicular autologous nerve grafting technique is still considered the “gold standard” for the repair of traumatic nerve defects (Geuna 2014).

The nerve graft acts providing a source of viable Schwann cells and empty endoneurial tubes through which the regenerating axons can cross the site of injury. The Schwann cells produce an immediate source of nerve growth factor, which helps to support the growth cone in the proximal stump. The graft, to be effective, must acquire a blood supply from the surrounding tissues. It has been shown that Schwann cells can survive 7 days, depending purely on diffusion. By 3 days after implantation, endothelial buds from the surrounding tissue bed get into the nerve graft, with evidence of high nerve blood flow in one week. Small-diameter grafts spontaneously revascularize, but large-diameter grafts do so incompletely; thick grafts undergo central necrosis with subsequent endoneurial fibrosis that is negative for the advancement of ingrowing axons. This is the reason for cable nerve grafts sutured or glued together to match the caliber of the recipient nerve are not for all surgeons the best option for bridging a nerve defect (Lundborg 2005).

Generally, it is used in case of secondary procedures. In an open injury when the nerve repair was not carried out immediately because of the type of injury (blunt or crush injuries), or the lack of microsurgical expertise, or because of iatrogenic lesions, the nerve stumps retracts requiring secondary grafting. In closed injury a stretching or blunt trauma often produce a neuroma in continuity that require secondary resection and nerve grafting. In *Figure 6* a cable nerve graft is shown.

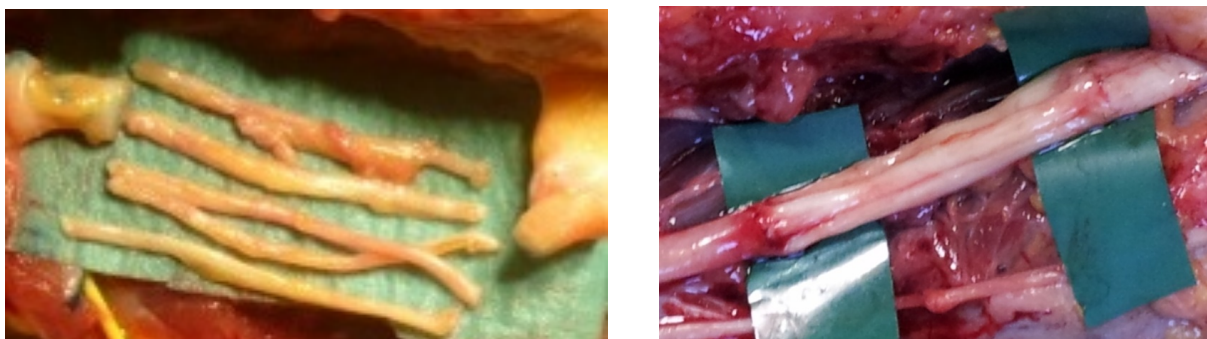


Fig. 6: nerve graft technique. On the left before the suture of all grafts to the nerve trunk. On the right at the end of the microsuture. Courtesy of Dr P. Tos.

Usually, nerve grafts could be harvested from sural nerve and medial brachial and anti-brachial cutaneous nerve, but other sensory nerves could be employed as source of autograft. The donor site morbidity is low and usually a few patients complain neuropathic pain or present problem due to the loss of sensibility in the dorso-lateral aspect of the foot or medial side of arm and forearm.

The diameter of the injured nerve is normally higher than that of the sural nerve, so that several graft segments are used until an equivalent diameter is obtained.

Each graft segment is addressed to each group of fascicles and a suture is performed between perineurium of the isolated abutment and the epineurium of the graft segment or, in small nerve with not clearly identifiable fascicles, epineurial suture could be performed between nerve stump and graft.

In this case, a few anchorage points (2 or 3) are sufficient among the single fascicles and the graft segment. At the end, fibrin glue is used to assemble the whole graft. Some authors proposed to do not use stitches, but only fibrin glue to fix the graft to the nerve stump, in order to do not create trauma on nerves, but there is no evidence of improvement of nerve regeneration using this technique.

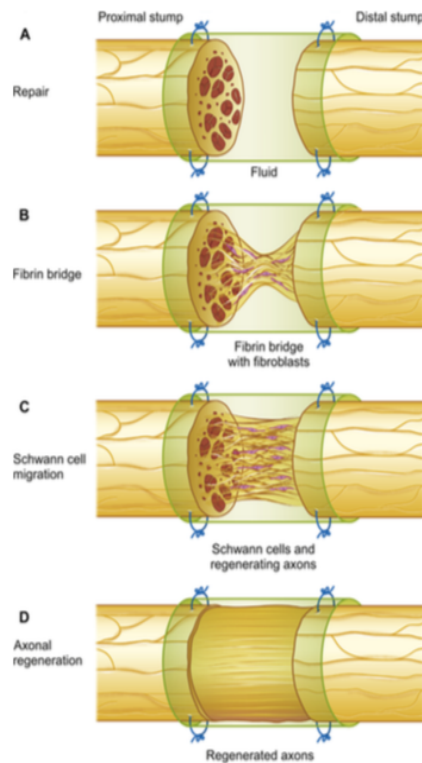
1.2.2.2. Nerve conduits

Nerve conduits are substitutes to nerve grafts used in nerve repair surgeries. They are either composed of biologic or synthetic materials, and are placed between the two nerve stumps as a regeneration scaffold. Conduits guide nerve regeneration across the defect toward the target organ and have the main advantage of not requiring the sacrifice of an autologous nerve.

Nerve conduits act connecting nerve stumps, creating a microenvironment in which neurotrophic and neurotropic factors can act, guiding the regenerating axons and protecting the nerve from the surrounding tissue (Sabongi 2015).

The concept of tubulization gives a way in which new extracellular matrix can grow providing functional scaffold for vessels, fibroblasts and SCs to form a new nerve structure (Siemionow 2009).

Nerve conduits can be differentiated according to their origin: biological conduits exist and can be autogenous and non-autogenous. Moreover, synthetic conduits are available for clinical use. Following the spreading of synthetic conduits, basic science is trying to ameliorate their regenerative capacity through engineering techniques. This last topic will be discussed later on.



In *Figure 7* is depicted how the nerve grows into an empty tube (Rinker 2014).

Fig. 7: The different phases of regeneration across the nerve tube. (A) Within hours of implantation, the lumen fills with fluid containing neurotrophic factors and various inflammatory cells. (B) Within days, a fibrin matrix is formed between the nerve stumps. (C) In weeks, Schwann cells, fibroblasts, and microvessels migrate along the fibrin matrix from both proximal and distal nerve ends. (D) In months, axons regenerate from the proximal nerve stump into the matrix (picture from (Rinker 2014, Vijayavenkataraman 2020, Huang 2023).

Autogenous conduits

Arteries, muscles and tendons have been studied as autologous alternatives for bridging nerve defects, but vein tubes have appeared to present the most advantages. Vein walls' are resilient enough to act as a barrier against scar ingrowth and have the permeability to allow diffusion of the proper nutrients. There is an ample supply for vein graft harvesting from many areas of the body, at a low cost, and with a relatively minor degree of additional injury compared with nerve grafts. Moreover, veins are nonimmunogenic, cause less inflammatory reaction compared to synthetic conduits and are available in a wide variety of sizes (Sabongi 2015). The use of intraluminal additives, filling the vein tube, reduce the risk of collapse. Such is the case for the Muscle-in-Vein (MIV) technique, which consists in harvesting a superficial vein with a diameter similar to that of the nerve requiring reconstruction, and a small strip of striated muscle fibers. The use of skeletal muscle in peripheral nerve reconstruction has been proposed because of its extracellular matrix components and highly oriented basal lamina tubes. These structures provide a suitable substrate for regenerating axons

(Battiston 2007). The muscle has the double function of sustaining the vein from the inside to avoid its walls from collapsing, and to help guiding the axonal regeneration process (Battiston 2009). The vein is sutured to the epineurium of the nerve stumps after their preparation. These procedures can be employed in patients with satisfactory clinical results for gaps up to 30 mm, with very impressive results especially for sensitive nerves (Tos 2012, Manoli 2014, Ederer 2023).

An example of MIV used to reconstruct a proper digital nerve is reported in figure 8.

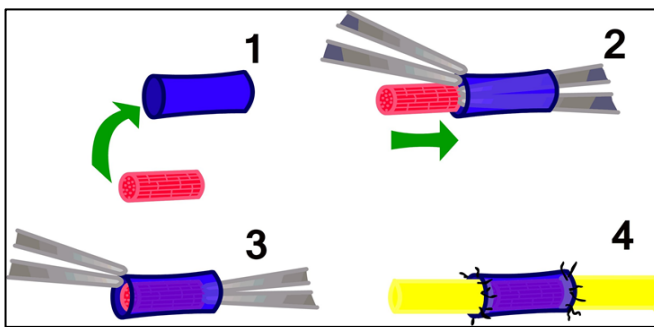


Fig. 8: a) Muscle-vein-combined graft technique; the muscle is withdrawn longitudinally in the sense of muscle fibers and well washed from blood. The muscle is inserted into the vein with the help of forceps. Finally, the graft is sutured into the gap as previously showed. B) clinical application of muscle in vein to reconstruct a 1.5 cm nerve gap of a digital collateral nerve.

Non-autogenous biological conduits

Nerve allograft consists on bridging a nerve gap with a decellularized nerve segment (Safa 2016). The decellularization process it is fundamental to remove all the immunogenic proteins inside the nerve, maintaining the structural components of the extracellular matrix to permit the axons to regenerate.

Allograft nerves provide a functional extracellular matrix (Carriel 2014). Researchers developed strategies of cryopreservation of allografts before the implantation. This strategy reduces the immunogenicity of the graft and its effectiveness is confirmed in experimental and clinical studies (Squintani 2013). Decellularization has been described as an efficient method for the generation of non-autogenous scaffolds. This technique removes cellular components from the tissue, but maintains intact the endoneurial collagen fibrils and the 3D architecture of the extracellular matrix (Deumens 2010).

Indeed, different nerve allografts derived from decellularization protocols show promising experimental results (Whitlock 2009), and some of them were approved for clinical use in humans by the FDA (Kehoe 2012). Despite the evidences reported by American manufactures of nerve allograft (Brooks 2012), different

decellularization techniques are being investigated and developed in order to reduce the cost of production of these promising nerve graft devices.

Clinical results are nowadays contradictory: it has been demonstrated their efficacy in reconstruct small nerve gaps in sensory nerves up to 3-4 cm with efficacy comparable to conduits and autograft. Whereas in longer gaps of motor or mixed nerves some authors reported impressive good results (Safa 2019). Others instead experienced no recovery in 4.5cm gap of mixed nerves (Huddleston 2021).

The human amniotic membrane and the rat small intestinal submucosa were used also. Tubular rolls of both cited tissues can promote and support peripheral axon regeneration, leading to a functional recovery similar to groups repaired with the autograft technique (Hadlock 2001, Riccio 2014).

The PhD program covered also this aspect. Chapter 3 contains a paper in which a new decellularization method has been investigated and applied to nerve segments from other animals. These xenografts were then employed to reconstruct a nerve gap in animal model.

Synthetic entubulation

It consists in the use of either absorbable or non-absorbable materials, completely overcoming the need for donor tissues. The downside to synthetic entubulation include the high costs. The ideal conduit should be made of a low-cost, biologically inert material that is, biocompatible, thin, flexible, transparent, inhibitor of inflammatory processes such fibrosis, gliomas, neuromas, swelling, ischemia, and adhesions, and facilitator of the processes that contribute to regeneration, accumulating of factors that promote nerve growth. No such synthetic conduit exists thus far. There are currently 7 US Food and Drug Administration (FDA)/Conformit Europe-approved synthetic nerve conduits: NeuraGen[®], NeuroMatrix[™], Neurolac[®], Neuroflex[™], Reaxon[®], Nerbridge[®] (Kehoe 2012). The used materials include woven polyglycolic acid (PGA), type I collagen, poly-DL-lactide-caprolactone (PCL). Most of these materials are biodegradable polymers, but carry the risk of foreign body reaction and extrusion, other than being costly. The non-absorbable materials include silicone scaffolds.

The major advantage of synthetic material is the possibility to modify the chemical and physical properties, improving resistance and flexibility. Indeed, synthetic materials are often devoid of the bioactive molecules necessary to promote cell-substrate interaction. Although synthetic biomaterials are suitable, they add expense to the surgical practice and increase the risk of foreign body reaction (Sabongi 2015).

Nerve conduits in general have emerged as alternatives to autologous nerve grafts, but their use in large-diameter nerve deficits (e.g., median, radial, and ulnar nerves) remains untested both experimentally and clinically. Currently, conduits are typically used for nerve gaps of less than 3 cm involving small-diameter, noncritical nerves as sensory digital nerves and branches of the radial sensory nerve (Moore 2009).

The nerve conduits are secured as follow in fig 9. A U-shaped stich is used to pull the nerve stumps into the tube, covering the nerve stumps under the tube edges.

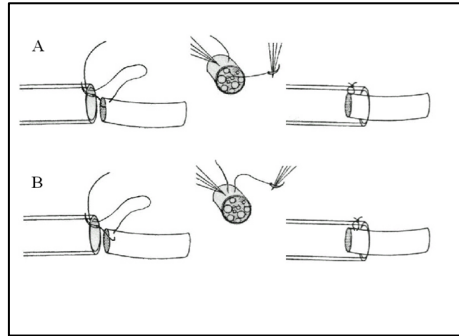


Fig. 9: different surgical techniques to insert the nerve 1-2 mm inside a nerve conduit to avoid dispersion of regenerating fibers; A: the needle pass through the nerve longitudinally; B the needle pass transversally on the epineurial tissue.

Chitosan conduits

Chitosan is a polymer of D-glucosamine and N-acetyl-D-glucosamine, obtained from full or partial N-deacetylation of chitin. It is a linear homopolymer composed of N-acetyl-D-glucosamine units that form beta-(1-4)-linkages (Freier 2005). Chitin is, after cellulose, the second most abundant polysaccharide in nature (Crompton 2007). This material is highly biocompatible, biodegradable and shows low toxicity. Moreover, chitosan is an attractive material to produce nerve guides because it can be easily blended with other materials or modified on its surface to better support axonal regrowth (Haastert-Talini 2013).

In vitro studies revealed the suitability to use chitosan membranes as substrate for survival and orienting the SCs and survival and differentiation of neuronal cells (Simoes 2011).

The study of chitosan-made tubes alone or in combination with other biomaterials in recent years, demonstrated the efficiency of such nervous guides for bridging peripheral nerve defects (Gnavi 2013 Shapira 2016). In *figure 10* is depicted the use of hollow chitosan conduit in repair of sciatic nerve gap in rat.

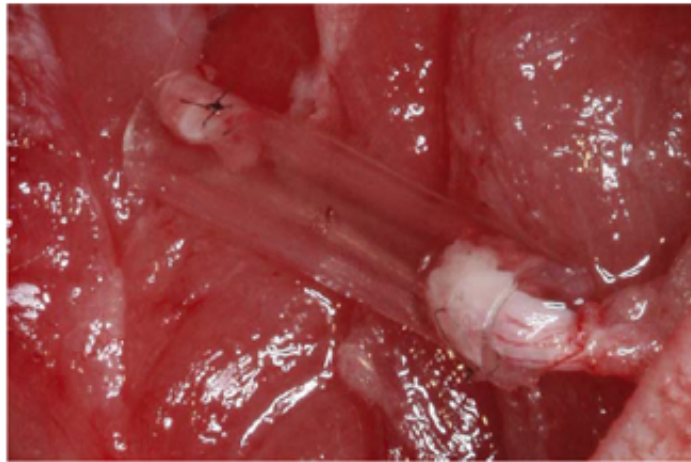


Fig. 10: Chitosan conduit employed in rat sciatic nerve. From (Shapira Y 2016).

The chitosan presents the possibility to change the degree of acetylation and it makes possible the modification of its mechanical properties and the degradation rate of the tube. Moreover, the possibility to change the microstructure leads to create 3D microstructures that could improve the physiology of nerve regeneration into conduits (Wang 2008).

In 2014 chitosan tubes have been accepted for clinical use in Europe (Reaxon[®] Nerve Guide, Medovent GmbH, Mainz, Germany). The clinical efficacy of this device was investigated in a randomized, double-blind, controlled, multicenter trial in different trauma centers in Germany and comprises cases of acute digital nerve injuries (up to 72 h from the injury) (Neubrech 2016).

PGA conduits

These scaffolds can degrade within a reasonable time-window, and the degradation products are totally absorbed with mild foreign body reaction. One of the most promising and effective material is Polyglycolic acid (PGA). It is a biodegradable polymer, and PGA-based conduits are currently the most applied nerve guides in the clinical and experimental practice. Moreover, PGA-based guides, NeurotubeTM, was the first approved nerve conduit for medical use in the human body (Belanger 2016).

In this chapter the most employed tubes in clinical practice were summarized. Considering the cited limits, lots of research programs are oriented towards improve efficacy of conduits, engineering them. Due to the complexity of this argument, a dedicated chapter is reserved later on.

1.2.2.3. Nerve transfer

When the characteristics of the nerve injury are such, due to the type and extent of the damage (root avulsion or tear), that it is not possible to use grafts for connecting the proximal and the distal stump, nerve transfers are indicated to reinnervate a denervated district. They are indicated when a nerve gap is longer than 10 cm and when the target organ is far from the reconstruction site, converting a high nerve injury to a lower-level lesion that is closer to the target muscles with a greater likelihood of timely and successful muscle reinnervation (Brown 2008).

Usually the neurotization is motor, but can also be sensory (radial pro median nerve). As stated above, nerve transfers are prevalently used in brachial plexus reconstruction. In such pathology accessory cranial nerve, intercostal nerves, triceps branch of the radial nerve, fascicles for the flexor carpi ulnaris of the proximal ulnar nerve are used as motor. Recently branches of the radial and median nerve have been described as motor for nerve transfer in the forearm to reanimate lower radial, median and ulnar nerve palsy (Brown 2008, Doi 2018).

From a 'technical' point of view, if the diameter of the recipient funiculus is similar to the contingent being transferred, a traditional end-to-end suture is the technique of choice.

In some situations, an end-to-side suture has been proposed. It consists on connecting by a terminolateral fashion method the distal stump of an injured nerve on a functional nerve with or without an epineurotomy. This technique presented very good results in preclinical setting, but not confirmed in clinical reconstruction. In clinical settings it is used as supercharging or babysitting procedure to boost the distal recovery of a proximal reconstructed or neurolysed nerve as for high ulnar nerve injury reconstruction or severe ulnar nerve compression at the elbow (Chuang 2018). In those cases, the anterior interosseous nerve can be sutured in end to side to the motor fascicles of the ulnar nerve at the elbow (Tos 2014).

Direct muscle neurotization

When a nerve trunk is torn from the muscle, excellent results have been achieved with the direct muscle neurotization described by Brunelli (Brunelli 1982). It consists in surgically implanting a nerve directly into a muscle: regenerating nerve fibers are able to re-establish functional connections with the muscle fibers forming new motor plates. Muscle fibers, following denervation, express receptors for acetylcholine over its entire surface, along which they can therefore be reinnervated.

Nerve transfer have been proposed also for autonomic reinnervation. Since the early 90's roots transfer for bladder reinnervation have been proposed in clinical practice following promising results obtained in animal models. The most investigated transfer involved has been L4 ventral root to L6 ventral root intradural transfer, in order to create a spinal reflex able to induce detrusor contracture (Xiao 1999). Following this

experience, extradural nerve transfers to pelvic nerve were tested in living models to improve bladder function (Ruggieri 2008).

The root transfer was tested not only for bladder recovery, but also for bowel control and erectile dysfunction.

More recently, to treat the latter issue, a direct organ neurotization has been proposed. In such procedure the femoral nerve was connected, through a sural nerve graft, to corpora cavernosa. This was used in patients affected by erectile dysfunction as a consequence of radical prostatectomy and the authors registered impressive positive results (Souza Trindade 2017).

Since part of this research project involves corpora cavernosa reinnervation and, moreover, few knowledges are now available on autonomic reinnervation and somatic to autonomic nerve transfer, a literature review on this topic has been finalized and presented in chapter 3.

1.3. COMPLICATIONS OF NERVE INJURIES AND REPAIRS

As written above, during the process of nerve repair and regeneration, pro fibrotic processes act in synergism with axons regrowth. The amount of scar and the site (perineural or intraneural) is dependent by the type of injury and how deeply the injury involves the nerve. Once the fibrotic process is ended, it can result in different pathological situation that can complicate nerve recovery. They can be divided in traction neuropathies when the scar connects the nerve to surrounding tissues, limiting its excursion during limbs movement; the other one is the so-called neuroma, an extended intraneural scar clew.

Both these pathological situations lead to pain and impaired nerve function.

1.3.1. Traction neuropathies

As a consequence of traumatic injuries and surgical procedures on peripheral nerve, a scar formation around the nerve can arise. This condition easily worsens the capacity of peripheral nerve to regenerate and give rise to traction neuropathy. Nerve tethering in the surgical scar is still the main cause of symptoms related to perineural scarring (Tos 2015) and the most frequent symptom complained by the patient is neuropathic pain. For instance, 7-20% of patients subjected to primary median nerve release report pain and symptom recurrence due to scar formation (Jones 2012).

When the scar connects a nerve to the surrounding tissue, the so called paraneurium, a conjunctiva-like structure (Lang 1962), is impaired and this reduce the possibility of nerve elongation. The consequence is the increasing of tension on the inner vessels and reduction of blood flow into the nerve. The evolution is a formation of edema and then intraneural scar. For this reason, traction neuropathy may be too narrow as definition. In fact, the condition is likely to a fibrotic response that is initially perineural and eventually

becomes intraneural due to chronic scarring compression. The repair process may subsequently lead to formation of an in-contiguity neuroma with residual nerve function whose symptoms also involve pain at rest (Elliot 2014). The histo-pathological consequence is the formation of a stage III or IV nerve injury according to Seddon and Sunderland classification.

Moreover, it is fundamental to report that preclinical studies have demonstrated that 8% increase in nerve tension induces a 50% reduction in intraneural blood flow, whereas tension exceeding 15% of the baseline value induces an 80% reduction in intraneural blood flow (Clark 1992).

The condition is difficult to manage, so much so that according to different reports compression symptoms persist after 40-90% of revision procedures, and 20% of patients actually require a third operation (Amadio 2009). In Figure 11 an example of post surgical scar around median nerve at the elbow is presented

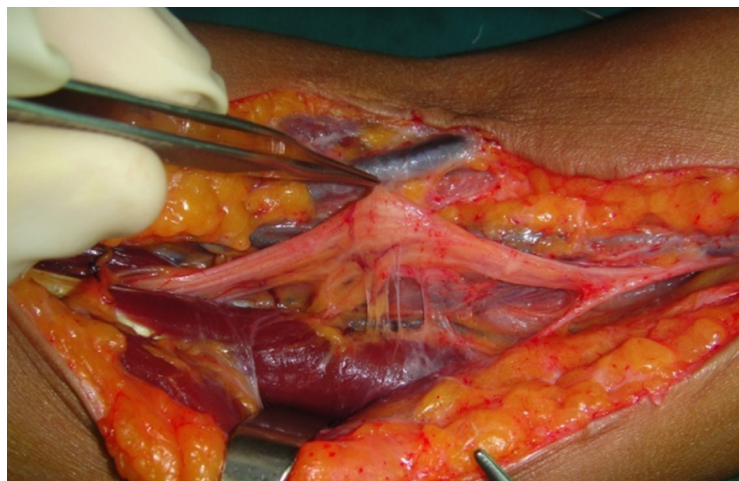


Fig. 11: Median nerve at the elbow entrapped in post-surgical scar. Courtesy of Dr. P. Tos and B. Battiston

Dignosis

History is crucial to establish the cause of symptoms, can be related to previous simple nerve decompression, reconstruction, direct trauma, or post-traumatic scarring. Physical examination and pain type - at rest or elicited by movement or mechanical stimuli - may provide information on lesion type.

Pain at rest commonly configures the presence of intraneural scar. Tinel's sign - the referred feeling of tingling during tapping over the course of a peripheral nerve - is invariably positive and the patient often has hyperalgesia and/or allodynia in the territory of the involved nerve.

As regards diagnostic imaging, ultrasound (US) provides reliable information on the actual extent of the nerve injury (due for instance to a previous procedure), the amount of scarring, and the state of the outer and inner connective tissue layers of the nerve trunk. It thus provides an indication for surgery by demonstrating the extension of scar tissue. In some cases, Magnetic Resonance Imaging (MRI) could add details, but actually a well conducted US study could be the main source of diagnostic imaging regarding this problem (Pitarokoili 2023).

Electromyography (EMG) examination is also important, because it documents the degree of peripheral nerve distress, and findings can be compared over time (preoperative, postoperative, follow-up examination).

1.3.2. Painful neuromas

A neuroma is part of the normal biological process in a transected and unreconstructed nerve. The axons sprout and grow, but without direction and form the neuroma, if there is no connection to a distal part of the nerve. Neuromas are provoked by axons sprout into the surrounding scar tissue.

A neuroma can be terminal, with or without the possibility of a distal reconnection (such in case of loss of substance) or can be in continuity (as in case of blunt trauma); another distinction has to be made between neuroma which determine or not a residual function.

It is absolutely unclear why a neuroma becomes a painful neuroma.

Two processes are responsible for pain: 1) persistent mechanical or chemical irritation of the axons within the neuroma and 2) the development of spontaneous and disturbing sensory symptoms caused by persistent stimulation of the axons within the neuroma and accompanied by the development of spontaneous activity of neurons within the dorsal root ganglion, dorsal horn of the spinal cord, or even more proximal level. It seems that an up-regulation of sodium channels, adrenergic and nicotinic cholinergic receptors lead to abnormal sensitivity and spontaneous activity of injured axons. During time a central sensitization in the spinal cord and sensory cortex take place. leading to a chronicity of the disorder. When this condition appears no more benefit from surgical procedure on peripheral nerve can be obtained (Smith 2023).

The true incidence of symptomatic neuroma is unknown is estimated at approximately between 2–60% of patients involved in peripheral nerve injury (Ducic 2008).

The neuroma can be:

- *terminal without possibility to a distal reconnection* (i.e. a digital neuroma or the distal nerve trunk is not available for multiple surgery, loss of substance);
- *terminal with the possibility to a connection* with a distal nerve stump (i.e. sensory radial nerve branch as a complication of surgery or traumatic transection of a nerve);
- *in continuity* (after a nerve suture or a trauma)
 - *without residual function*
 - *with a residual function.*

Diagnosis

The diagnosis of painful neuropathy is based on history and physical examination. Spontaneous pain, allodynia, hyperalgesia and cold intolerance are the main symptoms reported by the patient.

The history of a nerve injury is accompanied by pain and typical symptoms with a defined neural anatomic distribution often with cold intolerance. Another important information is the presence of a painful Tinel sign. A local anesthetic injection can be helpful to understand if the symptoms are related just to the neuroma of they are corticalized. Blocks provide patients with an idea of the potential area of altered sensation with nerve resection but does not guarantee operative success. On the other hand, if block doesn't reach the scope, it means that no surgical procedure can solve the problem and should be avoided.

Furthermore, instrumental examination - US or MRI - can confirm the diagnosis. It is suggested pairing a simple assessment of pain, like the visual analogue scale (VAS) with a more detailed pain and function questionnaire the DASH or PROMIS. Serial assessment with these forms facilitates tracking progress that is sometimes not apparent to the patients themselves (Smith 2023).

1.4. TECHNIQUES FOR TREATMENT OF TRACTION NEUROPATHIES AND PAINFUL NEUROMAS

1.4.1. Neurolysis and associated procedures

This is the treatment of choice when a symptomatic nerve tethering is diagnosed.

There is no consensus when the surgical therapy has the best role (Lipinski 2014). Nowadays, surgery is indicated when medical and physical therapy have failed to bring benefit.

The surgical intervention consists on surgical exploration, neurolysis under magnification, and adjunctive procedures aimed to prevent new scar formation such as flap coverage and application of anti-adhesion devices.

The first step consists on nerve identification in non-injured zone, after that the nerve is freed by the scar tissue by external neurolysis or, in few selected cases, by internal neurolysis. In Figure 12 the neurolysis of a scarred nerve is presented.

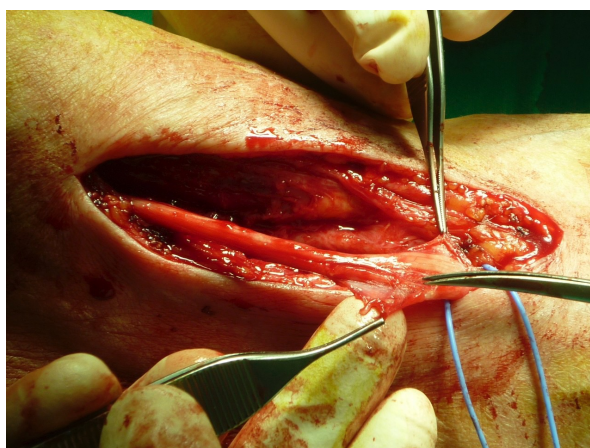


Fig. 12: external neurolysis of a median nerve at the elbow.

The second step involves relocation of the nerve tract involved in a “soft” vascularized bed enabling gliding (Lipinski 2014). To aim this goal the use vascularized or non-vascularized autologous tissue or anti-adhesion gel is described. However, there is no a clear indication about when anti-adhesion devices, flaps, or other autologous tissues have to be used or which have the best anti adhesion activity.

Commercial gels and anti-adhesion devices

The most easy and quick way to protect the nerve against scar recurrence is to apply these products around the nerve itself after neurolysis.

These devices are used to restore the lost gliding surface. The most employed products are composed by hyaluronic acid, carboxy-methylcellulose with polyethylene-oxyde or phosphatidylethanolamine and collagen.

However, it is not clear which of these products present the best anti adhesion activity either in pre-clinical and clinical settings.

Vein conduits

Elliot reported poor outcomes in neuromas-in-continuity of the palm and the fingers, describing pain recurrence at the site of treatment due especially to repeated trauma, because the thin vein wall does not adequately protect the nerve against external insults (Elliot D 2014). Actually, the usage of vein wrapping is increasing its popularity and good results, considering the low cost compared to artificial devices (Thakker 2021).

Flaps

A variety of flaps, pedicled (local) or free, are used for coverage after neurolysis: synovial, fascial, adipofascial, muscle and skin with subcutaneous tissue flaps.

Compared to vein wraps, gels, and other anti-adhesion devices, flaps have a dual function: to envelop the injured nerve in a highly vascular tissue to maximize nutrient supply, and to provide a bulk effect, i.e. protection against external mechanical insults. This approach is often used in patients where revision surgery has had poor outcomes or when the quality of local tissue does not allow performing simpler procedures.

Typical local flaps raised in patients with recurrences or sequelae of carpal tunnel syndrome (CTS) include the hypothenar fat pad flap first described by Crammer (Cramer 1985) and the palmaris brevis flap described by Rose (Rose 1991).

Thicker flaps can be raised from the volar forearm: the dorsal ulnar artery adipofascial flap described by Becker and Gilbert (Becker 1988) can be used as an adipofascial flap to wrap the nerve or as a fasciocutaneous flap to provide greater protection; the adipofascial radial artery perforator flap (Adani 2002) and the

adipofascial variant of the posterior interosseous flap raised from the dorsal portion of the forearm (Vogelin 2008) can be employed in the same way; the pronator quadratus muscle flap (Adani 2002) may be a useful solution when the injury is proximal to the wrist.

Numerous free vascularized flaps, described for coverage of freed nerves, are however rarely used. The free omental flap, lateral arm flap, scapular flap, and groin flap seem to be more effective than local flaps, yet the approach is recommended only for use in patients with severe conditions who have already been treated and in those with hand and forearm lesions where a local flap would impair hand use (Goitz 2005). Yamamoto and Koshima have gone further: they raised an anterolateral vascularized thigh flap that included the lateral cutaneous nerve of the thigh to reconstruct the median nerve, and described early pain resolution and full recovery of wrist and hand mobility five months from the procedure (Yamamoto 2014). We recommend such complex procedures only in patients with severe nerve injury and failure of multiple surgical procedures, where another local flap could result in local tissue damage. In *figure 13* a Becker flap and a pronator quadratus flap are presented.

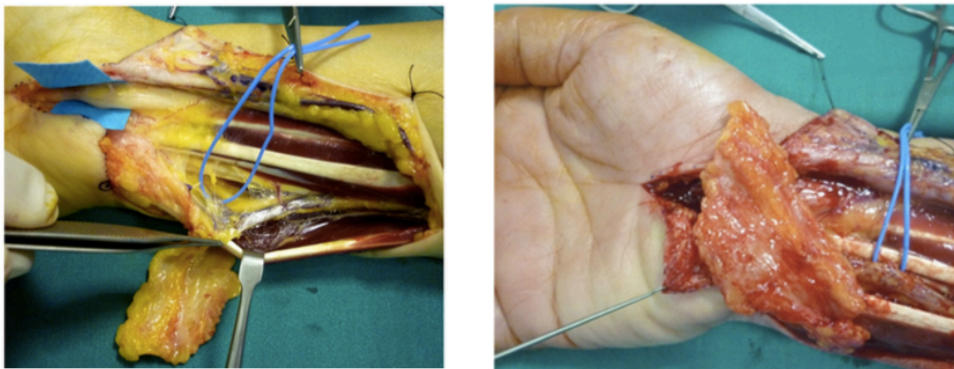


Fig. 13: a Becker flap is used to cover a neuroma with residual function of median nerve at the wrist.

Fat graft and allogenic tissues

Fat grafting properties are well known and have become more popular in last few years.

Several reasons could explain the efficacy of fat grafting as an anti-adherence barrier. The first and more immediate is the mechanical property of the fat. Lipoaspirate fat is similar to a gel and can easily surround an exposed nerve to protect it from adherence. Adipose-derived stem cells (ASCs) and other cells included in the stromal vascular fraction (SVF) survive with the lipografting (or fat grafting) technique. They donate a pro-regenerative pattern of characteristics that can be important for preventing neural damage or facilitating neural regeneration after a trauma (Faroni 2013).

In particular, ASCs have been used to re-populate decellularized nerve grafts used to repair rat nerve gap models (Liu 2011, Shen 2012). Moreover, after systemic injection of ASCs, few cells have been shown to migrate to the nerve injury site contributing inflammation reduction and nerve regeneration improvement (Saffari 2022).

The first attempt to protect a nerve in pre-clinical setting was made by Dumanian (Dumanian 1999). They showed the reduction of scar tissue formation after epineurectomy and mouse fat grafting. We compared lipografting to anti adhesion gel in reducing peripheral nerve scar, finding no differences, in animal model, between the two treatment (Cherubino 2017). Clinically, the use of lipografting have been more tested to treat painful neuromas either terminal or in continuity. Small case series and case reports reported interesting but variable results (Vaienti 2012, de Jongh 2020, Calcagni 2018), thus lipografting around a nerve to prevent scar neuropathies or painful neuromas it is not a defined treatment yet.

1.4.2. In continuity and terminal neuroma resection and associated procedures

In continuity neuroma with function

When an injured nerve maintains its function, but symptoms of nerve impairment are present, external neurolysis and eventual nerve relocation in deeper well vascularized and healthy tissues could be planned. This should be the first attempt (protection from mechanical and thermal injury and with the possibility to avoid adherences around the nerve). Sometimes symptoms persist and further surgical and non-surgical procedures should be considered. Usually this condition in hand and wrist appears as a complication of a previous surgery (carpal tunnel release, open reduction and internal fixation of distal radius fracture or phalanx). When the nerve maintains its function and the main symptoms is pain the indication to surgical decompression is indicated when no more benefit appears from physical therapy, usually it takes at least 6 months after primary surgery (Tos 2015).

In continuity neuroma without function

When no function is conserved and the patient presents insensibility distal to the site of injury or allodynia and motor impairment of the target muscles a resection and reconstruction of the injured nerve is recommended. Nerve reconstruction provides the nerve a biologic pathway through which to grow.

If the in-continuity neuroma affects a mixed nerve (median and ulnar nerve at the wrist) the reconstructive procedure should be indicated if, after 3-6 months from the trauma or initial surgery, there are no signs of recovery and such clinical evidence is supported by instrumental investigations.

If the gap is up to 3 cm of a sensory nerve, a nerve conduit can be used. Facing a mixed nerve gap the best reconstructive strategy is represented by autograft reconstruction, even in a short gap (3-4cm) (Rbia 2017).

When more than 10 to 12 months passed from the injury the possibility of motor recovery is unpredictable. According to the type of patient and functional requirements, nerve transfers or muscle transfer should be associated. They are indicated when reconstruction by nerve grafts is not possible, either due to an excessive gap or an excessively long period since the lesion (Chuang 2018).

Terminal painful neuromas

Terminal painful neuromas are still a challenging problem for hand surgeons. There is no a gold standard technique to solve pain and avoid recurrence risk. Actually, no evidences indicate that a technique is superior to another either in acute and elective condition (de Lange 2022). The first described technique consists in shortening the nerve and move the end in adjacent, helthy and non- "touching" area. To this, Gosset (Gosset 1962) associated electrical coagulation of the stump of the nerve (by slowly increasing the intensity of the current). This procedure was theorized observing that electrically burnt patients do not produce painful neuromas. In order to reduce the risk of neuroma formation, providing a target to transected axons seems to be a winning solution. So that, centro-central union (CCU) has been described. After neuroma resection, the nerve stumps can be sutured together. A vein segment can be added to cover the site of suture to avoid collateral sprouting. The axonal growth and neuroma formation are stopped when a continuous flow of axoplasm is present: suturing two ends of the same nerve together increases the axoplasm pressure that reduces the protein production and axoplasm flow in the neuron, acting to inhibit neuroma development (Belcher 2000). Another procedure, following the same principle, for terminal neuromas of the digits, is reverse end-to-side neurotization. The nerve stump may be coapted to the side of an adjacent intact nerve by means of an epineural window in the recipient nerve. Usually the sensory collateral digital nerve can be sutured to a dorsal sensory branch. Doing this, a pathway for regenerating axons is provided. In the last decade, following the principle expressed previously, the targeted muscle reinnervation (TMR) has emerged as one of the most promising treatments for neuroma pain and prevention in major limb amputations (Dumanian 2019). It is based on the connection of a transected sensory nerve to the motor nerve entry point for an expendable muscle. The authors reported satisfying results in terms of drugs reduction and recurrence with follow up extended to 20 months (Wimalawansa 2021). Parallel to this, another procedure was described to prevent neuroma recurrence. The principle is the same, a cuff of muscle is sutured around the nerve end as a graft. The so called regenerative peripheral nerve interface (RPNI) was firstly introduced in myoelectric prosthesis, but then was popularized in neuroma treatment due to its ability to treat associated pain and symptoms (Senger 2023). Other procedures as direct implantation of the nerve into the muscle belly or bone or nerve covering through epineural flap of cup either biological and artificial were proposed, without clear effectiveness in problem solution.

When an acute nerve injury happens, the surgeon as stated above, has principles to respect and ancillary procedures to perform in order to prevent the arise of a painful neuroma. Although lots of different procedures were tested and theorized to prevent and treat a painful neuroma, no one of them presented sure results in terms of pain reduction. For this reason, a groups of Italian hand surgeons were asked to

complete a survey to figure out which procedure should be the most appropriate and feasible to prevent them. The results are presented in the next section.

Non-surgical treatment of painful neuropathies of hand and wrist

When a painful neuroma arises after a terminalization of a finger or a painful neuropathy with residual function appears, appropriate medical treatment and physical therapy with dedicated operators should be continued for at least 6 months. Surgical procedures are indicated when no more benefit from those therapy can be obtained and there is no more evidences of symptoms improvement (Bates 2019).

In those patients in whom multiple surgeries failed to reduce pain, different approaches could be chosen by pain therapists. To treat chronic pain induced by a terminal neuroma or by an in-continuity neuroma with or without function, pulsed radiofrequency (PRF) may work. Radio waves are delivered to the targeted nerve through a needle. The frequency can be pulsed or continues (radio frequency ablation RFA) depending on the treated nerve (sensory or mixed). Especially following RFA complete loss of nerve function can be expected and the patient should be carefully informed. Pain neuromodulation could also be used when pain persists. With this technique the myelinated fibers are activated through nerve or spinal cord stimulators, reducing the synaptic efficacy. Pain due to peripheral nerve conditions is severe and should be always managed not only by the peripheral nerve surgeon, but in team with pain therapist and hand therapist (Bates 2019).

1.4.3. Role of intraoperative ultrasound study in nerve reconstruction

One of the mainstays of nerve reconstruction when a graft is planned is to reach a normal or near-normal histological architecture of proximal stumps. As stated in the first chapter the formation of a neuroma is the physiological respond to nerve trauma, either in case of nerve transection or crush injury (Neumeister 2020), thus an amount of intraneural fibrosis is predictable every time. The intra neural scar limits and blocks axon's regrowth, so it is imperative to remove as much as possible of scar tissue to put the nerve in the best condition for recovery. Actually, the identification of intraneural scar extension is still a challenge for every surgeon, in fact nerve section of proximal nerve stump is performed just with grossly evaluation (until bleeding is seen) and previous studies demonstrated that this kind of resection underestimates the extension of fibrous tissue into the proximal stump and the following nerve reconstruction could be limited and unsuccessful due to scar invasion (Malessy 1999).

In nerve diagnosis, the role of ultrasound (US) increased exponentially in the last few years. This technique is able to represent the anatomical components of a nerve in such an extremely detailed way.⁴⁻⁵⁻⁶

Koenig et al⁷ explored the use of intraoperative high-resolution US to examine nerve lesions continuously and found that it proved reliable, easy to use, and correlated well with electrophysiological investigations,

microsurgical dissection, and outcomes. Recently, further authors applied US in the operating field with aim to improve quality of nerve reconstruction (Cartwright 2008, Willsey 2017).

Inspired by these papers, we tried to introduce this technique in surgical practice on a cohort of patients. The results obtained are discussed in a research paper reported in chapter 3.

1.5. ROLE OF TRANSLATIONAL RESEARCH IN NERVE REPAIR

1.5.1. Experimental models of a peripheral nerve injury

1.5.1.1. Somatic nerve injury: the median nerve model

In pre-clinical research studies different kind of animal models have been used to simulate a somatic nerve injury. The nerve model was used to simulate crush injuries and nerve gaps. As in other fields of experimental surgery, employed animals vary from primate, sheep, pigs to rats and mice. The rat definitely represents the easiest and more translatable model, especially for studies evaluating regeneration across short nerve gaps, while for large nerve gaps the use of other larger animals would be recommended, even though, for large animals, facilities are not easily available and more ethical concerns are presents (Ronchi 2019). Classically the sciatic nerve has been, for decades, the most widespread model. Different downsides resulting from severing the sciatic nerve: at first, injury to the sciatic nerve may induce a paralysis of the hind limb and, often, in automutilation behaviour, such as biting and self-amputation of denervated toes and paw areas. Longer lasting paralysis (>4 weeks in the rat) often leads to joint contractures and stiffness. These side-effects reduce the reliability of functional tests, such as estimation of the sciatic function index or, in severe cases, will lead to exclusion of the respective animal from a study for ethical and animal welfare reasons. Furthermore, possibilities for evaluation functional recovery of motor skills after sciatic nerve lesion in the awaken animal are rather limited or need considerable efforts to be realised (Navarro 2016). As an alternative, the median nerve was progressively introduced as peripheral nerve injury model (Bertelli 2004, Ronchi 2009) because of several advantages. Transection injury of the rodent median nerve, results in only partial impairment of the upper limb function (Bertelli 1995). Incidence of automutilation is significantly lower in comparison to the sciatic nerve model, ulcerations are fewer and no joint contractures can be seen. This could happen thanks to the integrity of the ulnar and radial nerves that still preserve sensitivity and motor function in the forearm (Sinis 2006). An additional advantage of the rodent median nerve injury and repair model is that the hand functions require a fine finger movement that is quite similar between rodents and humans (Whishaw 1992). So that, specific and precise functional tests for motor recovery evaluation can be applied, enhancing the results of the under-investigation treatment. Non the less, a so called cross-chest

median nerve transfer has been proposed in rat to simulate gap longer than 4cm, reducing the requirement of larger animals (Sinis 2006). Recently a review about the median nerve as model of somatic nerve injury has been published considering the pros and cons of this model in different settings. As final remark, using the median nerve as pre-clinical experimental model to study nerve regeneration *in vivo is consistently encouraged* because of a better animal well-being, availability of different functional tests which make the results obtained more translatable into the clinic (Ronchi 2019). Still remains open the issue about nerve gap extension. In fact, the cross chest, whereas published, is not easily applicable in all experiments. One of the main problems still remain how to create a valuable autograft: a conjunction of two ulnar nerve was the technique proposed, but it differs from what it is used in clinical practice due to the presence of a further coaptation site usually not present. To solve this, further expedient are under investigation as the employment of allograft.

1.5.1.2. Autonomic nerve injury: the cavernous nerve model

Nerve injuries regards not only somatic nervous system, but also the autonomic one. This kind of injuries have been definitely less investigate compared to somatic nerve, but recently, thanks to the most sophisticated reconstructive techniques now available, increasing interest on this topic was noticed. As for somatic nerves, a pre-clinical model is required for deeply studying the regenerative processes of the autonomic nervous system and possible surgical strategies in case of injury. Since one of the targets of this project is erectile dysfunction recovery after NVB injury, a cavernous nerve injury model was adopted as described previously (Martinez- Pineiro 1994). Differently to the human anatomy, where an intricate nerve plexus is present, rats have got two cavernous nerves, one on each side of the prostate, that can be injured and repaired. Moreover, functional effect of the reinnervation can be tested through intracavernosal pressure measurement, whereas morphological and biomolecular analysis can be performed on reconstructed nerve segments and on the target organ. Moreover, further investigation on organ reinnervation could be planned to discover which processes sustain autonomic reinnervation.

1.5.2. Nerve conduits in peripheral nerve repair

As stated above, nerve conduits are now available for nerve reconstruction, with well identified application limits. They are useful for gap up to 3 cm in sensory nerve reconstruction. Since the biomaterials engineering is deeply involved in this field lot of researches are towards to ameliorate and push the power of these tools beyond the well-known intrinsic limit. Recently new materials from non-human biological sources are being developed; furthermore, biotechnologies are moving towards the use of growth factors and nanostructures to improve the regenerative capacity of these devices.

NOVEL MATERIALS

Silk fibroin and natural proteins

Derived from natural silk, the application of silk fibroin in biomedical fields is increased in recent years, because of the unique material properties of high tensile strength, elasticity, low immunogenicity, biodegradability in a reasonable time and an easy functionalization. In the field of peripheral nerve regeneration, silk fibroin has been used experimentally as biomaterial for nerve guides to clarify the biocompatibility with neural tissues *in vitro*, and for bridging nerve defects *in vivo* (Radtke 2016).

Other natural proteins like keratins have also been tested as natural biomaterial for nerve scaffold or as filler to support peripheral nerve regeneration (Pace 2013). During my research program a pre-clinical study about a silk-based conduit was completed and is reported in chapter 3. Now the FDA approval process for clinical use is ongoing.

ENGINEERED CONDUITS

One of the most important phase of peripheral nerve regeneration in gap injuries is the generation of the supportive structure needed to SCs migration. This is the principal limit of nerve conduit, especially in treatment of long nerve gaps. In fact, the production of extracellular matrix components during the early regeneration stages is inadequate, limiting SC migration into the lesion site, and consequently reducing the production of the trophic and topographical guidance structure (bands of Büngner) for regenerating axons. For this reason several tissue engineering approaches have been developed (Battiston 2009, Konofaos 2013, Carriel 2014).

Hollow nerve guides could be engineered and functionalized with structural components such as collagen and laminin-containing gels, internal frameworks, supportive cells, growth factors and conductive polymers (de Ruyter 2009, Deumens 2010, Thomson 2022) (Figure 14).

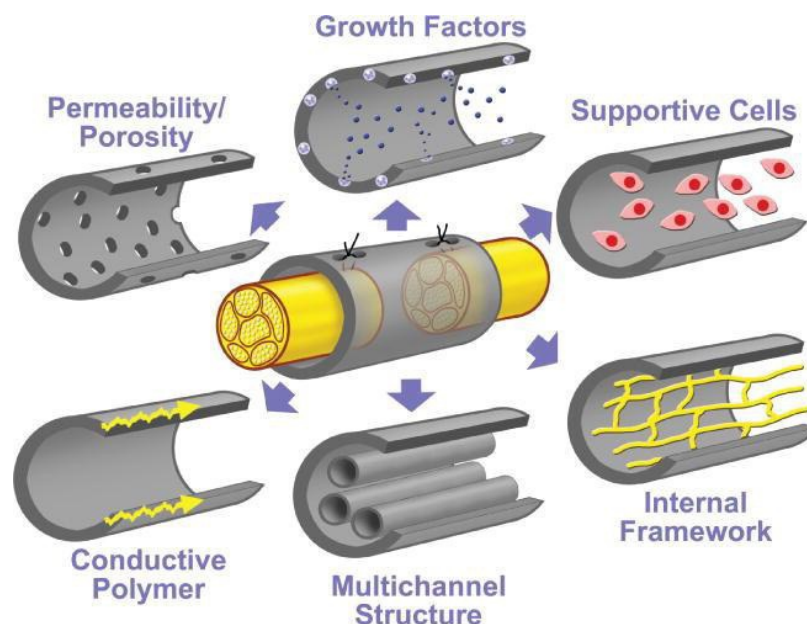


Fig 14: Modifications of hollow tube for peripheral nerve injury repair (de Ruyter GC 2009).

Presently, three different strategies are used to functionalized biomimetic conduits: (i) inclusion of bioactive molecules, later released; (ii) modification of material surface with ECM macromolecules or specific binding motifs; and (iii) nanoscale structural motif of the materials.

The introduction of appropriate internal filler or framework inside the conduit is an efficient strategy to improve the outcome of nerve regeneration (Deumens 2010, Carriel 2014). A simple way to potentiate synthetic conduits is to fill the tube with fibrin, laminin, collagen and other extracellular matrix components provided as hydrogel. These hydrogels favorite cell invasion and axon elongation inside the conduit, and allow neurotrophic factor diffusion. Moreover, hollow tubes can be enriched with internal fillers obtained from biological tissues such as denaturized (Dornseifer 2011) or fresh skeletal muscle fibers (Ronchi 2018, Crosio 2019).

Many studies demonstrated that autologous SCs seeded in a conduit can improve nerve regeneration (Dahlin 2007). Unfortunately, autologous or allogenic SCs are only viable after a long and difficult expansion time in vitro, making their clinical application arduous. An interesting alternative to SCs are mesenchymal stem cells (MSCs) derived from bone marrow (Mantovani 2010). These stem cells can differentiate to Schwann-like Cells (SLCs) and could improve the nerve regeneration significantly. It has been demonstrated the role of nerve fibroblasts that are greatly responsible of sNRG1 releasing. In future, fibroblasts could be grafted into critical gaps to induce Schwann cells dedifferentiation, process required during nerve repair and regeneration.

Adding growth factors to nerve tubes could be useful for axonal regeneration, especially in case of large nerve defects. A way to deliver growth factors could be by means of hydrogels, sponges, fibers, microspheres and immobilization on nanoparticles is usually preferred to ensure a prolonged and controlled factor release (Yasui 2016). Adding to conduits growth factors as NGF, GDNF, BDNF and NT-3, the stimulation of cells and re-growing axons could be obtained (Midha 2003, Regas 2020).

1.5.3. Other devices for peripheral nerve regeneration

Autonomic driven organs are innervated not only by a single nerve, but they are stimulated through a widespread plexus. Once the reconstruction is attempted it is not possible plan autografting or conduit in absence of a proximal and distal stump. For this reason, pro regenerative membranes have been produced, using some of the materials that demonstrate, in nerve conduits, to be efficient in promoting nerve regeneration. Previously the membrane was used in pre-clinical experiment to bridge a nerve gap with promising results (Fregnan 2016). In vitro researches confirmed the efficacy of the membrane in neurons regeneration (Muratori 2019). To further increase their efficacy, micro-structured chitosan membranes with

two different topographies were produced and tested at first *in vitro* to assess axonal outgrowth on immortalized and primary cultures of neurons. Part of this research program is directed to study autonomic system regeneration, so that chitosan membranes have been applied on cavernous nerve injury, comparing the efficacy of different micro-structured devices. Furthermore, considering the role of nerve transfer in organ recovery, a novel nerve transfer to reanimate corpora cavernosa after cavernous nerve injury were developed and results proposed in chapter 3.

1.5.4. Experimental model to simulate a traction neuropathy

Our research group over the years performed different type of pre-clinical studies in which CMC based gel and fat grafts were used to prevent perineural scar formation (Tos 2016, Cherubino 2017). Our researches were based on a perineural scar model on mice (Crosio 2014). Obtained results revealed comparable efficacy of both synthetic and biologic material in perineural scar prevention (Cherubino 2017). Unfortunately, in this field, so many different types of model were used to test the efficacy of anti-adhesion device, without the possibility to really compare their efficacy. So that a review of the literature about how to simulate a traction neuropathy was carried out and the results are reported later on.

2. AIMS OF THE STUDIES

Peripheral nerve repair and following regeneration is, up to now, a complex and even undisclosed argument. The possibility in clinical practice are limited and the rate of partial or no regeneration is still high. Considering this, the goal of these researches was to improve basic knowledges on peripheral nerve regeneration processes and to study surgical techniques and treatments able to ameliorate the outcome after nerve reconstruction. Both clinical and pre-clinical studies, keeping the focus on translation research, are presented in this thesis. Moreover, part of the research has been focused on the development of adequate experimental models to simulate different types of nerve injuries and neuropathies in order to study surgical techniques and regenerative processes.

In particular, in the paper presented in chapter 3.1, the role of sNRG1, released by fibroblasts, in promoting Schwann cell dedifferentiation to a "repair" phenotype, was investigated during regeneration in a chitosan hollow conduit used to repair a rat median nerve.

Nerve conduits amelioration is a topic of high interest in nerve repairs. Through this thesis two researches on novel nerve conduits are presented. Chapter 3.2 reports the results obtained in median nerve reconstruction by a processed nerve xenograft on animal model: this research was based on a novel decellularization method and investigate the possibility of nerve reconstruction by means of xenografts instead of allograft. Whereas in chapter 3.6 the preclinical experience with a new nerve conduit on rat median nerve is described.

Another technique to restore nerve function is nerve transfer. This technique is extensively used in muscle reinnervation, but autonomic driven organs reinnervation has been, over years, less investigated. To understand which is the state of the art about nerve transfer in autonomic reinnervation a literature review is presented in chapter 3.3. Furthermore, part of PhD program was directed to investigate cavernous nerve regeneration. To accomplish this goal an extensive research in which the efficacy of different types of chitosan membranes were tested on a rat model and, moreover, a new nerve transfer for corpora cavernosa reinnervation was described and compared to membranes. The results are reported in chapter 3.7.

Thus scar neuropathies are consequences of nerve injuries, a comprehensive review about method to simulate this condition in preclinical models was performed and presented in chapter 3.8.

Finally, two clinical researches are included in this thesis. Both are directed to improve treatment of secondary nerve reconstruction. Chapter 3.4 regards a consensus study about painful neuromas treatment and prevention. In chapter 3.5, instead, a case series in which a novel tool to improve nerve debridement was tested; intraoperative ultrasound was used to increase the ability to resect incontinuity neuromas, to have less scarred proximal and distal nerve stumps.

The order in which the papers are presented follows introductory chapters moving from pathophysiological aspect of nerve regeneration, to aspects regarding primary nerve repair, ending with topics regarding treatment of complications following peripheral nerve injuries.

3. RESULTS






3.1 Fibroblasts Colonizing Nerve Conduits Express High Levels of Soluble Neuregulin1, a Factor Promoting Schwann Cell Dedifferentiation

Fornasari BE, El Soury M, Nato G, Fucini A, Carta G, Ronchi G, Crosio A, Perroteau I, Geuna S, Raimondo S, Gambarotta G.

Cells. 2020 Jun 1;9(6):1366

Article

Fibroblasts Colonizing Nerve Conduits Express High Levels of Soluble Neuregulin1, a Factor Promoting Schwann Cell Dedifferentiation

Benedetta E. Fornasari ^{1,2}, Marwa El Soury ^{1,2}, Giulia Nato ^{2,3}, Alessia Fucini ¹, Giacomo Carta ^{1,2}, Giulia Ronchi ^{1,2}, Alessandro Crosio ^{1,2,4}, Isabelle Perroteau ¹, Stefano Geuna ^{1,2}, Stefania Raimondo ^{1,2} and Giovanna Gambarotta ^{1,2,*}

¹ Department of Clinical and Biological Sciences (DSCB), University of Torino, 10043 Orbassano (Torino), Italy; benedettaelena.fornasari@unito.it (B.E.F.); marwa.elsoury@unito.it (M.E.S.); alessia.fucini@edu.unito.it (A.F.); giacomo.carta@unito.it (G.C.); giulia.ronchi@unito.it (G.R.); alessandro.crosio@unito.it (A.C.); isabelle.perroteau@unito.it (I.P.); stefano.geuna@unito.it (S.G.); stefania.raimondo@unito.it (S.R.)

² Neuroscience Institute Cavalieri Ottolenghi (NICO), University of Torino, 10043 Orbassano (Torino), Italy; giulia.nato@unito.it

³ Department of Life Sciences and Systems Biology (DBIOS), University of Torino, 10123 Torino, Italy

⁴ Hand Surgery and Reconstructive Microsurgery, Gaetano Pini—CTO Hospital, 20122 Milano, Italy

* Correspondence: giovanna.gambarotta@unito.it; Tel.: +39-011-6705-436

Received: 25 April 2020; Accepted: 30 May 2020; Published: 1 June 2020



Abstract: Conduits for the repair of peripheral nerve gaps are a good alternative to autografts as they provide a protected environment and a physical guide for axonal re-growth. Conduits require colonization by cells involved in nerve regeneration (Schwann cells, fibroblasts, endothelial cells, macrophages) while in the autograft many cells are resident and just need to be activated. Since it is known that soluble Neuregulin1 (sNRG1) is released after injury and plays an important role activating Schwann cell dedifferentiation, its expression level was investigated in early regeneration steps (7, 14, 28 days) inside a 10 mm chitosan conduit used to repair median nerve gaps in Wistar rats. In vivo data show that sNRG1, mainly the isoform α , is highly expressed in the conduit, together with a fibroblast marker, while Schwann cell markers, including NRG1 receptors, were not. Primary culture analysis shows that nerve fibroblasts, unlike Schwann cells, express high NRG1 α levels, while both express NRG1 β . These data suggest that sNRG1 might be mainly expressed by fibroblasts colonizing nerve conduit before Schwann cells. Immunohistochemistry analysis confirmed NRG1 and fibroblast marker co-localization. These results suggest that fibroblasts, releasing sNRG1, might promote Schwann cell dedifferentiation to a “repair” phenotype, contributing to peripheral nerve regeneration.

Keywords: Neuregulin 1; nerve fibroblasts; nerve regeneration; Schwann cells; nerve guide; chitosan; peripheral nerve; nerve repair; nerve injury

1. Introduction

Traumatic injury to peripheral nerve represents a relevant clinical problem that can lead to permanent disability and functional impairment; indeed, it has been estimated that ~3% of all trauma involve peripheral nerves [1]. Unlike the central nervous system, peripheral nerves regenerate spontaneously after a crush (axonotmesis) or a clear cut (neurotmesis), when proximal and distal stumps remain in close contact, facilitating the formation of a bridge and axonal re-growth [2,3]. Nevertheless, after a clear cut, a microsurgical intervention is always recommended to guide the re-growing axons from the proximal to the distal stump and then to their target. If it is possible to connect the two stumps without tension, a direct suture is suggested; if, following nerve tissue

loss, a direct suture would cause a too high tension, it is necessary to insert a scaffold to bridge the two stumps without tension [4]. The length of the gap which needs bridging with a scaffold varies according to the characteristics of different nerves and their anatomical district [5].

Despite the progresses reached in nerve repair techniques during recent decades, peripheral nerve gap repair remains a significant clinical challenge. For severe injuries, the gold standard technique is the autograft, i.e., transplantation of an autologous nerve, but it presents some side effects, such as a secondary surgery and sensitivity loss [6]. A good alternative is the tubulization, where a tubular conduit is used to connect the gap between the nerve stumps. Different tubular conduits have been developed and several are commercially available, as recently reviewed [7,8]. Conduit repair efficiency is similar to the autograft for short distance repair, while for long distances the autograft remains the most effective technique [9,10]. Indeed, autograft, being a transplanted nerve, yet contains most of the players involved in Wallerian degeneration and nerve regeneration, while conduits require colonization by Schwann cells, fibroblasts, endothelial cells, and so on. A promising biomaterial widely used for peripheral nerve regeneration and recently approved for clinical use is chitosan, a polysaccharide of natural origins [10–12]. It is a highly versatile biomaterial, indeed it has been tested in several forms, such as hydrogels, films, or conduits used to repair nerve gap [13].

After a nerve cut, a bridge spontaneously forms between the proximal and the distal stumps; the analysis of the bridge showed that, during nerve regeneration, important roles are played by macrophages, endothelial cells, Schwann cells, and fibroblasts [14]. Initially, the bridge, composed by inflammatory cells and extracellular matrix released by fibroblasts, is poorly vascularized and becomes hypoxic: Macrophages, sensing hypoxia, release vascular-endothelial growth factor (VEGF) which attracts endothelial cells promoting angiogenesis; blood vessels provide a track for Schwann cell migration [14]. In the degenerating distal stump, Schwann cells, releasing soluble NRG1, might promote their de-differentiation from a myelinating to a “repair” phenotype, playing a key role in myelin debris clearing, macrophage attraction, neuron survival, and axonal re-growth [15]. Indeed, soluble NRG1 has been shown to play an important role for nerve regeneration [16], being highly, and transiently, over-expressed immediately after injury [17,18] and negatively affecting nerve regeneration when it is missing [18]. Different NRG1 isoforms obtained by alternative splicing were described [19]: They are mainly classified as transmembrane (expressed by axons and strongly involved in the regulation of myelination) or soluble (released by Schwann cells immediately after nerve injury), and as type α or type β , according to the C-terminus of EGF-like domain, the domain which is involved in the interaction with NRG1 receptors, namely ErbB3 and ErbB4 [20,21]. In Schwann cells, NRG1 signal transduction is mediated by the heterodimeric receptor ErbB2-ErbB3 [22].

While many studies have contributed to our knowledge about how peripheral nerves regenerate in case of mild injuries, such as crush (axonotmesis) or clear-cut transections (neurotmesis) followed by end-to-end repair, much less is understood about nerve regeneration after a severe injury with loss of nerve tissue. In particular, although tubulization is often and successfully used as a good alternative to autograft for short nerve gap repair [7,10,12,23–27], little is known about what happens during regeneration inside a conduit used to repair this kind of injury. A description of the different stages occurring inside a hollow conduit during nerve regeneration was carried out several years ago by means of electron microscopy analysis [28]: (1) The conduit is initially filled with plasma exudate which contains extracellular matrix molecules and neurotrophic factors; (2) fibrin filaments are formed; (3) fibroblasts and dedifferentiated Schwann cells colonize the gap, proliferate and align along the conduit forming the Bands of Büngner; (4) axons grow and reach their distal targets exploiting the biological cues supplied by Schwann cells; and (5) Schwann cells differentiate to a myelinating phenotype and myelinate axons [29].

Our aim was to further characterize the stages occurring inside a conduit using different techniques to identify the cells and the factors involved in the nerve regeneration, focusing our attention on the NRG1/ErbB system, with the idea that understanding what happens inside a nerve conduit might contribute to develop new strategies to further promote nerve repair.

2. Materials and Methods

2.1. Surgical Procedure

Eighteen adult female Wistar rats (ENVIGO, Milan, Italy), weighing about 200–250 g, were used. The total number includes animals used for uninjured control nerve withdrawal. Animals were kept under standardized and controlled conditions (12 h of light and 12 h of dark and free access to water and food). Surgeries were performed under general anesthesia through intraperitoneal injection of tiletamine HCl and zolazepam HCl (Zoletil Virbac, Milan, Italy) + xilazine (Rompun, Bayer, Leverkusen, Germany) ($40 \text{ mg kg}^{-1} + 5 \text{ mg kg}^{-1}$).

The median nerve was exposed and transected to establish a defect (8 mm of nerve was removed). Then, two experimental groups were obtained: the chitosan conduit group and the autograft group as previously described [30] (Figure S1).

1-for the chitosan conduit group a hollow 10 mm long chitosan tube was used to bridge the 8 mm nerve defect by inserting 1 mm of each nerve end inside the conduit (8 mm gap was chosen considering it). The nerve conduit was sutured with one 9/0 epineurial stitch (silk; Péters Surgicals, Bobigny, France) at each end. Chitosan-based conduits (Reaxon[®] Nerve Guides) were supplied by Medovent GmbH (Mainz, Germany).

2-for the autograft group, the transected median nerve segment was reversed (distal-proximal) and sutured to the nerve ends of the same animal with three 9/0 epineurial stitch at each end. Regenerated nerves were withdrawn 7, 14, and 28 days after the repair for biomolecular analysis ($n = 3-4$ for each group) and 7 days after the repair for morphological analysis; then, animals were sacrificed by anesthetic overdose ($>100 \text{ mg kg}^{-1}$ Zoletil and 30 mg kg^{-1} Rompun).

Control nerves were healthy median nerves obtained from 4 uninjured animals.

2.2. Ethics Approval and Consent to Participate

Animal study followed the recommendations of the Council Directive of the European Communities (2010/63/EU), the Italian Law for Care and Use of Experimental Animals (DL26/14), and are in agreement with the National Institutes of Health guidelines (NIH Publication No. 85-23, revised 1996). All animal experiments were carried out at the animal facility of Neuroscience Institute Cavalieri Ottolenghi (NICO) (Ministerial authorization DM 182 2010-A 3-11-2010). The current experimental study was reviewed and approved by the Ethic Experimental Committee of the University of Torino (Italian Ministry of Health approved project number: 864/2016/PR, 14-09-2016).

2.3. Schwann Cell Primary Culture

To obtain adult primary Schwann cell culture, 4 rat sciatic nerves were isolated for each biological replicate ($n = 3$). The *epineurium* was removed, nerves were cut into small pieces about 1 mm long, then were evenly distributed in a 3 cm diameter Petri dish and were incubated for 24 h in dissociation medium Dulbecco Modified Eagle Medium (DMEM, Gibco, Thermo Fisher Scientific, Waltham, MA, USA) containing 1 g/L glucose, 10% heat-inactivated fetal bovine serum (FBS; Invitrogen, Thermo Fisher Scientific), 100 units/mL penicillin, 0.1 mg/mL streptomycin, 10 μM Forskolin, 63 ng/mL recombinant NRG1 β 1 (#396-HB, R&D Systems, Minneapolis, MN, USA), 0.625 mg/mL collagenase IV, 0.5 mg/mL dispase II at 37 °C in a 5% CO₂ atmosphere saturated with H₂O.

After 24 h, mechanical dissociation was performed and the medium containing the dissociated nerves was collected in a tube, then the suspension was filtered through a cell strainer with 70 μm pores (Sartorius Stedim Biotech GmbH, Göttingen, Germany) and transferred into a new tube. Cells were centrifuged at 100 rcf for 5 min. The pellet obtained was resuspended in DMEM D-valine medium (Cell Culture Technologies, Gravesano, Switzerland) containing D-valine, 4.5 g/L glucose, 2 mM glutamine, 10% FBS, 100 units/mL penicillin, 0.1 mg/mL streptomycin, 10 μM Forskolin, and 63 ng/mL NRG1 β 1. Cells were grown in a cell culture dish pre-treated with poly-L-lysine (PLL) to allow Schwann cell adhesion, at 37 °C in a 5% CO₂ atmosphere saturated with H₂O. Medium was replaced every two days.

Cells (passage 1) were allowed to proliferate until confluence, then split and allowed to proliferate until confluence in a 6 cm diameter Petri dish (passage 2) for the subsequent extraction with TRIzol Reagent (Invitrogen, Thermo Fisher Scientific) to obtain RNA and protein, as described below.

DMEM D-valine medium was used to obtain Schwann cells, as the essential amino acid D-valine in this media can be exclusively metabolized by Schwann cells and not by fibroblasts, owing to the expression of the D-amino acid oxidase (DAAO) enzyme in Schwann cells. Since fibroblasts are not able to metabolize this isoform, they die after a few days in culture, due to the lack of an essential amino acid [31]. Unless specified, all reagents were purchased from Sigma-Aldrich, Merck, Darmstadt, Germany.

2.4. Nerve Fibroblast Primary Culture

To obtain adult primary nerve fibroblasts 2 rat sciatic nerves were isolated for each biological replicate ($n = 3$). The protocol is similar to that used for Schwann cell isolation, except for: (i) The epineurium was not removed from sciatic nerves, (ii) the culture medium DMEM (Sigma-Aldrich, Merck) contained L-valine, 4.5 g/L glucose, 10% FBS, 2 mM L-glutamine and 100 units/mL penicillin, 0.1 mg/mL streptomycin, and (iii) fibroblasts were cultured without any coating. Medium was replaced every two to three days. At least three passages were carried out to reduce the number of contaminating Schwann cells and to increase the purity of the primary culture. The purity of the culture was assessed by immunohistochemistry (data not shown). After reaching confluence, RNA and proteins were extracted for subsequent expression analysis, as described below.

Sciatic nerves to obtain Schwann cell and fibroblast primary cultures were withdrawn from nine uninjured animals, four of which were the animals used for control group median nerve withdrawal.

2.5. RNA Isolation, cDNA Preparation, and Quantitative Real-Time PCR

Total RNA extraction and retrotranscription, and quantitative real-time PCR (qRT-PCR), were performed as previously described [17], using 0.75 μg /sample for retrotranscription. Technical and biological triplicates were performed for in vitro sample analysis, while for in vivo sample analysis, biological replicates were 4. qRT-PCR data were analyzed using the “Livak $2^{-\Delta\Delta C_t}$ method” for the relative quantification [32]. Briefly, the threshold cycle (C_t) values of both the calibrator and the samples of interest were normalized to housekeeping genes to obtain ΔC_t , then ΔC_t were normalized to the calibrator to obtain $\Delta\Delta C_t$ and, following, the relative quantification ($2^{-\Delta\Delta C_t}$) representing the expression level of each sample relatively to the calibrator sample. As calibrator for the relative quantification the average of uninjured nerve was used. The geometric average of the two endogenous housekeeping genes ANKRD27 (Ankyrin repeat domain 27) and RICTOR (RPTOR Independent Companion Of MTOR, Complex 2) was used for data normalization [33].

Primer sequences for ErbB1, ErbB2, ErbB3, soluble NRG1, ANKRD27, RICTOR [17], ErbB4, NRG1 α , NRG1 β [30], S100, and p75 [34] were previously published. A new primer pair for Thy1 (accession number #NM012673, amplicon length 127 bp) was prepared: Thy1 forward: 5'-CTCCTGCTTTCAGTCTTGCAGATGTC-3'; Thy1 reverse: 5'-CATGCTGGATGGCAAGTTGGTG-3'.

2.6. Protein Extraction and Western Blot

After RNA extraction, total proteins were extracted by the TRIzol Reagent (Invitrogen, Thermo Fisher Scientific) according to manufacturer's instructions, then, protein pellet was dissolved in boiling LaemLi buffer (2.5% sodium dodecyl sulphate, 0.125 M Tris-HCl, pH 6.8). The Bicinchoninic Acid assay kit (Sigma-Aldrich, Merck) was used to determine protein concentration and equal amounts of proteins (50 μg) were loaded into each lane. Proteins were resolved by 8% SDS-PAGE. Western blot analysis was carried out as previously described [35]. The list of primary and secondary antibodies is reported in Table S1. Secondary antibodies are horseradish peroxidase-linked.

2.7. Immunohistochemistry

Seven days after the surgery, median nerves from each experimental group were withdrawn for the following immunohistochemistry (IHC) analysis. Before fixation chitosan conduits were removed with high precision in order to avoid loss of the tissue grown inside. Regenerated nerve specimens were fixed in 4% paraformaldehyde in PBS (phosphate buffered saline) (Sigma-Aldrich, Merck) for 2–3 h and stored in PBS at 4 °C. For the Cryo-embedding procedure, samples were cryo-protected with passages in solutions with increasing concentration of sucrose (Sigma-Aldrich, Merck, 7.5% for 1 h, 15% for 1 h, 30% overnight) in 0.1 M PBS. Next, samples were maintained in a solution of 30% sucrose and optimal cutting temperature medium (OCT, Electron Microscopy Sciences, Hatfield, PA, USA) in a ratio 1:1, for 30 min and then embedded in 100% OCT; samples were stored at –80 °C. Nine micrometer-thick cross sections of the nerve were obtained starting from the middle of the autograft or the middle of the new tissue grown inside the chitosan conduit.

For IHC, samples on slices were rinsed with PBS and then permeabilized and saturated in 0.01% Triton X-100, 10% normal donkey serum (NDS, Jackson ImmunoResearch, Philadelphia, PA, USA) in PBS for 1 h at room temperature in humid chamber. Samples were incubated with primary antibodies (Table S1, double staining were performed in single step, combined as follows: CD34 + S100 β , CD34 + NRG1, CD34 + RECA1) at 4 °C overnight in PBS containing 1% NDS, in humid chamber. Then, samples were rinsed three times with PBS and incubated 1h at room temperature in humid chamber with secondary antibodies (Table S1). After three washes in PBS, sections were covered with a mounting solution (Fluoromount, Sigma-Aldrich, Merck) and a glass coverslip was used to cover the section before observation. After drying for at least 3 days, samples were photographed using Leica (Wetzlar, Germany) TCS SP5 confocal microscope.

For specificity assessment, all these antibodies were previously checked by Western blotting, which showed a single band of staining (data not shown). These antibodies have been used for similar purposes in the literature. Anti-S100 β was used to label Schwann cells [36], anti-CD34 was used to specifically label nerve fibroblasts [37], even if it known to recognize also endothelial cells. As shown below in the immunohistochemistry panel 4C, no cells co-express S100 β and CD34, (indicating that these antibodies do not cross react). To specifically identify fibroblasts, anti-CD34 was coupled with anti-RECA1, a cell surface antigen which is expressed by endothelial cells [38,39].

To assess the expression of NRG1 in fibroblasts, slices were stained with anti-CD34 and anti-NRG1, a polyclonal antibody that recognizes the C-terminal of many different NRG1 isoforms (all isoforms with “type a” C terminus, which is common to many soluble isoforms) [19], used by several laboratories and acknowledged by the scientific community as a suitable antibody to assess NRG1 expression [18,40].

2.8. Statistical Methods

For in vivo experiments a priori power analysis performed with G*Power (v. 3.1.9.4; Heinrich-Heine-Universität Düsseldorf, Germany) [41] showed that a sample size of 12 samples ($n = 4$ for each group) for each time point was determined respecting an effect size of $d = 0.6$, with a power of 0.95 and α of 0.05 defining an actual power of 0.98 to limit the number of sacrificed animals.

Statistical analyses were performed with IBM SPSS Statistics 25 (IBM, Armonk, NY, USA) software. Data were expressed as mean \pm standard error of the mean (SEM). All data were tested for normal distribution in order to select the appropriate statistical test (Levene and Mauchly tests).

Analysis of variance (ANOVA) for repeated measures with Bonferroni’s correction was adopted to detect the effect of time, experimental groups, and their interaction and to highlight the overall significant differences among autograft group, chitosan group and uninjured control nerves and at each time point analyzed.

The two-tailed Student’s *t*-test for normally distributed data with comparable variances was used to highlight statistical differences between the two groups (Schwann cells and fibroblasts), while for data not showing normal distribution the nonparametric Mann–Whitney U-test was used.

The effect size of each factor was computed as partial eta-squared (η_p^2): a small effect was considered for a value of 0.010, a medium effect for value of 0.059 and a large effect for value of 0.138 [42].

3. Results

3.1. Soluble NRG1 Is Strongly Expressed in the Conduit after Nerve Repair, While ErbB2 and ErbB3 Are Missing

The expression of proteins belonging to the NRG1/ErbB system, which is strongly involved in peripheral nerve regeneration, was investigated in the new tissue grown inside the chitosan conduit ("chitosan" group) and compared with the grafted autologous nerve ("autograft" group), representing the surgery "gold-standard", or with healthy median nerve, used as control group, representing the starting point and the aimed final outcome (Figure 1).

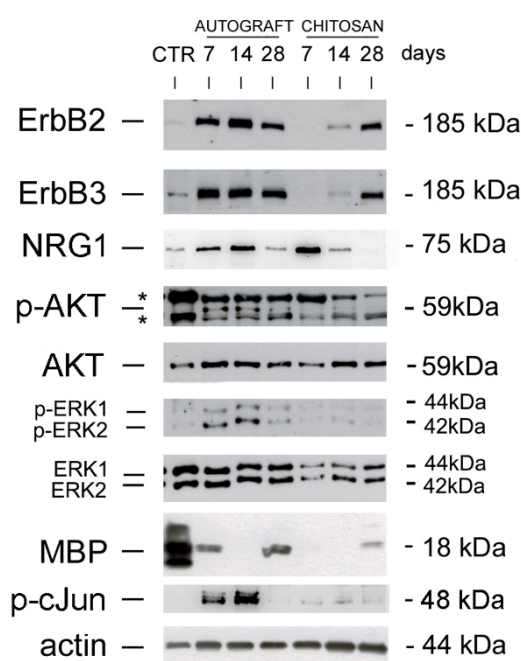


Figure 1. NRG1 and ErbB expression in autograft and chitosan groups. Western blot analysis of proteins extracted from healthy control nerves (CTR) and regenerating nerves belonging to autograft or chitosan groups withdrawn 7, 14, and 28 days after the repair and probed with antibodies for ErbB2, ErbB3, phospho-AKT, total-AKT, phospho-ERK, total-ERK, MBP, phospho-cJun; actin was used as a loading control. For NRG1, an antibody recognizing the C terminus fragment was used. Unspecific bands were identified with asterisks (*). Molecular weight (kDa) are shown on the right.

Our data show that ErbB2 and ErbB3 receptors were strongly up-regulated in the autologous nerve graft at all the time points analyzed (7, 14, and 28 days after the repair), while in the chitosan conduit ErbB2 and ErbB3 were not detectable 7 days after repair; they started to be detectable one week later, and were strongly expressed 28 days after the repair.

To detect soluble NRG1, an antibody which recognizes a 75 kDa band corresponding to the C terminal fragment of NRG1 was used [17,18]. NRG1 is strongly expressed 7 and 14 days after the repair in both groups, with a higher expression in the chitosan group 7 days after the repair. NRG1 expression strongly decreases 28 days after the repair in both experimental groups.

3.2. The PI3K/AKT and ERK/MAPK Pathways Are Activated in the Autograft, Not in the Conduit

AKT, ERK and cJun are strongly phosphorylated 7 and 14 days after repair with the autograft technique, while after 28 days their phosphorylation strongly decreases (AKT, ERK) or it is completely switched off (cJun). Inside the conduit, AKT phosphorylation is barely detectable 14 days after the repair, while ERK1/2 and cJun phosphorylation are not detectable; moreover, in the chitosan samples the total amount of ERK is lower than in the autograft.

Myelin basic protein (MBP) is strongly expressed in the uninjured median nerve; in the autograft group it is still present 7 days after injury (during Wallerian degeneration), disappears 14 days after repair (during axon regrowth) and it is present again 28 days after the repair (during axon remyelination). Within the chitosan conduit, where Wallerian degeneration does not occur, MBP starts to be present 28 days after the repair, during axon remyelination.

3.3. Fibroblast Markers Are Highly Expressed in the Chitosan Conduit

Western blot data analysis showed that in the chitosan conduit soluble NRG1 (usually highly expressed by Schwann cells after injury) was strongly expressed 7 days after nerve repair, while the NRG1 co-receptors ErbB2-ErbB3 were not. To identify the cells responsible for NRG1 release, we analyzed the expression of two Schwann cell (S100 β , p75) and one fibroblast (Thy1) markers within the chitosan conduit (Figure 2 and Table 1 for statistical analysis).

S100 β , a Schwann cell marker highly expressed by differentiated Schwann cells, is significantly down-regulated after injury in all samples. Our data show that at all the time points analyzed S100 β is significantly less expressed in conduit samples than in the nerve repaired through autologous graft. The effect size between all groups is significantly large for all time points analyzed (see Table 1). Multiple comparison analysis for S100 β revealed significant differences between autograft and chitosan groups ($p = 0.0056$, mean difference = 0.16, CI 95% = 0.06–0.26). The within subject test showed no significant effect for time ($p = 0.065$) and time x group factors ($p = 0.29$).

p75 is a Schwann cell marker highly expressed by dedifferentiated Schwann cells, known to be strongly up-regulated after nerve injury; accordingly, when compared with uninjured nerves, p75 expression is significantly higher in all autograft samples, while in the chitosan group it is significantly more highly expressed only 28 days after the repair (see Table 1). Data show that at all the time points analyzed p75 is significantly less expressed in the conduit group than in the nerve repaired through autologous graft. The effect size between experimental groups is large for all time points analyzed (see Table 1). Multiple comparison analysis for p75 revealed significant differences between the autograft and the chitosan groups ($p = 0.000016$, mean difference = 47.15, CI 95% = 36.93–57.37) and between the autograft and the control groups ($p = 0.000007$, mean difference = 54.43, CI 95% = 44.21–64.65). The within subject test revealed a significant effect for time ($p = 0.002$) and time x group ($p = 0.0004$) factors.

The nerve fibroblast marker Thy1 is significantly more highly expressed in the chitosan group, 14 and 28 days after the repair with a large effect size (see Table 1), in comparison with the autograft group and with uninjured nerves. Multiple comparison analysis for Thy1 revealed significant differences between the autograft and the chitosan groups ($p = 0.004$, mean difference = -6.5 , CI 95% = (-10.36) – (-2.62)), between the autograft and the control groups ($p = 0.012$, mean difference = 5.3, CI 95% = 1.49–9.23) and between the chitosan and the control groups ($p = 0.00017$, mean difference = 11.86, CI 95% = 7.98–15.72). The within subject test revealed a significant effect for time x group factors ($p = 0.01$), not for time alone ($p = 0.15$).

Soluble NRG1 is significantly higher in the chitosan group compared with the autograft group and with uninjured nerves 14 and 28 days after repair with large effect size (see Table 1). Multiple comparison analysis for soluble NRG1 revealed significant differences between chitosan and uninjured nerve groups ($p = 0.0002$, mean difference = 1.88, CI 95% = 1.18–2.58) and between chitosan and autograft groups ($p = 0.0002$, mean difference = 1.96, CI 95% = 1.21–2.70). The within subject test revealed a significant effect for time ($p = 0.006$) and time x group ($p = 0.000$) factors.

Soluble NRG1 isoforms (which are the most represented isoforms, at the mRNA level, in the peripheral nerve) include both α and β isoforms, whose regulation and activity can be different; therefore, we analyzed, separately, the expression of both isoforms.

NRG1 α is more highly expressed in the chitosan group, in comparison with the autograft group and with uninjured nerves, 14 and 28 days after the repair with large effect size (see Table 1). Multiple comparison analysis for soluble NRG1 α revealed significant differences between the chitosan and the uninjured nerve groups ($p = 0.002$, mean difference = 20.75, CI 95% = 10.29–31.19) and between the chitosan and the autograft groups ($p = 0.016$, mean difference = 13.48, CI 95% = 3.03–23.93). The within subject test revealed a significant effect for time x group factors ($p = 0.02$) not for time alone ($p = 0.16$).

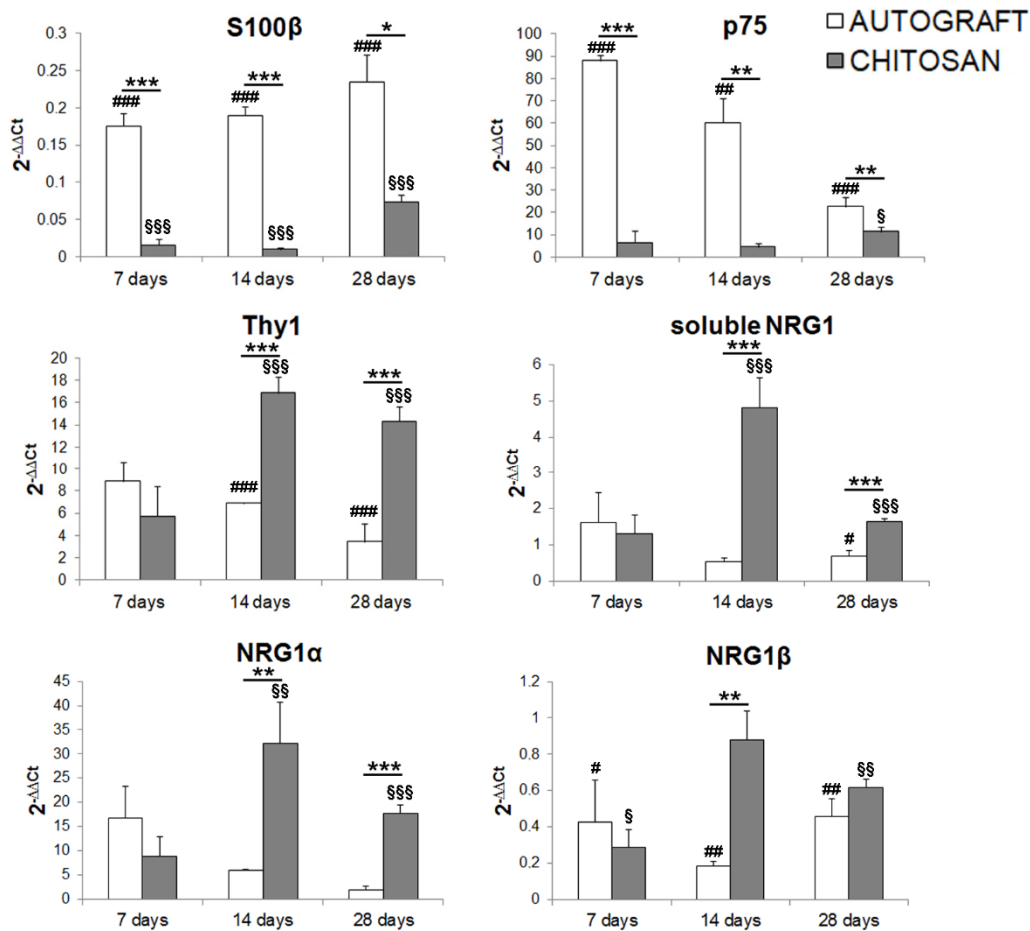


Figure 2. Quantitative expression analysis of Schwann cell and nerve fibroblast markers. Relative quantification ($2^{-\Delta\Delta C_t}$) of S100 β and p75 (Schwann cell markers), Thy1 (fibroblast marker), soluble NRG1, NRG1 α , and NRG1 β was evaluated by qRT-PCR. The geometric average of the housekeeping genes ANKRD27 and RICTOR was used to normalize data. Values in the graphics are expressed as mean + SEM ($n = 3-4$ for each group). ANOVA for repeated measures with Bonferroni's correction was adopted for statistical analysis; * denotes the significant differences between autograft and chitosan groups at each time point analyzed ($* p \leq 0.05$, $** p \leq 0.01$, and $*** p \leq 0.001$); # denotes the significant differences between autograft group and uninjured control nerves at each time point analyzed ($\# p \leq 0.05$, $## p \leq 0.01$, and $### p \leq 0.001$); § denotes the significant differences between chitosan group and uninjured control nerves at each time point analyzed ($\S p \leq 0.05$, $\S\S p \leq 0.01$, and $\S\S\S p \leq 0.001$). All data are calibrated to uninjured nerves (whose expression, not shown, is = 1).

Table 1. ANOVA for repeated measures with Bonferroni's correction.

	Autograft vs. Chitosan								
	7 Days			14 Days			28 Days		
	η_p^2	<i>p</i>	CI 95%	η_p^2	<i>p</i>	CI 95%	η_p^2	<i>p</i>	CI 95%
S100 β	0.85	0.001	0.1–0.24	0.87	0.001	0.11–0.25	0.63	0.02	0.35–0.26
p75	0.97	0.000	64.99–93.51	0.81	0.002	24.70–71.92	0.67	0.01	4.21–23.61
Thy1	0.05	0.59	(–5.67)–9.11	0.87	0.001	(–14.38)–(–6.27)	0.87	0.001	(–15.04)–(–6.70)
sNRG1	0.00	0.907	(–1.82)–2.02	0.93	0.000	(–6.16)–(–3.71)	0.85	0.000	(–1.43)–(–0.65)
NRG1 α	0.11	0.42	(–10.58)–22.33	0.69	0.01	(–51.10)–(–10.24)	0.94	0.000	(–19.71)–(–11.59)
NRG1 β	0.20	0.738	(–0.46)–0.61	0.78	0.004	(–1.20)–(–0.37)	0.47	0.06	(–0.51)–0.47
	Control vs. Autograft								
	7 Days			14 Days			28 Days		
	η_p^2	<i>p</i>	CI 95%	η_p^2	<i>p</i>	CI 95%	η_p^2	<i>p</i>	CI 95%
S100 β	0.99	0.000	0.92–1.11	0.99	0.000	0.92–1.06	0.99	0.000	0.82–1.04
p75	0.97	0.000	72.65–101.16	0.83	0.002	28.37–75.59	0.87	0.001	14.70–34.11
Thy1	0.4	0.09	(–13.5)–1.28	0.94	0.000	(–20.22)–(–12.12)	0.91	0.000	(–17.46)–(–9.12)
sNRG1	0.08	0.45	(–1.18)–2.41	0.10	0.4	(–1.59)–(–0.72)	0.50	0.033	(–0.77)–(–0.05)
NRG1 α	0.48	0.06	(–0.71)–32.21	0.06	0.57	(–15.39)–25.47	0.06	0.57	(–3.07)–5.05
NRG1 β	0.55	0.03	(–1.14)–(–0.06)	0.80	0.003	(–1.26)–(–0.42)	0.87	0.01	(–0.90)–(–0.41)
	Control vs. Chitosan								
	7 Days			14 Days			28 Days		
	η_p^2	<i>p</i>	CI 95%	η_p^2	<i>p</i>	CI 95%	η_p^2	<i>p</i>	CI 95%
S100 β	0.99	0.000	(–1.05)–(–0.91)	0.99	0.000	(–1.06)–(–0.92)	0.99	0.000	(–1.04)–(–0.82)
p75	0.22	0.237	(–21.91)–6.6	0.024	0.717	(–27.28)–19.94	0.54	0.04	(–20.21)–(–0.79)
Thy1	0.4	0.09	(–1.28)–13.5	0.94	0.000	12.12–20.22	0.91	0.000	17.46–0.91
sNRG1	0.06	0.52	(–2.31)–1.28	0.92	0.000	(–5.64)–(–3.34)	0.97	0.000	(–0.95)–(–0.27)
NRG1 α	0.26	0.19	(–26.34)–6.57	0.75	0.005	(–56.14)–(–15.28)	0.94	0.000	(–20.71)–(–12.57)
NRG1 β	0.61	0.022	0.14–1.22	0.02	0.75	0.36–0.48	0.73	0.007	0.16–0.66

Effect of time, experimental groups, and their interaction are reported at each time point analyzed. In this table the effect size (partial eta-squared, η_p^2), the significance (*p*) and the 95% confidence interval (CI) are shown. The effect of the experimental groups on the regulation of gene expression is significant and with an effect size higher than expected in most conditions.

NRG1 β is more highly expressed in the chitosan group compared with the autograft group 14 days after the repair with large effect size. NRG1 β expression in the chitosan group is significantly lower than in uninjured nerves at 7 and 28 days, with large effect size, while for the autograft group it is significantly lower at all the time points analyzed with large effect size (see Table 1). Multiple comparison analysis for soluble NRG1 β revealed significant differences between chitosan and uninjured nerve groups (*p* = 0.034, mean difference = –0.38, CI 95% = (–0.73)–(–0.03)) and between autograft and uninjured nerve groups (*p* = 0.0018, mean difference = –0.70, CI 95% = (–1.04)–(–0.35)).

The within subject test revealed a significant effect for time \times group factors (*p* = 0.035) not for time alone (*p* = 0.44).

3.4. Primary Cultures of Nerve Fibroblasts Express High Levels of NRG1 Isoforms, While NRG1 Receptors Are Not Expressed

As the expression of Schwann cell markers was very low in the chitosan conduit, while the fibroblast marker Thy1 and NRG1 were strongly expressed, we hypothesized that fibroblasts could be involved in NRG1 expression. To test this hypothesis, confluent primary cultures of fibroblasts and Schwann cells were obtained from adult rat sciatic nerves and were analyzed at both mRNA and protein level to investigate fibroblast involvement in NRG1 expression (Figure 3A,B).

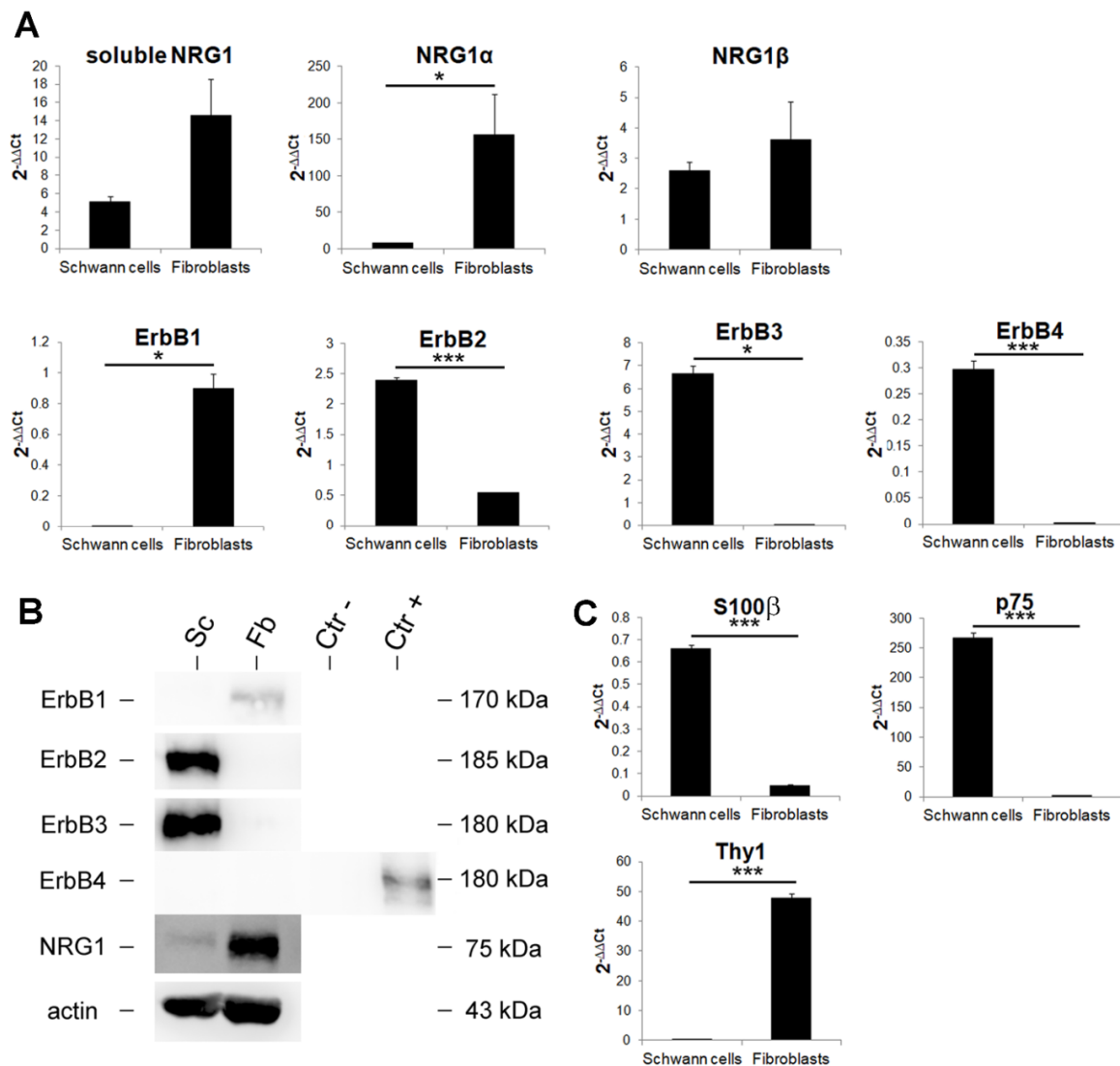


Figure 3. Nerve fibroblasts express high levels of soluble NRG1. **(A)** Quantitative analysis of the NRG1/ErbB system expression in primary cultures of Schwann cells and nerve fibroblasts. Relative quantification ($2^{-\Delta\Delta C_t}$) of different NRG1 isoforms (soluble, α , β), ErbB1, ErbB2, ErbB3, and ErbB4 was evaluated by qRT-PCR. **(B)** Western blot analysis of the NRG1/ErbB system. Proteins were extracted from primary cultures of Schwann cells (Sc) and nerve fibroblasts (Fb), separated on 8% acrylamide-bis-acrylamide gels and probed with antibodies for ErbB1, ErbB2, ErbB3, and ErbB4; for NRG1, an antibody recognizing the C terminus fragment was used. Actin was used as a loading control. Size markers are indicated on the right. Neural progenitor cells stably expressing ErbB4 or mock cells were used respectively as positive (Ctr+) and negative (Ctr-) controls for ErbB4. **(C)** Quantitative expression analysis of Schwann cell and nerve fibroblast markers. Relative quantification ($2^{-\Delta\Delta C_t}$) of S100 β and p75 (Schwann cell markers) and Thy1 (fibroblast marker) was evaluated by qRT-PCR to ensure the purity of the primary cultures. For panel A and C, the geometric average of housekeeping genes ANKRD27 and RICTOR was used to normalize data. All data were calibrated to healthy median nerves, whose expression, not shown, is = 1. Values in the graphics are expressed as mean + SEM ($n = 3$ for each group). For normally distributed data with comparable variances two-tailed Student's *t*-test was carried out, while for nonparametric data Mann–Whitney *U*-test was used; * $p \leq 0.05$, *** $p \leq 0.001$.

The identity of both cell types was confirmed by qRT-PCR using specific biomarkers: S100 β and p75 for Schwann cells and Thy1 for fibroblasts (Figure 3C).

At mRNA level we observed that NRG1 α is more highly expressed by nerve fibroblasts in comparison with Schwann cells, while soluble and β NRG1 isoforms are highly expressed in both cell types without significant differences (Figure 3A).

At the protein level, NRG1 is more highly expressed in nerve fibroblasts than in Schwann cells (Figure 3B); NRG1 was detected with an antibody which recognizes the 75-kDa band corresponding to the C terminal fragment of NRG1 [17,18].

Concerning ErbB receptor mRNA expression, ErbB1 is expressed by fibroblasts only, ErbB2 is more highly expressed by Schwann cells, ErbB3 and ErbB4 (NRG1 receptors) are only expressed by Schwann cells, at high and very low level respectively.

At protein level, fibroblasts express only ErbB1, Schwann cells express only ErbB2-ErbB3, ErbB4 is not detectable in both cell types; as a positive and negative controls for ErbB4 Western blot, neural progenitor cells stably expressing ErbB4 or mock cells were used [43].

3.5. Immunohistochemistry Analysis Shows that Nerve Fibroblasts Express NRG1

To assess in vivo the expression of NRG1 by nerve fibroblasts, immunohistochemistry analysis was carried out 7 days after nerve injury and repair, when at the protein level NRG1 is strongly expressed, while ErbB2 and ErbB3 are not detectable. The analysis was carried in the middle of the new tissue grown inside the conduit (the chitosan conduit was removed before fixation) and in the middle of the grafted autologous nerve.

In the autograft we found several cells positive for the Schwann cell marker S100 β (Figure 4A), while the signal of the fibroblast marker CD34 was very low; on the contrary, inside the conduit (Figure 4B), the signal of the Schwann cell marker was very low, while the signal of the fibroblast marker was highly detected. CD34 antibody was suitable for this analysis because it stains nerve fibroblasts [37], but not Schwann cells (as demonstrated in Figure 4, panels C-C''-C''').

Consistent with mRNA and protein analysis, several cells were stained with NRG1 antibody in the chitosan group (Figure 4, panels E-E'), while NRG1 staining in the autograft was very low (Figure 4, panels D-D'). At higher magnification, some cells were positive for both CD34 and NRG1 (Figure 4, panels F-F'-F''-G-G'-G'').

CD34 does not only recognize nerve fibroblast, but also endothelial cells [37]; usually, this does not represent a problem, because vessels are not very abundant in the nerve and blood vessel cross sections can be easily recognized for their rounded shape; nevertheless, because vessels in the chitosan were found to be very abundant, to unequivocally discriminate nerve fibroblasts from endothelial cells, we analyzed autograft and chitosan samples also with CD34 and RECA1 antibodies, as RECA1 antibody specifically stains endothelial cells. Data show that in the chitosan group (Figure 4, panels I-I'), unlike in the autograft (Figure 4, panels H-H'), there are several fibroblasts and several endothelial cells. At higher magnification (Figure 4, panels J-J'-K-K') it is possible to identify both cell types: endothelial cells that are positive for both CD34 and RECA1 staining (yellow signal) and nerve fibroblasts solely positive for CD34 staining (green signal).

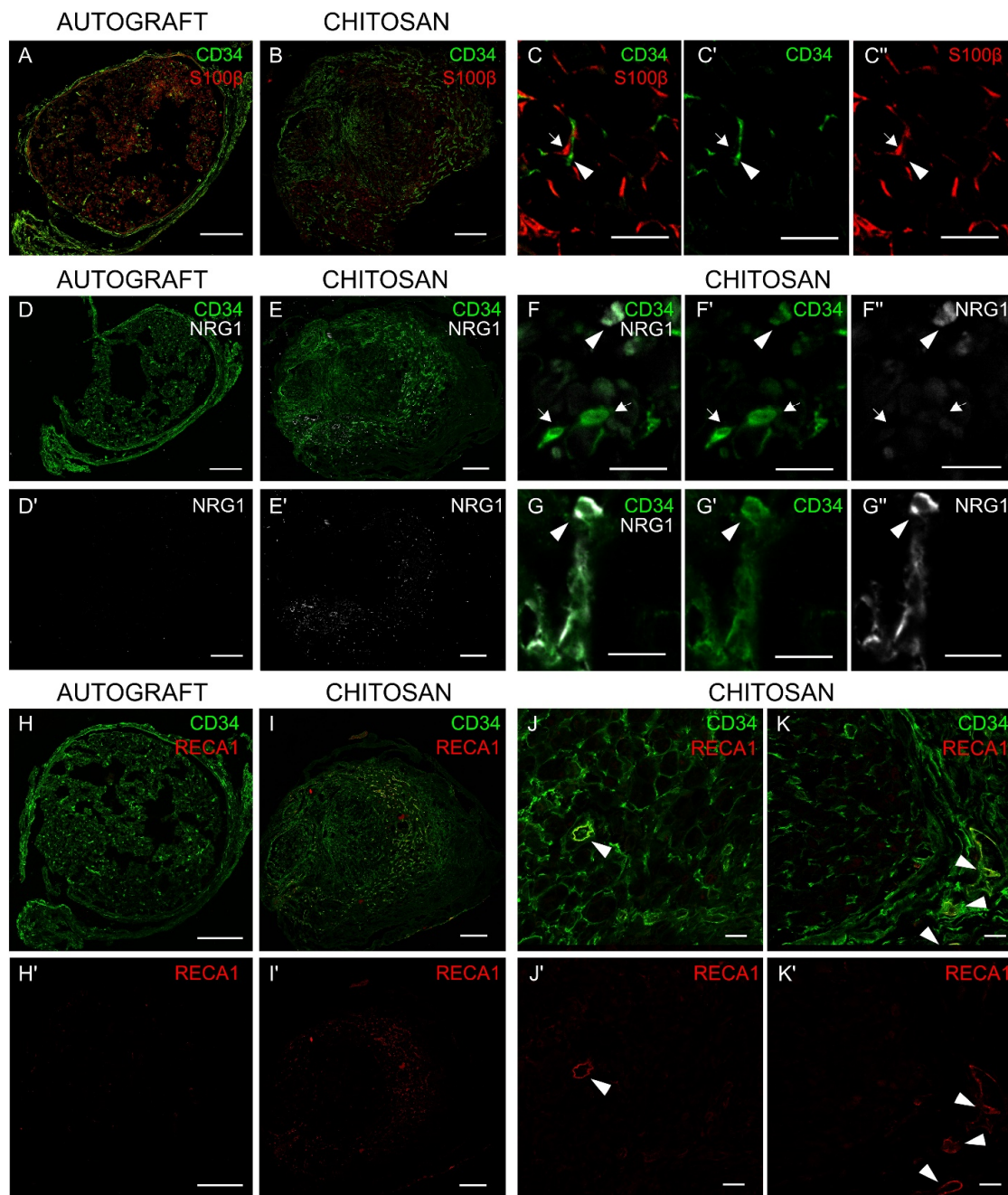


Figure 4. Nerve fibroblasts express NRG1 in vivo. Cross section of median nerves analyzed 7 days after repair with an autograft (A, D, D', H, H') or with a chitosan conduit (B, E, E', I, I'): (A,B) double-stained with S100 β (Schwann cell marker, red) and CD34 (fibroblast marker, green). (C, C', C'') Images at higher magnification show the absence of colocalization between S100 β and CD34; fibroblasts are pointed out by arrow heads, Schwann cells by arrows. (D,E) double-stained with CD34 (green) and NRG1 (white) or (D',E') single-stained with NRG1; (D') and (E') highlight different levels of NRG1 expression in the two different experimental models (higher in the chitosan group). (F, F', F'' and G, G', G'') Images at higher magnification show some CD34⁺ cells positive only to CD34 (arrow) and some CD34⁺ cells also positive to NRG1 (arrow head). (H,I) double-stained with CD34 (fibroblast and endothelial cell marker, green) and RECA1 (endothelial cell marker, red) or (H',I') single-stained with RECA1; (H') and (I') highlight different levels of RECA1 expression in the two different experimental models (higher in the

chitosan group). (J, J' and K, K') Images at higher magnification show some CD34⁺ cells also positive for RECA1, corresponding to endothelial cells (arrow heads), and several CD34⁺ cells positive only to CD34, corresponding to fibroblast cells. Scale bars: 200 μm (A, B, D, D', E, E', H, H', I, I'); 20 μm (J, J', K, K'); 10 μm (C, C', C'', F, F', F'', G, G', G'').

4. Discussion

For short nerve gap repair in human, up to 3 cm [8,9], tubulization is successfully used as a good alternative to autograft, especially in small diameter, noncritical sensory nerves [44], while short nerve gaps are successfully repaired in rat up to 1 cm [10,25,45]. Because several research groups [29], including ours [30], are making efforts to functionalize and enrich tubular conduits to further promote nerve regeneration in more complex situations, such as longer nerve gap or delayed repair, we focused our attention on investigating what occurs inside a hollow conduit after nerve gap repair.

Soluble NRG1 is one of the factors known to play an important role during nerve regeneration [16]; we and others previously showed [17,18,46] that soluble NRG1 transcript is strongly and transiently up-regulated in the distal portion of the nerve 1 day after injury and that the NRG1 receptor ErbB3 is strongly down-regulated 3 days after injury and up-regulated 7, 14, and 28 days after repair, while the expression of the co-receptor ErbB2, barely detectable in the healthy nerve, is up-regulated 7, 14, and 28 days after injury [17].

Here, we analyzed the expression of the NRG1/ErbB system inside a chitosan conduit 7, 14, and 28 days after injury and repair and we compared it with the autograft. Our data show that, while the expression of ErbB2 and ErbB3 is up-regulated in the autograft 7, 14, 28 days after injury, as occurs in the distal portion of the nerve after a crush injury or after an end-to-end repair [17], in the chitosan conduit ErbB2 and ErbB3 expression starts to be detectable 14 days after nerve repair and becomes high only 2 weeks later. The absence of ErbB expression one week after injury is consistent with the fact that the conduit needs time to be colonized by repair Schwann cells [28], which in the autograft play a key role either in the Wallerian degeneration, either in nerve regeneration, while in the conduit are mainly involved in nerve regeneration. Conversely, NRG1 expression is strongly detectable in both autograft and chitosan 7 days after nerve injury and repair. Moreover, it has been shown *in vitro* that NRG1 stimulation of Schwann cells activates ERK, AKT, and cJun phosphorylation [47–49]; the lack of ERK, AKT, and cJun phosphorylation in the chitosan samples, despite the presence of high levels of NRG1, might be due to the absence (or low presence) of Schwann cells.

We further confirmed this by analysis, at mRNA level, the expression of Schwann cell markers, together with a marker of nerve fibroblasts, which are supposed to colonize tubular nerve conduits earlier, as in the first stages conduits are filled with extracellular matrix and fibrin cables [28]. The high expression of NRG1 and of a fibroblast marker together with the low expression of Schwann cell markers led us to speculate that nerve fibroblasts might be the main source of soluble NRG1 detected within the conduit. As different soluble NRG1 isoforms are known to be expressed following a nerve injury [17], we analyzed at mRNA level the relative expression of soluble NRG1 and of NRG1 α and NRG1 β , two soluble NRG1 isoforms characterized by different expression pattern and activity [43]. Intriguingly, we found that the expression pattern of all soluble NRG1 isoforms has a trend similar to the expression of the fibroblast marker Thy1, especially NRG1 α , whose expression is strongly upregulated in the chitosan group 14 and 28 days after repair, like the fibroblast marker Thy1. The trend is similar also for NRG1 β , but its expression is lower. These data are highly reminiscent of our previous observation (carried out on the distal portion of different experimental rat models: Crush injury and cut followed by end-to-end repair) where we found that NRG1 α isoforms are more highly upregulated than NRG1 β isoforms [17], thus reinforcing the idea that α isoforms also might play a role in nerve regeneration [50].

Protein and mRNA data do not correspond exactly: At the protein level a stronger expression of NRG1 in the chitosan samples is observed 7 days after repair, while at the mRNA level the expression is higher 14 days after repair. This discrepancy might be explained in two ways: By the fact that

mRNA and protein expression could be different because of post-transcriptional and post-translational regulation or by the fact that at the mRNA level the expression of specific isoforms (soluble, α , β) is quantifiable, while no effective antibodies specific for the soluble fragment of NRG1 or for α or β isoforms are commercially available. The antibody used for Western blot analysis, acknowledged by the scientific community as a very good antibody to detect the C terminus of the transmembrane precursor of soluble NRG1 isoforms [18,40], recognizes only a subcategory of soluble NRG1 isoforms, but there are also isoforms expressed as soluble proteins without a transmembrane precursor or with a precursor with a different C terminus.

To identify the different NRG1 isoforms and NRG1 receptors and co-receptors expressed by nerve fibroblasts, an accurate mRNA and protein analysis was carried out on primary cultures of nerve fibroblasts and compared with primary cultures of Schwann cells and with healthy median nerves (used as calibrator). Our results show that nerve fibroblasts express high levels of different NRG1 isoforms: Soluble, type α and type β . Intriguingly, NRG1 α isoforms are significantly more highly expressed in fibroblasts than in Schwann cells and healthy nerve, while NRG1 β expression is more similar in the two primary cultures and in the healthy nerve, thus reinforcing the idea that the soluble NRG1 we observe upregulated in the chitosan might be mainly the NRG1 α expressed by fibroblasts.

Fibroblasts express ErbB1, while they do not express the NRG1 receptors ErbB3 and ErbB4 and the co-receptor ErbB2, thus suggesting that nerve fibroblasts are not able to activate a signal transduction pathway after NRG1 stimulation, which is in agreement with the lack of ERK, AKT and cJun phosphorylation. Schwann cells express only ErbB2-ErbB3 co-receptors; at mRNA level, a signal for ErbB4 is detectable, but at the protein level it is not expressed, as previously shown [51]. These results are consistent with literature data obtained from in vitro study showing that primary cultures of nerve fibroblasts can release soluble Schwann cell pro-migratory factors, including NRG1 [52,53]. However, our in vitro study demonstrated also that fibroblasts express both NRG1 α and NRG1 β , while Schwann cells express mainly NRG1 β . Our in vivo analysis, showing high levels of the fibroblast marker Thy1 and high levels of NRG1 α , suggests that nerve fibroblasts might be the main source of soluble NRG1 inside the conduit during nerve regeneration.

To further investigate NRG1 expression in vivo, immunohistochemistry analyses were carried out 7 days after injury and repair and it was observed a high NRG1 expression in the chitosan conduit samples, while in the autograft the NRG1 signal was lower, consistently with Western blot analysis. Moreover, in the autograft samples, Schwann cells were more abundant than fibroblasts, unlike in the chitosan samples, where fibroblasts were more abundant than Schwann cells.

To verify that the high amount of NRG1 observed in the conduit might be attributed to the high presence of fibroblasts, double labelling of a fibroblast marker and NRG1 was performed. Our data show that some fibroblasts were also positive for NRG1.

Thy1 is a good marker for mRNA analysis, but it is not suitable for IHC or Western blot analysis because it is also expressed by neurons [54]: When we analyze RNA in the distal portion of peripheral nerves (which does not include neuron cell bodies), we are analyzing RNA belonging to resident cells only (e.g., Schwann cells, fibroblasts, endothelial cells, and macrophages), while when we analyze proteins we detect proteins belonging to either the neurons, either resident cells, because neuron proteins are expressed also along the axons.

According to Richard and colleagues [55], the sialylated transmembrane glycoprotein CD34 is a good marker of nerve fibroblasts for IHC analysis, since it is not expressed by Schwann cells, macrophages, and perineurial cells. Nevertheless, CD34 is expressed not only by fibroblasts, but also by endothelial cells, which usually are not very abundant in the nerves and can be easily recognized for the rounded shape of blood vessels and capillary. To unequivocally discriminate between fibroblasts and endothelial cells, a double staining was carried out for CD34 and RECA1, which specifically detects endothelial cells, showing that inside the conduit there are several fibroblasts, but also several endothelial cells forming blood vessels. The presence of a high number of fibroblasts and blood vessels inside the chitosan conduit is consistent with the observation that fibroblasts might promote

angiogenesis by secreting cytokines [56]. Our data show that in the chitosan conduits blood vessels are highly abundant 7 days after injury and repair, while their presence is very low in the autograft samples. It has been shown by others [14] that in the bridge formed between proximal and distal stumps, when the gap is small, blood vessels provide a track for Schwann cell migration. The high presence of blood vessels in the conduit suggests that they could play here the same role. Moreover, as vascularization is also important to supply oxygen and nutrients for nerve tissue survival, different research groups are developing new strategies to further promote vessel formation inside conduits [57].

Although it has been previously demonstrated that fibroblasts accumulated at the injury site secrete extracellular matrix and form scar tissue, which might impair nerve regeneration [58], other authors demonstrated that grafted nerve fibroblasts can positively influence Schwann cell behavior during nerve repair [59]. Moreover, it has been shown that in the “nerve bridge”, formed between proximal and distal stumps after nerve injury, the interaction between nerve fibroblasts and Schwann cells—mediated by ephrinB2-EphB2—plays a key role for cell sorting and for Schwann cell cord formation [3].

Although hollow conduits are suitable for short gap repair, for long gaps they are unable to provide an adequate microenvironment for regeneration [60]; one possible reason might be that fibroblasts are not numerous enough to produce sufficient fibrin matrix, NRG1 and other factors. Indeed, it has been shown that matrix diameter is inversely proportional to the conduit length, deeply affecting the regenerative outcome after nerve transection [61] and that soluble NRG1 plays an important role in Schwann cell dedifferentiation, proliferation, and migration [16,18,62]. This study allows us to make two further methodological considerations:

1-The presence of Thy1 and NRG1 α also in the autograft samples, and the high levels of NRG1 α (together with NRG1 β) previously detected after crush injury or end-to-end repair [17] suggest that nerve fibroblasts might participate, together with Schwann cells, to NRG1 expression after nerve injury. The fact that soluble NRG1 might be produced not only by Schwann cells but also by fibroblasts, suggests that when CRE-lox technology is used to switch off NRG1 expression specifically in Schwann cells (using Schwann cell specific promoters for CRE expression), soluble NRG1 released by fibroblasts might be present in the environment and partially compensate for the absence of Schwann cell NRG1. To completely inactivate NRG1 expression (in, e.g., Schwann cells, neurons, and fibroblasts) we suggest to use inducible knockout animals, like those developed by Fricker and colleagues, ubiquitously expressing a tamoxifen inducible CRE protein which removes floxed NRG1 in all cells after tamoxifen treatment [63].

2-To obtain neuron specific gene expression or neuron specific CRE mediated gene inactivation, the neuron specific promoter Thy1 is often used, being expressed in motoneurons and DRG neurons [64]. Nevertheless, because Thy1 is expressed also by nerve fibroblasts, the use of this promoter could give rise to unspecific effects that need to be regarded, considering that fibroblasts might be involved in the regeneration process.

5. Conclusions

To conclude, our results suggest that nerve fibroblasts might contribute to the high level of soluble NRG1 observed after nerve injury and repair thus promoting Schwann cell dedifferentiation. Yet, it is possible to hypothesize that nerve fibroblast grafting within conduits might be a good strategy to further promote nerve regeneration after long gap and/or delayed nerve repair.

Supplementary Materials: The following are available online at <http://www.mdpi.com/2073-4409/9/6/1366/s1>, Figure S1: Macroscopic view of implantation sites; rat median nerve 8 mm defect was repaired with a 10 mm long chitosan conduit (A) or with autograft technique (B). Table S1. Antibodies used for Western blot and immunohistochemistry analysis.

Author Contributions: Conceptualization, B.E.F. and G.G.; Methodology, G.R., A.C., and S.R.; Validation, B.E.F.; Formal Analysis, B.E.F. and G.C.; Investigation, B.E.F., M.E.S., G.N., A.C., G.R., A.C., S.R., and G.G.; Data Curation, B.E.F. and G.G.; Writing—Original Draft Preparation, B.E.F., M.E.S., and G.G.; Writing—Review and Editing, G.R., I.P., S.G., S.R., and G.G.; Validation, B.E.F., and G.G.; Visualization, B.E.F., G.G., G.N., A.F., and G.C.; Supervision,

G.G.; Project Administration, B.E.F., and G.G.; Funding Acquisition, G.R., I.P., S.G., S.R., and G.G. All authors have read and agreed to the published version of the manuscript.

Funding: This study was supported by Compagnia di San Paolo, No. D86D15000100005 InTheCure project to S.R. and by grants from the University of Torino to I.P., S.G., S.R., and G.G.

Acknowledgments: Reaxon® Nerve Guides were supplied by Medovent GmbH (Mainz, Germany).

Conflicts of Interest: The authors declare no conflict of interest.

Abbreviations

ANKRD27	Ankyrin repeat domain 27
ANOVA	Analysis of variance
CI	confidence interval
DAAO	D-amino acid oxidase
DMEM	Dulbecco Modified Eagle Medium
GFAP	glial fibrillary acidic protein
η_p^2	partial eta-squared
ERK	extracellular signal-regulated kinase
FBS	fetal bovine serum
IHC	immunohistochemistry
MAPK	mitogen-activated protein kinase
MBP	Myelin basic protein
NDS	Normal Donkey Serum
NRG1	Neuregulin1
OCT	Optimal Cutting Temperature
PBS	Phosphate Buffered Saline
PI3K	Phosphoinositide 3-Kinase
PLL	poly-L-lysine
RICTOR	RPTOR Independent Companion Of MTOR, Complex 2
SEM	standard error of the mean
VEGF	Vascular-Endothelial Growth Factor.

References

1. Modrak, M.; Talukder, M.A.H.; Gurgenshvili, K.; Noble, M.; Elfar, J.C. Peripheral nerve injury and myelination: Potential therapeutic strategies. *J. Neurosci. Res.* **2020**, *98*, 780–795. [[CrossRef](#)]
2. Cattin, A.L.; Burden, J.J.; Van Emmenis, L.; MacKenzie, F.E.; Hoving, J.J.A.; Garcia Calavia, N.; Guo, Y.; McLaughlin, M.; Rosenberg, L.H.; Quereda, V.; et al. Macrophage-Induced Blood Vessels Guide Schwann Cell-Mediated Regeneration of Peripheral Nerves. *Cell* **2015**, *162*, 1127–1139. [[CrossRef](#)]
3. Parrinello, S.; Napoli, I.; Ribeiro, S.; Wingfield Digby, P.; Fedorova, M.; Parkinson, D.B.; Doddrell, R.D.S.; Nakayama, M.; Adams, R.H.; Lloyd, A.C. EphB signaling directs peripheral nerve regeneration through Sox2-dependent Schwann cell sorting. *Cell* **2010**, *143*, 145–155. [[CrossRef](#)]
4. Duffy, P.; McMahon, S.; Wang, X.; Keaveney, S.; O’Cearbhaill, E.D.; Quintana, I.; Rodríguez, F.J.; Wang, W. Synthetic bioresorbable poly- α -hydroxyesters as peripheral nerve guidance conduits; a review of material properties, design strategies and their efficacy to date. *Biomater. Sci.* **2019**, *7*, 4912–4943. [[CrossRef](#)]
5. Bahm, J.; Esser, T.; Sellhaus, B.; El-kazzi, W.; Schuind, F.T. Tension in peripheral nerve suture. In *Treatment of Brachial Plexus Injuries*; Vanaclocha, V., Sáiz-Sapena, N., Eds.; IntechOpen: London, UK, 2018; pp. 2–9.
6. Deumens, R.; Bozkurt, A.; Meek, M.F.; Marcus, M.A.E.; Joosten, E.A.J.; Weis, J.; Brook, G.A. Repairing injured peripheral nerves: Bridging the gap. *Prog. Neurobiol.* **2010**, *92*, 245–276. [[CrossRef](#)]
7. Belanger, K.; Dinis, T.M.; Taourirt, S.; Vidal, G.; Kaplan, D.L.; Egles, C. Recent Strategies in Tissue Engineering for Guided Peripheral Nerve Regeneration. *Macromol. Biosci.* **2016**, *16*, 472–481. [[CrossRef](#)]
8. Kornfeld, T.; Vogt, P.M.; Radtke, C. Nerve grafting for peripheral nerve injuries with extended defect sizes. *Wiener Medizinische Wochenschrift* **2018**, *169*, 240–251. [[CrossRef](#)]
9. Moore, A.M.; Kasukurthi, R.; Magill, C.K.; Farhadi, F.H.; Borschel, G.H.; Mackinnon, S.E. Limitations of conduits in peripheral nerve repairs. *Hand* **2009**, *4*, 180–186. [[CrossRef](#)]

10. Haastert-Talini, K.; Geuna, S.; Dahlin, L.B.; Meyer, C.; Stenberg, L.; Freier, T.; Heimann, C.; Barwig, C.; Pinto, L.F.V.; Raimondo, S.; et al. Chitosan tubes of varying degrees of acetylation for bridging peripheral nerve defects. *Biomaterials* **2013**, *34*, 9886–9904. [[CrossRef](#)]
11. Freier, T.; Montenegro, R.; Koh, H.S.; Shoichet, M.S. Chitin-based tubes for tissue engineering in the nervous system. *Biomaterials* **2005**, *26*, 4624–4632. [[CrossRef](#)]
12. Bağ, M.; Gutkowska, O.N.; Wagner, E.; Gosk, J. The role of chitin and chitosan in peripheral nerve reconstruction. *Polym. Med.* **2017**, *47*, 43–47. [[CrossRef](#)]
13. Boecker, A.; Daeschler, S.C.; Kneser, U.; Harhaus, L. Relevance and recent developments of chitosan in peripheral nerve surgery. *Front. Cell. Neurosci.* **2019**, *13*, 104. [[CrossRef](#)]
14. Cattin, A.L.; Lloyd, A.C. The multicellular complexity of peripheral nerve regeneration. *Curr. Opin. Neurobiol.* **2016**, *39*, 38–46. [[CrossRef](#)]
15. Jessen, K.R.; Arthur-Farraj, P. Repair Schwann cell update: Adaptive reprogramming, EMT, and stemness in regenerating nerves. *Glia* **2019**, *67*, 421–437. [[CrossRef](#)]
16. Fricker, F.R.; Bennett, D.L. The role of neuregulin-1 in the response to nerve injury. *Future Neurol.* **2011**, *6*, 809–822. [[CrossRef](#)]
17. Ronchi, G.; Haastert-Talini, K.; Fornasari, B.E.; Perroteau, I.; Geuna, S.; Gambarotta, G. The Neuregulin1/ErbB system is selectively regulated during peripheral nerve degeneration and regeneration. *Eur. J. Neurosci.* **2016**, *43*, 351–364. [[CrossRef](#)]
18. Stassart, R.M.; Fledrich, R.; Velanac, V.; Brinkmann, B.G.; Schwab, M.H.; Meijer, D.; Sereda, M.W.; Nave, K.A. A role for Schwann cell-derived neuregulin-1 in remyelination. *Nat. Neurosci.* **2013**, *16*, 48–54. [[CrossRef](#)]
19. Mei, L.; Xiong, W.C. Neuregulin 1 in neural development, synaptic plasticity and schizophrenia. *Nat. Rev. Neurosci.* **2008**, *9*, 437–452. [[CrossRef](#)]
20. Falls, D.L. Neuregulins: Functions, forms, and signaling strategies. *Exp. Cell Res.* **2003**, *284*, 14–30. [[CrossRef](#)]
21. Wen, D.; Suggs, S.V.; Karunakaran, D.; Liu, N.; Cupples, R.L.; Luo, Y.; Janssen, A.M.; Ben-Baruch, N.; Trollinger, D.B.; Jacobsen, V.L. Structural and functional aspects of the multiplicity of Neu differentiation factors. *Mol. Cell. Biol.* **1994**, *14*, 1909–1919. [[CrossRef](#)]
22. Newbern, J.; Birchmeier, C. Nrg1/ErbB signaling networks in Schwann cell development and myelination. *Semin. Cell Dev. Biol.* **2010**, *21*, 922–928. [[CrossRef](#)]
23. Gonzalez-Perez, F.; Cobianchi, S.; Geuna, S.; Barwig, C.; Freier, T.; Udina, E.; Navarro, X. Tubulization with chitosan guides for the repair of long gap peripheral nerve injury in the rat. *Microsurgery* **2015**, *35*, 300–308. [[CrossRef](#)]
24. Meyer, C.; Stenberg, L.; Gonzalez-Perez, F.; Wrobel, S.; Ronchi, G.; Udina, E.; Sukanuma, S.; Geuna, S.; Navarro, X.; Dahlin, L.B.; et al. Chitosan-film enhanced chitosan nerve guides for long-distance regeneration of peripheral nerves. *Biomaterials* **2016**, *76*, 33–51. [[CrossRef](#)]
25. Shapira, Y.; Tolmasov, M.; Nissan, M.; Reider, E.; Koren, A.; Biron, T.; Bitan, Y.; Livnat, M.; Ronchi, G.; Geuna, S.; et al. Comparison of results between chitosan hollow tube and autologous nerve graft in reconstruction of peripheral nerve defect: An experimental study. *Microsurgery* **2016**, *36*, 664–671. [[CrossRef](#)]
26. Boni, R.; Ali, A.; Shavandi, A.; Clarkson, A.N. Current and novel polymeric biomaterials for neural tissue engineering. *J. Biomed. Sci.* **2018**, *25*, 90. [[CrossRef](#)]
27. Subramanian, A.; Krishnan, U.M.; Sethuraman, S. Development of biomaterial scaffold for nerve tissue engineering: Biomaterial mediated neural regeneration. *J. Biomed. Sci.* **2009**, *16*, 108. [[CrossRef](#)]
28. Williams, L.R.; Longo, F.M.; Powell, H.C.; Lundborg, G.; Varon, S. Spatial-Temporal progress of peripheral nerve regeneration within a silicone chamber: Parameters for a bioassay. *J. Comp. Neurol.* **1983**, *218*, 460–470. [[CrossRef](#)]
29. Carvalho, C.R.; Oliveira, J.M.; Reis, R.L. Modern Trends for Peripheral Nerve Repair and Regeneration: Beyond the Hollow Nerve Guidance Conduit. *Front. Bioeng. Biotechnol.* **2019**, *7*, 337. [[CrossRef](#)]
30. Ronchi, G.; Fornasari, B.E.; Crosio, A.; Budau, C.A.; Tos, P.; Perroteau, I.; Battiston, B.; Geuna, S.; Raimondo, S.; Gambarotta, G. Chitosan Tubes Enriched with Fresh Skeletal Muscle Fibers for Primary Nerve Repair. *Biomed. Res. Int.* **2018**, *2018*, 9175248. [[CrossRef](#)]
31. Kaewkhaw, R.; Scutt, A.M.; Haycock, J.W. Integrated culture and purification of rat Schwann cells from freshly isolated adult tissue. *Nat. Protoc.* **2012**, *7*, 1996–2004. [[CrossRef](#)]
32. Livak, K.J.; Schmittgen, T.D. Analysis of relative gene expression data using real-time quantitative PCR and the 2- $\Delta\Delta$ CT method. *Methods* **2001**, *25*, 402–408. [[CrossRef](#)] [[PubMed](#)]

33. Gambarotta, G.; Ronchi, G.; Friard, O.; Galletta, P.; Perroteau, I.; Geuna, S. Identification and validation of suitable housekeeping genes for normalizing quantitative real-time PCR assays in injured peripheral nerves. *PLoS ONE* **2014**, *9*, e105601. [[CrossRef](#)] [[PubMed](#)]
34. Ronchi, G.; Cillino, M.; Gambarotta, G.; Fornasari, B.E.; Raimondo, S.; Pugliese, P.; Tos, P.; Cordova, A.; Moschella, F.; Geuna, S. Irreversible changes occurring in long-term denervated Schwann cells affect delayed nerve repair. *J. Neurosurg.* **2017**, *127*, 843–856. [[CrossRef](#)] [[PubMed](#)]
35. Gambarotta, G.; Garzotto, D.; Destro, E.; Mautino, B.; Giampietro, C.; Cutrupi, S.; Dati, C.; Cattaneo, E.; Fasolo, A.; Perroteau, I. ErbB4 expression in neural progenitor cells (ST14A) is necessary to mediate neuregulin-1beta1-induced migration. *J. Biol. Chem.* **2004**, *279*, 48808–48816. [[CrossRef](#)] [[PubMed](#)]
36. Zhou, L.N.; Cui, X.J.; Su, K.X.; Wang, X.H.; Guo, J.H. Beneficial reciprocal effects of bone marrow stromal cells and Schwann cells from adult rats in a dynamic co-culture system in vitro without intercellular contact. *Mol. Med. Rep.* **2015**, *12*, 4931–4938. [[CrossRef](#)] [[PubMed](#)]
37. Richard, L.; Védrenne, N.; Vallat, J.-M.; Funalot, B. Characterization of Endoneurial Fibroblast-like Cells from Human and Rat Peripheral Nerves. *J. Histochem. Cytochem.* **2014**, *62*, 424–435. [[CrossRef](#)]
38. Van Slooten, A.R.; Sun, Y.; Clarkson, A.N.; Connor, B.J. L-NIO as a novel mechanism for inducing focal cerebral ischemia in the adult rat brain. *J. Neurosci. Methods* **2015**, *245*, 44–57. [[CrossRef](#)]
39. Duijvestijn, A.; van Goor, H.; Klatter, F.; Majoor, G.; van Bussel, E.; van Breda Vriesman, P. Antibodies Defining Rat Endothelial Cells: RECA-1, a Pan-Endothelial Cell-Specific Monoclonal Antibody. *Lab. Investig.* **2012**, *66*, 459–466.
40. Fledrich, R.; Akkermann, D.; Schütza, V.; Abdelaal, T.A.; Hermes, D.; Schäffner, E.; Soto-Bernardini, M.C.; Götze, T.; Klink, A.; Kusch, K.; et al. NRG1 type I dependent autocrine stimulation of Schwann cells in onion bulbs of peripheral neuropathies. *Nat. Commun.* **2019**, *10*, 1467. [[CrossRef](#)]
41. Faul, F.; Erdfelder, E.; Lang, A.G.; Buchner, A. G*Power 3: A flexible statistical power analysis program for the social, behavioral, and biomedical sciences. *Behav. Res. Methods* **2007**, *39*, 175–191. [[CrossRef](#)]
42. Richardson, J.T.E. Eta squared and partial eta squared as measures of effect size in educational research. *Educ. Res. Rev.* **2011**, *6*, 135–147. [[CrossRef](#)]
43. Fornasari, B.E.; El Soury, M.; De Marchis, S.; Perroteau, I.; Geuna, S.; Gambarotta, G. Neuregulin1 alpha activates migration of neuronal progenitors expressing ErbB4. *Mol. Cell. Neurosci.* **2016**, *77*, 87–94. [[CrossRef](#)]
44. Meek, M.F.; Coert, J.H. US Food and Drug Administration /Conformit Europe- approved absorbable nerve conduits for clinical repair of peripheral and cranial nerves. *Ann. Plast. Surg.* **2008**, *60*, 466–472. [[CrossRef](#)]
45. Stenberg, L.; Kodama, A.; Lindwall-Blom, C.; Dahlin, L.B. Nerve regeneration in chitosan conduits and in autologous nerve grafts in healthy and in type 2 diabetic Goto-Kakizaki rats. *Eur. J. Neurosci.* **2016**, *43*, 463–473. [[CrossRef](#)]
46. Carroll, S.L.; Miller, M.L.; Frohnert, P.W.; Kim, S.S.; Corbett, J.A. Expression of neuregulins and their putative receptors, ErbB2 and ErbB3, is induced during Wallerian degeneration. *J. Neurosci.* **1997**, *17*, 1642–1659. [[CrossRef](#)]
47. Monje, P.V.; Bartlett Bunge, M.; Wood, P.M. Cyclic AMP synergistically enhances neuregulin-dependent ERK and Akt activation and cell cycle progression in Schwann cells. *Glia* **2006**, *53*, 649–659. [[CrossRef](#)]
48. Parkinson, D.B.; Bhaskaran, A.; Droggiti, A.; Dickinson, S.; D’Antonio, M.; Mirsky, R.; Jessen, K.R. Krox-20 inhibits Jun-NH2-terminal kinase/c-Jun to control Schwann cell proliferation and death. *J. Cell Biol.* **2004**, *164*, 385–394. [[CrossRef](#)]
49. Syed, N.; Reddy, K.; Yang, D.P.; Taveggia, C.; Salzer, J.L.; Maurel, P.; Kim, H.A. Soluble neuregulin-1 has bifunctional, concentration-dependent effects on Schwann cell myelination. *J. Neurosci.* **2010**, *30*, 6122–6131. [[CrossRef](#)]
50. de Souza, F.I.; Zumiotti, A.V.; da Silva, C.F. Neuregulins 1-alpha and 1-beta on the regeneration the peripheral nerves. *Acta Ortop. Bras.* **2010**, *18*, 250–254. [[CrossRef](#)]
51. Pascal, D.; Giovannelli, A.; Gnani, S.; Hoyng, S.A.; de Winter, F.; Morano, M.; Fregnan, F.; Dell’Albani, P.; Zaccheo, D.; Perroteau, I.; et al. Characterization of glial cell models and in vitro manipulation of the neuregulin1/ErbB system. *Biomed. Res. Int.* **2014**, *2014*, 310215. [[CrossRef](#)]
52. Dreesmann, L.; Mittnacht, U.; Lietz, M.; Schlosshauer, B. Nerve fibroblast impact on Schwann cell behavior. *Eur. J. Cell Biol.* **2009**, *88*, 285–300. [[CrossRef](#)]

53. van Neerven, S.G.A.; Pannaye, P.; Bozkurt, A.; Van Nieuwenhoven, F.; Joosten, E.; Hermans, E.; Taccola, G.; Deumens, R. Schwann cell migration and neurite outgrowth are influenced by media conditioned by epineurial fibroblasts. *Neuroscience* **2013**, *252*, 144–153. [[CrossRef](#)]
54. Caroni, P. Overexpression of growth-associated proteins in the neurons of adult transgenic mice. *J. Neurosci. Methods* **1997**, *71*, 3–9. [[CrossRef](#)]
55. Richard, L.; Topilko, P.; Magy, L.; Decouvelaere, A.V.; Charnay, P.; Funalot, B.; Vallat, J.M. Endoneurial fibroblast-like cells. *J. Neuropathol. Exp. Neurol.* **2012**, *71*, 938–947. [[CrossRef](#)]
56. Sorrell, J.M.; Caplan, A.I. Fibroblasts—a diverse population at the center of it all. *Int. Rev. Cell Mol. Biol.* **2009**, *276*, 161–214.
57. Muangsanit, P.; Shipley, R.J.; Phillips, J.B. Vascularization Strategies for Peripheral Nerve Tissue Engineering. *Anat. Rec. (Hoboken)* **2018**, *301*, 1657–1667. [[CrossRef](#)]
58. Atkins, S.; Smith, K.G.; Loescher, A.R.; Boissonade, F.M.; O’Kane, S.; Ferguson, M.W.J.; Robinson, P.P. Scarring impedes regeneration at sites of peripheral nerve repair. *Neuroreport* **2006**, *17*, 1245–1249. [[CrossRef](#)]
59. Wang, Y.; Li, D.; Wang, G.; Chen, L.; Chen, J.; Liu, Z.; Zhang, Z.; Shen, H.; Jin, Y.; Shen, Z. The effect of co-transplantation of nerve fibroblasts and Schwann cells on peripheral nerve repair. *Int. J. Biol. Sci.* **2017**, *13*, 1507–1519. [[CrossRef](#)]
60. Pabari, A.; Yang, S.Y.; Mosahebi, A.; Seifalian, A.M. Recent advances in artificial nerve conduit design: Strategies for the delivery of luminal fillers. *J. Control. Release* **2011**, *156*, 2–10. [[CrossRef](#)]
61. Zhao, Q.; Dahlin, L.B.; Kanje, M.; Lundborg, G. Repair of the transected rat sciatic nerve: Matrix formation within implanted silicone tubes. *Restor. Neurol. Neurosci.* **1993**, *5*, 197–204. [[CrossRef](#)]
62. El Soury, M.; Fornasari, B.E.; Morano, M.; Grazio, E.; Ronchi, G.; Incarnato, D.; Giacobini, M.; Geuna, S.; Provero, P.; Gambarotta, G. Soluble Neuregulin1 Down-Regulates Myelination Genes in Schwann Cells. *Front. Mol. Neurosci.* **2018**, *11*, 157. [[CrossRef](#)]
63. Fricker, F.R.; Antunes-Martins, A.; Galino, J.; Paramsothy, R.; La Russa, F.; Perkins, J.; Goldberg, R.; Brelstaff, J.; Zhu, N.; McMahon, S.B.; et al. Axonal neuregulin 1 is a rate limiting but not essential factor for nerve remyelination. *Brain* **2013**, *136*, 2279–2297. [[CrossRef](#)]
64. Moore, A.M.; Borschel, G.H.; Santosa, K.B.; Flagg, E.R.; Tong, A.Y.; Kasukurthi, R.; Newton, P.; Yan, Y.; Hunter, D.A.; Johnson, P.J.; et al. A transgenic rat expressing green fluorescent protein (GFP) in peripheral nerves provides a new hindlimb model for the study of nerve injury and regeneration. *J. Neurosci. Methods* **2012**, *204*, 19–27. [[CrossRef](#)]



© 2020 by the authors. Licensee MDPI, Basel, Switzerland. This article is an open access article distributed under the terms and conditions of the Creative Commons Attribution (CC BY) license (<http://creativecommons.org/licenses/by/4.0/>).

3.2 Exploring an innovative decellularization protocol for porcine nerve grafts: a translational approach to peripheral nerve repair

Muratori L, Crosio A, Ronchi G, Molinaro D, Tos P, Lovati A, Raimondo S

Under submission

EXPLORING AN INNOVATIVE DECELLULARIZATION PROTOCOL FOR PORCINE NERVE GRAFTS: A TRANSLATIONAL APPROACH TO PERIPHERAL NERVE REPAIR

Luisa Muratori¹, Alessandro Crosio^{1,2}, Giulia Ronchi¹, Debora Molinaro¹, Pierluigi Tos³, Arianna Lovati^{4§}, Stefania Raimondo^{1*§}.

¹*Department of Clinical and Biological Sciences, Neuroscience Institute Cavalieri Ottolenghi (NICO), University of Turin, Turin, Italy;*

²*UOC Traumatology-Reconstructive Microsurgery, Department of Orthopedics and Traumatology, AOU Città della Salute e della Scienza - CTO Hospital, Torino, Italy.*

³*Reconstructive Microsurgery and Hand surgery Unit, ASST Pini-CTO Milano, Italy;*

⁴*Cell and Tissue Engineering Laboratory, IRCCS Istituto Ortopedico Galeazzi, Milan, Italy.*

*Corresponding author

Stefania Raimondo

Department of Clinical and Biological Sciences,

Neuroscience Institute Cavalieri Ottolenghi (NICO)

Regione Gonzole 10, 10043 Orbassano (TO)

Tel +39 011 670 5433, fax +39 011 9038639,

E-mail address: stefania.raimondo@unito.it

§ Equally contributed

Abstract

Peripheral nerves are frequently affected by lesions caused by traumatic or iatrogenic damages, resulting in loss of motor and sensory function, crucial in orthopaedic outcomes and with a significant impact on patients' quality of life. Many strategies have been proposed over years to repair nerve injuries with substance loss, to achieve musculoskeletal reinnervation and functional recovery. Allograft have been tested as an alternative to the gold standard, the autograft technique, but nerves from donors frequently cause immunogenic response. For this reason, several studies are focusing to find the best way to decellularize nerves preserving either the extracellular matrix, either the basal lamina, as the key elements used by Schwann cells and axons during the regenerative process. This study focuses on a novel decellularization protocol for porcine nerves, aimed at reducing immunogenicity while preserving essential elements like the extracellular matrix and basal lamina, vital for nerve regeneration. The idea of using a porcine nerve graft arises from a translational point of view. This approach offers a promising direction in the orthopaedic field for nerve repair, especially in severe cases where conventional methods are limited.

The first aim of the present study was to test the efficacy of a decellularization method in order to evaluate its possible application to create efficient nerve grafts. The second aim was to evaluate the ability of the decellularized porcine nerve graft to repair median nerve lesions in rats.

To investigate the efficacy of the decellularization protocol to remove immunogenic cellular components of the nerve tissue and to preserve the basal lamina and extracellular matrix, morphological analysis was performed through Masson's Trichrome staining, immunofluorescence, high resolution light microscopy and transmission electron microscopy.

Morphological analysis was also used to study the ability of the porcine decellularized graft to support the nerve regeneration. Four weeks after injury, regenerating fibers colonized the graft suggesting a promising use to repair severe nerve lesions.

Keywords: peripheral nerve injuries, orthopaedic trauma, pig, nerve repair, decellularized nerve.

Introduction

Peripheral nerve injuries result in partial or total loss of function with significant consequences in orthopaedic outcomes and impairment in quality of life of affected patients (Lavorato et al. 2023). Even if peripheral nerves retain an intrinsic capability to regenerate spontaneously, this natural process is often unsatisfactory particularly in cases of severe injuries involving significant tissue loss. Therefore, achieving musculoskeletal reinnervation and improving the functional recovery are important medical challenges, with fully effective treatments yet to be established (Thibodeau et al. 2022). To date, the gold standard surgical procedure for nerve injuries with substance loss is the autograft technique. However, this approach has significant drawbacks, including limited graft availability, the necessity of a two-stage surgical process, and potential adverse effects that can lead to morbidity at the donor site (Hoben et al. 2018). In order to improve the outcome of such injuries, many attempts have been made to develop devices that can be used to bridge nerve gap and support nerve regeneration (Fornasari et al. 2020; Wu et al. 2023). Among these, an increasing number of strategies proposes the implantation of "decellularized nerve allografts" characterized by the removal of cellular antigens while maintaining the structure of a native nerve made of extracellular matrix (ECM), basal lamina, and endoneurial tubes. These components promote the regenerative process allowing Schwann cell (SC) proliferation, migration, and axonal elongation (Contreras et al. 2022; Contreras et al. 2023). Furthermore, ECM plays a role as a supportive structure through chemical interaction among SCs by soluble signalling, receptor pathways, and mechanotransduction (Prest et al. 2018; Xu et al. 2020; Urbanski et al. 2016; Armstrong et al. 2007). These evidences highlight the importance of ECM maintenance during nerve regeneration. Over time, numerous protocols have been developed that utilize a mix of chemical and biological agents along with physical methods to create effective decellularized nerve grafts, which can facilitate and ensure nerve regeneration (El Soury et al. 2021; Sondell, Lundborg, and Kanje 1998; Armstrong et al. 2007).

In this study, a novel decellularization protocol currently used to decellularize tendons (Bottagisio et al. 2019) was applied on porcine superficial peroneal nerves to obtain decellularized nerve grafts. The first aim of the present study was to assess the effectiveness of the decellularization procedure applied for the first time on superficial peroneal pig nerves. The secondary goal was to conduct *in vivo* experiments using these decellularized porcine nerve grafts to repair median nerve injuries in rats, to determine the potential of this xenograft model in supporting nerve regeneration.

2- Materials and methods

2.1 Study design

Four superficial peroneal nerves (SPN) were harvested from two 6-months old pigs as waste anatomical tissues from subjects euthanized for an unrelated study (Authorization #771/2020-PR, ID 185D1.6.EXT.0). Each nerve was cut to create nerve segments of 1 cm length and a total of 18 nerve segments were obtained. Nine nerve segments were used as controls, and nine segments underwent the decellularization procedure. Once obtained decellularized grafts, they were divided into two study groups, one for the analysis of the efficacy of the decellularization procedure and the second for the application of the porcine decellularized nerve graft *in vivo* to repair median nerve injuries in rats (Figure 1).

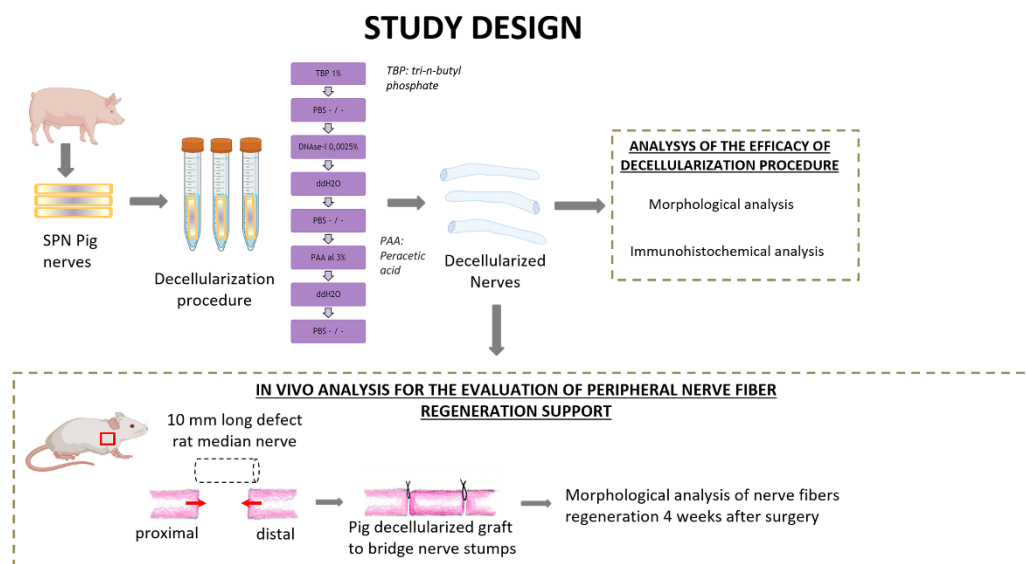


Fig. 1 Schematic representation of experimental design and analysis. Created with [BioRender.com](https://www.biorender.com).

2.2 Decellularization protocol

The decellularization of the nerve segments followed a method outlined for tendons in a previous study (Bottagisio et al. 2019). In summary, nerves were treated with 1% tri-n-butyl phosphate (TBP) in a Tris-HCl buffer, followed by rinsing and storage steps to eliminate detergents. DNase-I and 3% peracetic acid (PAA) treatments were then applied to further process the samples (Figure 1). Subsequent rinses in distilled water and PBS were conducted before their use. Specifically, some samples were fixed in 4% paraformaldehyde for histological analyses, and 2.5% glutaraldehyde for TEM. Samples dedicated to the *in vivo* study were stored at -80°C until use.

2.3 Morphological evaluation of decellularized porcine nerves

To evaluate the effectiveness of the decellularization protocol applied on porcine superficial peroneal nerves, morphological analysis has been carried out comprising Masson's Trichrome staining, immunofluorescence, high resolution light microscopy and Transmission Electron Microscopy (TEM).

2.3.1 Paraffin embedding

Nerve samples were fixed by immediate immersion in 4% paraformaldehyde for 2 h, washed in a solution of 0.2% glycine in 0.1 M phosphate buffer (pH 7.2), and embedded in paraffin. Specimens were cut 10 µm thick using a Leica RM2125 microtome and processed for histological and immunofluorescence analysis.

2.3.2 Masson's trichrome staining

For Masson's trichrome staining, a Masson trichrome with aniline blue kit (Bio-Optica) was used. This method is a three-colour staining that allows to identify collagen (blue), cytoplasm (red) and nuclei (black). As a first step, a mixture of Weigert's iron haematoxylin (solution A+B) were combined together to stain slides. After an incubation with alcoholic picric acid and a wash in distilled water, sections were stained with Ponceau acid fuchsin, and lastly with aniline blue for collagen detection. As a final step, sections were rapidly dehydrated in ethanol, cleared in xylol/Bioclear (Bio-Optica) and mounted in DPX (Fluka).

2.3.3 Immunofluorescence and Confocal Microscopy

Sections were rinsed in PBS, blocked with normal goat serum (1% in PBS–Triton 0.1%) for 1 h and incubated overnight with the primary antibody. After primary antibody(ies) incubation, sections were washed three times in PBS and incubated for 1 h in a solution containing the secondary antibodies: Alexa 488 anti-Mouse, Cy3 anti-Rabbit (Life Technologies) in order to recognize the species of primary antibodies. After three washes in PBS, sections were mounted with a Dako fluorescence mounting medium and stored at 4 °C before being analyzed. The sections were incubated in a solution containing the following primary antibodies: anti-PAN-NF (monoclonal, mouse, Sigma Aldrich), anti S-100 (polyclonal, rabbit, Sigma Aldrich), anti-peripherin (polyclonal rabbit, Sigma Aldrich). Nuclei were stained with 4,6-diamidino-2-phenylindole (DAPI, Sigma) diluted 1:1000 in PBS. Finally, sections were mounted with a Dako fluorescence mounting medium. Images were acquired using a Zeiss LSM800 confocal laser microscopy system (Zeiss, Jena, Germany).

2.3.4 Resin embedding, High resolution light microscopy and Transmission electron microscopy (TEM)

Native and decellularized superficial peroneal nerves were fixed by immediate immersion in 2.5% glutaraldehyde (SIC, Società Italiana Chimici) in 0.1 M phosphate buffer (pH 7.4) for 5–6 h, at 4 °C. Samples were then post-fixed in 2% osmium tetroxide (SIC, Società Italiana Chimici) for 2 h and dehydrated in passages in ethanol (Sigma Aldrich) from 30% to 100% (5 minutes of each passage). After two 7 min passages in propylene oxide and overnight in a 1:1 mixture of propylene oxide (Sigma Aldrich) and Glauerts' mixture of resins, the samples were embedded in Glauerts' mixture of resins (made of equal parts of Araldite M and Araldite Harter, HY 964, Sigma Aldrich). Into the resin mixture, 0.5% of the plasticizer dibutyl phthalate (Sigma Aldrich) was added. For the final step, 2% of accelerator 964 was added to the resin in order to promote the polymerization of the embedding mixture, at 60 °C. Semi-thin sections (2.5 µm thick) were cut using an Ultracut UCT ultramicrotome (Leica Microsystems, Wetzlar, Germany) and stained with 1% toluidine blue and 2% borate in distilled water for high resolution light microscopy. A DM4000B microscope equipped with a DFC320 digital camera was used for high resolution light microscopy.

For transmission electron microscopy analysis (TEM), ultrathin (70 nm thick) sections were obtained with the same ultramicrotome, stained with a solution of 4% UAR-EMS uranyl acetate replacement in distilled water, and analysed using a JEM-1010 transmission electron microscope (JEOL, Tokyo, Japan) equipped with a Megaview-III digital camera and a Soft-Imaging-System (SIS, Münster, Germany) for the computerised acquisition of the images.

2.4 In vivo study

To study the ability of porcine decellularized nerves graft to support peripheral nerve regeneration, decellularized nerves graft were implanted and used to repair median nerve injuries with substance loss in rats.

2.4.1 Ethic statement

A total of 3 adult Wistar rats weighing approximately 230–250 g (Charles River Laboratories, Milan, Italy) were used for this study. Animals were housed in large cages at the animal facility of Neuroscience Institute Cavalieri Ottolenghi (NICO; Ministerial authorization DM 182 2010-A 3–11-2010) in a humidity and temperature-controlled room with 12 h light/dark cycles. Free access to water and standard chow was provided. Human endpoint criteria were adopted to adequately measure and minimise any animal pain, discomfort, or distress. The study conditions conformed to the guidelines of the European Union's Directive EU/2010/63. In addition, approval by the Ethic Experimental Committee of the University of Turin (Ministry of Health project number 692/2020) was obtained before the research began.

2.4.2 Surgical procedure

Surgeries were performed under general anaesthesia, with ketamine hydrochloride (2.5 mg/kg) and xylazine (50mg/kg) by intraperitoneal injection. All surgical procedures were carried out under a high magnification surgical microscope. Nerve lesion was performed on median nerves. The median nerve of both forelimbs was severed and a nerve segment of 10 mm was removed and repaired with decellularized superficial peroneal nerve. The nerve graft was sutured with 9/0 epineural stitch at each end (Figures 2A–B). After 4 weeks, rats were euthanized through anaesthetic overdose of ketamine and xylazine by intraperitoneal injection. The surgical site was exposed, regenerated nerve samples were harvested and processed for morphological evaluation of nerve regeneration.



Fig. 2. Surgical procedure: median nerve resection (10 mm gap) (A); repair with porcine decellularized superficial peroneal nerve graft (B); regenerated nerve harvested 4 weeks after implantation (C).

2.4.3 Resin embedding, high resolution light microscopy and TEM

Regenerated nerves were processed for resin embedding, high resolution light microscopy and TEM according to the aforementioned procedures (see paragraph 2.3.4). Particularly for the *in vivo* study, in order to understand if regenerated fibers reached the end of the graft, only the distal portions of the sample were cut and analysed by high resolution light microscopy and TEM.

2.4.4 Histological procedures

Samples were processed for paraffin embedding as previously described (see paragraph 2.3.1), transversal cross sections (10 μ m thickness) of the whole nerve were obtained starting from the distal portion until the proximal, in order to evaluate the course of the regenerated fibers on the whole sample.

2.4.5 Immunofluorescence

In order to identify the presence of regenerated nerve fibers and ECM components, immunofluorescence analysis was performed on the proximal, middle and distal portions of

regenerated nerves. For this purpose, sections were dewaxed, rinsed in PBS, blocked with normal goat serum (1% in PBS–Triton 0.1%) for 1 h and incubated overnight with primary antibodies. After primary incubation, the sections were washed three times in PBS and incubated for 1 h in a solution containing the secondary antibodies: Alexa 488 anti-Mouse, Cy3 anti-Rabbit (Life Technologies) in order to recognize the species of primary antibodies. After three washes in PBS, sections were mounted with a Dako fluorescence mounting medium and stored at 4 °C before being analysed. The sections were incubated in a solution containing the following primary antibodies: anti-PAN-NF (monoclonal, mouse, Sigma Aldrich), anti S-100 (polyclonal, rabbit, Sigma Aldrich), anti-laminin (polyclonal rabbit, Sigma Aldrich). Nuclei were stained with 4,6-diamidino-2-phenylindole (DAPI, Sigma) diluted 1:1000 in PBS. Finally, sections were mounted with a Dako fluorescence mounting medium. Images were acquired using a Zeiss LSM800 confocal laser microscopy system (Zeiss, Jena, Germany).

3. Results

The first aim of the present study was to test the efficacy of the decellularization method currently used to decellularize horse tendons in order to evaluate its possible application as a nerve graft. The procedure effectiveness was assessed by determining if immunogenic nuclear and cellular components of the nerve tissue were removed, and whether the ECM was preserved.

The second aim was to evaluate the ability of the porcine decellularized nerve graft to support nerve regeneration after injury using it to repair median nerve lesions in rats.

3.1 Evaluation of overall nerve morphology and connective tissue structure after decellularization protocol.

In order to evaluate the overall morphology and connective tissue structure of porcine decellularized superficial peroneal nerve, Masson's Trichrome staining was performed on decellularized and native nerves.

Transversal cross sections of superficial peroneal nerves displayed the typical histological organization of a healthy nerve characterized by many nerve fascicles, each surrounded by perineurium, and adipose tissue between fascicles, held together by epineurium, the outermost layer of connective tissue (Fig. 3A-B).

High resolution light microscopy on semi- thin cross sections stained with Toluidine Blue, highlights the morphology of nerve fibers within nerve fascicles. Moreover, adipose tissue is well detectable (Fig. 3C). Ultrastructural analysis, performed using TEM, allows to identify the presence of

unmyelinated and myelinated fibers (Fig. 3D); at higher magnifications, an axon surrounded by a Schwann cell to form myelin sheath with lamellae spirally arranged is detectable (Fig. 3E).

In decellularized nerves, Masson's Trichrome staining allowed to verify that the outer epineurium was still present as well as the perineurium that surrounded each fascicle (Fig. 3F). The amount of adipose tissue decreased. At higher magnifications (Fig. 3G), nerve fibers were barely detectable compared with native nerves.

To further evaluate the effectiveness of the decellularization protocol on porcine superficial peroneal nerves, high resolution light microscopy and TEM analyses were performed (Fig. 3H-O): native nerve displayed axons surrounded by myelin sheath, adipose tissue and blood vessels (Fig. 3C), in decellularized nerve myelin sheath is not clearly identifiable, however the presence of connective tissue around nerve fascicles was still present (Fig. 3H) Ultrastructural analysis displayed empty space and scattered myelin around degenerating axons (Fig. 3I-J, asterisks), collapsed axons with enlarged disintegrated myelin sheath were detectable (Fig. 3K-M, red arrows). At the same time, a well-preserved collagen made of collagen fibrils was clearly visible (Fig. 3N-O, black arrows).

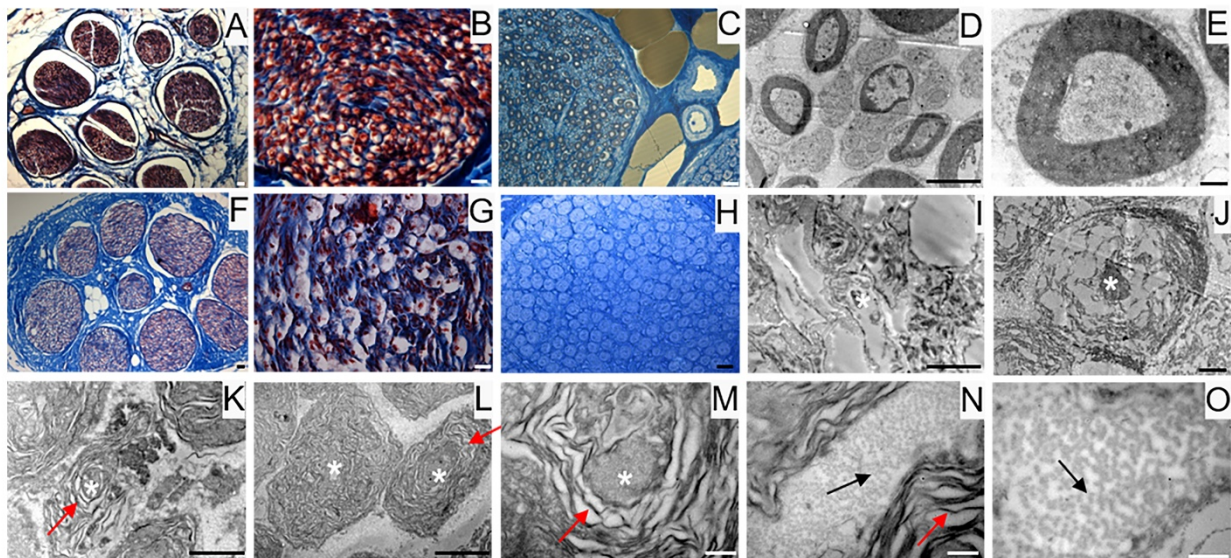


Fig. 3: Masson's Trichrome Staining (A-B, F-G), High resolution light microscopy (C, H) and Transmission electron microscopy (D, E, I-O) performed on native (A-E) and decellularized (F-O) porcine superficial peroneal nerves. Scale bar A, B, C, F, G, H= 20 μm ; D, I = 10 μm ; E, J = 0,2 μm ; K= 2 μm , L= 1 μm ; M-O= 0,5 μm . Asterisk marks degenerating axons; red arrows mark enlarged lamellae; black arrows mark collagen fibrils.

3.2 Evaluation of axonal and glial components after the decellularization protocol

In order to detect immunogenic components such as axonal filaments, nuclei and myelin, specific axonal, glial and nuclear markers were tested in native and decellularized porcine nerves.

For glial components an immunostaining with S100 was performed and DAPI as nuclear staining. Native porcine nerves showed the normal morphology in which Schwann cells form myelin sheath around axons; many nuclei were clearly visible in blue (DAPI) (Fig. 4A-B). In decellularized nerves, no immunostaining was found for S100 and DAPI (Fig. 4C-D).

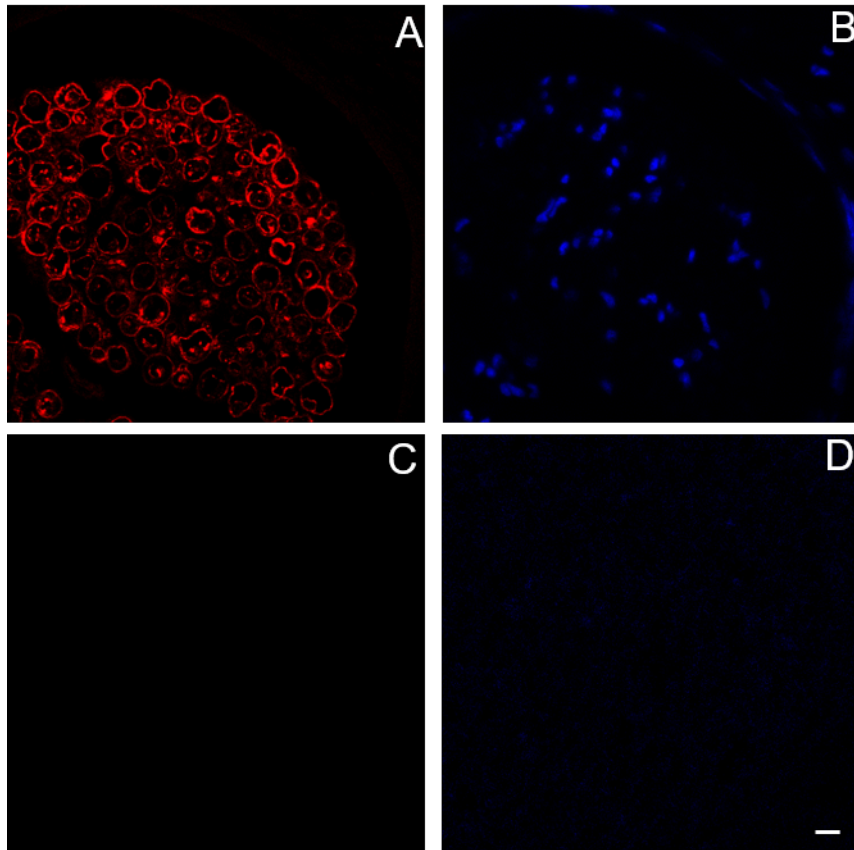


Fig. 4: Immunofluorescence analysis to detect glial cells (S100 in red -A and C) and nuclei (DAPI in Blue – B and D) in native (A-B) and decellularized porcine nerves (C-D). Scale bar= 20 μ m

To investigate the presence of axonal components, anti-neurofilament -a typical protein expressed by axons - and peripherin -a type III intermediate protein expressed by unmyelinated fibers - were used in a double immunostaining either on native (Fig. 5A-D) and decellularized nerves (Fig. 5E-H). Results revealed the presence of a few axons immunopositive for peripherin (red) and neurofilament (green) in decellularized nerve demonstrating a low presence of this axonal proteins. In native nerves, the same staining showed the presence of axonal neurofilament and peripherin according to the expected morphology.

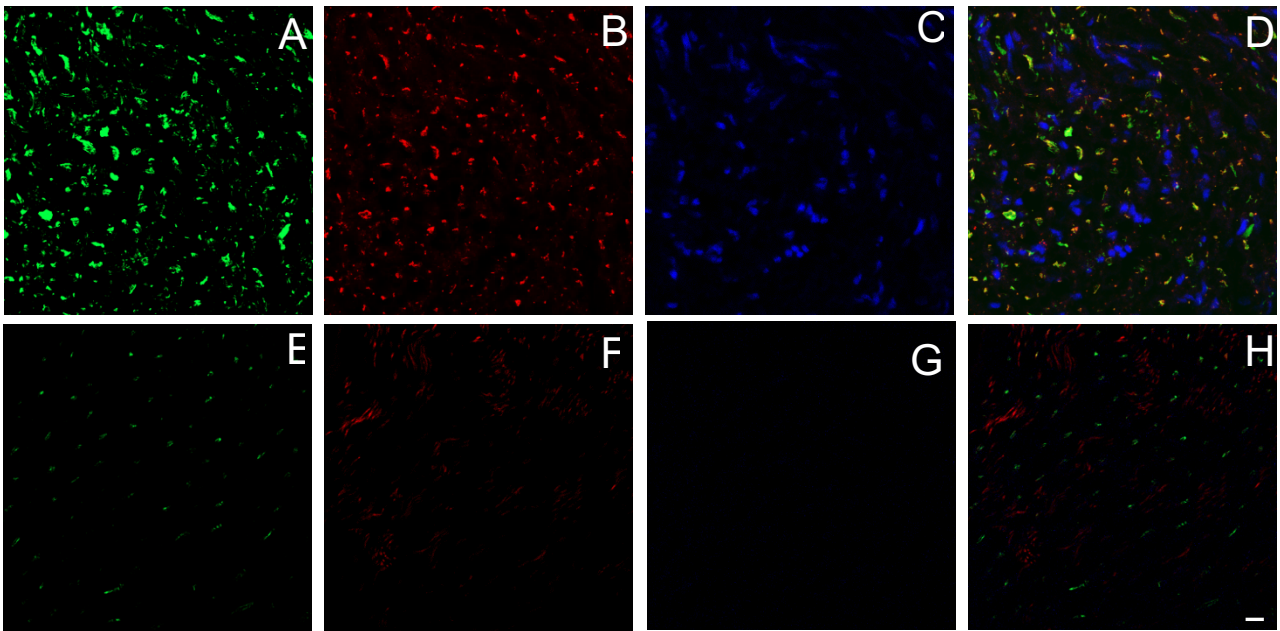


Fig. 5: Immunofluorescence analysis to detect axonal components and nuclei in native (A-D) and decellularized nerves (E-H). Green: neurofilament (A, E); red: peripherin (B, F); DAPI: blue (C, G); Merged (D, H). Scale bar= 20 μ m

3.4 Morphological assessment of nerve regeneration along the decellularized nerve graft

Rat median nerves repaired with decellularized porcine superficial peroneal nerve graft were harvested four weeks after implantation to investigate the ability of the decellularized graft to support nerve regeneration.

In order to study the morphological pathway of regenerated fibers, three different portions of the regenerated graft were analysed: proximal, middle and distal.

Masson's trichrome staining was employed to assess the overall structure of the regenerated nerve at different portions, showing the morphology of the connective tissue surrounding nerve fascicles and the presence of red staining within the regenerated nerve (Fig. 6A-D-G).

In the proximal portion (Fig. 6A), decellularized fascicles were not detectable compared with the other portions (Fig. 6D, G). At higher magnifications, regenerated fascicles were clearly visible together with a large regenerated red zone detectable by Masson's Trichrome staining (Fig. 6B).

In order to identify the presence of newly regenerated nerve fibers, immunofluorescence analysis using axonal (Neurofilament) and glial markers (S100) allowed to clearly detect axons and Schwann cells at the proximal portion (Fig. 6C). Results clearly showed the typical morphology of a regenerated nerve fully colonized by new nerve fibers immunopositive for S100 and Neurofilament (Fig. 6C).

Shifting toward the centre of the regenerated graft, decellularized fascicles became visible (Fig. 6D) and colonized by regenerated nerve fibers identifiable either within porcine fascicles or among them (Fig. 6E). Immunostaining confirmed the presence of regenerated fibers (Fig. 6F).

Considering the distal portion (Fig. 6G-I), the presence of large nerve fascicles was identified, corresponding to the decellularized porcine nerve, characterised by weak red staining (Fig. 6G). Interestingly among these, many regenerated axons were detectable by an intense red staining and surrounded by connective tissue (Fig. 6H). The immunofluorescence analysis reported in Fig. 6I demonstrated that regenerated fibers, stained with neurofilaments and glial markers, reached the distal portion of the graft.

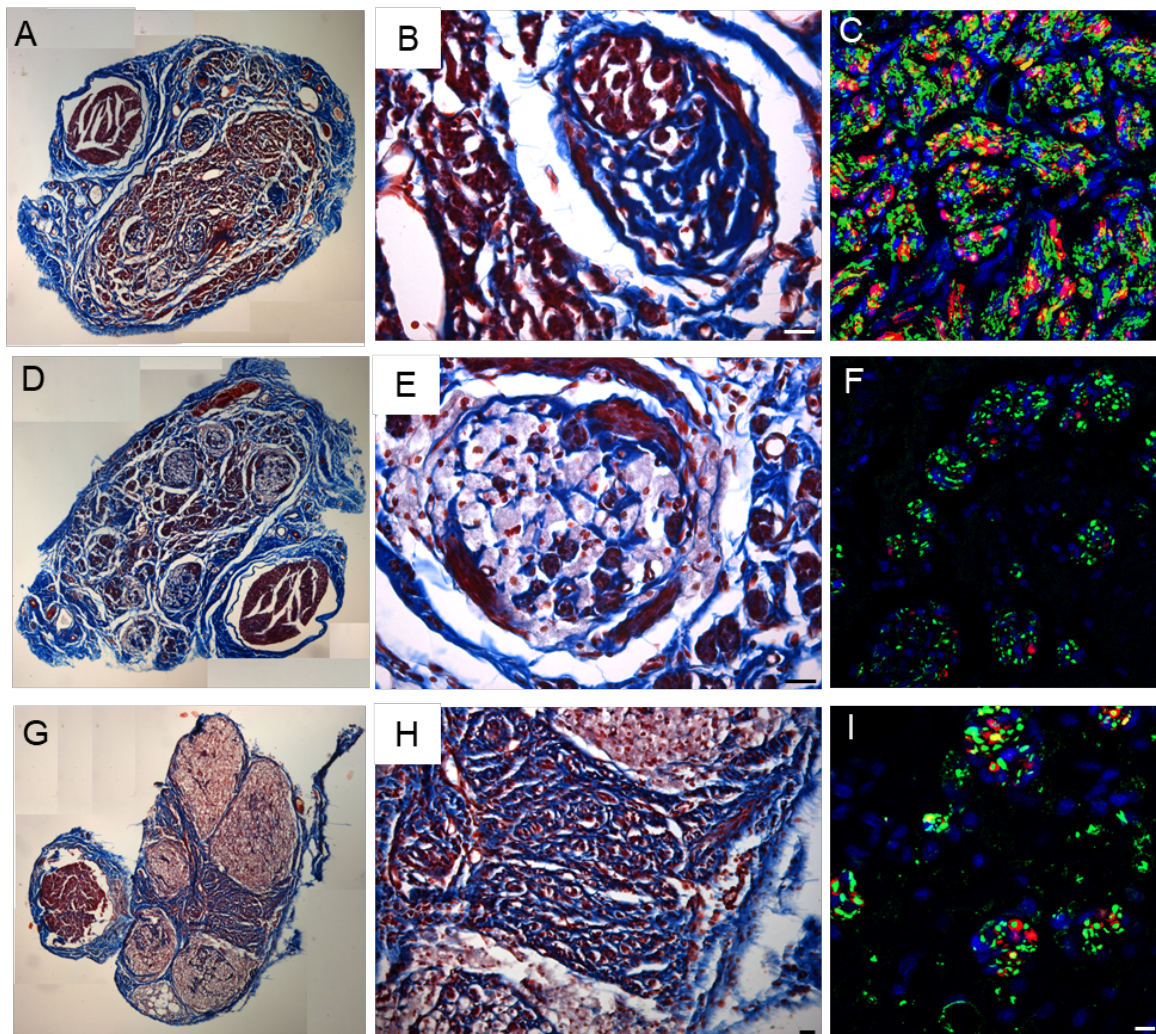


Fig. 6: Masson's Trichrome Staining (A, B, D, E, G, H) and IHC for Neurofilament (Green) and S100 (red), DAPI in Blue (C, F, I) performed to identify the presence of regenerated fibers on proximal (A-C), middle (D-F) and distal (G-I) level. Scale bar= 20 μ m

3.5 Ultrastructural analysis of regenerated nerve

High resolution light microscopy on transversal cross-section of rat median nerve repaired with decellularized superficial peroneal nerve graft revealed the presence of cells, nuclei and blood vessels at distal portions 4 weeks after implant (Fig. 7A-C). Interestingly, a well-defined bundle of nerve fibers surrounded by connective tissue was clearly evident within the regenerated nerve (Fig. 7C). To further improve the morphological evaluation of the regenerated nerve, TEM analysis enabled the study of its ultrastructural features characterised by both myelinated and unmyelinated fibers (Fig. 7 D-F).

Myelinated fibers were also randomly detectable within the nerve (Fig. 7G), and an enveloping Schwann cell during the early phase of axonal myelination (Fig. 7I-J, red arrows). Finally, ultrastructural features of packed lamellae made of Schwann cells membrane were easily detectable (Fig. 7K, blue arrow) together with blood vessels with erythrocytes (Fig. 7L, asterisk).

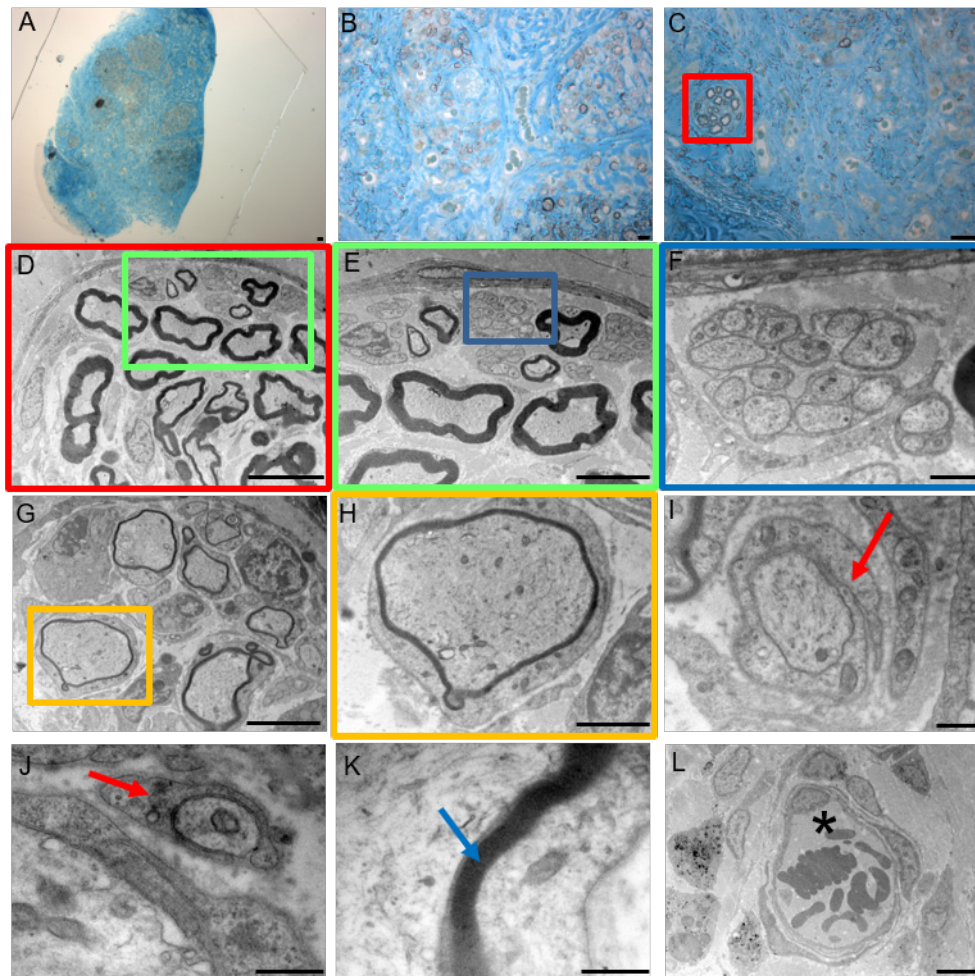


Fig. 7: High resolution light microscopy (A-C) and Transmission Electron microscopy (D-L) at distal portion of the regenerated nerve 4 weeks after surgery. Scale bar: A-C= 20 μm ; D= 10 μm ; E-G= 5 μm ; F= 1 μm ; H= 2 μm ; I-J-K-L= 0,5 μm . Red arrows mark enveloping Schwann cells; blue arrow marks myelin; asterisk marks a blood vessel.

3.6 Evaluation of extracellular matrix preservation

Because ECM (extracellular matrix) molecules play a crucial role in creating a specific and supportive physical and chemical environment for cell survival, as well as for the proliferation and migration of Schwann Cells during nerve regeneration, the study focused on preserved laminin. (Armstrong et al. 2007; de Luca et al. 2014), Indeed, laminin is a significant substrate not only for Schwann cell functions but also for the axonal elongation.

Immunolabeling for anti-laminin in the decellularized porcine superficial peroneal nerve indicated the preservation of this crucial ECM component post-decellularization (Fig. 8A). Similarly, in the rat median nerve repaired with the decellularized graft, a comparable immunopositivity was observed. This was evident in the proximal (Fig. 8B), middle (Fig. 8C), and distal (Fig. 8D) portions of the regenerated nerve, where many neurofilament-positive axons (green) were seen within endoneurial tubes that also showed positive immunoreactivity for laminin.

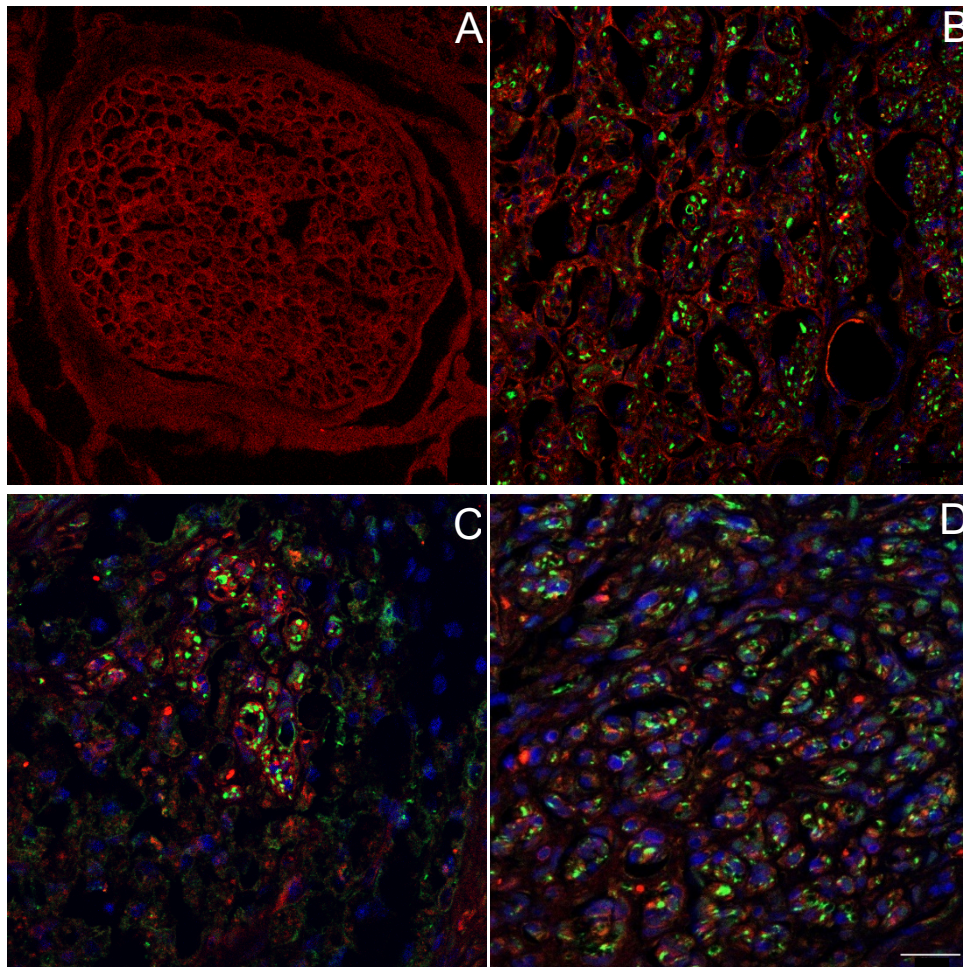


Fig. 8: The immunoreactivity for laminin in decellularized porcine nerve (A) and in proximal (B), middle (C), distal (D) portion of the regenerated nerve displaying the preservation of the ECM (red) colonized by regenerating axons (green) and cellular nuclei (DAPI). Scale bar=20 μ m

DISCUSSION

In the field of tissue engineering, the development of decellularized nerve grafts is a topic of ongoing research. These grafts are being explored as potential alternatives to the traditional autograft technique, especially for repairing nerve injuries with longer gaps (over 3 cm). Studies involve assessing the regenerative potential of various decellularization protocols on animal models to understand their effectiveness in nerve regeneration. This research is crucial for advancing the treatment of severe nerve injuries where traditional methods may not be sufficient (Garcia-Garcia et al. 2023). Decellularized nerve grafts should provide a suitable substrate for nerve regeneration in which the conservation of ECM components plays a crucial role for peripheral nerve regeneration and axonal guidance (Mahdian et al. 2023; Hsu et al. 2023). The currently available decellularized methods are time and effort consuming (El Soury et al. 2021). Consequently, there is an ongoing effort to develop and propose new decellularization procedures and strategies. In this study, a novel decellularization method already used to obtain decellularized tendons (Bottagisio et al. 2019) was applied for the first time on porcine nerves in order to study its effectiveness to create a valid decellularized nerve graft able to support nerve regeneration in case of injury with substance loss in rats. Since nerves and tendons share common features, such as scarcely tissue permeability (El Soury et al. 2021), it was hypothesized that the use of this decellularization protocol in nerves could efficiently produce biocompatible and well-structured decellularized nerve grafts. The study successfully demonstrated that the decellularization method used for horse tendons can be effective in preparing porcine superficial peroneal nerves for grafting. This indicates a potential application in nerve grafts, as evidenced by the removal of immunogenic components and preservation of the ECM. Detailed morphological assessments through various staining and microscopy techniques revealed significant insights into the structural integrity and changes post-decellularization. The preservation of key nerve structures alongside some level of degradation points to areas for further optimization. Morphological analysis performed on decellularized porcine nerves showed that glial components have been successfully removed together with nuclei. The absence of immunogenic and glial markers in decellularized nerves indicates successful decellularization. This is a crucial factor in preventing host immune response post-transplantation. Masson's trichrome staining highlighted the preservation of the overall connective tissue structure made of epineurium that surround the whole nerve, perineurium surrounding nerve fascicles and endoneurium surrounding individual nerve fibres. Ultrastructural analysis performed by TEM confirmed the conservation of collagen fibrils within the decellularized graft.

The second aim of this study was to evaluate the ability of the decellularized nerve graft to support nerve regeneration *in vivo* using a xenograft model in which a decellularized porcine nerve was used

to repair a median nerve injury in rats. The use of decellularized porcine nerve grafts in rat median nerve injury models showed promising results. Despite the limitation of this study is related to the number of rats employed, it represents an initial proof of concept of the efficacy of decellularized xenografts in nerve repair. Indeed, the study observed nerve regeneration, suggesting that these grafts can effectively support nerve repair processes. Masson's Trichrome staining allowed to identify the organisation of regenerated nerve fibers and connective tissue conditions in regenerated nerve showing a substantial presence of nerve fibers starting from the proximal toward the distal portion of the nerve. In order to demonstrate the presence of such regenerated fibers, immunofluorescence analysis allowed the detection of axons, SC forming myelin and nuclei at the proximal, middle and distal portions. Particularly, according to the regenerative time (4 weeks of follow-up), TEM revealed the presence of many unmyelinated fibers, enveloping SC forming myelin sheath and myelinated fibers at the distal portion. Finally, the preservation of laminin in porcine nerve graft after decellularization and in regenerated median nerve of rats strengthened the specificity of the protocol to preserve ECM components that play a key role for SC proliferation, migration and axonal elongation (Armstrong et al. 2007). The preservation of ECM components like laminin, essential for nerve regeneration, underscores the potential of this decellularized graft in clinical applications. This is further supported by the successful colonization and regeneration of nerve fibers in the graft. Taken together the results achieved in this study demonstrated either the effectiveness of the decellularization protocol in removing the native nerve components, or its supporting role as nerve graft to promote axonal elongation and fibre regeneration.

The translational value of this study lies in the use of a xenograft model, a technique that involves transplanting tissue from one species to another. This approach holds significant promise in the field of regenerative medicine for replacing damaged tissues, highlighting its potential impact and utility. A previous study (Hopf et al. 2022) successfully investigated a new method to decellularize large-diameter porcine nerves combining a mild chemical disruption of cellular components with enzymatic degradation: a large acellular nerve scaffold was obtained with a preserved ECM structure, supporting the possible application of porcine nerve graft in the clinical context of nerve repair.

Indeed, actually, many porcine tissues are efficiently transplanted in human, i.e. porcine dermis used as a graft to support the repair of large skin loss after burned condition (Haller et al. 2021), or decellularized porcine heart valve scaffolds successfully implanted for heart valve tissue engineering (Leyh et al. 2003).

In conclusion, the study presents significant advancements in the field of nerve repair, especially regarding the use of decellularized grafts. While promising, these findings also highlight the need for continued research to refine these methods for clinical applications. The study sets a foundation for

future investigations into optimizing decellularization protocols and assessing long-term outcomes in nerve regeneration.

References:

- Armstrong, S. J., M. Wiberg, G. Terenghi, and P. J. Kingham. 2007. 'ECM molecules mediate both Schwann cell proliferation and activation to enhance neurite outgrowth', *Tissue Eng*, 13: 2863-70.
- Bottagisio, M., D. D'Arrigo, G. Talo, M. Bongio, M. Ferroni, F. Boschetti, M. Moretti, and A. B. Lovati. 2019. 'Achilles Tendon Repair by Decellularized and Engineered Xenografts in a Rabbit Model', *Stem Cells Int*, 2019: 5267479.
- Contreras, E., S. Bolivar, N. Nieto-Nicolau, O. Farinas, P. Lopez-Chicon, X. Navarro, and E. Udina. 2022. 'A novel decellularized nerve graft for repairing peripheral nerve long gap injury in the rat', *Cell Tissue Res*, 390: 355-66.
- Contreras, E., S. Traserra, S. Bolivar, N. Nieto-Nicolau, J. Jaramillo, J. Fores, E. Jose-Cunilleras, X. Moll, F. Garcia, I. Delgado-Martinez, O. Farinas, P. Lopez-Chicon, A. Vilarrodona, E. Udina, and X. Navarro. 2023. 'Decellularized Graft for Repairing Severe Peripheral Nerve Injuries in Sheep', *Neurosurgery*, 93: 1296-304.
- de Luca, A. C., S. P. Lacour, W. Raffoul, and P. G. di Summa. 2014. 'Extracellular matrix components in peripheral nerve repair: how to affect neural cellular response and nerve regeneration?', *Neural Regen Res*, 9: 1943-8.
- El Soury, M., O. D. Garcia-Garcia, M. Moretti, I. Perroteau, S. Raimondo, A. B. Lovati, and V. Carriel. 2021. 'Comparison of Decellularization Protocols to Generate Peripheral Nerve Grafts: A Study on Rat Sciatic Nerves', *Int J Mol Sci*, 22.
- Fornasari, B. E., G. Carta, G. Gambarotta, and S. Raimondo. 2020. 'Natural-Based Biomaterials for Peripheral Nerve Injury Repair', *Front Bioeng Biotechnol*, 8: 554257.
- Garcia-Garcia, O. D., M. El Soury, F. Campos, D. Sanchez-Porras, S. Geuna, M. Alaminos, G. Gambarotta, J. Chato-Astrain, S. Raimondo, and V. Carriel. 2023. 'Comprehensive ex vivo and in vivo preclinical evaluation of novel chemo enzymatic decellularized peripheral nerve allografts', *Front Bioeng Biotechnol*, 11: 1162684.
- Haller, H. L., S. E. Blome-Eberwein, L. K. Branski, J. S. Carson, R. E. Crombie, W. L. Hickerson, L. P. Kamolz, B. T. King, S. P. Nischwitz, D. Popp, J. W. Shupp, and S. E. Wolf. 2021. 'Porcine Xenograft and Epidermal Fully Synthetic Skin Substitutes in the Treatment of Partial-Thickness Burns: A Literature Review', *Medicina (Kaunas)*, 57.
- Hoben, G. M., X. Ee, L. Schellhardt, Y. Yan, D. A. Hunter, A. M. Moore, A. K. Snyder-Warwick, S. Stewart, S. E. Mackinnon, and M. D. Wood. 2018. 'Increasing Nerve Autograft Length Increases Senescence and Reduces Regeneration', *Plast Reconstr Surg*, 142: 952-61.
- Hopf, A., L. Al-Bayati, D. J. Schaefer, D. F. Kalbermatten, R. Guzman, and S. Madduri. 2022. 'Optimized Decellularization Protocol for Large Peripheral Nerve Segments: Towards Personalized Nerve Bioengineering', *Bioengineering (Basel)*, 9.
- Hsu, M. W., S. H. Chen, W. L. Tseng, K. S. Hung, T. C. Chung, S. C. Lin, J. Koo, and Y. Y. Hsueh. 2023. 'Physical processing for decellularized nerve xenograft in peripheral nerve regeneration', *Front Bioeng Biotechnol*, 11: 1217067.
- Lavorato, A., G. Aruta, R. De Marco, P. Zeppa, P. Titolo, M. R. Colonna, M. Galeano, A. L. Costa, F. Vincitorio, D. Garbossa, and B. Battiston. 2023. 'Traumatic peripheral nerve injuries: a classification proposal', *J Orthop Traumatol*, 24: 20.
- Leyh, R. G., M. Wilhelmi, T. Walles, K. Kallenbach, P. Rebe, A. Oberbeck, T. Herden, A. Haverich, and H. Mertsching. 2003. 'Acellularized porcine heart valve scaffolds for heart valve tissue engineering and the risk of cross-species transmission of porcine endogenous retrovirus', *J Thorac Cardiovasc Surg*, 126: 1000-4.
- Mahdian, M., T. S. Tabatabai, Z. Abpeikar, L. Rezakhani, and M. Khazaei. 2023. 'Nerve regeneration using decellularized tissues: challenges and opportunities', *Front Neurosci*, 17: 1295563.
- Prest, T. A., E. Yeager, S. T. LoPresti, E. Zygelyte, M. J. Martin, L. Dong, A. Gibson, O. O. Olutoye, B. N. Brown, and J. Cheetham. 2018. 'Nerve-specific, xenogeneic extracellular matrix hydrogel promotes recovery following peripheral nerve injury', *J Biomed Mater Res A*, 106: 450-59.
- Sondell, M., G. Lundborg, and M. Kanje. 1998. 'Regeneration of the rat sciatic nerve into allografts made acellular through chemical extraction', *Brain Res*, 795: 44-54.

- Thibodeau, A., T. Galbraith, C. M. Fauvel, H. T. Khuong, and F. Berthod. 2022. 'Repair of peripheral nerve injuries using a prevascularized cell-based tissue-engineered nerve conduit', *Biomaterials*, 280: 121269.
- Urbanski, M. M., L. Kingsbury, D. Moussouros, I. Kassim, S. Mehjabeen, N. Paknejad, and C. V. Melendez-Vasquez. 2016. 'Myelinating glia differentiation is regulated by extracellular matrix elasticity', *Sci Rep*, 6: 33751.
- Wu, S., W. Shen, X. Ge, F. Ao, Y. Zheng, Y. Wang, X. Jia, Y. Mao, and Y. Luo. 2023. 'Advances in Large Gap Peripheral Nerve Injury Repair and Regeneration with Bridging Nerve Guidance Conduits', *Macromol Biosci*, 23: e2300078.
- Xu, Z., J. A. Orkwis, B. M. DeVine, and G. M. Harris. 2020. 'Extracellular matrix cues modulate Schwann cell morphology, proliferation, and protein expression', *J Tissue Eng Regen Med*, 14: 229-42.

3.3 Somatic to autonomic nerve transfer: review of the literature and future perspectives.

Crosio A, Fregnan F, Muratori L, Falcone F, Tos P, Raimondo S, Ciclamini D.

Under submission

SOMATIC TO AUTONOMIC NERVE TRANSFER: REVIEW OF THE LITERATURE AND FUTURE PERSPECTIVES

Alessandro Crosio^{1,2*}, Federica Fregnan², Luisa Muratori², Marco Falcone³, Pierluigi Tos⁴, Stefania Raimondo², Davide Ciclamini¹

¹*Orthopedics and Traumatology 2 - Hand Surgery and Reconstructive Microsurgery, AOU Città della Salute e della Scienza, CTO Hospital, Torino, Italy.*

²*Department of Clinical and Biological Sciences, Neuroscience Institute Cavalieri Ottolenghi (NICO), University of Turin, Turin, Italy;*

³*Urology Department, AOU Città della Salute e della Scienza, CTO Hospital, Torino, Italy.*

⁴*Reconstructive Microsurgery and Hand surgery Unit, ASST Pini-CTO Milano, Italy;*

*Corresponding author

Abstract

Nerve transfer is a technique widely used in muscle reanimation under certain conditions. It required a sacrifice of healthy nerve or part of it. In the last 20 years attempts of nerve transfer in autonomic driven functions have been performed with variable results. Whereas in somatic nerve a lot of informations are known about the mechanics of nerve regeneration, function gaining and neural plasticity, few and fragmentary informations are available in literature regarding somatic-to-autonomic (StA) nerve transfer.

An extensive query has been performed through PubMed. The identified papers have been screened by title and abstract, those who passed the screening process was then analyzed. 266 papers were identified, 15 passed the screening process. Papers were divided in clinical and pre-clinical. Bladder dysfunction, bowel dysfunction and erectile dysfunction were the topics treated. Bladder and bowel dysfunctions were consequence of spinal cord injury (SCI) or medullary pathologies as spina bifida (SB) or myelomeningocele. ED was secondary to cavernous plexus or nerve injury in pelvic area.

The treatment was performed by L5-S1 to S2-S3 ventral roots (VR) transfer for BD and AD.

The aim of this review is to identify the StA transfers described in literature, focusing the attention on what is known about the effect of somatic nerve on autonomic driven organ and summarize the actual application of this procedure in humans.

Keywords: nerve transfer, autonomic nerve system, erectile dysfunction, bladder dysfunction

Introduction:

Autonomic system disorders following denervation due to trauma correlated to spinal cord injury, dysmorphism of the spinal cord, or secondary to iatrogenic injury in the pelvic area are debilitating events for affected patients. The consequences related to uro-genital or bowel system dysfunction can lead to devastating complications and however forced patients to continuous self-catheterization and bowel self-evacuation. In case of iatrogenic or post traumatic erectile dysfunction (ED) the clinical consequences are definitely not life threatening, but can affect seriously the patients' quality of life.

Different strategies have been attempted among years to restore these essential functions, in the last 20 years some authors proposed and investigated the efficacy of autonomic reinnervation using somatic donor nerve, in which an intact somatic nerve is selected for coaptation to the distal stump of the injured autonomic nerve. In this case, to connect the two stumps, an end-to-end (EtoE) or end-to-side (EtoS) technique can be applied. This procedure is classified as nerve transfer (NT). It is a widespread procedure actually used in the treatment of brachial plexus and peripheral nerve injuries (Chuang 2005, Doi 2018). To gain a success, some principles have to be respected, as performing the NT into a time limit from injury and suturing the donor nerve as close as possible to the target.

In treatment of bladder and bowel dysfunction following a SCI (spinal cord injury), root transfer was firstly proposed by Xiao (Xiao 1994, Xiao 1999) in the late 90's. Through root transfer the authors proposed a new spinal reflex supposed to be able to induce bladder emptying in response to skin stimulation of the corresponding dermatome. To this, many papers succeeded with contrasting results both in animal model and clinical trials.

NT was tempted also in treatment of ED. One paper described the root transfer procedure in an animal models, but most of the authors tried to solve the problem caused by surgeons during radical prostatectomy (RP) in which frequently iatrogenic damage to the periprostatic neurovascular bundles (NVBs) occurs (Dangerfield 2023). Before NT was attempted, two authors demonstrated the inefficacy of cavernous nerve reconstruction after RP (Davis 2009) either monolateral or bilateral (Kung 2015). Moreover, preclinical

researches also failed to restore erectile function through nerve graft (Bessede 2014). In this field, other authors proposed and obtained promising results using Chitosan membrane (CS-Me) to promote nerve regeneration after RP. Otherwise no evidences of clear nerve regeneration were obtained (Tuite 2018). So that, some authors performed a real NT to reinnervate directly corpora cavernosa bypassing the NVBs (Souza – Trindade 2017). This solution is giving the most encouraging and promising results in ED recovery. Despite the potentiality of nerve transfer in autonomic system reanimation, few notions are known about the biomolecular aspects that drive the autonomic system reinnervation through somatic motor axons.

In this paper we would like to review the existing literature who described a somatic to autonomic nerve transfer, gathering what is known about the process, analyzing the methods used in animal models to investigate the recovery and proposed further research to clarify this fascinating novel approach.

Methods:

An extensive literature review was performed on Medline with the following search phrase “somatic to autonomic and erectile dysfunction or bladder dysfunction or anorectal dysfunction or bowel dysfunction”. Only time filter was applied, limiting the research to the last 20 years. The found papers have been screened by title and abstract. The selected works were then divided in animal research and clinical research. For pre-clinical papers type of nerve transfer, type of suture (EtE or EtS), number of animals, timepoint for recovery evaluation, outcomes measures, results obtained were resumed and compared. In clinical research papers other than the type of nerve transfer and the type of suture, also time intercurrent between the injury and nerve transfer were analyzed as well as time of follow up and outcome measures.

Results:

The retrieving process resulted in 261 papers. The screening process by title and abstract ended in 17 papers that were included in final reviewing. In table 1 and table 2 the papers finally included in the review were summarized.

Author	Year	Topic	Technique	Transfer	Animal
Dong	2016	Erectile Dysfunction	EtS	L6VR to L4VR (donor)	36 Rats
Sun	2010	Anorectal dysfunction	EtE	L4VR to L6 VR	16 rats
Dong	2012	Anorectal dysfunction	EtS	L6VR to L4VR (donor)	40 rats
Wang	2007	Bladder dysfunction	EtE	L4VR to L6 VR	15 rats
Ruggieri	2008	Bladder dysfunction	EtE	GF nerve to PN (denervation through S1S2VR section)	13 dogs
Ruggieri	2008	Bladder dysfunction	EtE	CG nerve to S1 and S2 GF nerve to PN	10 dogs
Ruggieri	2011	EUS dysfunction EAS dysfunction	EtE	FN to Pudendal nerve	9 dogs
Gao	2011	Bladder dysfunction	EtS	L6VR to L4VR (donor)	30 Rats
Gomez-Amaya	2014	Bladder dysfunction	EtE	GF to PN	41 dogs
Gomez-Amaya	2015	Bladder dysfunction	EtE	GF to PN	37 dogs
Zerhau	2016	Bladder dysfunction	EtE	L5S1 to S2S3	17 rabbits

Tab 1: pre clinical papers included in the review.

Author	Year	Topic	Technique	Transfer	Patients	Time from injury	Follow up
Rasmussen	2015	Bowel dysfunction	EtE	L5 or S1 VR to S2VR	10, supraconal SCI	Between 1 and 18 years (4 years)	18 months
Xiao	2003	Bladder dysfunction	EtE	L5VR to S2 VR	15, suprasacral SCI	mean 7 years from injury	1-6-12-18-26 months
Xiao	2005	Bladder dysfunction	EtE	L5VR to S3 VR	20 spina bifida		12 months
Tuite	2013	Bladder dysfunction	EtE	L5VR to S2S3 VR	1 SCI	9 years	2 years
Peters	2014	Bladder dysfunction Bowel dysfunction	EtE	Lumbar VR according to stimulation (L5-S1) to S3	13 spina biphida	/	3 years
Rasmussen	2015	Bladder dysfunction	EtE	L5 or S1 VR to S2VR	10, supraconal SCI	between 1 and 18 years (4 years)	18 months
Tuite	2016	Bladder dysfunction	EtE	S1VR to S2S3 VR vs spinal cord detethering	20 patients in 2 groups (double blind, MM and LMM)	/	3 years
Sievert	2016	Bladder dysfunction	EtE	L5VR to S2S3 VR	8 SCI	mean 7 years from injury	71 months (mean)
Souza-Trindade	2017	ED	EtS + sural nerve graft	FN to corpora cavernosa and dorsalis penis	10 ED post RP	2 years from denervation (RP)	6-12-18 months
Reece	2019	ED	EtS + sural nerve graft	Selective fibers from FN to Corpora cavernosa	17	2.2 years from non NS RP	18 months

						2.4 years from NS RP	
Dangerfield	2023	ED	EtS + sural nerve graft		4	2 years	18 months
Cystectoprostectomy and Neobladder Formation, TURP, Abdoperineal Resection, Salvage Radiotherapy Post-Radical Prostatectomy (NS)							

Tab 2: clinical papers included in the review. MM = myelomeningocele, LMM= lipomyelomeningocele, NS RP= nerve sparing radical prostatectomy.

Bladder dysfunction: it has been so far the most investigated topic. Of the 11 papers who passed the first line screening process, 6 are pre-clinical studies, whereas the remaining 5 are clinical trials.

Anorectal dysfunction: only 2 papers on animal model were focused on anorectal function recovery. Some of the papers on bladder dysfunction cited improvement of bowel function following the surgical procedure.

Erectile dysfunction: only one paper investigated the effect of somatic to autonomic transfer in animal model, otherwise three case series have been published, until now, in humans.

Type of nerve transfer

Bladder dysfunction

In pre-clinical papers two types of transfer were tested.

In the intra-dural nerve transfer after lumbar spine exposure, the dura mater is incised and lumbar and sacral roots are exposed. According to the technique, the donor and receiving ventral roots are selected, the donor root is transected and the nerve coaptation performed in EtS or EtE. Donor roots are usually L4 or L5 and are transferred to L6 or S2. Through this novel connection, contraction of the target organ should be induced stimulating the skin innervated by the dorsal horns of the donor root. A particular mention should be reserved to (Zerhau 2016). He chose the donor and receiving roots basing of intraoperative electrical

stimulation of both muscles and detrusor response. In its paper donor roots were L5 to S1 VR and receiving S2 or S3 VR.

A distal nerve transfer was also proposed. The main difference in this case consists moving the donor nerve closer to the target organ, reducing the time required for reinnervation. Coccygeal nerve (CG) to S1 and S2 and genitofemoral nerve (GF) and femoral nerve (FN) to pelvic nerve (PN) connected through an EtE suture have been described. Gomez-Amaya and colleagues chose to transfer only the femoral nerve branch to gracilis to reduce as much as possible risk of gait impairment (Gomez-Amaya 2015).

Considering the clinical practice most of the case series were based on the so-called Xiao's procedure (Xiao 1999) in which an intradural anastomosis between L5VR and S2 or S2 and S3VR was performed.

Anorectal dysfunction

The two papers from Sun and Dong (Sun 2010, Dong 2013) evaluated the recovery of anorectal function following the intradural anastomosis between L4VR and L6VR. The former in end to end fashion, the latter in end to side.

Erectile dysfunction

Dong in 2016 investigated the effect of L4VR to L6VR in EtS to recover erectile function in rats.

In clinical practice, in 2017, a sural nerve graft in EtS between the FN and corpora cavernosa and dorsalis penis nerve was tested (Souza Trindade 2017), furthermore a simplification of this procedure was proposed by Reece in 2019 and was repeated recently Dangerfield 2023.

In figure 1 a schematic example of intradural and distal nerve transfer are reported to clarify the procedures

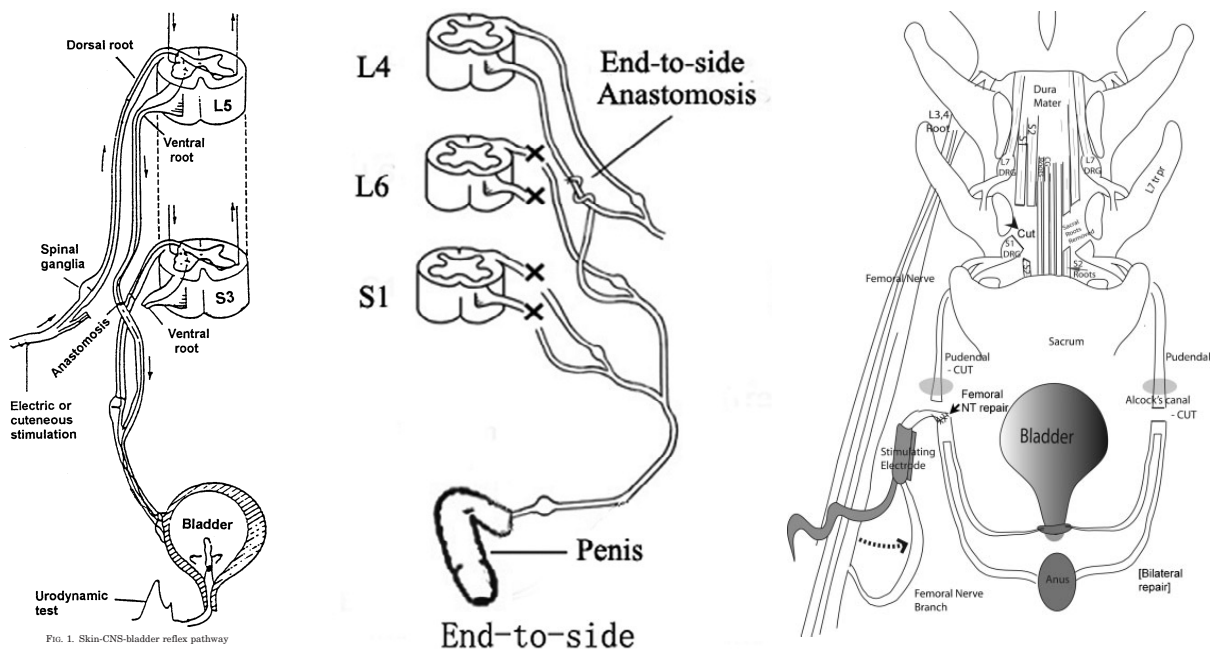


Fig. 1: on the left the Xiao procedure in which L5 VR is transferred to S3 VR (Xiao 1999), center the EtS transfer described by Dong (Dong 2016), on the right side the femoral to pudendal nerve transfer reported by Ruggieri in 2011 (Ruggieri 2011)

Animal models and outcomes measures

Most of the authors tested nerve transfer on rats except Ruggieri and his group and Zheuru who operated respectively dogs and rabbits.

The mean interval time between surgery and final evaluation was included between 4 and 14 months. Some authors (Wang 2007 and Sun 2010) performed the nerve transfer followed, few months later (3 months), by spinal cord transection above the transfer to simulate a post traumatic SCI.

In all of the treated animals the pressure inside the bladder, rectus and corpora cavernosa were measured at the last time point inducing distal reaction by electric stimulation above and below the nerve coaptation site.

Most of the authors used the retrograde nerve tracing (RNT) technique to show the new connection between somatic neural body in anterior horn and parasympathetic ganglia. Fluorogold (FG), fast blue (FB) or Dil 4 mg/mL (1,1'-dioctadecyl-3,3,3',3'-tetramethylindocarbocyanine perchlorate) were injected into major pelvic ganglia to trace retrogradely the axon to the neural body into the spinal cord. Sun injected dextran

tetramethylrhodamine (TMR) into external anal sphincter to trace in a proximal direction also the post ganglionic fibers. Moreover, Wang associated polyclonal choline acetyltransferase (ChAT) primary anti-body to the Dil staining to *highlight the neurons producing Acth in the spinal cord*.

The morphology of nerve anastomosis, the counting of myelinated and unmyelinated fiber as well as the morphology and weight of skeletal muscles innervated by donor nerve were frequently included as outcome measure. Toluidin-blue and hematoxylin-eosin were used to achieve morphological analysis.

Moreover, some authors added specific investigations typical of the type of function inspected: Wang described the regenerated post ganglionic nerve fibers into the detrusor muscle using acetylcholin-esterase staining (Wang 2007). Gomez-Amaya in 2015 investigated the presence of nicotinic receptors into the bladder using anti alfa1 and anti ppg9.5 antibodies. Dong used the mating test to confirm the recovery of induced ED (Dong 2016).

Results of nerve transfer in animal models

Bladder dysfunction

The results should be grouped depending to type of nerve transfer. Most of the authors who performed a root transfer registered muscle contraction in detrusor at final follow up. Despite this, no artificial micturition nor external urethral sphincter (EUS) release were recorded both during nerve stimulation or during skin stimulation (Zerahu 2016). Those who studied EtS L4VR to L6VR transfer (Gao 2012) registered intravesical pressure up to 53% compared the control group. Both the studies in which L4 to L6 was obtained revealed by retrograde nerve tracing new connections between sympathetic ganglia and ventral horn of the donor root and microscopical analysis demonstrated axon's regrowth into anastomosis site. Comparing EtE and EtS suture, no differences were described.

The research group held by Ruggieri tested a more distal nerve transfer. First in 2008 coccygeal nerve to S1 and S2 were compared to genitofemoral nerve to pudendal nerve (Ruggieri 2008(1), Ruggieri 2008(2), Ruggieri 2011). The authors didn't show any significant differences between techniques. They concluded that also mixed sensory/motor nerve may have the same efficacy than a pure motor nerve. Subsequently they compared the GF transfer to FN transfer concluding that FN transfer induced more intense detrusor

contraction following electrical stimulation than that induce stimulating GF nerve. Moreover in 2015 they demonstrated the presence of alfa 1 nicotinic receptor in reinnervated bladder that is a sign of muscle plasticity as a consequence of somatic nerve fibers regrowth (Gomez-Amaya 2015).

Anorectal dysfunction

Only L4VR to L6VR both in EtE and EtS were compared and described. Both the techniques reported in animals a synergy leading to contraction of the rectum and relaxation of the external anal sphincter (EAS) following electrical stimulation of transferred nerve. The retrograde nerve tracing confirmed the new nerve connection into the spinal cord.

Erectile dysfunction

Dong in 2016 (Dong 2016) applied the same transfer as indicated above investigating the recovery of penile erection. All the outcomes were successfully, reaching half the intracavernous pressure of control group in treated group and reporting a positive mating test in transfer group. The RNT technique revealed motor neurons in ventral horn of donor root and morphological analysis showed myelinated and unmyelinated axons in PN in nerve transfer group, whereas no axons was present in control denervated group.

Complications

In animal models no changes in post-operative gaiting were reported nor significant changes in microscopical appearance of skeletal muscle fibers or muscle weight regarding the donor nerves were observed. The only exception was Zerahu. He reported that 18% of the operated animals had hind limb paresis and 12% showed paraparesis.

Results of nerve transfer in human

Bladder dysfunction

Xiao in 2003 and in 2005 reported the results of intradural L5 to S2-S3 transfer for SCI and spina bifida. About 67% of the patients affected by SCI recovered bladder storage and emptying function via skin reflex in cutaneous territory of L5. Furthermore, he noted the reduction of hyperreflexic bladder and solution of detrusor-EUS dyssynergia. The mean time from injury to surgery was 7 years. In cohort of patients affected

by spina bifida, 17 of 20 recovered at 12 months complete control of bladder. Only 5 patients had muscular wasting secondary to L5 denervation.

Then Tuite in 2013 reported a single case of SCI in which the Xiao procedure was performed. The surgery was performed about 9 years after the injury. The patient was followed up for 2 years, concluding with no recovery of bladder control. The anastomosis was then microscopically analyzed when a kidney transplant was performed (3 years after Xiao procedure) and a neuroma at the level of nerve coaptation site was discovered. The same author in 2016 published the results of a double-blind cohort study in which the patients treated through Xiao procedure presented at 2 years of follow up no differences in bladder control and voiding compared to patients treated with only spinal cord de-tethering (Tuite 2016).

Even further Sievert in 2016 reported the negative results of Xiao procedure on 8 patients with bladder dysfunction as consequence of SCI. The nerve transfer was done at a mean of 7 years after injury and they were followed up until 70 months. The authors finally had not any improvement of bladder control at final follow up nor following skin stimulation nor in videourodynamic test.

Erectile dysfunction

All three clinical papers reported the results of sural nerve graft between FN and corpora cavernosa. Patients underwent nerve transfer procedure after about 2 years from denervation (radical prostatectomy or demolitive surgery in pelvic area). The first work showed rigid erection in 7 among 10 patients 9 months after surgery. Patients improved their general and orgasmic satisfaction from baseline at 6 and 12 months after surgery and the IIEF score improved at each follow up point.

Reece in 2019 proposed a slightly modified technique in 17 patients. At final follow up, 18 months after surgery, 70% of patients had good results as reported by IIEF-5 and EPIC-26 score.

The more recent paper reported good results in 4 patients treated with Reece procedure after a follow up of 18 months according to IIEF-5 and EPIC-26 score.

Discussion

Nerve transfer (NT) is a surgical option that intentionally divides a physiologically active nerve (with low donor morbidity) and transfers it to a distal, more important, but irreparable, paralyzed nerve (Chuang 2005). This concept increased its popularity over time in limbs reconstruction, demonstrating its superiority, in some circumstances, to traditional proximal nerve graft and becoming part of the standard armamentarium in reconstruction of brachial plexus or peripheral nerves (Chuang 2018). Actually, NTs are more frequently used in treatment of cervical spinal cord injury (Bertelli 2017).

Their main indications are reanimation of huge nerve gaps (> 10 cm) or situations in which unhealthy proximal nerve stumps is found. In certain situation, however, the outcomes of NT have not been so satisfactory (Doi 2018).

When a NT is performed a three stages regenerative process begin: (1) the transection of healthy donor nerves, (2) the regeneration of donor nerves into the targeted muscles or skin areas (morphological reinnervation), and (3) transformation from morphological reinnervation to functional reinnervation (Shen 2022).

NTs have optimal results when the donor and acceptor nerves are close one to each other in the motor areas, sharing some corticospinal projections from the motor cortex. The transfer probably switches on some silent connections, leading to an optimal result (Peters 2017). Otherwise, when the neurons in the primary motor cortex are distant, then it takes time to create a relay between the donor and acceptor neurons, inducing moderate results as for intercostal to musculocutaneous transfer (Mano 1995).

Different is for sensibility: topographies in the primary somatosensory cortex are relatively stable and their preservation does not depend on peripheral sensory inputs even after years from the procedure (Makinand 2017).

Despite NTs are very well introduced in treatment of peripheral nerve injuries, their use in autonomic disorders is quite new and a lot of uncertain aspects exist and have to be revealed.

Since the end of 90's NTs in autonomic system reinnervation were undergone. Bladder reinnervation have been the first to be experimented. Xiao and colleague performed in animal models the transfer of L5VR to S2-S3VR (Xiao 1999)

Their efforts induced more authors to reproduce and modify that procedure to further investigate the efficacy and the mechanisms that rule the functional recovery, if any. The papers included in this review regarding root transfer for voiding recovery demonstrated axon regrowth along the suture site, the presence of a connection between the MPG and the donor horn of the spinal cord through RNT technique, but they failed to demonstrated a restoration of voluntary or induced voiding nor the recovery of detrusor-EUS synergism. This fundamental aspect was highlighted by Gomez-Amaya in animal models and, more clearly, by Zerhau who stated not to use this technique in clinical practice due to the lack of efficacy.

Meanwhile the research group by Ruggieri and colleagues investigated the possibility to reinnervate bladder using a distal nerve transfer. They performed and compared GF and FN transfer to PN. As for the previous papers the authors did not described or reported the restoration of voiding, even though good outcomes at final follow up were presented. Interestingly, Gomez-Amaya described a novel aspect of smooth cell plasticity. After somatic reinnervation the muscle fibers of detrusor started to express nicotinic receptors instead muscarinic ones.

In humans, however, the attempts of bladder reinnervation due to SCI or other spinal disorders such as spina-biphida were attempted following the positive results in animal models and cohort of patients published by Xiao and colleague (Xiao 1993, Xiao 2005). Despite the initial enthusiasm, a double-blind clinical trial and a cohort of patients with long follow up showed inconsistent results, as for animal models (Sievert 2016, Tuite 2016). The root nerve transfer failed to reestablish the voiding reflex. The reason why it is unknown and was not clearly investigated. Sievert commented the papers by Xiao concerning the modality of roots selection as receiver, stating the high variability in detrusor innervation. Moreover, in animal models the SCI were performed after the nerve transfer, otherwise in clinics the SCI is first of all. The creation of a nerve transfer before the SCI could induce nerve regeneration and should be influenced by the descending axons from

upper levels, things that can't happen in patients. Lastly, patients treated in cohort studies suffered the trauma 4 to 9 years before the NT. This fact could interfere with the final outcome: a nerve transfer for skeletal muscle should be done within 1 year from injury (Doi 2018). It is possible to argue that a long-lasting bladder denervation could influence negatively the recovery due to obscured and uninvestigated pathophysiological aspects.

Interestingly, the two papers who concentrate their attention to bowel recovery both showed a synergism between rectus contraction and EAS release following electrical stimulus. No further papers were published on this, but it would be interesting to understand the reason why a synergism was described in anorectal reinnervation and not in bladder reinnervation, using the same NT. The solution could stand in neuro anatomy, maybe due to the presence of closest connection between motor nerve in the ventral horn of L4 and EAS releasing system. Improve the understanding of what is the mechanism here, could give a solution for bladder reinnervation.

Different are the attempts to treat ED. As one of the main drawbacks of RP, end-to-end nerve grafting of cavernous nerve were attempted. Thus, a randomized controlled trial failed to demonstrate any benefit of unilateral CN reconstruction contextually of RP (Davis 2009). The same findings were also reported by Kung and colleague (Kung 2015) who outperformed both unilateral and bilateral interposition end-to-end sural nerve grafting. In 2014 the inefficacy of CN reconstruction was also noted in an animal model in which a vein graft failed to induce erectly function recovery in rats (Bessede 2015). This failure could be attributable to the "web-like" nature of the CN bundles (Anderson 2011) and the deal is even more difficult in humans, in whom the CN consists of multiple fibers interwoven in a plexus. Dong in 2016 was the first who investigated the possibility to restore penile erection through a nerve transfer in a rat model in an EtoS fashion. He demonstrated erection recovery through the mating test, further the intracavernous pressure increased to half the normal pressure in consequence of transferred nerve stimulation. This model shows the possibility to recover in an animal model the erectile function through an EtS anastomosis. It still remains a very proximal nerve transfer that could be supposed to perform in case of SCI, but it is not usable in case of RP or any other injury to CN. Moreover, in case of SCI the root transfer should be supposed to work based on a

local reflex as for voiding, but it still remains a troublesome field. An innovative procedure was proposed by Souza-Trindade in 2017. They grafted directly the femoral nerve into corpora cavernosa, pushing the concept of nerve transfer directly into the target organ, bypassing the coaptation between donor and receiving nerve. They had incredible results as shown in results section. Reece and, more recently, Dangerfield confirmed the findings proposed in 2017. From a technical point of view the former connected both the nerve graft on an epineurotomy of the femoral nerve and passed one graft into the corpora cavernosa, the other was sutured to dorsalis penis nerve. The latter instead used only the distal connection to corpora cavernosa, excluding the dorsalis penis nerve and whereas the proximal stump was sutured to a neurotomized fascicle of the femoral nerve. Despite the surgical technique, all of them had impressive results: erectile function was recovered in 70% of patients 2 years after surgery. Patients undergone a RP with or without nerve sparing technique and no differences seemed to be between groups. It is difficult to certainly indicate that the NT procedure is the only responsible of erectile function recovery (Chung 2021) as far as more aspects co-act in recovery. Moreover, nothing is known about the mechanism of penile reinnervation and even less is known about neuroplasticity in somatic to autonomic transfer. Some concerns can be moved to the above procedure: first both sural nerves have to be harvested with risk of donor site morbidity, second a long course is required to reach the target, third the end to side neurotomy it is not certainly feasible in mixed nerve reconstruction, but in this field it seems to be more trustable than in other. Considering this pioneering papers, maybe local nerve transfer could be hypothesized to reach the same goal. Furthermore, animal models replicating or improving this technique should be planned to better understand the mechanism that underline somatic reinnervation of autonomic driven organs.

Of course, the recovery of synergistic processes as voiding or anorectal function is even more complex, not secondary they are caused by SCI, meaning that there is a complete disconnection from the higher control center, so that only local reflex can be, up to now, proposed. Maybe bio engineering could help this via electrostimulations. Instead, a lower injury with intact spinal cord could be helped by lower nerve transfer maybe directly into the target organs as proposed by Souza-Trindade and colleagues.

In conclusion this review demonstrated the possibility to create a functional somatic to autonomic connection. Artificial spinal reflexes under some aspects work, but, actually, can't replace the complex synergism between bladder, rectum and their external sphincters. The animal models in this field showed some interesting aspect of somatic to autonomic reinnervation as the expression of nicotinic receptors in smooth muscle fibers of the detrusor after somatic reinnervation. In penile reinnervation the astonishing clinical results should be the starting point to better understand what happens inside corpora cavernosa. More knowledges on biomolecular changes induced by somatic to autonomic reinnervation are required and maybe could open a gate on a novel surgical procedures giving new hopes in patients whose life was dramatically changed.

REFERENCES

Andersson KE. Mechanisms of penile erection and basis for pharmacological treatment of erectile dysfunction. *Pharmacol Rev* 2011;63:811–59

Bertelli JA and Ghizoni MF. Nerve transfers for restoration of finger flexion in patients with tetraplegia. *Journal of Neurosurgery. Spine*, vol. 26, no. 1, pp. 55–61, 2017

Bessede T, Moszkowicz D, Alsaïd B, Zaitouna M, Diallo D, Peschard F, Benoit G, Droupy S. Inside-out autologous vein grafts fail to restore erectile function in a rat model of cavernous nerve crush injury after nerve-sparing prostatectomy. *Int J Impot Res*. 2015 Mar-Apr;27(2):59-62.

Chuang DCC. Nerve transfers in adult brachial plexus injuries: my methods. *Hand Clin* 2005;21(01):71–82

Chuang DC. Distal Nerve Transfers: A Perspective on the Future of Reconstructive Microsurgery. *J Reconstr Microsurg*. 2018 Nov;34(9):669-671

Dangerfield DC, Coombs CJ. 'Case of the Month' from the University of Melbourne, Melbourne, Australia: treatment of iatrogenic erectile dysfunction with somatic-to-autonomic sural nerve grafting. *BJU Int*. 2023 Sep;132(3):262-265

Davis JW, Chang DW, Chevray P, et al. Randomized phase II trial evaluation of erectile function after attempted unilateral cavernous nerve-sparing retropubic radical prostatectomy with versus without unilateral sural nerve grafting for clinically localized prostate cancer. *Eur Urol* 2009;55:1135–43

Doi K. Distal Nerve Transfer: Perspective of Reconstructive Microsurgery. *J Reconstr Microsurg*. 2018 Nov;34(9):675-677

Dong C, Gao W, Jia R, Li S, Shen Z, Li B. Reconstruction of anorectal function through end-to-side neurorrhaphy by autonomic nerves and somatic nerve in rats. *J Surg Res*. 2013 Apr;180(2):e63-71

Dong C, Dong Z, Xie Z, Zhang L, Xiong F, Wen Q, Fan Z, Peng Q. Functional Restoration of Erectile Function Using End-to-side Autonomic-to-somatic Neuroorrhaphy in Rats. *Urology*. 2016 Sep;95:108-14

Gao WS, Dong CJ, Li SQ, Kunwar KJ, Li B. Re-innervation of the bladder through end-to-side neuroorrhaphy of autonomic nerve and somatic nerve in rats. *J Neurotrauma*. 2012 May 20;29(8):1704-13

Gomez-Amaya SM, Barbe MF, Brown JM, Lamarre NS, Braverman AS, Massicotte VS, Ruggieri MR Sr. Bladder reinnervation using a primarily motor donor nerve (femoral nerve branches) is functionally superior to using a primarily sensory donor nerve (genitofemoral nerve). *J Urol*. 2015 Mar;193(3):1042-51

Gomez-Amaya SM, Barbe MF, Lamarre NS, Brown JM, Braverman AS, Ruggieri MR Sr. Neuromuscular nicotinic receptors mediate bladder contractions following bladder reinnervation with somatic to autonomic nerve transfer after decentralization by spinal root transection. *J Urol*. 2015 Jun;193(6):2138-45

Kung TA, Waljee JF, Curtin CM, Wei JT, Montie JE, Cederna PS. Interpositional nerve grafting of the prostatic plexus after radical prostatectomy. *Plast Reconstr Surg Glob Open* 2015;3:e452

Makinand TR, Bensmaia SJ. Stability of sensory topographies in adult cortex. *Trends in Cognitive Sciences*, vol. 21, no. 3, pp. 195–204, 2017

Mano Y, Nakamuro T, Tamural R. Central motor reorganization after anastomosis of the musculocutaneous and intercostal nerves following cervical root avulsion. *Annals of Neurology*, vol. 38, no. 1, pp. 15–20, 1995

Peters AJ, Lee J, Hedrick NG, O'Neil K, Komiyama T. Reorganization of corticospinal output during motor learning. *Nature Neuroscience*, vol. 20, no. 8, pp. 1133–1141, 2017

Reece JC, Dangerfield DC, Coombs CJ. End-to-side Somatic-to-autonomic Nerve Grafting to Restore Erectile Function and Improve Quality of Life After Radical Prostatectomy. *Eur Urol*. 2019 Aug;76(2):189-196

Ruggieri MR, Braverman AS, D'Andrea L, McCarthy J, Barbe MF. Functional reinnervation of the canine bladder after spinal root transection and immediate somatic nerve transfer. *J Neurotrauma*. 2008 Mar;25(3):214-24 (1)

Ruggieri MR, Braverman AS, D'Andrea L, Betz R, Barbe MF. Functional reinnervation of the canine bladder after spinal root transection and genitofemoral nerve transfer at one and three months after denervation. *J Neurotrauma*. 2008 Apr;25(4):401-9 (2)

Ruggieri MR Sr, Braverman AS, Bernal RM, Lamarre NS, Brown JM, Barbe MF. Reinnervation of urethral and anal sphincters with femoral motor nerve to pudendal nerve transfer. *Neurourol Urodyn*. 2011 Nov;30(8):1695-704

Sievert KD, Amend B, Roser F, Badke A, Toomey P, Baron C, Kaminsky J, Stenzl A, Tatagiba M. Challenges for Restoration of Lower Urinary Tract Innervation in Patients with Spinal Cord Injury: A European Single-center Retrospective Study with Long-term Follow-up. *Eur Urol*. 2016 May;69(5):771-4

Shen J. Plasticity of the Central Nervous System Involving Peripheral Nerve Transfer. *Neural Plast*. 2022 Mar 18;2022:5345269

Souza Trindade JC, Viterbo F, Petean Trindade A, Fávaro WJ, Trindade-Filho JCS. Long-term follow-up of treatment of erectile dysfunction after radical prostatectomy using nerve grafts and end-to-side somatic-autonomic neurography: a new technique. *BJU Int*. 2017 Jun;119(6):948-954

Sun F, Chen M, Li W, Xiao C. Effect of the artificial somato-autonomic neuroanastomosis on defecation after spinal cord injury and its underlying mechanisms. *J Huazhong Univ Sci Technolog Med Sci*. 2010 Aug;30(4):490-3

Tuite GF, Storrs BB, Homsy YL, Gaskill SJ, Polsky EG, Reilly MA, Gonzalez-Gomez I, Winesett SP, Rodriguez LF, Carey CM, Perlman SA, Tetreault L. Attempted bladder reinnervation and creation of a scratch reflex for

bladder emptying through a somatic-to-autonomic intradural anastomosis. *J Neurosurg Pediatr.* 2013 Jul;12(1):80-6

Tuite GF, Polsky EG, Homsy Y, Reilly MA, Carey CM, Parrish Winesett S, Rodriguez LF, Storrs BB, Gaskill SJ, Tetreault LL, Martinez DG, Amankwah EK. Lack of efficacy of an intradural somatic-to-autonomic nerve anastomosis (Xiao procedure) for bladder control in children with myelomeningocele and lipomyelomeningocele: results of a prospective, randomized, double-blind study. *J Neurosurg Pediatr.* 2016 Aug;18(2):150-63

Wang HZ, Li SR, Wen C, Xiao CG, Su BY. Morphological changes of cholinergic nerve fibers in the urinary bladder after establishment of artificial somatic-autonomic reflex arc in rats. *Neurosci Bull.* 2007 Sep;23(5):277-81

Xiao CG, Godec CJ. A possible new reflex pathway for micturition after spinal cord injury. *Paraplegia*, 32: 300, 1994 4.

Xiao, C. G., De Groat, W. C., Godec, C. J., Dai, C. and Xiao, Q.: "Skin-CNS-bladder" reflex pathway for micturition after spinal cord injury and its underlying mechanisms. *J Urol*, 162: 936, 1999

Xiao CG, Du MX, Dai C, Li B, Nitti VW, de Groat WC. An artificial somatic-central nervous system-autonomic reflex pathway for controllable micturition after spinal cord injury: preliminary results in 15 patients. *J Urol.* 2003 Oct;170(4 Pt 1):1237-41

Xiao CG, Du MX, Li B, Liu Z, Chen M, Chen ZH, Cheng P, Xue XN, Shapiro E, Lepor H. An artificial somatic-autonomic reflex pathway procedure for bladder control in children with spina bifida. *J Urol.* 2005 Jun;173(6):2112-6

Zerhau P, Mackerle Z, Husár M, Sochůrková D, Brichtová E, Gopfert E, Faldyna M, Kubát M, Plánka L. Experimental Electrophysiological and Pressure Responses of Urinary Bladder Detrusor to Lumbar to Sacral Nerve Rerouting - An Animal Study with Negative Results. *Urol Int.* 2016;97(4):421-428

3.4 Prevention of symptomatic neuroma in traumatic digital amputation: A RAND/UCLA appropriateness method consensus study.

Crosio A, Albo E, Marcoccio I, Adani R, Bertolini M, Colonna MR, Felici N, Guzzini M, Atzei A, Riccio M, Titolo P, Tos P.

Injury. 2020 Dec;51 Suppl 4:S103-S107



Prevention of symptomatic neuroma in traumatic digital amputation: A RAND/UCLA appropriateness method consensus study[☆]

Alessandro Crosio^{a,*}, Erika Albo^b, Ignazio Marcoccio^c, Roberto Adani^d,
Maddalena Bertolini^e, Michele Rosario Colonna^f, Nicola Felici^g, Matteo Guzzini^h,
Andrea Atzeiⁱ, Michele Riccio^j, Paolo Titolo^e, Pierluigi Tos^a

^a Hand Surgery and Reconstructive Microsurgery Department. ASST Gaetano Pini - CTO, P.zza A. Ferrari 1, 20122 Milan, Italy

^b Orthopaedic and Traumatology Department. Università Campus Bio-Medico - via Álvaro del Portillo 200, 00128 Rome, Italy

^c Orthopaedic Microsurgery and Upper Limb Surgery. Istituto Clinico Città di Brescia - Via Bartolomeo Gualla 15, 25128 Brescia, Italy

^d Hand Surgery Department. Azienda Ospedaliero Universitaria di Modena, Largo del Pozzo 71, 41125 Modena, Italy

^e Orthopaedic and Traumatology 2 Surgery for the Upper Limb and Reconstructive Microsurgery. AOU Città della Salute e della Scienza. PO CTO. Via Zuretti 29, 10126 Turin, Italy

^f Plastic Surgery Department. Policlinico di Messina. Via Consolare Valeria 1, 98147 Messina, Italy

^g Reconstructive Surgery of the Limbs. AO San Camillo-Forlanini. Circonvallazione Gianicolense, 87, 00152 Rome, Italy

^h Orthopaedic and Traumatology Department. AOU Sant'Andrea. Via di Grottarossa 1035/1039, 00189, Rome, Italy

ⁱ Hand Surgery. Koelliker Hospital. Corso G. Ferraris 247, 10134 Turin, Italy

^j Reconstructive and Hand Surgery Department. AOU Ospedali Riuniti di Ancona. Via Conca 71, 60020 Ancona, Italy

ARTICLE INFO

Article history:

Accepted 7 March 2020

Keywords:

Traumatic amputation
Neuroma
Finger

ABSTRACT

Introduction: The appearance of a symptomatic neuroma following finger amputation is a devastating consequence for patient's quality of life. It could be cause of chronic neuropathic pain. The prevention of neuroma formation is a challenging effort for hand surgeons. The biological mechanisms leading to neuroma formation are mostly unknown and different preventing procedures have been tried without certain results. In this paper, a panel of Italian hand surgeons have been asked to express appropriateness about potentially preventive techniques of neuroma formation following the RAND/UCLA appropriateness protocol.

Methods: A literature review was preliminarily performed identifying the most employed methods to reduce the pathologic nerve scar. Afterwards, the selected panelists were asked to score the appropriateness of each procedure in a double scenario: in case of a sharp amputation or in a tear injury. The appropriateness was evaluated according to RAND/UCLA protocol.

Results: Nine Italian hand surgeons were included in the panel. Of them 5 were orthopaedic surgeons, 4 plastic surgeons. The identified appropriate procedures were: revision amputation should be done in operating room, the neurovascular bundles should be identified and is mandatory to treat surrounding soft tissues. Only in case of clean-cut amputation, it is appropriate to perform a proximal extension of the dissection, to use diathermocoagulation and coverage with local flaps. Procedures such as shortening in tension of the nerve stump, bone shortening, implantation of the nerve end in the soft tissue, treatment in the emergency room and, in both scenarios, certain results are evaluated as uncertain.

Discussion: In order to prevent the formation of a distal stump neuroma few methods were judged appropriate. It is mandatory to identify the neurovascular bundles and treat also the surrounding tissues, but no certain results could be obtained with local flap, bone shortening and other ancillary surgical

[☆] This paper is part of a Supplement supported by the European Federation of Societies of Microsurgery (EFSM).

* Corresponding author.

E-mail addresses: alessandro.crosio@asst-pini-cto.it (A. Crosio), e.albo@unicampus.it (E. Albo), info@ignaziomarcoccio.it (I. Marcoccio), adani.roberto@policlinico.mo.it (R. Adani), pierluigi.tos@asst-pini-cto.it (P. Tos).

acts. Moreover, it is not possible to guarantee the non arising of neuroma in any cases, also when every procedure has been temped.

Conclusions: The prevention of distal neuroma is actually a challenge, without a well known strategy due to the variability of response of nervous tissue to injury.

© 2020 Elsevier Ltd. All rights reserved.

Introduction

Digital amputations account for 69% of all traumatic upper limb amputations presenting at Emergency Department, with higher frequency for fingertip and partial digit injuries [1]. A good initial management is essential to prevent local complications that could compromise the return to normal daily activities and require further surgical treatments. Finger amputations are frequently burdened with local complications, with a rate that amounts to 20% [2]. Among these, peripheral nerve lesions and traumatic neuroma formations are invariably present. However, symptomatic amputation neuroma, one of the most challenging clinical problems in hand surgery, is diagnosed in about 7% of patients [3]. When a nerve is cut, it begins a regenerative process through axonal sprouting from the proximal stump toward its distal target. In patients that sustained a digital amputation, since neuroorrhaphy is impossible during revision surgery due to the absence of the distal stump, the axonal outgrowth escapes in a disorganized way in the surrounding tissues. This attempt results in the formation of a neuroma that can cause severe pain and hypersensitivity in the distribution of the involved nerve [4]. A painful digital neuroma can limit the overall function of the upper limb, requiring further surgical treatments to relieve patient's symptoms [5,6]. In literature, a variety of surgical techniques have been proposed, including resection and implantation of the nerve stump in muscle tissue, ligation, capping and bipolar diathermy. Because of the high failure rate and poor outcomes after revision surgery, currently there is no consensus about the best surgical choice [7]. The aim of this study is to identify the most appropriate surgical techniques on a non-replantable digital amputation that allow the prevention of painful neuroma during a stump regularization procedure, using the instructions described by the RAND/UCLA protocol [8,9].

Materials and methods

RAND/UCLA appropriateness method

The RAND/UCLA Appropriateness Method [8], an established approach for the development of health indicators, was used to identify the appropriate surgical procedures on a non-replantable digital amputation in order to prevent a painful neuroma. This Method is aimed to provide a consensus opinion about the appropriateness of a medical procedure combining the collective judgment of a panel of experts with the best available scientific evidence. To achieve this purpose, panel members are provided with an overview of relevant research evidence and hypothetical scenarios in which patients are classified in terms of clinical variables that are relevant in the decision-making process leading to recommend a particular procedure.

Review of the literature

MEDLINE (through www.pubmed.com), CINAHL (<http://www.ebscohost.com/cinahl/>), Google Scholar (<http://scholar.google.com/>) and The Cochrane Library (<http://www.thecochranelibrary.com/view/0/index.html>) databases were accessed to perform a comprehensive research of articles published in the last 28 years about

prevention and treatment of digital amputation neuroma. We performed different searches using the following keywords “neuroma”, “finger”, “amputation” and “digit”, isolated or combined using Boolean operators. Regarding the language filter, we selected articles in English and Italian given the linguistic capabilities of the research team. At the first electronic search, 284 papers were identified and, according to their abstract, only 28 studies were considered eligible to be further investigated. When full text articles were obtained and reviewed, 6 papers were selected to identify the procedures that can be applied on a non-replantable digital amputation in order to prevent a painful neuroma [10–15]. A research evidence document was drawn up to synthesize the latest available scientific evidence that experts were advised to consult. During this phase, also a list of the hypothetical clinical scenarios and the surgical options was formulated.

Recruitment of panelists

We recruited 13 orthopedics and plastic surgeons who daily manage traumatic hand emergencies in major centers of Hand Surgery and Microsurgery in Italy. The list of the panelists was selected by the senior author (PT). Each expert member was provided with results of the literature review and was initially asked to evaluate the hypothetical scenarios and the guidelines established by the team to give them the opportunity to suggest changes.

Generation of scenarios

Scenarios were developed by expert members of the research team (PT and AC), considering that the procedures were applied in an ideal situation in which all the resources were available and all techniques listed below could be performed, the medical history of the patient was known and the clinical examination gave unequivocal indication to regularization of the digital amputation stump. Moreover, amputations proximal to the metacarpo-phalangeal joint and thumb injuries were excluded.

At the end of the formulation and modification process including panelists suggestions, two distinct scenarios were finally identified: guillotine amputation with clean-cut complete detachment (scenario 1) and avulsion amputation with extensive tissues damage and nerve tear from the proximal stump (scenario 2). For each scenario, the panelists were asked to evaluate the location for injury management and the possible surgical techniques for nervous lesions treatment and the eventual procedures for soft tissues management finalized to neuroma prevention. Tables 1 and 2 were sent to the panelists and anonymously completed and re sent to the senior author.

The rating process and analysis

The clinical scenarios were sent to the panelists in August 2019. Panelists were invited to give their opinion about clinical scenarios and treatment methods. Adjustments of different items were done according to panelists' suggestions. For each scenario, panelists were asked to score the appropriateness of the treatment in

Table 1
Guillotine amputation with equal distribution of proximal and distal nerve stump between the two amputation stumps.

Management	Score								
Treatment in operating room	1	2	3	4	5	6	7	8	9
Treatment In ER box	1	2	3	4	5	6	7	8	9
treatment of nervous tissue									
Identification of vascular bundle	1	2	3	4	5	6	7	8	9
Proximal Dissection on healthy tissue	1	2	3	4	5	6	7	8	9
Non in tension shortening of proximal nerve stump	1	2	3	4	5	6	7	8	9
Embedding nerve stump in soft tissue	1	2	3	4	5	6	7	8	9
Tensioned section of proximal nerve stump	1	2	3	4	5	6	7	8	9
Diathermocoagulation	1	2	3	4	5	6	7	8	9
Direct neurorrhaphy of proximal nerve stump	1	2	3	4	5	6	7	8	9
Epineural ligature	1	2	3	4	5	6	7	8	9
Epineural flap	1	2	3	4	5	6	7	8	9
Epineural graft	1	2	3	4	5	6	7	8	9
Local soft tissue treatment	1	2	3	4	5	6	7	8	9
If you scored "Local Soft Tissue Treatments" 4 or more, judge the following points									
Soft tissue treatment	1	2	3	4	5	6	7	8	9
Coverage flap	1	2	3	4	5	6	7	8	9
Expected results									
Express the degree of appropriateness about the following sentence:Applying all the procedures that are thought appropriate, you can guarantee the results	1	2	3	4	5	6	7	8	9

Table 2
Tear injury with nerve stump more in the distal part than in the proximal part.

Management	Score								
Treatment in operating room	1	2	3	4	5	6	7	8	9
Treatment in ER box	1	2	3	4	5	6	7	8	9
Treatment of nervous tissue									
Identification of vascular bundle	1	2	3	4	5	6	7	8	9
Proximal dissection on healthy tissue	1	2	3	4	5	6	7	8	9
Non in tension shortening of proximal nerve stump	1	2	3	4	5	6	7	8	9
Embedding nerve stump in soft tissue	1	2	3	4	5	6	7	8	9
Tensioned section of proximal nerve stump	1	2	3	4	5	6	7	8	9
Diathermocoagulation	1	2	3	4	5	6	7	8	9
Direct neurorrhaphy of proximal nerve stump	1	2	3	4	5	6	7	8	9
Epineural ligature	1	2	3	4	5	6	7	8	9
Epineural flap	1	2	3	4	5	6	7	8	9
Epineural graft	1	2	3	4	5	6	7	8	9
Local soft tissue treatment	1	2	3	4	5	6	7	8	9
If you scored "Local soft tissue treatments" 4 or more, judge the following points									
Soft tissue treatment	1	2	3	4	5	6	7	8	9
Coverage flap	1	2	3	4	5	6	7	8	9
Expected results									
Express the degree of appropriateness about the following sentence:Applying all the procedures that are thought appropriate, you can guarantee the results	1	2	3	4	5	6	7	8	9

each scenario from 1 (highly inappropriate) to 9 (highly appropriate). All data returned from panelists were analysed for areas of agreement and disagreement. By definition, a procedure was classified as "appropriate" if the median rating was 7 to 9, with agreement; "inappropriate" if the median rating was 1 to 3, with agreement; and "uncertain" if the median rating was 4 to 6, with agreement or if any median without agreement was found. For definition of agreement/disagreement, the following parameters were calculated: median, interpercentile range (IPR), lower IPR, upper IPR, IPR ratio, central point of IPR (IPRCP), asymmetry index (AI), Interpercentile Range Adjusted for Symmetry (IPRAS) and disagreement index (DI) as reported in RAND/UCLA manuscript [8].

Results

Of the 13 experts involved in this study, 9 completed the questionnaires and were included in the panel. We included 5 Orthopaedic Surgeons and 4 Plastic Surgeons, whose clinical practice focuses exclusively on Hand Surgery and Reconstructive Microsurgery in Italian major centers of Hand Surgery and Microsurgery. Panelists reached consensus for 9 questions in scenario 1 (56%) and for 6 questions in scenario 2 (38%). Therefore, there was lack of consensus for 7 questions in scenario 1 and 10 questions in sce-

nario 2. Tables 3 and 4 resume the questions according to the final response.

Panelists found appropriate in both scenarios the injury treatment in operating room, the identification of neuro-vascular bundles and the treatment of the surrounding soft tissues. Only in case of clean-cut amputation, it is appropriate to perform a proximal extension of the dissection, to use diathermocoagulation and coverage with local flaps. In any case, accessory procedures carried out on the nerve stump (epineural graft, epineural flap and epineural ligation) were inappropriate. Procedures such as shortening in tension of the nerve stump, bone shortening, implantation of the nerve end in the soft tissue, treatment in the emergency room and, in both scenarios, certain results are evaluated as uncertain.

Guillotine amputation

In scenario 1, panelists evaluated as appropriate (A): treatment in the operating room, identification of nerve vascular bundles, proximal extension of dissection in healthy tissue, diathermocoagulation, treatment of surrounding soft tissues and cover flaps. Treatment in the emergency room, shortening of the non-tensioned nerve stump, implantation of the nerve end in the soft tissue, section in tension of the stump, termino-terminal neurorra-

Table 3

Results of appropriateness in guillotine injury. table caption: A - Appropriate, U - Uncertain, I - Inappropriate.

Management	Median	Results
Treatment in operating room	<u>9.0</u>	A
Treatment in operating room	<u>3.0</u>	U
Treatment of nervous tissue		
Identification of vascular bundle	<u>9.0</u>	A
Proximal dissection on healthy tissue	<u>8.0</u>	A
Non in tension shortening of proximal nerve stump	<u>7.5</u>	U
Embedding nerve stump in soft tissue	<u>7.0</u>	U
Tensioned section of proximal nerve stump	<u>7.5</u>	U
Diathermocoagulation	<u>7.0</u>	A
Direct neurorraphy of proximal nerve stump	<u>4.5</u>	U
Epineural ligature	<u>3.0</u>	I
Epineural flap	<u>3.0</u>	I
Epineural graft	<u>3.0</u>	I
Local soft tissue treatment	<u>7.5</u>	A
If you scored "local soft tissue treatments" 4 or more, judge the following points		
Soft tissue treatment	<u>7.0</u>	U
Coverage flap	<u>8.0</u>	A
Expected results		
Express the degree of appropriateness about the following sentence:		
Applying all the procedures that are thought appropriate, you can guarantee the results	<u>3.0</u>	U

Table 4

Results of appropriateness in tear injury table caption: A - Appropriate, U - Uncertain, I - Inappropriate.

Management	Median	Results
Treatment in operating room	<u>9.0</u>	A
Treatment in operating room	<u>3.0</u>	U
Treatment of nervous tissue		
Identification of vascular bundle	<u>9.0</u>	A
Proximal dissection on healthy tissue	<u>8.0</u>	U
Non in tension shortening of proximal nerve stump	<u>3.5</u>	U
Embedding nerve stump in soft tissue	<u>6.0</u>	U
Tensioned section of proximal nerve stump	<u>5.0</u>	U
Diathermocoagulation	<u>6.0</u>	U
Direct neurorraphy of proximal nerve stump	<u>4.5</u>	U
Epineural ligature	<u>3.0</u>	I
Epineural flap	<u>3.0</u>	I
Epineural graft	<u>3.0</u>	I
Local soft tissue treatment	<u>8.0</u>	A
If you scored "Local Soft Tissue Treatments" 4 or more, judge the following points		
Soft tissue treatment	<u>3.0</u>	U
Coverage flap	<u>8.0</u>	U
Expected results		
Express the degree of appropriateness about the following sentence Applying all the procedures that are thought appropriate, you can guarantee the results	<u>3.0</u>	U

phy, bone shortening and certain result were considered uncertain (U) options. Three procedures were considered inappropriate (I): epineural ligation, epineural flap and epineural graft.

Avulsion amputation

In scenario 2, panelists evaluated as appropriate (A): treatment in the operating room, identification of neuro-vascular bundles and treatment of surrounding soft tissues. Treatment in the emergency room, proximal extension of dissection in healthy tissue, shortening of the non-tensioned nerve stump, implantation of the nerve end in the soft tissue, section in tension of the stump, diathermocoagulation, termino-terminal neurorraphy, bone shortening, cover flaps and certain result were considered uncertain (U) options. Three procedures were considered inappropriate (I): epineural ligation, epineural flap and epineural graft.

Discussion

A panel of 9 expert hand surgeons, using the RAND/UCLA Appropriateness Method, collaborated to identify the appropriate process of care for patients with traumatic non-replantable digital amputations in order to prevent the formation of a painful neuroma. They were asked to express a judgment of appropriateness on different surgical techniques and strategy of neuroma prevention both in guillotine and avulsion amputations. No guidelines are available for this type of injury that are mostly treated on the basis of the single surgeon experience.

Symptomatic amputation neuroma is currently one of the major complications of digital amputations. It occurs in about 7% of patients and in all cases determines various degrees of disability that could require further surgical treatments [4,6,13]. Factors involved in pain onset are extremely variable. Consequently, several expedients have been described in the literature to prevent this complication, without establish an effective technique. One of the

main reasons for these failures is that we are not aware of the local mechanisms underlying neuroma formation. It is known that factors such as α -SMA and NGF are involved and that a local pro-inflammatory environment is crucial for stimulation of nociceptive receptors and residual nerve fibers. However, the complete biological process is not fully understood [16].

Various studies demonstrated that the best option for neuroma prevention is direct nerve repair, when it is possible. The reconnection between distal and proximal nerve stump support the regenerative process of axonal sprouting from the proximal nerve end toward its distal target [17]. In literature, termino-terminal neurotaphy is reported as an effective techniques with a good outcomes but data did not allow to consider this method certainly appropriate [18]. Some papers reported satisfactory results with procedures such as flap to cover the amputation stump or epineural graft to cover the nerve end [7]. On the contrary, panelists judged this techniques inappropriate in every situation.

In the study of Vlot and colleagues [19], no difference was observed about the onset of a painful neuroma between patients initially treated in the operating room or in the emergency room. In our study, the experts have indicated as appropriate the surgical revision of the amputation stump in the operating room, while the use of the emergency room could be considered only in case of inaccessibility of the operating room.

As reported in literature, useful procedure in neuroma prevention were section in tension of the nerve end and implantation of the nerve stump in the surrounding soft tissue ore bone, with a demonstrated efficacy in 70% of cases if performed immediately [20]. Panel members did not confirm this statement and considered outcomes of these procedures as uncertain.

On the contrary, there is a complete agreement about the appropriateness of surrounding soft tissue treatment. Amputation could be considered as an exposed fracture that require bone and soft tissue debridement in order to reduce necrotic or potentially necrotic tissue [21]. In this way, local inflammatory processes and risk of nervous end incorporation in scar tissue are reduced.

Local flaps, although useful in distal injuries, are considered a more complex treatment that often requires an extensive dissection of soft tissues with potential further lesions of the residual digital nerve [22].The panel of experts considers this procedure appropriate in clean-cut digital injury, while of uncertain efficacy in avulsion lesions.

The divergence that emerges between the appropriate and uncertain procedures in guillotine and avulsion amputation groups is confirmed by the literature. If it is known that a painful neuroma is more frequent in avulsion amputations, it could be stated that all the procedures aimed at neuroma prevention did not assure good outcomes.

Conclusions

In conclusion, identification of the neuro-vascular bundles, use of the operating room and debridement of surrounding soft tis-

ues of the amputation stump are the unique procedures defined as appropriate for symptomatic neuroma prevention by the panel members. However, even if promptly applied, this techniques can not assured the absence of neuroma formation.

Declaration of Competing Interest

All authors declare no conflict of interest.

References

- [1] Win TS, Henderson J. Management of traumatic amputations of the upper limb. *Bmj* 2014;348:g255.
- [2] Conolly WB, Goulston E. Problems of digital amputations: a clinical review of 260 patients and 301 amputations. *Aust N Z J Surg* 1973;43:118–23.
- [3] Weng W, Zhao B, Lin D, Gao W, Li Z, Yan H. Significance of alpha smooth muscle actin expression in traumatic painful neuromas: a pilot study in rats. *Sci Rep* 2016;6:23828.
- [4] Vernadakis AJ, Koch H, Mackinnon SE. Management of neuromas. *Clin Plast Surg* 2003;30:247–68 VII.
- [5] Mackinnon SE. Evaluation and treatment of the painful neuroma. *Tech Hand Up Extrem Surg* 1997;1:195–212.
- [6] Watson J, Gonzalez M, Romero A, Kerns J. Neuromas of the hand and upper extremity. *J Hand Surg Am* 2010;35:499–510.
- [7] Wu J, Chiu DT. Painful neuromas: a review of treatment modalities. *Ann Plast Surg* 1999;43:661–7.
- [8] Fitch K.BSJ, Aguilar, M.D., Burnand B., LaCalle J.R., Lázaro P., van het Loo M. et al. The rand/ucla appropriateness method user's manual. Santa Monica, CA: RAND.
- [9] Bell BG, Spencer R, Avery AJ, Campbell SM. Tools for measuring patient safety in primary care settings using the RAND/UCLA appropriateness method. *BMC Fam Pract* 2014;15:110.
- [10] Yuksel F, Kislaoğlu E, Durak N, Ucar C, Karacaoglu E. Prevention of painful neuromas by epineural ligatures, flaps and grafts. *Br J Plast Surg* 1997;50:182–5.
- [11] Belcher HJ, Pandya AN. Centro-central union for the prevention of neuroma formation after finger amputation. *J hand surg* 2000;25:154–9.
- [12] Blair JW, Moskal MJ. Revision amputation achieving maximum function and minimizing problems. *Hand Clin* 2001;17:457–71 IX.
- [13] van der Avoort DJ, Hovius SE, Selles RW, van Neck JW, Coert JH. The incidence of symptomatic neuroma in amputation and neurotaphy patients. *J Plast Reconstr Aesthet Surg* 2013;66:1330–4.
- [14] Peterson SL, Peterson EL, Wheatley MJ. Management of fingertip amputations. *J Hand Surg Am* 2014;39:2093–101.
- [15] Honeyman CS, Wiberg A, Sen SK. Simple glove guard to protect soft tissues during digital amputation. *Ann R Coll Surg Engl* 2016;98:343.
- [16] Lu C, Sun X, Wang C, Wang Y, Peng J. Mechanisms and treatment of painful neuromas. *Rev Neurosci* 2018;29:557–66.
- [17] Gorkisch K, Boese-Landgraf J, Vaubel E. Treatment and prevention of amputation neuromas in hand surgery. *Plast. Reconstr. Surg.* 1984;73:293–9.
- [18] Smahel J. Some thoughts and observations concerning the prevention of neuroma. *Acta Chir Plast* 1998;40:12–16.
- [19] Vlot MA, Wilkens SC, Chen NC, Eberlin KR. Symptomatic neuroma following initial amputation for traumatic digital amputation. *J Hand Surg Am* 2018;43:86 e1–e8.
- [20] Dellon AL, Mackinnon SE, Pestronk A. Implantation of sensory nerve into muscle: preliminary clinical and experimental observations on neuroma formation. *Ann Plast Surg* 1984;12:30–40.
- [21] Friedrich J.B., Vedder, N.B. Mangled upper extremities in green's operative hand surgery. 7th edition ed: Elsevier.
- [22] Foucher G, Sammut D, Greant P, Braun FM, Ehrler S, Buch N. Indications and results of skin flaps in painful digital neuroma. *J Hand Surg* 1991;16 25-9.

3.5 Intraoperative ultrasound study of traumatic nerve injury: current applications and future perspectives.

Crosio A, Verga L, Locatelli F, Magnani M, Clemente A, Odella S, Tos P.

Under submission

INTRAOPERATIVE ULTRASOUND STUDY OF TRAUMATIC NERVE INJURY: CURRENT APPLICATIONS AND FUTURE PERSPECTIVES

Alessandro Crosio^{1*}, Lucia Verga², Francesco Locatelli¹, Mauro, Magnani¹, Alice Clemente¹,
Simona Odella¹, Pierluigi Tos¹

1 Hand Surgery and Reconstructive Microsurgery, ASST Gaetano Pini – CTO, Milan

2 Radiology department, ASST Gaetano Pini – CTO, Milan

*Corresponding author

Abstract

The identification of intraneural scar tissue is a challenge for every surgeon who is treating nerve injuries. For nerve reconstruction it has been proposed that normal histological architecture of proximal stump is mandatory to obtain good functional results. Actually, nerve section of proximal nerve stump is performed just with grossly evaluation. Previous studies demonstrated that this kind of resection underestimates the extension of fibrous tissue into the proximal stump and the following nerve reconstruction could be limited and unsuccessful due to scar invasion. To ameliorate this procedure, intraoperative ultrasound study of nerve stumps has been proposed.

In this study we performed intraoperative ultrasound of the stump neuromas in 6 patients with traumatic nerve injury treated by debridement and reconstruction. The debridement was performed until a normal proximal and distal stump appeared. Furthermore, stumps were also investigated by ultrasound directly in the field. Compared to eye-guided resection, the ultrasound showed hyperechoic fibrotic tissue interposed between fascicles and fascicle appeared to be edematous at least 0.5 cm more proximal to where the macroscopical-guided

cute would have been done. This procedure led to a recut of both stumps of at least 0.5 cm and, in some patients, induced to perform different surgical procedure. The intra-operative findings were compared to histological appearance, revealing a qualitative correlation between ultrasound and microscopy.

In the presented case series, a protocol of intraoperative sonographic study is reported. This tool seems to be feasible and helpful in nerve reconstruction. In all cases greater nerve resection was induced by ultrasound appearance of nerve stumps, reducing the amount of intraneural scar. Further studies are required to correlate quantitatively sonohistology to histological findings, further increasing the accuracy of nerve resection before reconstruction.

Keywords

Peripheral nerve, ultrasound, nerve reconstruction, intra operative ultrasound.

Introduction

One of the main concerns in nerve reconstruction is to obtain valid proximal and distal nerve stumps through nerve resection. It means to reach a condition in which the entire section is occupied by fascicles, no areas of scar tissue are present and punctate bleeding is seen. Actually, nerve section of proximal nerve stump is performed just with gross evaluation, with the only help of magnification instruments. Previous studies demonstrated that this kind of resection underestimates the extension of fibrous tissue into the proximal stump and the following nerve reconstruction could be limited and unsuccessful due to scar invasion¹. Intraoperative histological scar tissue quantification can help the surgeon to perform a scar free cut on the proximal nerve end, but this procedure is time spending and required available experienced peripheral nerve pathologist.

Considering the increasing capacity of ultrasound (US) to study pathologies afflicting peripheral nerves, Koenig et al² explored the use of intraoperative high-resolution US to examine nerve lesions founding a correlation between what ultrasound described, previous electrophysiological investigations, microsurgical dissection, and outcomes. Recently, further authors applied US in the operating field with aim to improve quality of nerve reconstruction²⁻³⁻⁴⁻⁵.

In this paper the authors report their experience with the use of ultrasound directly on the nerve stumps during debridement with the aim to improve the quality of the debrided nerve. Morphological differences between ultrasound guided and macroscopical-guided resection are reported and its effect on functional outcomes is analyzed.

Methods

Patient selection

A retrospective evaluation of patients treated between 2016 and 2021 was performed. Intraoperative ultrasound was performed in those patients who were treated for a peripheral nerve palsy following an open or close trauma either in the upper and lower extremity with clinical and instrumental diagnosis of neuroma in continuity without function. They were treated by means of neuroma in continuity resection and appropriate reconstruction. Differences in nerve gap between macroscopical and ultrasound sectioning was evaluated comparing the two methods.

Intraoperative ultrasound equipment

In all patients the MyLab x8 and a linear 4-15 MHz transducer (Esaote - Via E. Melen, 77 16152 Genova Italy) was used at maximal frequency. The transducer, once needed, was covered by a sterile drape, the tip of the drape was filled in by ultrasound gel. To enhance the ultrasound window, the field was flood by sterile saline solution, leaving the stumps in site. The axial and longitudinal scans were obtained moving the transducer from the center of neuroma to a proximal and distal direction, leaving the nerve stumps into the operating field, after microsurgical dissection.

Surgical technique

Once the neuroma in continuity was identified, a progressive 3 mm cut in a proximal and distal direction was done. It stopped when macroscopically the cross-section areas appeared to be occupied only by fascicles, without any fibrotic areas and with punctate bleeding. This procedure was carried out using n 11 knife and magnification using 3.5x loupes and in all

patients was performed by two authors (PT and AC). The last slice obtained by macroscopical cut was marked.

After macroscopic evaluation, ultrasound axial and longitudinal scans were obtained. Another mark was placed where the nerve stump presented slight hyperechoic epineurium and every fascicle countered by hyperechoic perineurium⁶, this kind of appearance was defined as a normal nerve ultrasound anatomy.

The ultrasound study was conducted by an expert radiologist in nerve ultrasound (LV). Before nerve withdrawal, the delta between nerve gap according to macroscopic and ultrasound evaluation was registered. The marked segments were sent to histological analysis to compare the extension of intraneural scar in macroscopical and ultrasound section. The nerve gaps were then reconstructed with nerve grafts or direct suture as required and suture sites were protected by means of fibrine sealant (Tisseel - Baxter International Inc. One Baxter Parkway Deerfield, IL 60015-4633).

Every segment was embedded in paraffin. Then the slices were stained with hematoxylin-eosine to emphasize collagen fibers and intra neural scar.

Outcome measures

Histological sections were described qualitatively by expert muscle-skeletal pathologists, providing differences between macro guided and ultrasound guided sections.

Each patient was followed up monitoring recovery of reinnervated muscles according to MRC scale for muscle strength, sensory recovery was registered through sensory scale. The Numerical Rating Scale for pain was added also at the last follow up visit.

Results

Patients' characteristics

In the investigated period 6 patients were included. In table 1 clinical notices about each patient are reported. The median interval between trauma and surgery was 8 months (between 6 and 48 months). The mean nerve gap after macroscopical resection was 5,1 cm (between 2 and 8 cm). The gap increased to 5.7cm after intraoperative ultrasound evaluation (between 2 and 9 cm). In three patients over five the ultrasound induced to resect 1 cm more. The nerve gaps were reconstructed by means of sural nerve graft (4 patients), medial brachial and antebrachial cutaneous nerve (1 patient) and direct suture in 1 other patient.

Patient 1: was affected by circular saw wound treated in emergency in other hospital. The patient came to our attention about 5 months after the injury due to pain and no recovery. Pre-operative ultrasound study demonstrated a terminal neuroma of median and ulnar nerve (not previously repaired), confirmed by electrophysiological studies who reported no signs of nerve recovery. Flexor tendons appeared to be adhered in heavy scar tissue.

Patient 2: he suffered a lacerated wound by metal film on the ulnar border of middle third/distal forearm, treated in other hospital. The patient came to our outpatient clinic due to pain in ulnar nerve innervation territory, claw hand and atrophy of intrinsic muscles 3 years and a half after trauma. Intense Tinel sign at the level of the wound was present. Ultrasound study demonstrated a terminal neuroma of the ulnar nerve and occluded ulnar artery. A local anesthetic block above the neuroma demonstrated a relief of pain so that a reconstruction of the ulnar nerve was programmed for sensory recovery and a Zancolli 2 procedure was performed to reduce the claw. No transfer for adduction of the thumb was proposed because was not required by the patient.

Patient 3: closed brachial plexus injury due to motor vehicle accident with humeral shaft fracture. Ultrasound appearance of the radial nerve showed a neuroma in continuity with signs of axonotmesis, confirmed also by electrophysiological studies. A reconstruction of the radial nerve, after recovery of the brachial plexus was planned

Patient 4: supracondylar humeral fracture treated by closed reduction and K wire fixations. Clinically persisted a high median nerve palsy, ultrasound study showed the median nerve entrapped in bone callus at the distal third of the humerus. Electrophysiological studies confirmed the presence of high grade axonotmesis injury.

Patient 5: farm machine trauma in the left leg treated emergently in other hospital. The patient still continued to have pain and sensory impairment in the tibial nerve territory. She arrived at our institution one year and a half after trauma. Ultrasound showed a terminal neuroma of the tibial nerve in the middle third of the leg, confirmed by electrophysiological studies who demonstrated an axonotmesis type of injury. In this patient a good response to local anesthetic block induced us to reconstruct the tibial nerve with the intent of pain reduction and plantar foot sensory recovery.

Patient 6: knife wound at the distal leg, a misdiagnosed partial injury to the tibial nerve above the tarsal tunnel was then assessed about 7 months after injury due to pain and numbness in the innervation territory of the tibial nerve. Ultrasound evidence of in continuity neuroma with pain and incomplete tibial nerve palsy 10 months after the injury confirmed the clinical suspicion.

Patient	Age	Nerves	Intervention	Time from trauma (months)	Date of surgery	Nerve gap macro (cm)	Nerve gap after US resection (cm)	Delta (cm)	Other procedures	Last follow up	Follow up time	Muscle recovery MRC	Sensory recovery S	NRS
1	59	Median fa	Sural graft	6	feb-20	4,5	5.5	1	Camitz	1/12/2023	34	M1	Median S2	3
		Ulnar fa	Sural graft						Flexor tenolysis				Ulnar S2	
									EPI proponente (jul 2022)					
2	37	Ulnar fa	MACN	48	feb-20	4,8	6	1,2	vein graft for ulnar artery Zancolli II	1/12/2023	34	M1	S2+	2
3	24	Radial arm	Sural graft	10	jan-20	6	6	0	Tendon transfer for radial nerve after 2 year for no recovery (2021)	1/12/2023	24	M0	S1	0
4	8	Median elbow	Direct suture	6	feb-21	2	2	0		7/4/2023	26	M4	8mm	0
5	33	Tibial	Sural graft	12	set-21	8	9	1	TMR tibial nerve 09/2023	22/09/2023	22	M0	S0	8
6	32	Tibial	Sural graft	7	apr-23	4	4,5	0,5	TMR/RPNI 09/2023	set-23	5	M0	S0	8
Median				14,8		5,5		0,75			24,2			3,50
Mean				8		6		0,6			26			2

Table 1: patients' characteristics and differences between macroscopical and ultrasound guided resection.

Note that 0.6 cm more of nerve stump were resected through ultrasound evaluation. Fa = forearm, MACN = medial antebrachial cutaneous nerve

Ultrasound and histopathological appearance

In all treated patients the ultrasound scan induced to cut at least 0.5 cm more both in proximal and distal stump compared to macroscopical guided cut.

The histological slices found absence of edema between nerve fascicles in ultrasound guided slices at distal stump, providing a better-quality stump for nerve regeneration. In figure 1 a comparison of histological appearance between ultrasound guided section and macroscopical section is showed.

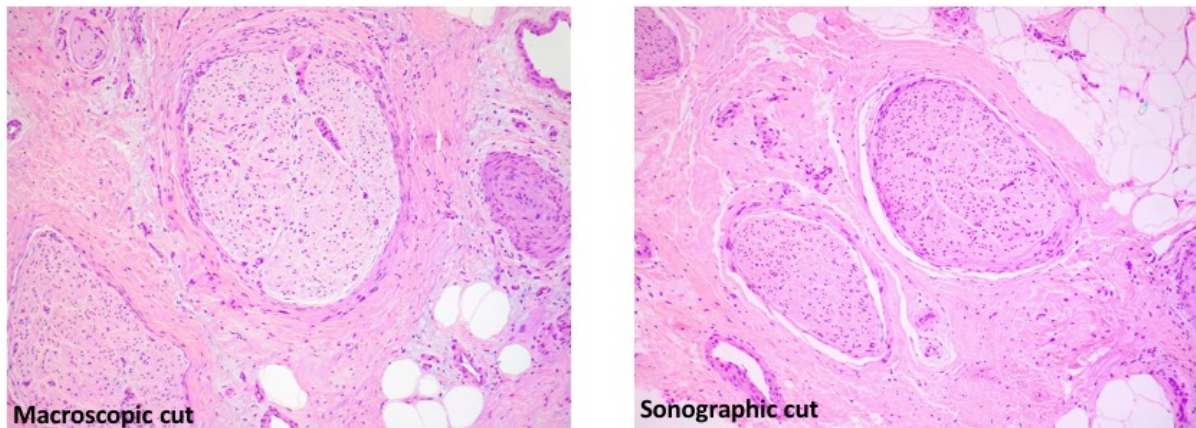


Fig. 1: right sections of distal nerve stump after ultrasound guided sections. Left section after macroscopical guided cut. Note in macro cut the presence of oedema, not present on the right, where fascicles are better represented.

Patients' outcome

In table 1 the type of reconstruction of resected neuromas and clinical results at last follow up or last follow up before any other surgery are reported.

Three out of six patients didn't require any other surgical procedure. Three of them required a revised surgical procedure due to no recovery or pain. Two of them was revised at about 2 years after first procedure, the other one developed a painful neuroma at the proximal suture site and was revised due to terrible neuropathic pain 5 months after index procedure. One patient didn't show any sign of functional recovery, so that tendon transfer for radial nerve palsy was performed about 24 months after index procedure.

The other three patients didn't require any other procedure, the child obtained at two years a very good recovery. The other two patients were satisfied by their recovery, without pain and with a satisfiable recovery of the hand, even if not complete.

Discussion

The intraoperative use of ultrasound in the resection of nerve lesions is relatively young. Literature data are poor. Koenig et al have successfully evaluated the use of intraoperative ultrasound on 19 traumatic nerve lesions, correlating the ultrasound, clinical, electromyographic, surgical and histological data². Lee et al confirmed the usefulness of the ultrasound during the surgical approach to six neural lesions⁷. Haldeman et al successfully employed the ultrasound scanner in five cases of post-traumatic neuroma and schwannoma/neurofibroma⁸. Burks et al finally report 3 cases of post-traumatic neuromas with an attempt of correlation between ultrasound image and histological finding⁹. Osorio et al published an interesting study in which in a cohort of 13 patients with a variety of nerve injuries (entrapment syndromes, post-traumatic neuromas, neural tumors) ultrasound is used pre-operatively to inject methylene blue into the nerve lesion. Methylene blue is mainly picked up by nerve funicles, which are thus highlighted¹⁰.

In our case series, histological sections performed where nerve trimming was performed according to the indications given by intraoperative ultrasonography result in a condition in which less edema around fascicles were observed.

In the operative field emerges that, due to the greater resolution capacity than the human eye and the possible intrafascicular characterization of the lesion, ultrasound suggests sacrificing a few more millimeters of nerve, compared to macroscopic evaluation. Our case histories showed that, usually, for peripheral nerve lesions, the resection margin should be increased, on average, by about 5 mm. It could correspond to a longer recovery time and ideally to a best functional outcome. The advantage of this procedure seems to be especially related to more accurate nerve resection. Considering the results obtained in our case series a real advantage on clinical results cannot be expressed clearly. The patient who obtained the

best result is a child in which, fortunately, an end to end suture of the median nerve was performed and a good result could have been supposed. Certainly, ultrasound allowed us to describe more clearly the injury and confirmed the resection level supporting the possibility of a direct suture. Two patients were treated for a neuroma in continuity one following a closed trauma of the subclavian brachial plexus and the other one for an open medio cubital injury at the forearm. In both cases, tendon transfers were required due to an incomplete recovery. These patients were treated with nerve graft after 6 and 10 months from trauma, a time frame that in most cases could be easily associated to an unsuccessful result as well. Three patients were affected by a neuroma in continuity. Two of them suffered intense pain for non-less than 6 months. Nerve reconstruction didn't solve pain even the increased nerve resection. This suggests that in this kind of pathology, where the pain is present, aspects that can't be observed through instrumental imaging are responsible for the symptomatic condition.

Certainly, a larger number of cases and a more homogenous population will allow us to better define the efficacy of the ultrasound applied into the operative field. Another limitation of the study is that we used a linear 4-15 MHz transducer. Nowadays high frequency transducers are available, but not in the operating room of our institution. Increasing the probe frequency, will increase the resolution of image.

Moreover, given the long learning curve required to clearly identify differences in intraneural architecture, it is mandatory, at least for the treatment of the first patients, the support of a radiologist specialized in peripheral nerves evaluation.

Furthermore, in this paper, just a qualitative evaluation of histological sections was performed. A better and precise correlation between the ultrasound and histological data

could be obtained through an objective quantification of the fibrotic and scar area at the level of an ultrasound and histological cross section, evaluated in the same position.

A promising field of application could be plexopathies, where even a few millimeters of resection become crucial in terms of clinical outcome. For this, an high frequency transducer of small dimension would be required considering the depth of the surgical field. In the very first cases, the support by an expert radiology in the field is fundamental to maximize the results.

The ultrasound can be effectively used to implement nerve debridement compared to macroscopical guided debridement. The more extended resection seems not to be able to increase the clinical results at least in our case series. This could possibly mean that even with a more accurate nerve resection and better quality of nerve stumps, other factors such as time from trauma, influence greatly recovery capacity. This concept is even more important in treating in-continuity painful neuromas. Our findings greatly reinforce how complex is the treatment of painful neuromas. Even a whit a specific tool able to better confirm the healthiness of neural stump, it is not possible to predict a good result.

According to our findings the use of intraoperative ultrasound during surgical procedures on post traumatic nerve injuries could increase the ability of the surgeon to better reconstruct and understand the extension of intraneural scar tissue. Sometimes this tool could influence the decision-making process, but is not able to guarantee better results.

REFERENCES

1. M. J. Malessy, S. G. van Duinen, H. K. Feirabend, and R. T. Thomeer, "Correlation between histopathological findings in C-5 and C-6 nerve stumps and motor recovery following nerve grafting for repair of brachial plexus injury.," *J. Neurosurg.*, vol. 91, no. 4, pp. 636–44, Oct. 1999
2. R. W. Koenig et al., "Intraoperative high-resolution ultrasound: a new technique in the management of peripheral nerve disorders.," *J. Neurosurg.*, vol. 114, no. 2, pp. 514–21, Feb. 2011
3. F. C. Lee, H. Singh, L. N. Nazarian, and J. K. Ratliff, "High-resolution ultrasonography in the diagnosis and intraoperative management of peripheral nerve lesions.," *J. Neurosurg.*, vol. 114, no. 1, pp. 206–11, Jan. 2011
4. M. Willsey, T. J. Wilson, P. T. Henning, and L. J.-S. Yang, "Intraoperative Ultrasound for Peripheral Nerve Applications.," *Neurosurg. Clin. N. Am.*, vol. 28, no. 4, pp. 623–632, Oct. 2017
5. H. Kubiena, M. Hörmann, W. Michlits, M. Tschabitscher, K. Groszschmidt, and M. Frey, "Intraoperative imaging of the brachial plexus by high-resolution ultrasound.," *J. Reconstr. Microsurg.*, vol. 21, no. 7, pp. 429–33, Oct. 2005
6. Lawande AD, Warriar SS, Joshi MS. Role of ultrasound in evaluation of peripheral nerves. *Indian J Radiol Imaging.* 2014;24(3):254-258
7. F. C. Lee, H. Singh, L. N. Nazarian, and J. K. Ratliff, "High-resolution ultrasonography in the diagnosis and intraoperative management of peripheral nerve lesions.," *J. Neurosurg.*, vol. 114, no. 1, pp. 206–11, Jan. 2011
8. C. L. Haldeman, C. D. Baggott, and A. S. Hanna, "Intraoperative ultrasound-assisted peripheral nerve surgery.," *Neurosurg. Focus*, vol. 39, no. 3, p. E4, Sep. 2015

9. S. S. Burks, I. Cajigas, J. Jose, and A. D. Levi, "Intraoperative Imaging in Traumatic Peripheral Nerve Lesions: Correlating Histologic Cross-Sections with High-Resolution Ultrasound.," *Oper. Neurosurg.* (Hagerstown, Md.), 2017 Apr 1;13(2):196-203
10. Osorio. JA et al., "Ultrasound-guided percutaneous injection of methylene blue to identify nerve pathology and guide surgery," *Neurosurg. Focus*, vol. 39, no. 3, 2015

3.6 Preclinical Validation of SilkBridge™ for Peripheral Nerve Regeneration

Fregnan F, Muratori L, Bassani GA, Crosio A, Biagiotti M, Vincoli V, Carta G, Pierimarchi P, Geuna S, Alessandrino A, Freddi G, Ronchi G.

Front Bioeng Biotechnol. 2020 Aug 7;8:835



Preclinical Validation of SilkBridge™ for Peripheral Nerve Regeneration

Federica Fregnan^{1,2*†}, Luisa Muratori^{1,2†}, Giulia A. Bassani³, Alessandro Crosio^{1,4}, Marco Biagiotti³, Valentina Vincoli³, Giacomo Carta^{1,2}, Pasquale Pierimarchi⁵, Stefano Geuna^{1,2}, Antonio Alessandrino³, Giuliano Freddi³ and Giulia Ronchi^{1,2}

¹ Department of Clinical and Biological Sciences, University of Turin, Turin, Italy, ² Neuroscience Institute Cavalieri Ottolenghi, University of Turin, Turin, Italy, ³ Silk Biomaterials Srl, Lomazzo, Italy, ⁴ Department of Orthopaedics and Traumatology for Hand, ASST Gaetano Pini, Milan, Italy, ⁵ Institute of Translational Pharmacology, National Research Council, Rome, Italy

OPEN ACCESS

Edited by:

Chiara Tonda-Turo,
Politecnico di Torino, Italy

Reviewed by:

Giovanni Vozzi,
University of Pisa, Italy
Stephanie K. Seidlits,
University of California, Los Angeles,
United States
Victor Carriel,
University of Granada, Spain

*Correspondence:

Federica Fregnan
federica.fregnan@unito.it

†These authors have contributed
equally to this work

Specialty section:

This article was submitted to
Biomaterials,
a section of the journal
Frontiers in Bioengineering and
Biotechnology

Received: 04 March 2020

Accepted: 29 June 2020

Published: 07 August 2020

Citation:

Fregnan F, Muratori L,
Bassani GA, Crosio A, Biagiotti M,
Vincoli V, Carta G, Pierimarchi P,
Geuna S, Alessandrino A, Freddi G
and Ronchi G (2020) Preclinical
Validation of SilkBridge™
for Peripheral Nerve Regeneration.
Front. Bioeng. Biotechnol. 8:835.
doi: 10.3389/fbioe.2020.00835

Silk fibroin (*Bombyx mori*) was used to manufacture a nerve conduit (SilkBridge™) characterized by a novel 3D architecture. The wall of the conduit consists of two electrospun layers (inner and outer) and one textile layer (middle), perfectly integrated at the structural and functional level. The manufacturing technology conferred high compression strength on the device, thus meeting clinical requirements for physiological and pathological compressive stresses. As demonstrated in a previous work, the silk material has proven to be able to provide a valid substrate for cells to grow on, differentiate and start the fundamental cellular regenerative activities *in vitro* and, *in vivo*, at the short time point of 2 weeks, to allow the starting of regenerative processes in terms of good integration with the surrounding tissues and colonization of the wall layers and of the lumen with several cell types. In the present study, a 10 mm long gap in the median nerve was repaired with 12 mm SilkBridge™ conduit and evaluated at middle (4 weeks) and at longer time points (12 and 24 weeks). The SilkBridge™ conduit led to a very good functional and morphological recovery of the median nerve, similar to that observed with the reference autograft nerve reconstruction procedure. Taken together, all these results demonstrated that SilkBridge™ has an optimized balance of biomechanical and biological properties, which allowed proceeding with a first-in-human clinical study aimed at evaluating safety and effectiveness of using the device for the reconstruction of digital nerve defects in humans.

Keywords: silk fibroin, nerve conduit, mechanical properties, *in vivo*, long-term biocompatibility, biodegradation, nerve regeneration, functional recovery

INTRODUCTION

Peripheral nerves are widely spread throughout the body and are therefore highly vulnerable to injury as a consequence of multiple causes, i.e., car accidents, domestic falls, military and sports injuries. Iatrogenic injuries and injury associated with degenerative conditions or diabetes are also very frequent (Dahlin et al., 2008a; Dahlin et al., 2008b; Cederlund et al., 2009; Haastert-Talini and Dahlin, 2018).

Peripheral nerve injuries affect 2,8% of trauma patients, many of which acquire lifelong disability (Noble et al., 1998; Taylor et al., 2008; Miranda and Torres, 2016). More than 300.000 peripheral nerve injuries are reported each year in Europe and over one million worldwide (Daly et al., 2012)

and represent a major cause for morbidity, bringing to total or partial loss of motor, sensory and autonomic functions, with a devastating impact on a patients' quality of life, especially for severe nerve injury. Associated healthcare costs are higher than €2.2 billion/year (Ciardelli and Chiono, 2006), and include not only the treatment, but also care and rehabilitation.

Although the peripheral nervous system has an intrinsic capacity to regenerate, this ability is often not sufficient and microsurgical intervention is therefore required. For short gap injuries (<5 mm), a direct end-to-end tension-free repair between the two nerve ends is usually the chosen treatment. For longer gaps (>5 mm), a graft must be used to bridge the gap between the two nerve stumps and to guide regenerating axons towards target organs. Autologous nerve graft still represents the "gold standard" technique for bridging nerve defects and provides the best properties for best achievable functional restoration (Siemionow and Brzezicki, 2009; Kornfeld et al., 2019). However, it is associated with some drawbacks, including donor nerve morbidity, the need of an additional surgery to harvest the donor nerve that may be harmful to the patients, mismatch of donor nerve size with recipient site due to structural differences and limited availability of graft material (Ray and Mackinnon, 2010; Kornfeld et al., 2019).

Is therefore necessary to develop new strategies to find a suitable alternative to autologous nerve graft. In the last decades, research has focused on developing artificial nerve guide conduits (NGCs) in terms of materials selection and design that act as guide, stimulating and accelerating regrowth of the transected nerve and additionally forming a barrier to ingrowth of connective tissue (Faroni et al., 2015; Du et al., 2018).

To date, a wide variety of new synthetic polymers and biopolymers have been evaluated. Scaffolds of natural origins provide several advantages compared to the synthetic ones, such as biocompatibility, biodegradability, non-toxic degradation products and the minimal foreign body response induction (Carriel et al., 2014).

Silk fibroin (SF) is a natural polymer produced from the silkworm and it is one of the oldest materials used in medical applications. It is a highly biocompatible material known for its ability to promote cell adhesion and proliferation and to stimulate tissue regeneration *in vivo*, with a unique combination of biological and mechanical properties (Altman et al., 2003; Rockwood et al., 2011; Catto et al., 2015; Thurber et al., 2015).

We have recently developed a new conduit made by silk fibroin (SilkBridge™ nerve conduit) consisting of a hybrid tubular structure composed by two electrospun layers (ES, made of regenerated silk fibroin fibers of sub micrometer size) coupled with an intermediate textile layer (TEX, made of native silk fibroin microfibrils) (Alessandrino et al., 2019b). This novel multi-layered SF-based nerve conduit resulted in a perfectly integrated and mechanically resistant structure with a light weight and a high porosity level in the low pore size range, all features important for an optimal nerve conduit. In the previous work, we have demonstrated the biocompatibility and biomimeticity of SilkBridge™ nerve conduit, both *in vitro* and *in vivo*. SilkBridge™ nerve conduit was able to sustain Schwann cell proliferation, neuronal differentiation and axonal elongation

in vitro. *In vivo* pilot tests conducted at 2 weeks post implantation revealed a perfect cellular colonization of the conduit and the progressive growth of the regenerating nerve fibers.

Given these promising results, in the current study we evaluated the efficiency of SilkBridge™ nerve conduit in sustaining nerve regeneration at mid (4 weeks) and longer (12 and 24 weeks) time points, in a model of rat median nerve injury, using the autologous nerve repair approach as control.

MATERIALS AND METHODS

Manufacturing of SilkBridge™

The three-layered SF-based nerve conduit (SilkBridge™) was manufactured as previously reported (Alessandrino et al., 2019a; Alessandrino et al., 2019b). Briefly, two electrospun layers (ES) were assembled onto the inner and outer faces of a tubular textile braid (TEX) according to a patented process (Alessandrino, 2017). Coupling of the TEX layer with the two ES layers was made during electrospinning, by means of a welding medium comprising a solution of 15% w/w SF dissolved in an ionic liquid (1-ethyl-3-methylimidazolium acetate; EMIMAc). After electrospinning, the hybrid ES-TEX tubular structure was consolidated by immersion in aqueous ethanol (80 vol%), followed by overnight washing with distilled water and drying. Finally, the device was purified by microwave assisted extraction with ethanol to remove processing aids, packaged under a laminar flow cabinet, and sterilized with ethylene oxide (EtO).

The main characteristics of the SilkBridge™ conduits used in the present study are: total length of the device 30 mm (reduced for the *in vivo* implantation to a length of 12 mm); inner diameter 1.60 ± 0.15 mm; wall thickness 0.50 ± 0.15 mm; weight per unit length of about 8 mg cm^{-1} ; wall porosity of about 80%; ES:TEX percent weight ratio of 60:40%.

Mechanical Characterization

Ultimate tensile strength and suture retention strength were determined on SilkBridge™ conduits, under submersed conditions (in water at 37°C), by using an All-electric Dynamic Test Instrument ElectroPuls E3000 (Instron), equipped with a 250 N load cell and a thermostatic bath (BioPuls). Both tests were performed in accordance with the provisions of the ISO 7198:2016 standard, which specifies the requirements for the evaluation of the mechanical properties of prosthetic devices with tubular shape.

For the measurement of the ultimate tensile strength, six specimens with a total length of 50 mm were used. The gage length was 30 mm, a preload of 0.5 N was applied, and the tests were run at 50 mm min^{-1} crossbar rate.

The suture retention strength is the force necessary to pull a suture from the device while pulling a suture inserted through the wall. The conduit was cut normal to the long axis and a suture was inserted 2 mm from the end of the device through the wall to form a half loop. The device was clamped in the lower fixed grip and the suture thread in the upper moving grip which was pulled at the rate of 50 mm min^{-1} . The force required to pull the suture through the device was recorded.

Animal Care, Experimental Groups and Surgery

For this study, a total of 36 adult female Wistar rats (weight approximately 200 g) were used. Animals were housed in a room with controlled conditions (temperature and humidity), with a regular light/dark cycle (12 h of light and 12 h of dark) and free access to food and water. Every attempt was made to reduce animal suffering. The study conditions were conformed to the guidelines of the European Union's Directive EU/2010/63 for animal experiments. All animal experiments were performed at the animal facility of Neuroscience Institute Cavalieri Ottolenghi (NICO) (Ministerial authorization DM 182 2010-A 3-11-2010). The current experimental study was reviewed and approved by the Ethic Experimental Committee of the University of Turin (Ministry of Health project number 864/2016).

Analyses of nerve regeneration were carried out at three time points: 4, 12, and 24 weeks. The shortest time point (4 weeks) was planned with the aim to explore the outcome of middle endpoints, i.e., middle-stage tissue response to the conduit, extracellular matrix deposition, infiltration of Schwann cells, and axon regeneration. Animals ($n = 4$) with bilateral implantation of the SilkBridge™ conduit were used. Medium-to-long term time points (12 and 24 weeks) were designed to follow the regeneration process until the steady state was achieved in terms of biological tissue response, healing of the injured nerve, and complete functional recovery. Animals ($n = 10$ for each time point) were implanted monolaterally with SilkBridge™ conduits. Control animals ($n = 6$ for each time point) with autograft implants were also included in this part of the study.

Surgeries were performed under general anesthesia, with Zolazepam (Zoletil, Virban) + Xilazina (Bayer) by intraperitoneal injection (40 mg/kg +5 mg/kg). All surgical procedures were carried out under a high magnification surgical microscope, in a clean room. Nerve lesions were performed on the median nerves. The median nerve of both forelimbs of the 4 weeks experimental group was transected (10-mm gap) and a 12-mm long SilkBridge™ conduit was used to bridge the nerve defect by inserting 1 mm of each nerve end inside the conduit. The nerve conduit was sutured with one 9/0 epineural stitch at each end (Figures 2A–D). SilkBridge™ conduits were immersed in sterile saline for at least 5 min before implantation.

In all the other animals (12 and 24 weeks experimental and control groups), the median nerve of the right forelimb was approached from the axillary region to the elbow, the nerve was transected at the middle third of the brachium and its proximal stump was sutured with 9/0 epineural stitch to the *pectoralis major muscle* to avoid spontaneous reinnervation. Afterwards, the left median nerve was transected and immediately repaired according to the experimental group. For the SilkBridge™ conduit group, the gap was bridged with a 12-mm long conduit as described above (Figures 2A–D). For the autograft group, the 10-mm nerve segment was cut out, reversed (distal – proximal), and sutured to the nerve ends with 9/0 epineural stitches. At the end of the surgical procedure, the skin was sutured with a 3/0 stitch. At day 0, 1, 2, and 3 post-surgery, analgesic therapy with Rymadil (4 mg/Kg, Zoetis Italia) was administered by subcutaneous

injection, while at day-1 pre-surgery, 2 and 5 post-surgery, the antibiotic treatment (Rubrocillina 0.05 ml/500 g, MSD animal health) was administered by intramuscular injection. The general health status of animals was evaluated by experienced personnel considering the following parameters: shine rat fur, reactivity, general health, and aspect of surgical wound. Animals were observed at day-7 pre-implantation, at day 0 before surgery, and at day 1, 2, and 3 post-surgery. From the 2nd week after surgery weekly routine monitoring was carried out regularly. Weight evolution of animals was also recorded at day-1 and every 3 weeks post-surgery. The last observation coincided with the last day of procedure.

The last day of procedure rats were sacrificed through anesthetic overdose of Zoletil + Xilazina (>60 and >10 mg/kg) by intraperitoneal injection. The surgical site was exposed, and the nerve samples were harvested and processed for further examination. The *superficialis flexor muscles* were harvested and weighted.

Evaluation of Nerve Regeneration After 4 Weeks: Histological Procedures

Four nerve samples harvested after 4 weeks were fixed in 4% paraformaldehyde for 2 h, washed in a solution of 0.01 M PBS (pH 7.2) for 30 min. For Crio-embedding procedure, specimens were rehydrated with PBS (Sigma) and cryo-protected with three passages in increasing solutions of sucrose (Sigma) (7.5% for 1 h, 15% for 1 h, 30% overnight) in 0.1 M PBS. Thereafter, specimens were maintained in a 1:1 solution of sucrose 30% and optimal cutting temperature medium (OCT, electron microscopy sciences) for 30 min and then embedded in 100% OCT. Sections were cut 10 μ m thick and processed for Masson's trichrome staining or immunofluorescence. The other four nerve samples were fixed by immediate immersion in 2.5% glutaraldehyde (SIC, Società Italiana Chimici) in 0.1 M phosphate buffer (pH 7.4) for 5.6 h, at 4°C and subjected to resin embedding, high resolution light microscopy and transmission electron microscopy.

Masson's Trichrome Staining

Masson's trichrome staining was performed on cryo-embedded longitudinal section according to Masson trichrome with aniline blue kit (Bio-Optica). After staining, slides were washed in distilled water, rapidly dehydrated in ethanol and cleared in xylol/Bioclear (Bio-Optica). Finally, samples were mounted with DPX mountant (Fluka).

Immunofluorescence and Confocal Laser Microscopy

Crio-embedded longitudinal sections were permeabilized, blocked with 0.1% triton X-100, 10% normal goat serum for 1 h and incubated overnight with the primary antibodies anti-NF 200 kDa (monoclonal, mouse, Sigma Aldrich) and S-100 (polyclonal, rabbit, Sigma Aldrich). After primary antibodies incubation, sections were washed three times in PBS and incubated for 1 h in a solution containing the secondary antibodies Alexa 488 anti-Mouse and Cy3 anti-Rabbit (Life Technologies). Nuclei were stained with 4,6-diamidino-2-phenylindole (DAPI, Sigma) diluted 1:1000 in PBS. After three washes in PBS, sections were mounted with a Dako fluorescent mounting and

analyzed using a Zeiss LSM800 confocal laser microscopy system (Zeiss, Jena, Germany).

High Resolution Light Microscopy and Transmission Electron Microscopy

The nerve samples fixed in 2.5% glutaraldehyde were post-fixed in 2% osmium tetroxide (SIC, Società Italiana Chimici) for 2 h and dehydrated in passages in ethanol (Sigma Aldrich) from 30 to 100% (5 min each passage). After two passages of 7 min in propylene oxide, one passage of 1 hour in a 1:1 mixture of propylene oxide (Sigma Aldrich) and Glauerts' mixture of resins, samples were embedded in Glauerts' mixture of resins (made of equal parts of Araldite M and the Araldite Harter, HY 964, Sigma Aldrich). In the resin mixture, 0.5% of the plasticizer dibutyl phthalate (Sigma Aldrich) was added. For the final step, 2% of accelerator 964 was added to the resin in order to promote the polymerization of the embedding mixture, at 60°C. Transverse semi-thin sections (2.5 μm thick) were cut inside the conduit (both proximally and distally) using an Ultracut UCT ultramicrotome (Leica Microsystems, Wetzlar, Germany) and stained with 1% toluidine blue for high resolution light microscopy using a DM4000B microscope equipped with a DFC320 digital camera. Ultra-thin sections (70 nm thick) were cut with the same ultramicrotome. Sections were analyzed using a JEM-1010 transmission electron microscope (JEOL, Tokyo, Japan) equipped with a Mega-View-III digital camera and a Soft-Imaging-System (SIS, Münster, Germany) for the computerized acquisition of the images.

Evaluation of Nerve Regeneration After 12 and 24 Weeks

Grasping Test

The grasping test on 12 and 24 weeks experimental and control groups was performed every 3 weeks. The last observation coincided with the last day of procedure. The aim of the test was to evaluate the functional recovery of the operated nerve by assessing the flexor muscle strength. The animal was gently lifted by holding its tail and allowing it to grasp a grid connected to an electronic balance (BS-GRIP Grip Meter). The quantitative assessment was made by measuring the maximum weight that the rat was able to hold before losing its grip. Each animal was tested three times and the average was considered.

Quantitative Assessment of Myelinated Regenerated Nerve Fibers

Transverse semi-thin sections (2.5 μm thick) were cut distally to the conduit/autograft and stained with 1% toluidine blue for high resolution light microscopy examination and design-based stereology. A DM4000B microscope equipped with a DFC320 digital camera and an IM50 image manager system (Leica Microsystems, Wetzlar, Germany) was used for section analysis. For the stereological analysis, the following parameters were evaluated: (i) number of fibers; (ii) density of fibers; (iii) diameter of fibers and axons; (iv) myelin thickness; and (v) axon diameter/fiber diameter ratio (g-ratio). Sections were randomly selected and analyzed for the measurement of the total cross-sectional area of the nerve. The stereological assessment was

performed according to a previously described method (Geuna, 2000; Geuna et al., 2000). 2D dissector probes were also used to select unbiased representative samples of myelinated nerve fibers.

Assessment of Biomaterial Behavior After Implantation

Analysis of New-Generated Vessels

The process of angiogenesis within the SilkBridge™ conduits was assessed by quantifying new blood vessel formation in resin-embedded transverse semi-thin sections. On one randomly selected semi-thin section taken in the central portion of the conduit, 8–10 fields were selected using a systematic random sampling protocol, with a magnification of 40 \times . The two-dimensional dissector procedure was adopted for the quantification (Geuna, 2000). Blood vessel density was then calculated. Finally, the diameter of the vessels was measured, and the vessel diameter distribution was obtained.

Biomaterial Degradation

SilkBridge™ conduit degradation was evaluated both qualitatively and quantitatively. For qualitative analysis, the behavior of the conduit wall (consisting in three layers: inner and outer electrospun layers and middle textile layer) was carefully analyzed in semi-thin cross sections in order to observe and describe any variation compared to the non-implanted conduit.

Quantitative analysis of conduit degradation was focused on the two electrospun layers (inner and outer), since they are in direct contact with surrounding tissue (outside) and regenerating nerve fibers (inside). These two layers are made by silk fibroin fibers of sub micrometer size, and the analysis was therefore done with the transmission electron microscopy on ultra-thin cross sections. 15–20 fields were selected using a systematic random sampling protocol, with a magnification of 20000 \times , and a total of 350 fibers for each group were measured. As control, we used SilkBridge™ conduits implanted for 2 weeks.

Statistical Analysis

Statistical analysis was performed using R Statistical Software (Foundation for Statistical Computing, Vienna, Austria). After data normality was tested (Levene and Mauchly tests), one-way analysis of variance (ANOVA) and ANOVA for repeated measures tests with Tukey's correction were adopted to detect the effect of time, experimental groups, and their interaction and to highlight the significant differences among the Autograft group and the SilkBridge™ group at each time point tested. Two one-sided tests (TOST) equivalence test was used to assess the effect of the two different interventions (**Supplementary Material**). The Cohen's *d* obtained between beginning and end values of the Autograft group was adopted as the smallest effect size and set as a reference for the TOST test. The two sided paired Student's T test was adopted to compare data on vessel morphology and 95% Confidence Intervals (CI) were reported (Mascha and Sessler, 2011). The effect size was defined for each factor as partial eta-squared (η^2) small 0.02, medium 0.13 and large 0.26. The level of significance was set at $p \leq 0.05$ (*), $p \leq 0.01$ (**), $p \leq 0.001$ (***), and $p \leq 0.000$ (****). Values were expressed as mean \pm SD (standard deviation).

RESULTS

Mechanical Characterization

The mechanical characterization discussed in this paper complements the results previously reported (Alessandrino et al., 2019a; Alessandrino et al., 2019b) which referred specifically to the behavior of the conduit subjected to transversal stresses in the compression mode. Here, the mechanical properties of the SilkBridge™ conduit are investigated in the longitudinal direction, by testing the ultimate tensile strength and the suture retention strength. The results of tensile and suture retention strength are listed in **Supplementary Table S1**. **Figure 1B** shows typical load-elongation curves of the SilkBridge™ conduit measured under submersed condition at 37°C. A schematic representation of the 3D architecture of the conduit is also presented in **Figure 1A**.

The SilkBridge™ conduit breaks at high strength values when subjected to a force applied in the longitudinal direction, thanks to its hybrid electrospun/textile architecture (**Supplementary Table S1**). The braided TEX structure encased between the two ES layers is the load-bearing component of the device (**Figure 1A**). In terms of ultimate tensile strength, SilkBridge™ outperforms not only natural peripheral nerves (Chiono and Tonda-Turo, 2015), but also many other nerve conduit devices made only by electrospun fibers, either based on SF (Dinis et al., 2015) or on other polymers such as PLGA (Hou et al., 2019), PCL (Quan et al., 2019), and PU/gelatin (Salehi et al., 2018). With reference to other nerve conduits with a braided texture made of native SF microfibers (Pillai et al., 2019) or other polymer fibers (PLA/PGA) (Ichihara et al., 2015), the mechanical performance may be similar or better depending on the construction parameter of the textile structure (yarn and fiber size, knit density, etc.). Usually, the denser and thicker the textile texture, the stiffer the device, which might become a drawback in terms of biomechanical compliance at the site of implantation. In fact, when a load is first applied to a resting natural nerve, its length increases with minimal increase of the tensile load as a result of straightening of the wavy

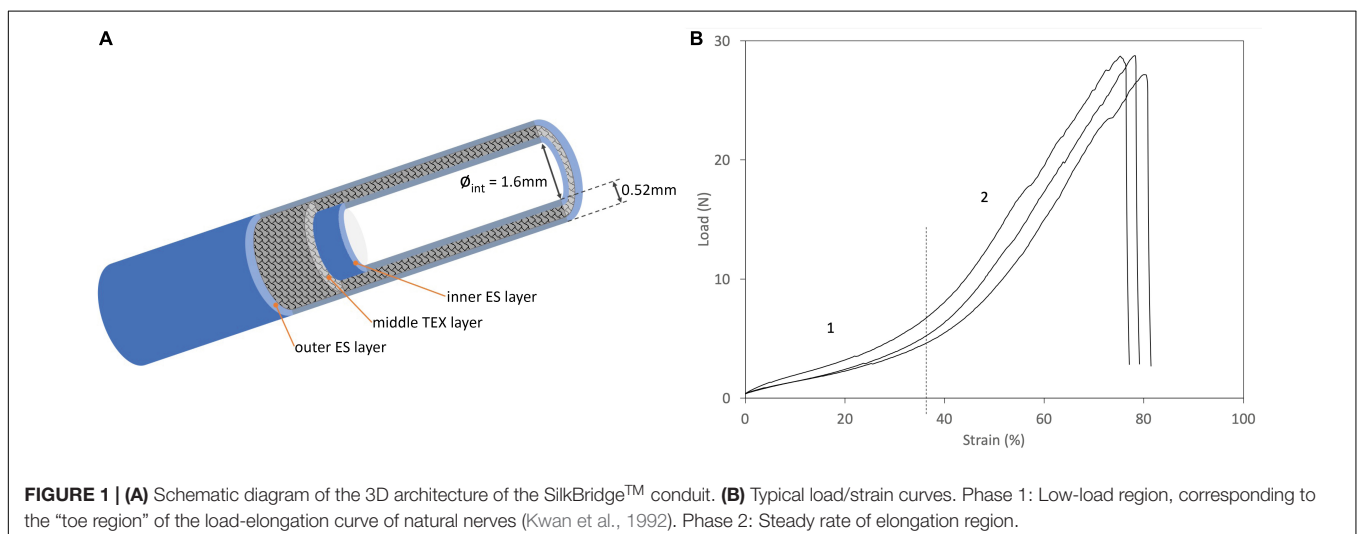
connective tissue and axons in the endoneurial compartment (Topp and Boyd, 2006). This is called the “toe region” of the load-elongation curve of natural nerves (Kwan et al., 1992). As the tensile load is further increased, the nerve elongates at a steady rate, showing a steeper linear region of the load-elongation curve before ultimate failure. Interestingly, the combination of two electrospun layers with an open-texture textile layer of braided silk microfibers results in a load-elongation curve with two distinct phases (**Figure 1B**) that mimics the tensile behavior of natural nerves (Kwan et al., 1992), as well as of other soft tissues (Holzapfel and Weizsacker, 1998). Therefore it is possible to deduce that the SilkBridge™ conduit, which displays a balanced combination of strength and elasticity, might be more biomechanically compliant with natural nerves than other devices where a much higher ultimate tensile strength was reached at the expenses of a dramatic loss of elasticity, especially in correspondence of the “toe region” of the natural nerve (Zhang et al., 2019).

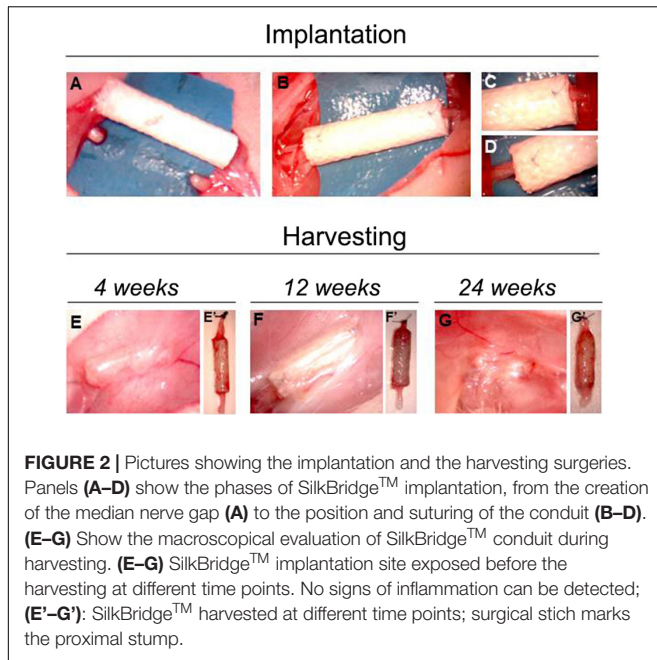
The hybrid electrospun/textile structure of SilkBridge™ is also beneficial for the achievement of high values of suture retention strength (**Supplementary Table S1**). With the 9/0 suture, the same used for implanting the device in the animal study, the test ends with the failure of the suture at about 117 gf (**Supplementary Table S1**). Failure of the device occurred at about 460 gf using a thicker suture stich (5/0). These results confirm that the suturing process can be easily and safely performed during the grafting surgery, and that failure after surgery can be reasonably considered an unexpected event for the SilkBridge™ conduit.

Assessment of Medium and Long-Term Nerve Regeneration

Surgical Procedures, Animal Welfare, and Macroscopic Evaluations

As already demonstrated in a previous work (Alessandrino et al., 2019b) SilkBridge™ showed optimal mechanical parameters during surgery, including easy handling and suturability, and





adequate stiffness and flexibility. During post-operative period, all animals were in good health. None of them showed signs of inflammation, pain, discomfort or auto-mutilation of the operated arm. As an indicator of animal welfare, the body weight was measured. No sudden decrease in weight was observed and animals showed a physiological increase in body mass throughout the experiment (data not shown).

At the time of sample harvesting, all conduits were still clearly recognizable. They were encapsulated in a thin layer of connective tissue. No signs of inflammation, foreign body reactions or scar tissue formation around the conduit was detected, confirming the good biocompatibility of SilkBridge™ (Figures 2E–G).

Medium-Term Nerve Regeneration

We observed the nerve morphology in the medium period of regeneration (4 weeks post-surgery) using histological staining, immunohistochemical labeling and electron microscopy analysis (Figure 3).

Longitudinal sections stained with Masson's trichrome staining revealed a thin layer of connective tissue surrounding the outer side of SilkBridge™ and the absence of scar tissue formation. Moreover, a reach cellular population colonizing the full length of the conduit was observed (Figure 3A).

Immunohistochemical examination revealed many neurofilament positive regenerated nerve fibers surrounded by S-100 positive Schwann cells, especially in the proximal and mid portion of the conduit (Figures 3B–E) indicating the progression of nerve regeneration throughout the conduit.

In the proximal portions of the conduit, semi-thin toluidine blue-stained transverse sections revealed many well-myelinated axons (Figures 3G,H), visualized also through electron microscopy analysis (Figure 3I). In the distal portions of the

conduit, semi-thin toluidine blue-stained transverse sections did not allow the visualization of regenerated myelinated nerve fibers (Figure 3M). However, electron microscopy analysis revealed numerous unmyelinated fibers and few regenerating fibers with a thin myelin sheath, indicating that the myelination process was still in progress in the distal portion of the conduit (Figures 3N,O).

Finally, many blood vessels, some of them with big diameter, were detected not only in the lumen of the conduit (Figures 3H–M) but also among the layers of the wall throughout the full length of the conduit (not shown).

Long-Term Nerve Regeneration

The effectiveness of SilkBridge™ in stimulating nerve regeneration was then evaluated at long-term time points (12 and 24 weeks) and was compared to the “gold standard” technique (Autograft).

Functional recovery was investigated starting from 3 weeks until 12 or 24 weeks by means of the grasping test. The graph in Figure 4 (Figure 4A) reports the post-traumatic time course of functional recovery. The function of the finger flexor muscles innervated by the median nerve started recovering faster in the Autograft group, as indicated by the statistically different performance recorded at weeks 6 ($p < 0.000$) and 9 ($p < 0.001$) after lesion. Animals implanted with SilkBridge™ started recovering at weeks 6 and then progressively improved. With exception of the weeks 15 ($p < 0.002$) time point, where SilkBridge™ and Autograft groups still showed a statistically significant difference, at 12 weeks ($p = 0.105$) and then from 18 weeks ($p = 0.152$) until the end of the test, no significant differences were possible to be observed between the two experimental groups (21 weeks: $p = 0.086$; 24 weeks: $p = 0.153$). The within subjects test revealed a significant effect for time ($F[8,196] = 262.91$, $p < 0.000$, $\eta^2 = 0.91$), treatment ($F[1,196] = 85.11$, $p < 0.000$, $\eta^2 = 0.30$) and time x group ($F[8,196] = 9.64$, $p < 0.000$, $\eta^2 = 0.28$) factors.

As an additional indicator of motor recovery, the forelimb *finger flexor superficialis* muscles were harvested from both SilkBridge™ and Autograft animals and their fresh weight was determined (Figure 4B). The weight of the muscles increased significantly from 12 to 24 weeks ($F[1,26] = 9.997$, $p < 0.003$, $\eta^2 = 0.28$), but no significant differences were observed between the two groups ($F[1,26] = 0.507$, $p < 0.483$, $\eta^2 = 0.02$) and within time ($F[1,26] = 0.183$, $p < 0.673$, $\eta^2 = 0.01$). This result that underscores the good performance of animals that underwent nerve reconstruction by means of the SilkBridge™, is in good agreement with the trend evidenced by functional recovery tests.

Stereological and morpho-quantitative analysis of regenerated nerve fibers were performed on toluidine blue-stained semi-thin cross sections, just distally to the graft. At 12 weeks after nerve reconstruction, regenerated nerves from SilkBridge™ and Autograft groups showed many re-growing myelinated fibers organized in microfascicles, with well-defined axoplasm and well-organized myelin sheaths (Figures 5A–D). Quantitative stereological analysis of semi-thin sections revealed that the cross-sectional area of the nerve regenerated (Figure 5E) decreased but not significantly from 12

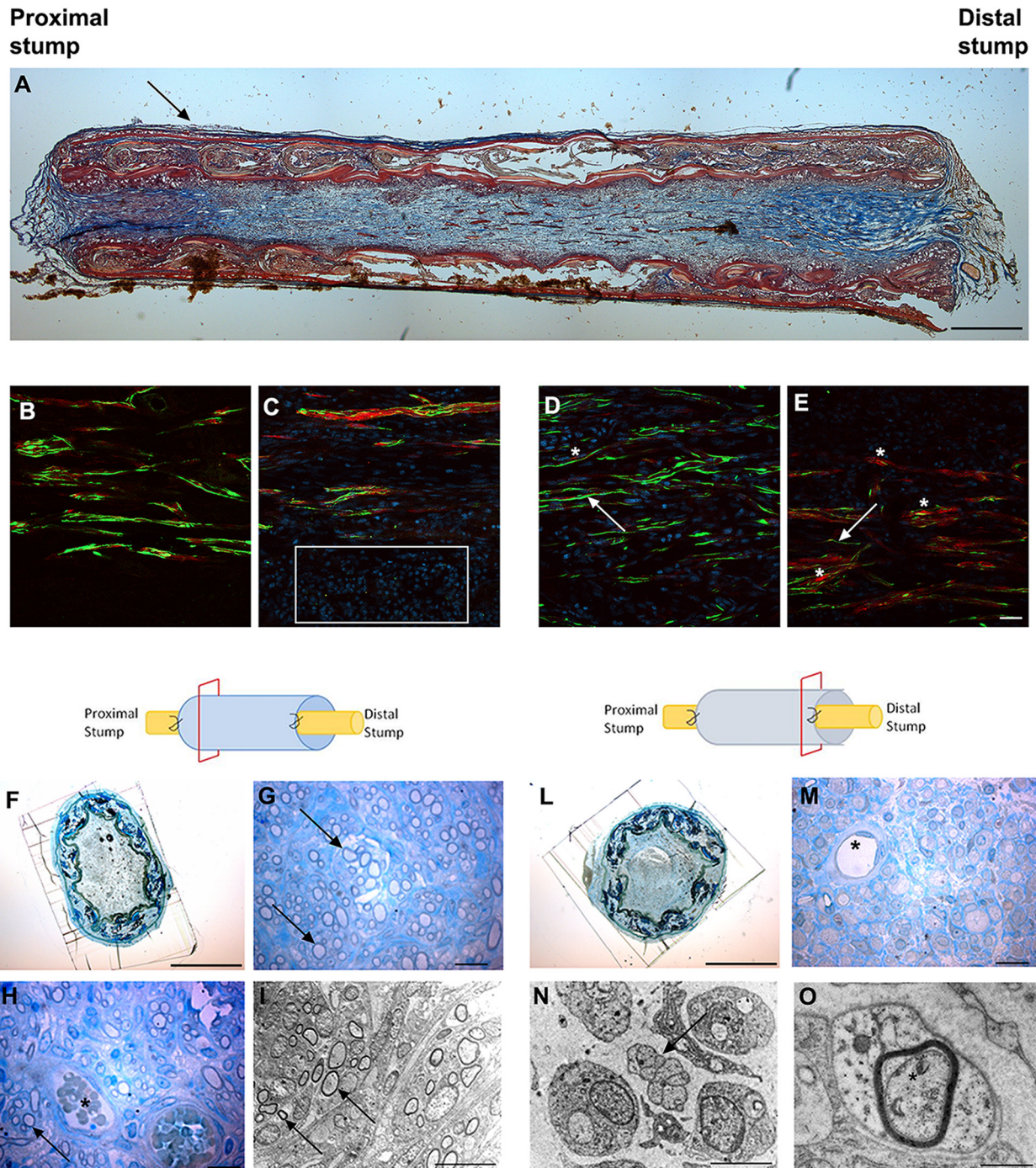
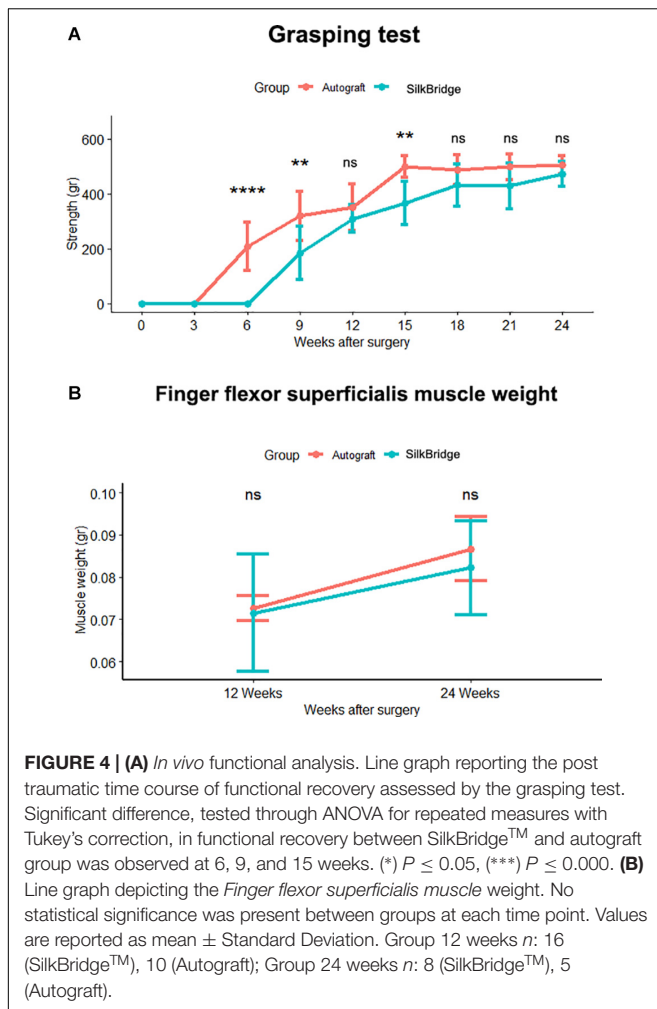


FIGURE 3 | Images showing the morphological evaluation of nerve regeneration inside SilkBridge™ nerve conduit at 4 weeks. **(A)** Representative longitudinal section of repaired median nerve analyzed by Masson's trichrome staining. Black arrow indicates the layer of connective tissue. Scale bar: 1000 μm . **(B–E)** Representative immunofluorescence staining performed on proximal and central part of SilkBridge™ conduit. Scale bar: 20 μm ; **(B)** Nerve fibers and Schwann cells in the proximal stump; **(C)** Several nuclei (DAPI-blue, white box) and regenerated nerve fibers localized within the conduit; **(D,E)** Positive neurofilament fibers surrounded by S-100 positive Schwann cells in the center of the conduit. White arrows indicate nerve fibers (green); asterisk indicate the Schwann cells (red). **(F–H)** Representative high resolution light micrographs of toluidine blue-stained semi-thin proximal cross sections; **(G,H)** Black arrows indicate regenerated nerve fibers in the proximal part of the conduit, while blood vessels are marked by asterisks. **(I)** Representative electron microscopy images of regenerated median nerve (nerve fibers black arrows) taken inside the grafts, proximally. **(L,M)** Representative high resolution light micrographs of toluidine blue-stained semi-thin distal cross sections; **(N,O)** Representative electron microscopy images of regenerated median nerve taken inside the grafts, distally, at different magnifications. Black arrows underlie the presence of unmyelinated fibers, the asterisk marks the presence of a myelinated fiber with a thin myelin sheath. **(H–M)** Asterisk indicates blood vessels. Scale bar **(F,L)**: 1000 μm ; Scale bar **(G,H,M)**: 20 μm ; Scale bar **(I,N)**: 10 μm ; Scale bar **(O)**: 1 μm .



to 24 weeks ($F[1,22] = 0.971$, $p = 0.335$, $\eta^2 = 0.04$), inside the SilkBridge™ conduit (and measured distally to the conduit). It was significantly smaller than that of the Autograft group ($F[1,22] = 8.745$, $p < 0.007$, $\eta^2 = 0.28$) but, no significant differences were observed between the two groups and within time ($F[1,22] = 0.278$, $p < 0.604$, $\eta^2 = 0.01$).

The density of myelinated fibers was similar in both groups (**Figure 5F**) and no effect of time ($F[1,22] = 1.057$, $p = 0.315$, $\eta^2 = 0.05$), treatment ($F[1,22] = 1.116$, $p = 0.302$, $\eta^2 = 0.05$) and time by treatment was significant ($F[1,22] = 3.947$, $p = 0.060$, $\eta^2 = 0.15$).

The total number of myelinated fibers showed no significant difference between the two groups ($F[1,22] = 3.933$, $p = 0.060$, $\eta^2 = 0.152$) and no time ($F[1,22] = 4.096$, $p = 0.055$, $\eta^2 = 0.157$) nor time by treatment effect was detected ($F[1,22] = 0.714$, $p = 0.407$, $\eta^2 = 0.031$; **Figure 5G**). The highest density of myelinated fibers in the Autograft group of about 1033.26 n/fibers was not significantly superior to the SilkBridge™ conduit group ($p = 0.061$, 95% CI: $-47.20-2113.73$).

Noteworthy, g-ratio (**Figure 5H**), one of the more reliable morphological predictors of nerve recovery, was significantly different between the two time points ($F[1,22] = 9.978$, $p < 0.005$,

$\eta^2 = 0.312$) but, no significant effect was detectable for type of intervention ($F[1,22] = 2.440$, $p = 0.133$, $\eta^2 = 0.10$) and intervention by time factor ($F[1,22] = 0.075$, $p = 0.787$, $\eta^2 = 0.003$). The mean difference of g-ratio between Autograft and SilkBridge™ conduit group of about 0.001 is not significant ($p = 0.132$, 95% CI: $-0.01-0.03$).

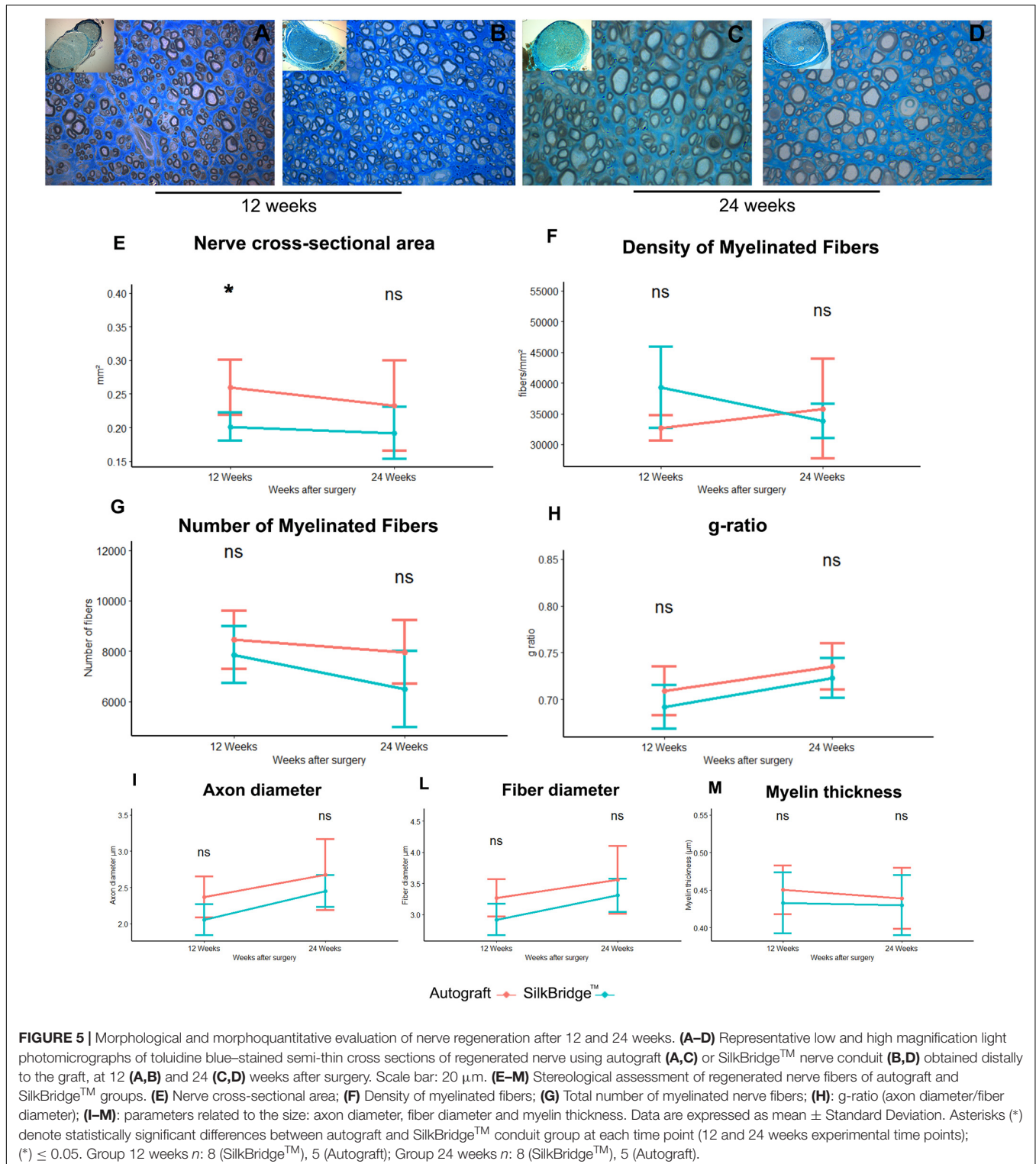
After 24 weeks, the regenerating nerves continued their maturation process in terms of fiber size and myelin organization, as evidenced by the histological details (**Figures 5C,D**). The stereological parameter that were significantly different at 12 weeks between SilkBridge™ and Autograft groups (nerve cross-sectional area) resulted to be similar at 24 weeks (**Figure 5E**). Furthermore, myelin thickness was not affected by treatment ($F[1,22] = 0.409$, $p = 0.7$, $\eta^2 = 0.007$), time ($F[1,22] = 0.152$, $p = 0.7$, $\eta^2 = 0.007$) or interaction between those factors ($F[1,22] = 0.068$, $p = 0.797$, $\eta^2 = 0.003$). The mean difference of myelin thickness between Autograft and SilkBridge™ conduit group of about 0.013 is not significant ($p = 0.408$, 95% CI: $-0.02-0.05$). Considering the fiber diameter a significant effect was detected for time and treatment factors ($F[1,22] = 7.125$, $p < 0.014$, $\eta^2 = 0.245$; and $F[1,22] = 4.864$, $p = 0.038$, $\eta^2 = 0.181$) but not for their interaction ($F[1,22] = 0.138$, $p = 0.713$, $\eta^2 = 0.006$). The fiber diameter in the Autograft group was significantly superior to the SilkBridge™ group of about $0.298 \mu\text{m}$ ($p < 0.038$, 95% CI: $-0.02 - 0.05$). Referring to the axons diameter a significant effect was detected for time and treatment factors ($F[1,22] = 9.739$, $p < 0.005$, $\eta^2 = 0.307$; and $F[1,22] = 5.159$, $p = 0.033$, $\eta^2 = 0.190$) but not for their interactions ($F[1,22] = 0.124$, $p < 0.728$, $\eta^2 = 0.006$). The axon diameter in the Autograft group was significantly superior to the SilkBridge™ group of about $0.271 \mu\text{m}$ ($p < 0.024$, 95% CI: $0.02-0.052$).

Biomaterial *in vivo* Long-Term Implantation

Morphometrical Analysis of New-Generated Vessels

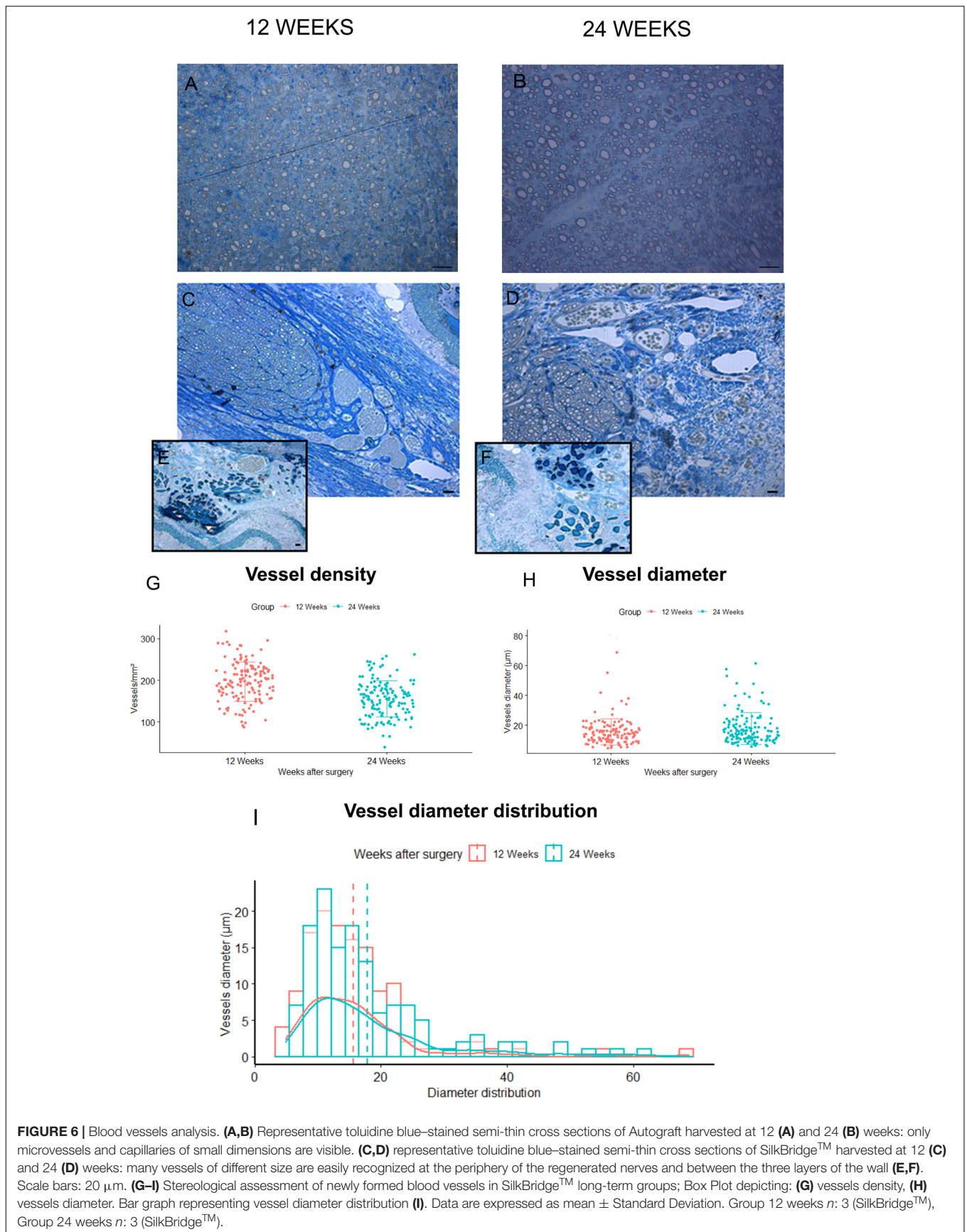
The morphological aspect of the regenerated tissue inside the grafts was assessed through toluidine blue-stained semi-thin cross sections obtained from the mid-portion of SilkBridge™ experimental groups (**Figures 6C-F**). Micrographs at low magnifications (**Figures 6C,D**) showed that regenerated myelinated axons grown inside SilkBridge™ were organized and packed in the central part of the conduit. Extracellular matrix, cells and blood vessels colonized the portion between the wall of the conduit and the regenerated fibers. On the other hand, the whole cross-section of the Autograft was full of regenerated fibers (**Figures 6A,B**).

Regarding blood vessels in the SilkBridge™ experimental groups, a quantitative analysis was conducted in order to estimate their density and size (**Figures 6G-I**). In particular, blood vessel with a diameter bigger than $7 \mu\text{m}$ (and therefore easily recognizable in toluidine blue-stained sections) were considered. It has been observed with interest that, in the two regenerative timepoints examined a large number of newly formed blood vessels were found in SilkBridge™ (**Figures 6G-I**). Despite no significant differences were detected between 12 and 24 weeks



(Figures 6G,H) considering vessels density ($t[1,135] = 7.62$, $p = 0.063$, 95% CI: $-52.4 - -31.2$) and diameter ($t[1,135] = 0.47$, $p = 0.068$, 95% CI: $-0.16 - 4.58$) a slight tendency to vessel maturation was observed over time (Figure 6H). Their localization was particularly found at the periphery of the

regenerated tissue, very close to the wall (Figures 6C–D) and in addition, blood vessels of varying dimensions were also found between the three layers of the conduit wall (Figures 6E,F). No vessels of this dimension were found in Autograft groups, only microvessels and capillaries of small dimensions (Figures 6A,B).



Biomaterial Degradation

The degradation of SilkBridge™ was evaluated qualitatively by high resolution light microscopy and quantitatively by transmission electron microscopy. The morphological analysis was performed in order to highlight the interaction between the conduit, the cells, and the extracellular matrix as well as to evidence any discontinuity of its original shape and structure; the stereological analysis was performed to evaluate changes in electrospun fibers diameter overtime. The 2 week timepoint, the shortest post-operative timepoint tested *in vivo* and described in Alessandrino et al. (2019b), was chosen as control for the comparison of degradation. This allowed to observe a sample not yet degraded but bearing some structural modifications caused by the *in vivo* environment.

In non-implanted SilkBridge™ the three layers of the conduit wall (the outer-ES-o, the inner-ES-i and the middle textile-TEX layer) are well defined and organized (Figure 7A); at higher magnification more details are detectable: the two ES layers are homogeneous and packed with TEX in the middle (Figures 7B,C).

After 2 weeks of nerve repair through SilkBridge™ conduit the wall structure is still conserved: at low magnification a thin layer of connective tissue is visible on the ES-o layer suggesting an integration of the conduit with the surrounding tissue (Figure 7D); at higher magnification many cells and extracellular matrix colonized both the ES-o and ES-i layers (Figures 7E,F). After 12 weeks of implantation, a morphological integrity of the structure (Figure 7G) can still be appreciated at low magnification. Interestingly, at higher magnification, large portions of the ES-o layer appeared still compact, whereas more boundary regions started losing their compactness with extracellular matrix growing between the electrospun fibers sub-layers (Figure 7H). The same is detectable on the ES-i, proving an onset of degradation with variable intensity, with flaked areas at different degrees (Figure 7I). After 24 weeks, the ES-o layer was still continuous, displaying regions of high compactness, and others with flaked ES-o sub-layers forming two or more arrays of thinner layers (Figure 7L). At higher magnification, electrospun fibers at the outer limit of the ES-o layer progressively lost contact with each other. The extracellular matrix filled the inter-fiber areas, showing only a slight progression compared to the 12 weeks-time point (Figure 7M). On the contrary, the ES-i layer underwent greater modification since discontinuities along its circumferential path were observed in various regions. Moreover, the initial layer compactness was sensibly lost and individual electrospun fibers were fully embedded in the extracellular matrix showing a full integration of the material with the regenerated tissue (Figure 7N).

The conduit degradation analysis was continued with the quantification of the electrospun fibers diameter of the inner and outer ES layers at 2, 12, 24 weeks post implantation (Figure 7O).

Results showed a reduction of the SilkBridge™ electrospun fibers diameter of both inner and outer ES layers overtime. In particular the inner ES layer had shown a significant difference between 12 and 24 weeks ($t[1,30] = 3.87, p < 0.01$) and the outer ES layer between 2 and 12 weeks ($t[1,30] = 3.25, p < 0.03$). Those data are in complete agreement with what was observed in the morphological analysis (Figure 7P).

DISCUSSION

Despite the intrinsic ability of peripheral nerve to regenerate, clinical and experimental evidence shows that regeneration is often unsatisfactory especially following severe nerve injury (Navarro et al., 2007). For lesions with loss of substance, the nerve autograft represents the surgical gold standard, despite the secondary effects of this technique (additional surgery, scarring, donor-site morbidity, and limited source of donor nerves) (Battiston et al., 2009).

Over the past ten years, advances in tissue engineering have led to obtain decellularized nerve allografts (Philips et al., 2018; Chato-Astrain et al., 2020) which allow to maintain the three-dimensional structure to sustain axonal growth, while being cleaned of the antigenic component. Recent papers reported the advantages of this technique and the achievement of some regenerative parameters obtained with allograft (Lovati et al., 2018; Chato-Astrain et al., 2020). However, further research is needed to optimize preparation protocols, improve effectiveness, especially for the repair of long nerve defects.

In parallel, a wide variety of new synthetic polymers and biopolymers have been evaluated. Scaffolds of natural origins are able to provide biocompatibility, biodegradability, non-toxic degradation products and a minimal foreign body response induction (Carriel et al., 2014). Authors have reported of biologically active devices whose lumen has been enriched through nanostructures and/or stem cells, capable of directing axonal growth and providing trophic factors and molecules in support of mechanical cues (Chato-Astrain et al., 2018).

When a simple biomaterial of natural origin, like silk, is also bioactive, the creation of a conduit equipped with a multi-layered wall can be a simple but effective response in a repair intervention of nerve damage with loss of substance (Alessandrino et al., 2019b).

SilkBridge™ conduit is a tubular device whose wall is made by silk fibroin, a natural polymer produced by the silkworm *Bombyx mori*, that displays an optimum combination of strength and elasticity to withstand clinical operation stresses, such as manipulation and suturing during implantation, to resist deformation caused by biomechanical *in vivo* stresses, and to avoid channel collapse since compression can result in damage to the growing axon (Altman et al., 2003; Rockwood et al., 2011; Catto et al., 2015; Thurber et al., 2015). The wall of SilkBridge™ is composed by three layers manufactured using a new combination of electrospinning and textile technologies that allows combination of micro- (to optimize the mechanical properties) and sub micro- (to maximize the biological characteristics of the material) fibrous elements (Alessandrino et al., 2019a; Alessandrino et al., 2019b).

In a previous work (Alessandrino et al., 2019b), the mechanical, structural and biological properties of SilkBridge™ have been demonstrated. The wall thickness of about 0.5 mm and the wall porosity > 80% fall in the optimum range of geometric parameters able to ensure nutrient, oxygen, and metabolite transport and exchange with the surrounding environment, thus providing support to the regenerating axon (Kokai et al., 2009; Nectow et al., 2012; Chiono and Tonda-Turo, 2015). The conduit presents an optimal capability to resist to compression

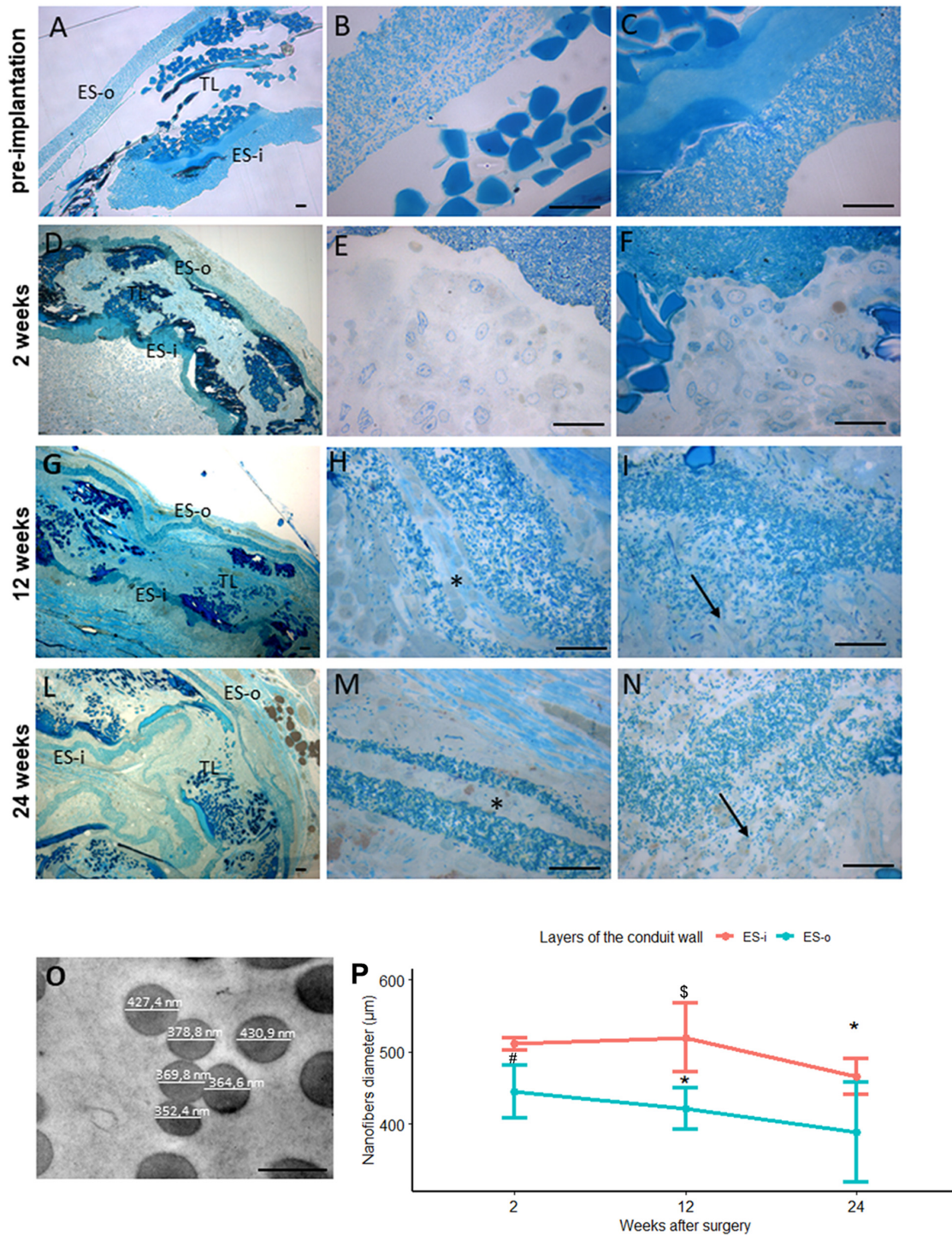


FIGURE 7 | Evaluation of biomaterial degradation. **(A–N)** Representative high resolution light photomicrographs of toluidine blue–stained semi-thin cross sections showing the behavior of the SilkBridge™ conduit wall at different time points. **(A–C)** SilkBridge™ not implanted; **(D–F)** SilkBridge™ implanted for 2 weeks, **(G–I)** for 12 weeks and **(L–N)** for 24 weeks. **(A,D,G,L)** low magnification showing the three layers of SilkBridge. Scale bars: 20 µm; **(B,E,H,M)**: magnification of the outer ES-o layer. Scale bars: 20 µm; **(C,F,I,N)**: magnification of the inner ES-i layer. Scale bar: 20 µm; **(O)**: representative image of electrospun fibers of the ES layer with diameter measurements. Scale bar: 0,5 µm. ES-o: ES outer layer; ES-i: ES inner layer; TL: TEX layer. **(H,M-asterisks)** the ES outer layer that in some cases divides in two thinner layers; **(I,N-arrows)** the electrospun fibers dispersion in the ES inner layer. **(P)** Line graph depicting the quantification of the electrospun fiber diameter constituting the external ES wall (ES-o) and the internal ES wall (ES-i) of the SilkBridge conduit. Data are expressed as mean ± Standard Deviation. Significant differences within each time point are reported (*) $P \leq 0.05$. \$ indicates the statistically significant difference in fibers diameter of inner ES layer between 12 and 24 weeks; #Indicates the statistically significant difference in fibers diameter of outer ES layer between 2 and 12 weeks. n :350 fibers analyzed for each experimental group.

stresses, being able to resist to both physiological and pathological compressive stresses (Topp and Boyd, 2006), thus meeting an indispensable property for clinical application. From the biological point of view, the conduit has proven to be a good substrate for Schwann cells growth and proliferation, as well as for the differentiation and axonal elongation of neurons *in vitro*. Moreover, 2 weeks after implantation *in vivo* the conduit demonstrated a good integration with the surrounding tissues, absence of inflammation and scar formation.

In the current study we confirmed the optimal mechanical and biological properties, as well as the *in vivo* biocompatibility of the novel SilkBridge™ conduit, which showed its great potential to sustain peripheral nerve regeneration at mid (4 weeks) and longer (12 and 24 weeks) time points in a model of rat median nerve injury. Indeed, histological analysis at 4 weeks showed the progression of nerve regeneration process alongside the conduit, demonstrated by the presence of many myelinated fibers in the proximal and mid portion of the conduit, and the approaching at the distal portion, and the good integration with the surrounding tissue, demonstrated by the whole colonization of both the lumen and the wall of the conduit by extracellular matrix and different cell types, the presence of a thin layer of connective tissue surrounding the outer side of the conduit, the formation of many blood vessels and the absence of any foreign body reaction.

At longer time points (12 and 24 weeks), the SilkBridge™ conduit led to a very good functional and morphological recovery of the median nerve, similar to that observed with the reference autograft nerve reconstruction. The functional recovery, assayed by means of the grasping test and muscle weight, showed a stably motor performance of the finger flexor muscles, with no statistically nor clinically relevant difference in the SilkBridge™ conduit group and in the Autograft group. The delay of functional recovery of the experimental group with respect to the control autograft group can be justified by the different repair technique and it is in line with the reconstruction through different conduits (Geuna et al., 2016). Morphological and morphometric analyses reflected the good performance of functional tests. Indeed, after 24 weeks, nerve fibers size, maturation, and organization of experimental and control groups levelled, suggesting a positive outcome of the regeneration process driven by the SilkBridge™ conduit. To be noticed, in the case of axon diameter and fiber diameter outcomes the statistically significant differences between the two groups that were detected refers to dimensions less than a micrometer, with no reliable confidence intervals, that could be considered clinically irrelevant.

Finally, special attention was paid to analyze the behavior of the silk material once implanted *in vivo*, with a particular regard to integration with regenerating tissues and to degradation over time. In the time points investigated, a large number of newly formed blood vessels were found in the SilkBridge™ conduit during nerve regeneration and these vessels were mainly located at the periphery of the regenerated tissue, very close to the multi-layered wall and also between the three layers of the wall. The absence of this situation in the control group, at both experimental times, suggests that

SilkBridge™ through formation of blood vessels may have created a favorable oxygen-glucose environment in the nerve conduit, being therefore partly responsible for such a positive pro-regenerative effect (Wang et al., 2018; Chouhan and Mandal, 2020). A very important feature of tissue design is the rate of the scaffold degradation, the importance of the balance between the decomposing time of the biomaterial and the rate of tissue regeneration. Moreover, in case of silk fibroin, the velocity and the extent of degradation may be strictly connected with the structural characteristics of the polymers, the biological site of implantation, and the presence of different sources of mechanical and chemical stresses (Taddei et al., 2006). In this context and given the complex structure of SilkBridge™ with its multilayer wall, a careful high-resolution optical analysis and a quantification through ultrastructure images have allowed to appreciate the first degradation phenomena, which in SilkBridge™ have been observed at the level of ES-o and ES-i wall layers. The layers of the conduit wall, consisting of silk electrospun fibers, were in fact firstly intercalated with new cellular elements and extracellular matrix, thus losing their original compactness and subsequently, at long times after implantation, their electrospun fibers significantly reduced in the diameter.

Altogether, the present results and the previous ones (Alessandrino et al., 2019b) represent an important achievement for the implementation of clinical studies aimed at investigating the safety and efficacy of the newly designed SF-based nerve conduit, which is intended as an “off-the-shelf” device to be used as it is, without the need of adding neurotrophic and/or angiogenic factors or cells. These very encouraging results allowed us to proceed quickly towards the submission of a first-in-human clinical study aimed at evaluating the reconstruction of digital nerve defects in humans using SilkBridge™ nerve conduit (ClinicalTrials.gov identifier: NCT03673449). The study has already started at the Department of Plastic Surgery and Hand Surgery of the University Hospital of Zurich. Four out of 15 patients have been enrolled and implanted with SilkBridge™ nerve conduit to repair a digital nerve gap.

DATA AVAILABILITY STATEMENT

The datasets generated for this study are available on request to the corresponding author.

ETHICS STATEMENT

The animal study was reviewed and approved by the Ethic Experimental Committee of the University of Turin (Ministry of Health project number 864/2016).

AUTHOR CONTRIBUTIONS

FF supported the surgery, carried out analysis, contributed to designed experiments and the data analysis, wrote, and revised

the manuscript. LM performed *in vivo* functional experiments, carried out the morphological and stereological analysis, wrote, and revised the manuscript. AC carried out surgery on animals. GR performed surgery, carried out stereological and morphological analysis, wrote and revised the manuscript, and contributed to designed experiments. SG supported the study, designed experiments, and contributed to the data analysis. AA carried out the manufacturing and the mechanical characterization of SilkBridge™, revised the manuscript, and contributed to design the experiments. GF and GB carried out the manufacturing and the mechanical characterization of SilkBridge™, contributed to designed experiments, and provided guidance throughout the entire study. MB, VV, and PP supported the manufacturing and the mechanical characterization of SilkBridge™ conduit. All authors contributed to the article and approved the submitted version.

FUNDING

The authors declare that this study received funding from Silk Biomaterials srl. The funder had the following involvement with the study: carried out the manufacturing and mechanical characterization of SilkBridge™, revised the manuscript, and contributed to the discussion for designing experiments.

ACKNOWLEDGMENTS

This research did not receive any specific grant from funding agencies in the public, commercial, or not-for-profit sectors.

REFERENCES

- Alessandrino, A. (2017). Process For The Production Of A Hybrid Structure Consisting Of Coupled Silk Fibroin Microfibers And Nanofibers, Hybrid Structure Thus Obtained And Its Use As Implantable Medical Device. Google Patents.
- Alessandrino, A., Chiarini, A., Biagiotti, M., Dal Pra, I., Bassani, G. A., Vincoli, V., et al. (2019a). Three-layered silk fibroin tubular scaffold for the repair and regeneration of small caliber blood vessels: from design to *in vivo* pilot tests. *Front. Bioeng. Biotechnol.* 7:356. doi: 10.3389/fbioe.2019.00356
- Alessandrino, A., Fregnan, F., Biagiotti, M., Muratori, L., Bassani, G. A., Ronchi, G., et al. (2019b). SilkBridge: a novel biomimetic and biocompatible silk-based nerve conduit. *Biomater. Sci.* 7, 4112–4130. doi: 10.1039/c9bm00783k
- Altman, G. H., Diaz, F., Jakuba, C., Calabro, T., Horan, R. L., Chen, J., et al. (2003). Silk-based biomaterials. *Biomaterials* 24, 401–416.
- Battiston, B., Papalia, I., Tos, P., and Geuna, S. (2009). Chapter 1: peripheral nerve repair and regeneration research: a historical note. *Int. Rev. Neurobiol.* 87, 1–7. doi: 10.1016/s0074-7742(09)87001-3
- Carriel, V., Alaminos, M., Garzon, I., Campos, A., and Cornelissen, M. (2014). Tissue engineering of the peripheral nervous system. *Expert. Rev. Neurother.* 14, 301–318.
- Catto, V., Fare, S., Cattaneo, I., Figliuzzi, M., Alessandrino, A., Freddi, G., et al. (2015). Small diameter electrospun silk fibroin vascular grafts: mechanical properties, *in vitro* biodegradability, and *in vivo* biocompatibility. *Mater. Sci. Eng. C Mater. Biol. Appl.* 54, 101–111. doi: 10.1016/j.msec.2015.05.003
- Cederlund, R. I., Thomsen, N., Thrainsdottir, S., Eriksson, K. F., Sundkvist, G., and Dahlin, L. B. (2009). Hand disorders, hand function, and activities of daily

SUPPLEMENTARY MATERIAL

The Supplementary Material for this article can be found online at: <https://www.frontiersin.org/articles/10.3389/fbioe.2020.00835/full#supplementary-material>

FIGURE S1 | Equivalence test on functional analysis. **(A)** Grasping test: The equivalence test was statistically significant ($t[169.44] = -29.660, p < 0.000$) and the null-hypothesis test was statistically significant ($t[169.44] = 2.881, p < 0.004$) revealing that the observed effect of Autograft superior to SilkBridge™ of about 80.2 gr ($p = 0, 95\% \text{ CI: } 63.99\text{--}96.42$), can be considered overlapped. **(B)** Finger flexor superficialis muscles weight: The equivalence test was not statistically significant ($t[27] = 5.773, p < 0.000$) and the null-hypothesis test was statistically not significant ($t[27] = -0.734, p = 0.469$) revealing that the observe higher weight in Autograft group 0.003 gr is not statistically different ($p = 0.483, 95\% \text{ CI: } -0.00\text{--}0.01$).

FIGURE S2 | Equivalence test on morphoquantitative evaluation of nerve regeneration. **(A)** Cross-sectional area: The equivalence test ($t[12,53] = 1.489, p = 0.919$) and the null-hypothesis test ($t[27] = -0.734, p = 0.469$) revealed that the Autograft had a higher cross-sectional area of about 0.049 mm² ($p < 0.007, 95\% \text{ CI: } 0.01\text{--}0.08$). **(B)** Density of myelinated fibers: The equivalence test ($t[18,87] = 0.323, p = 0.375$) and the null-hypothesis test ($t[18,87] = -0.990, p = 0.335$) revealed an higher density of myelinated fibers in the SilkBridge™ conduit group of about 2293 fibers/mm²; not statistically relevant ($p = 0.302, 95\% \text{ CI: } -2208.85\text{--}6796.35$). **(C)** Total number of myelinated fibers: the equivalence test and the null-hypothesis test were not a significant ($t[22,43] = 0.963, p = 0.827; t[22,43] = 1.982, p = 0.061$). **(D)** g-Ratio: the equivalence test and the null-hypothesis test were not a significant ($t[18,71] = -1.173, p = 0.128; t[18,71] = 1.347, p = 0.194$). **(E)** Axons diameter: the equivalence test and the null-hypothesis test were not a significant ($t[14,7] = -0.045, p = 0.483; t[14,7] = 1.811, p = 0.0906$). **(F)** Fiber diameter: the equivalence test and the null-hypothesis test were not a significant ($t[23,28] = -0.233, p = 0.591; t[23,28] = -1.937, p = 0.0645$). **(G)** Myelin thickness: the equivalence test and the null-hypothesis test were not a significant ($t[20,85] = -0.262, p = 0.398; t[20,85] = 0.949, p = 0.353$).

TABLE S1 | Mechanical properties of SilkBridge™ conduit.

- living in elderly men with type 2 diabetes. *J. Diabetes Complicat.* 23, 32–39. doi: 10.1016/j.jdiacomp.2007.09.002
- Chato-Astrain, J., Campos, F., Roda, O., Miralles, E., Durand-Herrera, D., Saez-Moreno, J. A., et al. (2018). *In vivo* evaluation of nanostructured fibrin-agarose hydrogels with mesenchymal stem cells for peripheral nerve repair. *Front. Cell Neurosci.* 12:501. doi: 10.3389/fbioe.2019.00501
- Chato-Astrain, J., Philips, C., Campos, F., Durand-Herrera, D., Garcia-Garcia, O. D., Roosens, A., et al. (2020). Detergent-based decellularized peripheral nerve allografts: an *in vivo* preclinical study in the rat sciatic nerve injury model. *J. Tissue Eng. Regen. Med.* 14, 789–806. doi: 10.1002/term.3043
- Chiono, V., and Tonda-Turo, C. (2015). Trends in the design of nerve guidance channels in peripheral nerve tissue engineering. *Prog. Neurobiol.* 131, 87–104. doi: 10.1016/j.pneurobio.2015.06.001
- Chouhan, D., and Mandal, B. B. (2020). Silk biomaterials in wound healing and skin regeneration therapeutics: from bench to bedside. *Acta Biomater.* 103, 24–51. doi: 10.1016/j.actbio.2019.11.050
- Ciardelli, G., and Chiono, V. (2006). Materials for peripheral nerve regeneration. *Macromol. Biosci.* 6, 13–26.
- Dahlin, L. B., Lithner, F., Bresater, L. E., Thomsen, N. O., Eriksson, K. F., and Sundkvist, G. (2008a). Sequelae following sural nerve biopsy in type 1 diabetic subjects. *Acta Neurol. Scand.* 118, 193–197. doi: 10.1111/j.1600-0404.2008.01000.x
- Dahlin, L. B., Stenberg, L., Luthman, H., and Thomsen, N. O. (2008b). Nerve compression induces activating transcription factor 3 in neurons and Schwann cells in diabetic rats. *Neuroreport* 19, 987–990. doi: 10.1097/wnr.0b013e328302f4ec
- Daly, W., Yao, L., Zeugolis, D., Windebank, A., and Pandit, A. (2012). A biomaterials approach to peripheral nerve regeneration: bridging the peripheral

- nerve gap and enhancing functional recovery. *J. R. Soc. Interf.* 9, 202–221. doi: 10.1098/rsif.2011.0438
- Dinis, T. M., Elia, R., Vidal, G., Dermigny, Q., Denoed, C., Kaplan, D. L., et al. (2015). 3D multi-channel bi-functionalized silk electrospun conduits for peripheral nerve regeneration. *J. Mech. Behav. Biomed. Mater.* 41, 43–55. doi: 10.1016/j.jmbm.2014.09.029
- Du, J., Chen, H., Qing, L., Yang, X., and Jia, X. (2018). Biomimetic neural scaffolds: a crucial step towards optimal peripheral nerve regeneration. *Biomater. Sci.* 6, 1299–1311. doi: 10.1039/c8bm00260f
- Faroni, A., Mobasser, S. A., Kingham, P. J., and Reid, A. J. (2015). Peripheral nerve regeneration: experimental strategies and future perspectives. *Adv. Drug Deliv. Rev.* 8, 160–167. doi: 10.1016/j.addr.2014.11.010
- Geuna, S. (2000). Appreciating the difference between design-based and model-based sampling strategies in quantitative morphology of the nervous system. *J. Comp. Neurol.* 427, 333–339. doi: 10.1002/1096-9861(20001120)427:3<333::aid-cne1>3.0.co;2-t
- Geuna, S., Raimondo, S., Fregnan, F., Haastert-Talini, K., and Grothe, C. (2016). In vitro models for peripheral nerve regeneration. *Eur. J. Neurosci.* 43, 287–296.
- Geuna, S., Tos, P., Battiston, B., and Guglielmo, R. (2000). Verification of the two-dimensional disector, a method for the unbiased estimation of density and number of myelinated nerve fibers in peripheral nerves. *Ann. Anat.* 182, 23–34. doi: 10.1016/s0940-9602(00)80117-x
- Haastert-Talini, K., and Dahlin, L. B. (2018). Diabetes, its impact on peripheral nerve regeneration: lessons from pre-clinical rat models towards nerve repair and reconstruction. *Neural Regen. Res.* 13, 65–66.
- Holzzapfel, G. A., and Weizsacker, H. W. (1998). Biomechanical behavior of the arterial wall and its numerical characterization. *Comput. Biol. Med.* 28, 377–392. doi: 10.1016/s0010-4825(98)00022-5
- Hou, Y., Wang, X., Zhang, X., Luo, J., Cai, Z., Wang, Y., et al. (2019). Repairing transected peripheral nerve using a biomimetic nerve guidance conduit containing intraluminal sponge fillers. *Adv. Healthc. Mater.* 8:e1900913.
- Ichihara, S., Facca, S., Liverneaux, P., Inada, Y., Takigawa, T., Kaneko, K., et al. (2015). Mechanical properties of a bioabsorbable nerve guide tube for long nerve defects. *Chir. Main.* 34, 186–192. doi: 10.1016/j.main.2015.05.004
- Kokai, L. E., Lin, Y. C., Oyster, N. M., and Marra, K. G. (2009). Diffusion of soluble factors through degradable polymer nerve guides: controlling manufacturing parameters. *Acta Biomater.* 5, 2540–2550. doi: 10.1016/j.actbio.2009.03.009
- Kornfeld, T., Vogt, P. M., and Radtke, C. (2019). Nerve grafting for peripheral nerve injuries with extended defect sizes. *Wien. Med. Wochenschr.* 169, 240–251. doi: 10.1007/s10354-018-0675-6
- Kwan, M. K., Wall, E. J., Massie, J., and Garfin, S. R. (1992). Strain, stress and stretch of peripheral nerve. Rabbit experiments in vitro and in vivo. *Acta Orthop. Scand.* 63, 267–272. doi: 10.3109/17453679209154780
- Lovati, A. B., D'arrigo, D., Odella, S., Tos, P., Geuna, S., and Raimondo, S. (2018). Nerve repair using decellularized nerve grafts in rat models. a review of the literature. *Front. Cell Neurosci.* 12:427. doi: 10.3389/fnec.2019.00427
- Mascha, E. J., and Sessler, D. I. (2011). Equivalence and noninferiority testing in regression models and repeated-measures designs. *Anesth. Analg.* 112, 678–687. doi: 10.1213/ane.0b013e318206f872
- Miranda, G. E., and Torres, R. Y. (2016). Epidemiology of traumatic peripheral nerve injuries evaluated with electrodiagnostic studies in a tertiary care hospital clinic. *Proc. R Health Sci. J.* 35, 76–80.
- Navarro, X., Vivo, M., and Valero-Cabre, A. (2007). Neural plasticity after peripheral nerve injury and regeneration. *Prog. Neurobiol.* 82, 163–201. doi: 10.1016/j.pneurobio.2007.06.005
- Nectow, A. R., Marra, K. G., and Kaplan, D. L. (2012). Biomaterials for the development of peripheral nerve guidance conduits. *Tissue Eng. Part B Rev.* 18, 40–50. doi: 10.1089/ten.teb.2011.0240
- Noble, J., Munro, C. A., Prasad, V. S., and Midha, R. (1998). Analysis of upper and lower extremity peripheral nerve injuries in a population of patients with multiple injuries. *J. Trauma* 45, 116–122. doi: 10.1097/00005373-199807000-00025
- Philips, C., Campos, F., Roosens, A., Sanchez-Quevedo, M. D. C., Declercq, H., and Carriel, V. (2018). Qualitative and quantitative evaluation of a novel detergent-based method for decellularization of peripheral nerves. *Ann. Biomed. Eng.* 46, 1921–1937. doi: 10.1007/s10439-018-2082-y
- Pillai, M. M., Kumar, G. S., Houshyar, S., Padhye, R., and Bhattacharyya, A. (2019). Effect of nanocomposite coating and biomolecule functionalization on silk fibroin based conducting 3D braided scaffolds for peripheral nerve tissue engineering. *Nanomedicine* 24:102131. doi: 10.1016/j.nano.2019.102131
- Quan, Q., Meng, H., Chang, B., Hong, L., Li, R., Liu, G., et al. (2019). Novel 3-D helix-flexible nerve guide conduits repair nerve defects. *Biomaterials* 207, 49–60. doi: 10.1016/j.biomaterials.2019.03.040
- Ray, W. Z., and Mackinnon, S. E. (2010). Management of nerve gaps: autografts, allografts, nerve transfers, and end-to-side neurotaphy. *Exp. Neurol.* 223, 77–85. doi: 10.1016/j.expneurol.2009.03.031
- Rockwood, D. N., Preda, R. C., Yucel, T., Wang, X., Lovett, M. L., and Kaplan, D. L. (2011). Materials fabrication from *Bombyx mori* silk fibroin. *Nat. Protoc.* 6, 1612–1631. doi: 10.1038/nprot.2011.379
- Salehi, M., Naseri-Nosar, M., Ebrahimi-Barough, S., Nourani, M., Khojasteh, A., Farzamfar, S., et al. (2018). Polyurethane/gelatin nanofibrils neural guidance conduit containing platelet-rich plasma and melatonin for transplantation of schwann cells. *Cell Mol. Neurobiol.* 38, 703–713. doi: 10.1007/s10571-017-0535-8
- Siemionow, M., and Brzezicki, G. (2009). Chapter 8: current techniques and concepts in peripheral nerve repair. *Int. Rev. Neurobiol.* 87, 141–172. doi: 10.1016/s0074-7742(09)87008-6
- Taddei, P., Arai, T., Boschi, A., Monti, P., Tsukada, M., and Freddi, G. (2006). In vitro study of the proteolytic degradation of *Antheraea pernyi* silk fibroin. *Biomacromolecules* 7, 259–267.
- Taylor, C. A., Braza, D., Rice, J. B., and Dillingham, T. (2008). The incidence of peripheral nerve injury in extremity trauma. *Am. J. Phys. Med. Rehabil.* 87, 381–385. doi: 10.1097/phm.0b013e31815e6370
- Thurber, A. E., Omenetto, F. G., and Kaplan, D. L. (2015). In vivo bioresponses to silk proteins. *Biomaterials* 71, 145–157. doi: 10.1016/j.biomaterials.2015.08.039
- Topp, K. S., and Boyd, B. S. (2006). Structure and biomechanics of peripheral nerves: nerve responses to physical stresses and implications for physical therapist practice. *Phys. Ther.* 86, 92–109. doi: 10.1093/ptj/86.1.92
- Wang, C., Jia, Y., Yang, W., Zhang, C., Zhang, K., and Chai, Y. (2018). Silk fibroin enhances peripheral nerve regeneration by improving vascularization within nerve conduits. *J. Biomed. Mater. Res. A* 106, 2070–2077. doi: 10.1002/jbm.a.36390
- Zhang, L., Xu, L., Li, G., and Yang, Y. (2019). Fabrication of high-strength mecobalamin loaded aligned silk fibroin scaffolds for guiding neuronal orientation. *Coll. Surf. B Biointerf.* 173, 689–697. doi: 10.1016/j.colsurfb.2018.10.053

Conflict of Interest: This study is sponsored by Silk Biomaterials srl. GF is stock owners and consultant of the sponsoring organization. AA is stock owners and employee of the sponsoring organization. GB, MB, and VV are employees of the sponsoring organization. FF, LM, GC, GR, and SG are consultants of the sponsoring organization.

The remaining authors declare that the research was conducted in the absence of any commercial or financial relationships that could be construed as a potential conflict of interest.

Copyright © 2020 Fregnan, Muratori, Bassani, Crosio, Biagiotti, Vincoli, Carta, Pierimarchi, Geuna, Alessandrino, Freddi and Ronchi. This is an open-access article distributed under the terms of the Creative Commons Attribution License (CC BY). The use, distribution or reproduction in other forums is permitted, provided the original author(s) and the copyright owner(s) are credited and that the original publication in this journal is cited, in accordance with accepted academic practice. No use, distribution or reproduction is permitted which does not comply with these terms.

3.7 Strategies for cavernous nerve repair in animal model: regeneration through chitosan membrane vs sciatic nerve to corpora cavernosa transfer.

Crosio A, Fregnan, F, Muratori L, Ciclamini D, Tos P, Raimondo S.

Under submission

STRATEGIES FOR CAVERNOUS NERVE REPAIR IN ANIMAL MODEL: REGENERATION THROUGH CHITOSAN MEMBRANE VS SCIATIC NERVE TO CORPORA CAVERNOSA TRANSFER

Alessandro Crosio^{1,2}, Federica Fregnan², Luisa Muratori², Davide Ciclamini¹, Pierluigi Tos³, Stefania Raimondo¹.

¹*Orthopedics and Traumatology 2 - Hand Surgery and Reconstructive Microsurgery, AOU Città della Salute e della Scienza, CTO Hospital, Torino, Italy*

²*Department of Clinical and Biological Sciences, Neuroscience Institute Cavalieri Ottolenghi (NICO), University of Turin, Turin, Italy*

³*Reconstructive Microsurgery and Hand surgery Unit, ASST Pini-CTO Milano, Italy*

ABSTRACT

Erectile dysfunction (ED) following radical prostatectomy is a frequent and debilitating complication. Even robotic prostatectomy seems to be more accurate in nerve sparing, it can prevent ED in all patients. Positive results have been published in human using chitosan membrane on the prostatic bed after excision, revealing better functional results compared to those patients in which the membrane was not applied. Another recent strategy to solve ED has been a direct corpora cavernosa neurotization using a bilateral sural nerve graft sutured to femoral nerve. None is known about the effective of chitosan membrane in cavernous plexus regeneration and either none is known about reinnervation of autonomic organ by means of somatic nerves. So that in this paper we proposed a pre-clinical study in which a bilateral cavernous nerve injury in rats is treated by chitosan membrane bridging. Different types of membrane are tested: flat membrane and nanostructured membrane . On the other side in one group corpora cavernosa in directly neurotized with a branch of the sciatic nerve. After 4 months morphological and biomolecular analysis are performed to evaluate nerve recovery and corpora cavernosa reinnervation. Results showed that axons can growth all along the membrane from proximal to distal stump and that nanostructures facilitate axons polarization. Morphologically, reduction of muscle component into corpora cavernosa is evident as well as cavern enlargement compared to control group. In nerve transfer gene expression analyses in the target organ described expression of pro regenerative molecules. In this paper the mechanism of nerve regeneration through chitosan membrane is seen and described and a novel somatic to autonomic nerve transfer is created, further studies are needed to understand which procedure gives the best results in term of functional recovery.

INTRODUCTION

In developed and industrialized countries, prostate cancer is one of the most frequent. Its incidence increases progressively with the age of the patient: more than ¼ of men over 75 are affected by this disease. Due to the growing proportion of elderly people in the world population, this cancer is set to become an increasingly

important public health burden. However, it can also be diagnosed in patients younger than 40-50 years. In EU countries, the incidence rate of prostate cancer is 55 cases per 100,000 males.

The current treatment of localized prostate cancer is radical prostatectomy with frequent iatrogenic damage to periprostatic neurovascular bundles that can lead to erectile dysfunction (Porpiglia, Fiori, et al., 2018). One strategy to protect and promote regeneration of damaged fibres of periprostatic neurovascular bundles after surgery is the application of flat membranes. The use of a dehydrated human amniotic membrane allograft wrapped around the periprostatic neurovascular bundles after robot-assisted radical prostatectomy accelerates normal functional recovery (Patel et al., 2015). Our research groups have shown that the application of a chitosan membrane is safe and able to promote faster recovery (Porpiglia, Bertolo, et al., 2018; Porpiglia et al., 2019; Muratori et al., 2019).

Chitosan is a chitin derivative, obtained from the exoskeleton of crustaceans, which is garnering some interest in both basic research and clinical settings. Its chemical structure (a polysaccharide composed of D-glucosamine and N-acetyl-D-glucosamine linked to the β (1-4) bond) makes it an excellent candidate for applications in medicine due to its biocompatibility, bioavailability and lack of toxicity. For these reasons, chitosan is effectively used in the periodontal and orthopedic fields (in implantable and injectable form), in drug delivery systems, as an agent to promote tissue healing, as a pulmonary surfactant additive, as a scaffold for the regeneration of various tissues (nerve, skin, bone, cartilage), and is also approved by the Food and Drug Administration (FDA) for clinical use (ref).

Pro-regenerative devices are currently engineered to improve their efficacy. The interaction of glial and neuronal cells with micro/nano-topographies has been extensively studied by Prof. Geuna's research group (Gnavi et al., 2015, 2018). Polymeric nano/micro-grooves have been shown to promote neurite orientation (Wieringa et al., 2012), consolidating aligned neurites and destabilising misaligned ones (Ferrari et al., 2010). Furthermore, micropatterning of chitosan can induce and regulate Schwann cell growth (Li et al., 2014).

Another strategy to solve erectile dysfunction after prostatectomy was the reinnervation of corpora cavernosa through a bilateral sural nerve graft connected in end-to-side with motor fibers of femoral nerve. The new technique reported impressive results about 2 years after surgery (Souza-Trindade JC 2017, Reece J 2019, Dangerfield D 2023). Despite these good results, nerve grafting is prone to loss of sensory function, to risk of painful neuromas and, not secondly, the time of recovery is prolonged according to the graft length. In modern nerve surgery nerve transfers are preferred for irreparable nerve injuries to reanimate skeletal muscles; their main advantage is to connect the donor nerve close to the target muscle reducing time of reinnervation (Chuang DCC 2005, Doi K 2018). In literature distal nerve transfer was attempted for bladder reinnervation as described by Ruggieri 2008, 2011, and Gomez Amaya who used genitofemoral nerve (GF) to pudendal nerve (PN), coccygeal nerve (CG) to S1 or obturator nerve (ON) to PN pelvic nerve in animal models. Due to lack of knowledges on the mechanism of cavernous nerve repair through chitosan membrane, in this paper an animal model of cavernous nerve injury was used to firstly evaluate the effect of flat chitosan

membranes on nerve regeneration. Moreover, micro-structured membranes were also used to understand whether nanotechnologies can bust regenerative capacity of the device. Nanostructured membranes showed in vitro their efficacy in promotion of neurite elongation (results not showed here).

Considering the efficacy of nerve transfer in humans, a novel experimental surgical model of nerve transfer in rat, without the requirement of nerve graft, is presented here and its efficacy is compared to the treatment with chitosan membrane for the recovery of induced erectile dysfunction.

MATERIALS AND METHODS

Animals and In Vivo Surgery.

Adult male Wistar rats approximately weighing 250–350 g (Envigo Laboratories, Udine, Italy) were used in the present study, animals were divided into the following experimental groups:

Group 1 (pilot study): two adults male wistar rats were used to evaluate the feasibility and safety of the surgical procedure and to evaluate the protocol in terms of nerve regeneration.

Group 2: six adults male wistar rats were included in the second study in which different types of Cs membranes were used to bridge the cavernous nerve gap in a bilateral surgery as follow:

- 4 FLAT membranes;
- 4 membranes with GRATING topography;
- 4 membranes with SCA topography;

Group 3: on four adults male wistar rats, a bilateral sciatic nerve to corpora cavernosa transfer was performed.

Group 4: three adult wistar rats were used as negative control (denervation control). Both cavernous nerves were sectioned as described above, here a bigger nerve gap was performed and distal stump was flipped distally in order to prevent spontaneous regeneration.

Surgical procedure

Cavernous nerve injury

The surgical interventions were carried out under deep anaesthesia using Tiletamine (052019, Bayer, Milano, Italy) + Zolazepam (Zoletil) (A101580025, Virbac, Milano, Italy) (40 and 5 mg/kg). After trichotomy, the abdominal cavity was accessed by making a medial cut at the umbilical level as far as the pelvic region; the prostatic region was then reached with isolation of the gland itself on whose dorsal lateral walls it was possible to identify bilaterally the presence of the prostatic ganglion containing motor neurons and the cavernous nerve, whose fibers are responsible for innervation of the corpora cavernosa and erectile function. Once the cavernous nerve was isolated (Fig. 1A), a bilateral resection of a 3mm-long nerve segment was performed.

Chitosan membrane implantation

In rat from group 1 and 2, the two nerve stumps derived from the resection of each nerve were sutured to the chitosan membrane (Fig. 1B) to allow regeneration of the nerve fibers on the biomaterial. In total, two membranes were implanted for animal, one on each side.

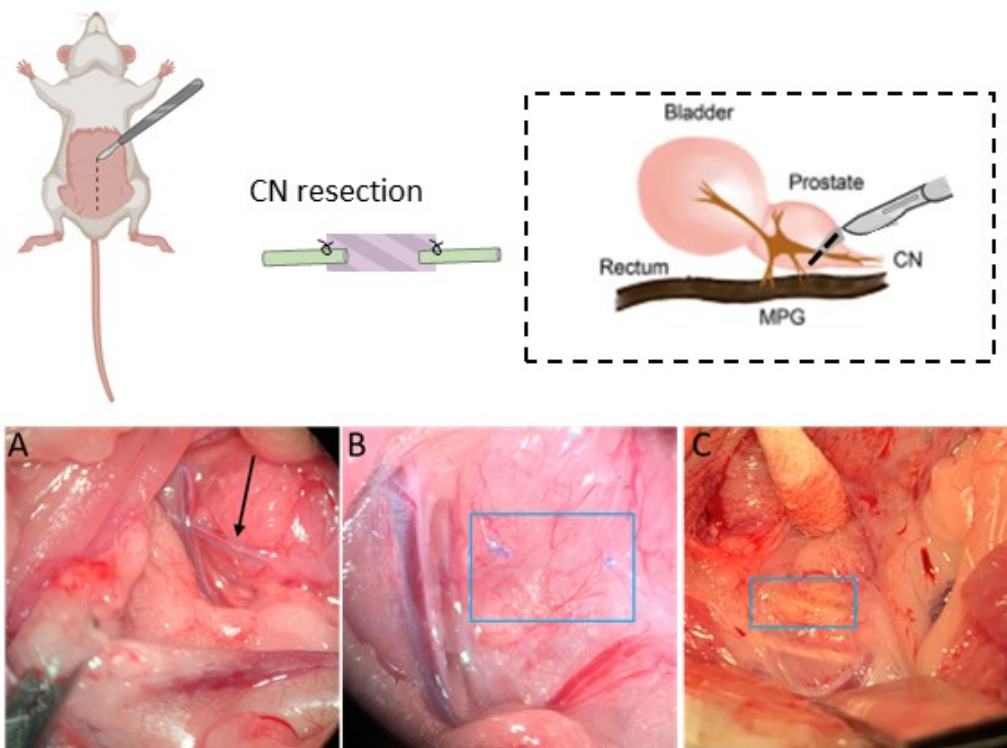


Figure 1: The image shows the different stages of the surgical procedure. A: identification of the cavernous nerve (arrow); B: application of the chitosan membrane after resection of the nerve and application of the sutures; C: removal of the membrane 30 days after surgery, the integration of the membrane with the surrounding tissue can be seen.

Nerve transfer surgery

After cavernous nerve injury, a posterior approach to bilateral thighs was performed, the sciatic nerve was identified bilaterally and traced distally, the branch to anterior tibialis muscle was dissected and transected as close as possible to the muscle entry point. The freed nerve was dissected proximally. In the proximal part of the posterior thigh a soft tissue tunnel was created to allow the free part of sciatic nerves to be transposed anteriorly. The free ends were then introduced for few millimeters into corpora cavernosa through a small

incision of the tunica albuginea and secured with an 8-0 stich in both sides. Details regarding surgical procedure are reported in figure 2.

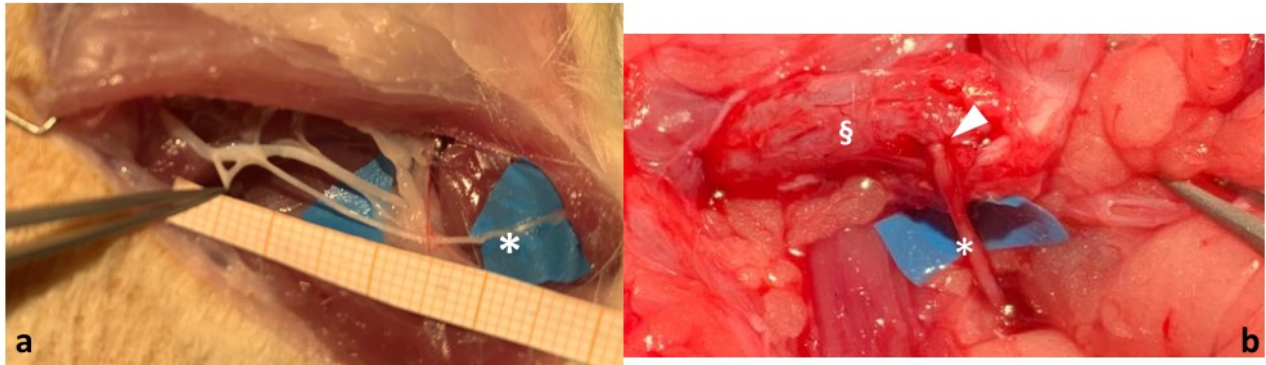


Figure 2: In a the branch to the tibial anterior is freed until the entry point into the muscle () for 3.5 cm. The nerve is passed from posterior to anterior towards a soft tissue tunnel and sutured (b) into corpora cavernosa (arrow tips) of the penis (§).*

In the days following the surgery, animals were monitored to evaluate the state of health and general well-being: macroscopically no signs of suffering were highlighted, the surgical wound showed no signs of infection and accumulation of liquid in the abdominal cavity wasn't observed.

Samples harvesting

Group 1: after a period of 30 days following the surgical procedure, the regenerated membranes were harvested. At the time of sampling, the two membranes were isolated from the surrounding tissue and each membrane was correctly found at the implantation site (Fig 1C).

Group 2, 3, 4:

After a period of 60 days following the surgical procedure, regenerated membranes were sampled as described above for group 2. Penises from all groups were taken from each rat in order to perform qualitative and quantitative analyses on the target organ innervated by the cavernous nerves.

Fixation, Immunohistochemistry and Confocal Microscopy Group 1: following collection, regenerated membranes were fixed in 4% paraformaldehyde for approximately three hours and then maintained in PBS at 4°C until analysis.

Group 2 : the regenerated membranes 3 were treated according to iDISCO technology to be able to three-dimensionally visualize the course of the regenerated nerve fibers on the chitosan membranes. The 'iDISCO' technique developed and fine-tuned by Renier et al., (Renier et al., 2014) was used, allowing a 3D reconstruction of the entire immunolabelled sample. The first step of the iDISCO procedure involves processing the samples in order to make the tissues optically transparent; achieving transparency is of paramount importance as it reduces differences in the refractive index of the tissue allowing

immunofluorescence analysis to be performed in order to visualize the course of the labelled structures. Immunolabelling is a fundamental technique in many areas of biological research and medical diagnosis, making it possible to study the morphology of. The combined approach of transparency and whole-sample immunolabelling made it possible to visualize the course of regenerated fibers on smooth and nanostructured membranes.

iDISCO

Regenerated cavernous nerves on different chitosan membranes were treated with a protocol of iDISCO+, adapted by Renier et al., 2016, to obtain three dimensional images and a perspective of regeneration.

iDISCO+ is an organic solvent-based tissue clearing technique which allows the immunolabeling of whole organs and their subsequent high quality three-dimensional acquisition confocal microscopy.

The peculiarity of iDISCO clearing is that it allows a better antibody tissue penetration thanks to the additional pretreatment step with methanol. Then, samples are immunolabeled with different antibodies and cleared using dichloromethane for lipid extraction, to limit the shrinking and preserve morphology. At last, the dibenzyl-eter is used to match the RI of the sample to the imaging solution (Renier et al 2014).

The iDISCO+ steps are summarized as follows:

- 1) Dehydration: Samples were treated in sequential solutions of increasing methanol concentration.
- 2) Bleaching: Sample were depigmented by oxygen water.
- 3) Rehydration: Samples were treated in sequential solutions of decreasing methanol concentration.
- 4) Blocking and permeabilization: Samples were treated with solution containing TritonX-100 and DSMO to facilitate antibody penetration.
- 5) Antibody labelling: Sample were incubated 14 days with primary antibodies (S100 β and PAN Neurofilament) to recognize cellular target and 7 days with secondary antibodies (Alexa 488 and Alexa 647) to permit the acquisition at confocal microscope.
- 6) Clearing: After the dehydration, as describe before, the samples were cleared with dichloromethane and, at last, transfer in dibenzyl-eter solution.

The samples were then acquired with confocal microscopy (Leica, SP5) in oil-immersion mode with 20x object and reconstruction of the whole sample was performed.

Processing and analysis of penises

In order to assess the effect of reinnervation on target organ function, penises belonging to rats undergoing bilateral cavernous nerve injury followed by repair by means of flat and nanostructured chitosan membranes were taken and processed for morphological and immunofluorescence analysis by means of a specific anti-smooth muscle marker.

Following collection and fixation, the penile samples were embedded in paraffin: after a series of passages in alcohols of increasing gradation, they were incubated in XyloI (two passages of 30 minutes) and finally placed overnight in paraffin in an oven at 60°. The following day the samples were moved to paraffin two for one hour and finally left at room temperature to allow the paraffin to solidify. Microtome cutting was performed, resulting in 10 µm thick sections.

Some sections were processed by means of Masson's Trichrome staining, which allowed the morphology of the tissue to be assessed.

Since penile erection is a phenomenon caused by the relaxation of smooth muscle leading to increased blood flow inside the corpora cavernosa, it was necessary to proceed with the qualitative and quantitative analyses of this muscular component by means of an anti-SMA antibody.

RESULTS

Macroscopically there were no signs of distress, the surgical wound showed no signs of infection or formation of fluid in the abdominal cavity, allowing a good general state of health to be maintained in the days following the operation. In nerve transfer group one of the rats presented a transitory palsy of muscles innervated by sciatic nerve, but recovered in 2 weeks. No others complications were observed during the post-operative period.

Group 1. Bilateral cavernous nerve injury repaired with a flat cs membrane. Experimental time-point: 1 month

Morphological analysis using confocal microscopy allowed the identification of numerous nuclei labelled with a nuclear intercalant (DAPI) and nerve fibers labelled by means of the PAN neurofilament antibody that showed the course of the fibers on the membranes (Fig. 3).

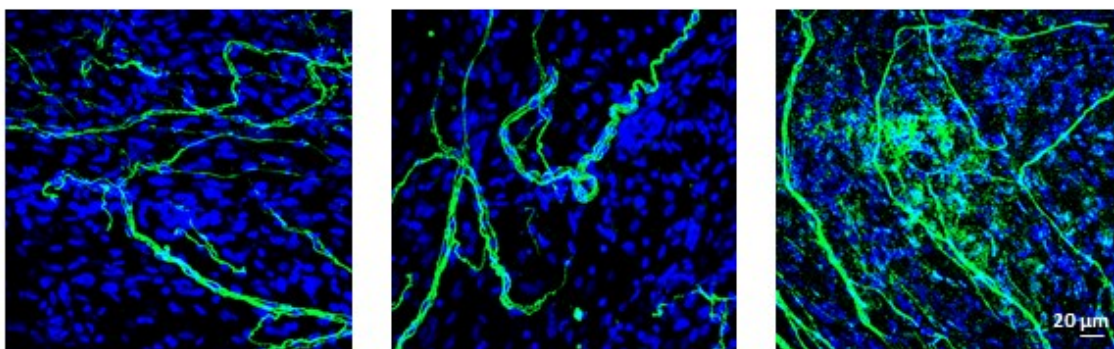


Figure 3: The image shows the presence of identifiable nerve fibers in green (positive for the marker pan neurofilament) and their course on the chitosan membrane and numerous nuclei of cells that colonized the membrane, identified in blue (DAPI).

Group 2 : Bilateral cavernous nerve injury repaired with a flat/SCA/grating cs membranes. Experimental time-point: 2 month

As shown in the images (Fig.4,5,6) the regenerated nerve fibers are easily identifiable on the different membranes analyzed.

Fig 4 shows the course of the nerve fibers on the FLAT Cs membrane in which fascicles of nerve fibers are easily identifiable along the entire membrane. At higher magnification it is possible to assess the morphology of the nerve fascicles consisting of axons that can be seen in green and numerous Schwann cells that can be seen in red (Fig.4 A-D).

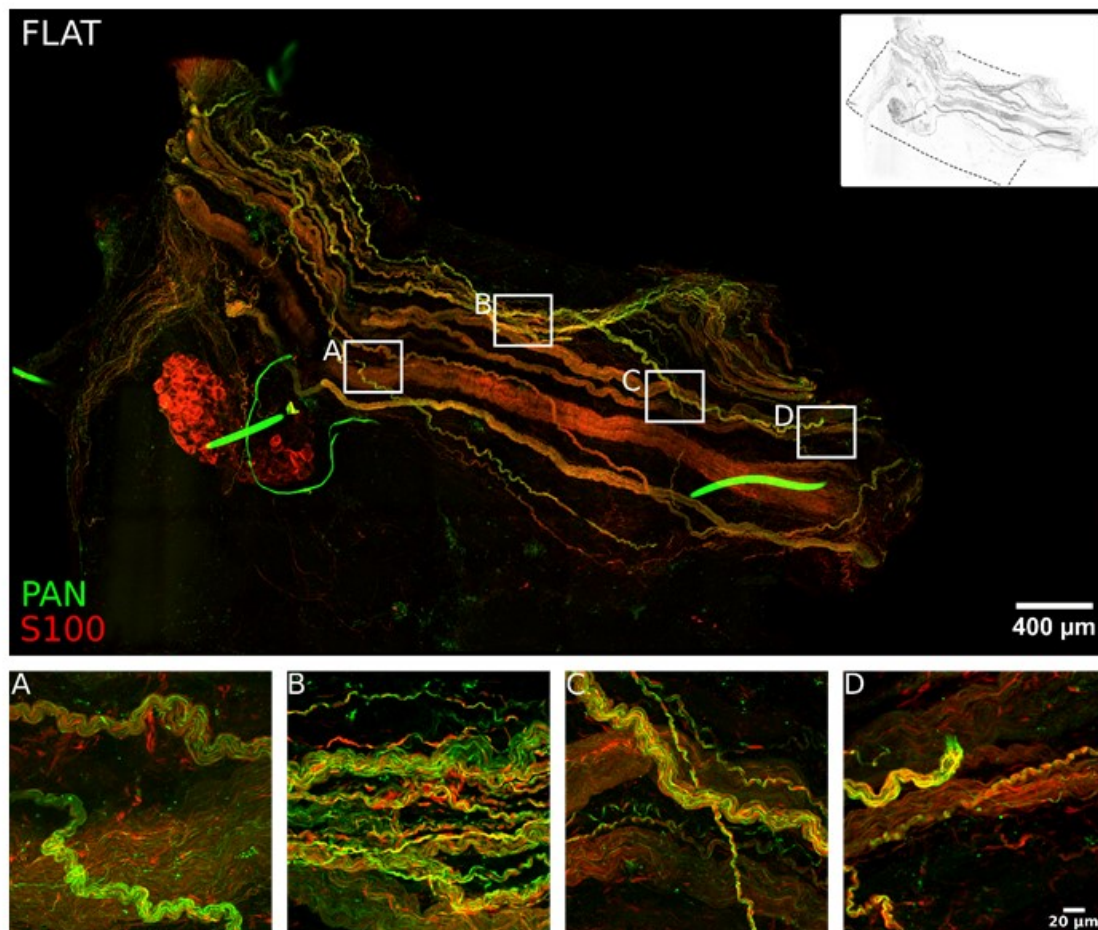


Figure 4: Chitosan membrane explant 2 months after cavernous nerve repair surgery. The image shows the presence of identifiable nerve fibres in green (positive for the pan-neurofilament marker) and their course on the chitosan membrane, which has no microstructure (FLAT) and numerous S100 marker positive glial cells in red. The first image shows the whole explant that was processed, using the i-Disco technique, to visualise

nerve regeneration and the boxes (A-D) indicate the proximal, intermediate and distal points at which enlargements were made.

The morphological analysis carried out on the membrane with GRATING microstructure shows numerous fascicles oriented from the proximal to the distal point located mainly on the upper and lower margins of the membrane (Fig. 5, reconstruction), however, it is possible to assess the presence of numerous fascicles crossing the entire membrane surface.

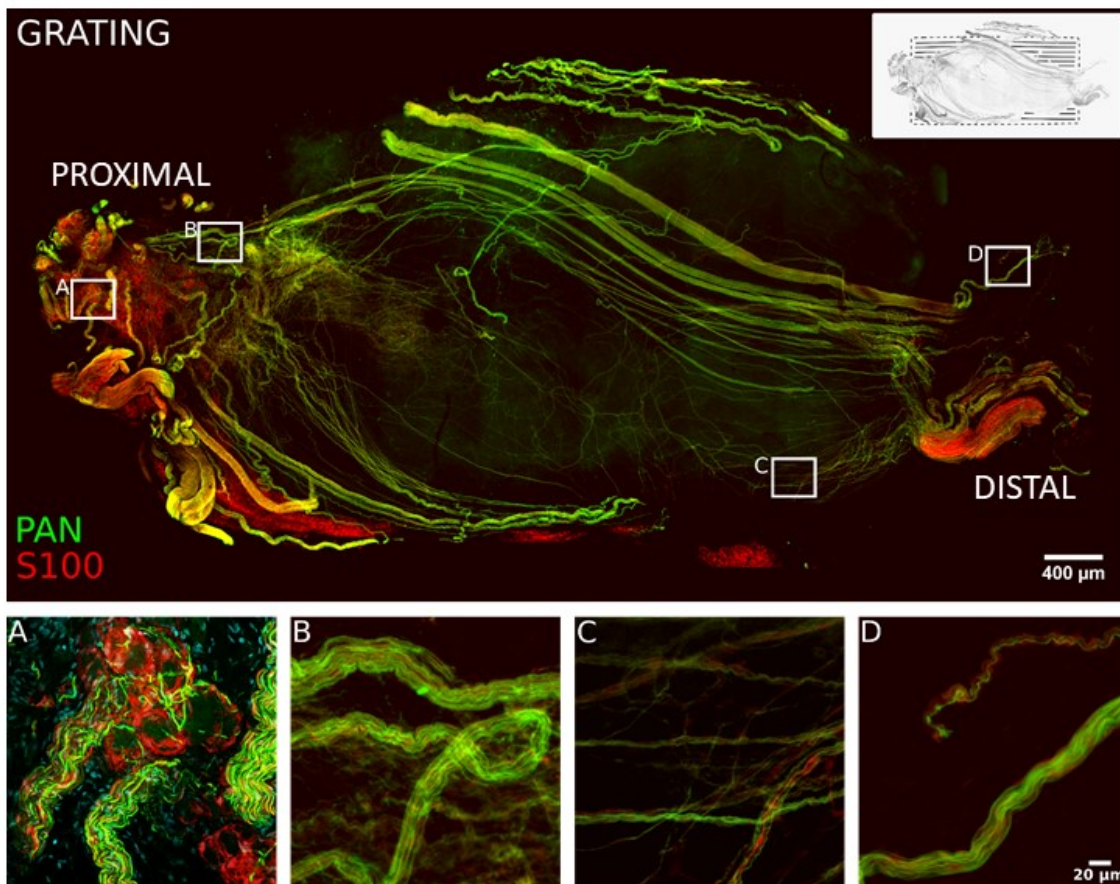


Fig. 5

Figure 5: Chitosan membrane explant 2 months after cavernous nerve repair surgery. The image shows the presence of identifiable nerve fibres in green (positive for the pan-neurofilament marker) and their course on the chitosan membrane, which shows a microstructure with parallel lines (grating layout) and numerous glial cells positive for the S100 marker in red. The first image shows the whole explant that was processed, using the i-Disco technique, to visualise nerve regeneration and the boxes (A-D) indicate the proximal, intermediate and distal points where enlargements were made.

Finally, immunolabelling of the whole specimen performed on the SCA membrane made it possible to identify the presence of regenerated nerve fibers with proximal-distal orientation also on this type of topography (Fig. 6, reconstruction). At higher magnification regenerated fascicles are easily identifiable (Fig. 6 A-D), especially image D shows nerve fibers that have reached the distal edge of the membrane.

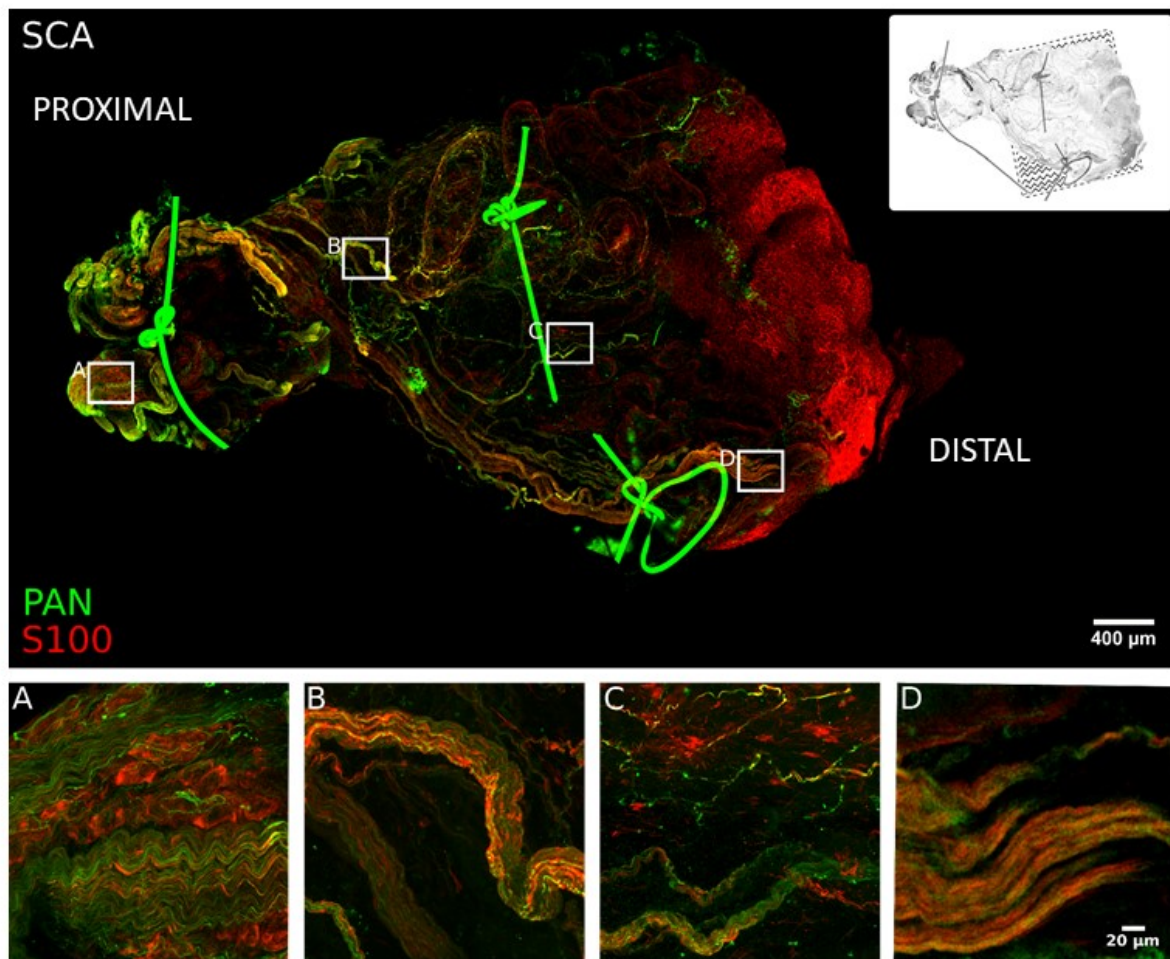


Figure 6: Chitosan membrane explant 2 months after cavernous nerve repair surgery. The image shows the presence of identifiable nerve fibres in green (positive for the pan-neurofilament marker) and their course on the chitosan membrane, which shows a ziz-zag microstructure (SCA layout) and numerous glial cells positive for the S100 marker in red. The first image shows the whole explant that was processed, using the i-Disc technique, to visualise nerve regeneration and the boxes (A-D) indicate the proximal, intermediate and distal points where enlargements were made.

TARGET ORGAN ANALYSIS

Figure 7 shows the results obtained from the analysis by means of Masson's Trichrome staining, which made it possible to assess the morphology of the penile tissue. The morphological analysis performed on the control tissue showed the typical morphology of the penis, in which the presence of cavernous tissue responsible for the erectile function of the organ is identified. Clearly distinguishable are the caverns (Fig.7, asterisks) representing the areas where physiologically blood accumulates to allow erection, the presence of a strong connective tissue component viewable in blue and the smooth muscle component viewable in red both around the caverns and between the connective tissue component (Fig.7 A).

Penile specimens subjected to injury and repaired with chitosan membranes show a very different labelling with a strong diffuse red component and a decrease in connective tissue (blue). The caverns appear defined although the muscular component is less identifiable (Fig.7 B,C,D).

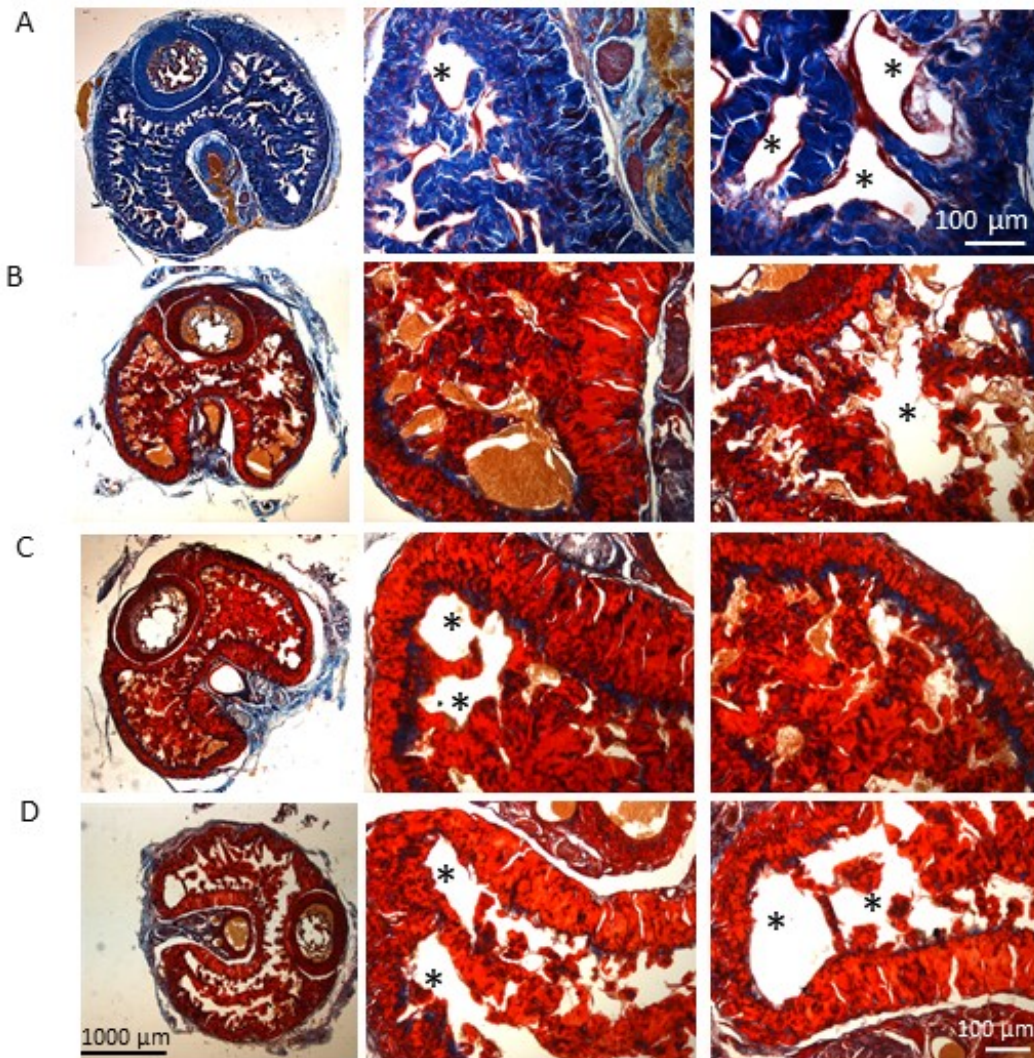


Figure 7: Representative images of cross-sections of penis subjected to Masson's Trichrome. (A) Control (B) penis corresponding to cavernous nerve repaired with FLAT chitosan membrane; (C) penis corresponding to cavernous nerve repaired with Grating chitosan membrane; (D) penis corresponding to cavernous nerve repaired with SCA chitosan membrane. The enlargements highlight the region of the corpora cavernosa ().*

To further investigate the muscular component of the target organ, it was necessary to proceed with the qualitative and quantitative analysis of this muscular component by means of an anti-SMA antibody. The qualitative analysis performed by confocal microscopy showed the presence of smooth muscle in both the

control and the injured and repaired samples. Quantitative analysis of the muscle component labelled with the anti-SMA antibody showed a slight decrease in the regenerated samples compared to the controls (Fig.8).

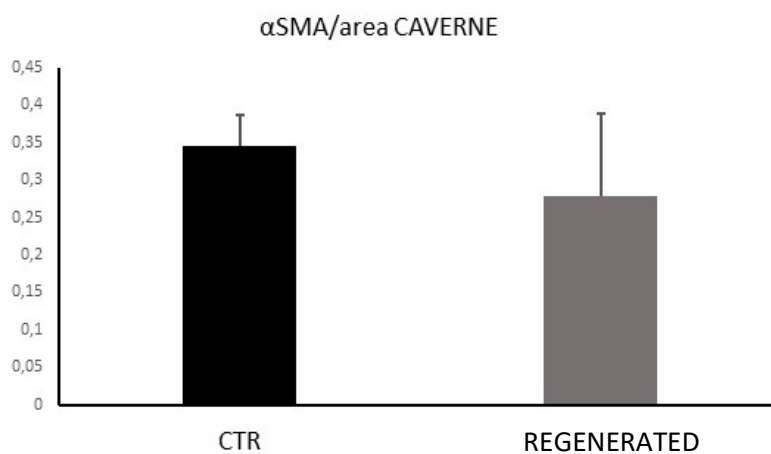
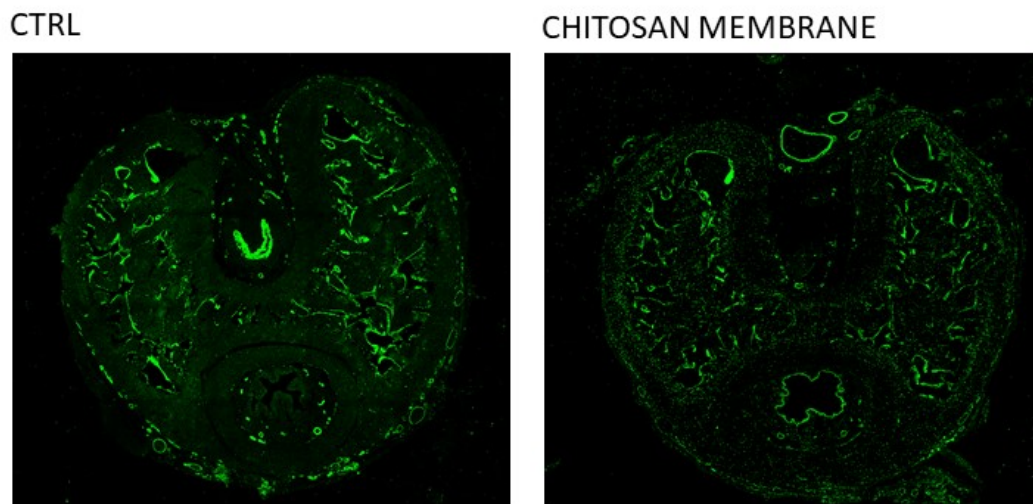


Fig. 8

Figure 8: Representative images of cross-sections of penis labelled with anti-SMA antibody and relative quantification of the muscle component.

Group 4

The harvested branch of the sciatic nerve from the muscle entry point to the more proximal site in which the branch can be dissected was 3.5 cm long. While organ harvesting no breakdown of the suture was noted. Gene expression analyses on target organ are still ongoing.

DISCUSSION:

In this study, an effective model of nerve injury to the cavernous nerve in the rat was developed in order to further study nerve regeneration able of restoring erectile function. This is to mimic as much as possible what happens following iatrogenic damage to the periprostatic plexus following radical removal of the prostate in men.

Reconstruction of cavernous nerve in living model by means autograft has been tested already with promising results, despite good results obtained, it is not possible to translate in humans due to the different anatomy of prostate innervation, in fact autograft reconstruction of cavernous plexus dramatically failed (Davis JW 2009). On the other hand, human experience with chitosan membranes used to cover the bed of autonomic plexus revealed their capacity to induce erectile recovery. Due to the absence of clear evidence of nerve regeneration along the implanted device, a pre-clinical study has been designed to depict, from a morphological point of view, nerve regeneration among chitosan membrane. Our results revealed axon growth along the membrane after four weeks, explaining what is also happened in patients.

One of the main drawbacks related to flat membranes is the absence of edges that may drive axons during elongation. Moreover, has been demonstrated the advantage induced by micro/nano-topographies in axons regrowth. The protocol for the production of nanostructured membranes was developed and published by Scaccini et al. (Scaccini L., et al., *Int J Mol Sci.* 22:7901, 2021) and those devices were implanted and tested in this study. It appears that axons follow the shape of microstructures along the membrane. No differences are evident and further greater samples are required to define differences between membranes type. The target organ was also analyzed; antiSMA antibody draw well the edges of each cavern, giving the possibility to measure their area. After 2 months a slight reduction in cavern volume in reconstructed group can be noted, further time points are required to figure out variation in volumes among the period of reinnervation. Certainly, a slight reduction of cavern is expected following denervation.

To further reinforce our findings a greater number of samples is required in each group to be able to perform morphological and gene expression analysis both on nerves and target organs. In future a functional analysis will be included to confirm the effectiveness of axons regrowth. .

Nerve transfer for autonomic driven organs have been proposed since late '90s by the pioneering research from Xiao and colleagues (Xiao CG 1999) who tried to reinnervate bladder through proximal root transfer. Considering the contrasting results obtained, in humans, with this transfer, different authors proposed the so-called distal nerve transfer, moving the donor nerve closer to the target. The first results obtained on bladder through GF to PN or CG to S1 have been positive on animal models (Ruggieri MR 2008, Gomez-Amaya S 2015). Interestingly, the authors noted the presence of nicotinic receptors in the reinnervated detrusor muscle, that is a prerogative of skeletal muscle fibers, highlighting the plasticity of muscles to different innervations. Despite these procedures were not translated in humans, two different groups attempted the

reinnervation of corpora cavernosa through femoral nerve bridge by a bilateral sural nerve graft. They obtained impressive results in term of erectile dysfunction recovery. In our mind the cited procedure could present many drawbacks: both sural nerves are required, nerve coaptation was obtained through and end to side suture, a kind of suture that presents well known limits and moreover the length of the graft could limit the quality of recovery. Moving by these considerations we started from an animal model to theorized the feasibility of a nerve transfer procedure for corpora cavernosa reinnervation, sparing a nerve graft. The choice was made on the branch of sciatic nerve for tibialis anterior in order to choose only a pure motor nerve, simulating what was done in humans, maintaining the sensory innervation of the rear limbs, preventing painful neuromas and self-amputation. This choice made the procedure even more difficult, a posterior to anterior tunnel is required, but no valid options were present in rats. What is expected in future is to describe corpora cavernosa reinnervation through functional, biomolecular and morphological analysis and all this represents the main limitation of this paper in which only surgical technique and survival rate at 4 months is presented. Moreover, this technique should be compared in terms of erectile dysfunction recovery, to the cavernous nerve reconstruction by means of chitosan membrane. The advantage of the here described technique is that completely bypass the injured nerve, fact that is closer to what happens in humans after radical prostatectomy, where no nerve stumps are available for reconstruction. Considering what is already done in humans, a nerve transfer for corpora cavernosa could be planned and compared to nerve transfer obtained through nerve grafting.

CONCLUSIONS

Cavernous nerve injury model on rat is a feasible model to test the efficacy of chitosan membrane. The devices are still in place after 2 months and axons can elongate among them. According to our pilot study we can argue that microstructured membranes are able to guide axons regrowth as well as flat membranes, but the use of these nanostructured chitosan membranes is useful for the oriented growth of regenerating fibers. Further studies are required to identify any advantage bring by microstructures.

Moreover, this pilot study demonstrates the feasibility of a nerve transfer in animal model for corpora cavernosa reinnervation. No complications were noted so that a more comprehensive study with more animals divided in different groups could be planned to better understand the effectiveness of this novel method for reinnervation of autonomic driven organs.

BIBLIOGRAPHY

- Adhikari, H.S. & Yadav, P.N. (2018) Anticancer Activity of Chitosan, Chitosan Derivatives, and Their Mechanism of Action. *Int. J. Biomater.*, **2018**, 2952085.
- Brown, M.A., Daya, M.R., & Worley, J.A. (2009) Experience with chitosan dressings in a civilian EMS system. *J. Emerg. Med.*, **37**, 1–7.
- Chuang DCC. Nerve transfers in adult brachial plexus injuries: my methods. *Hand Clin* 2005;21(01):71–82
- Chen, W., Mi, R., Haughey, N., Oz, M., & Höke, A. (2007) Immortalization and characterization of a nociceptive dorsal root ganglion sensory neuronal line. *J. Peripher. Nerv. Syst.*, **12**, 121–130.
- Dangerfield DC, Coombs CJ. 'Case of the Month' from the University of Melbourne, Melbourne, Australia: treatment of iatrogenic erectile dysfunction with somatic-to-autonomic sural nerve grafting. *BJU Int.* 2023 Sep;132(3):262-265.
- Davis JW, Chang DW, Chevray P, et al. Randomized phase II trial evaluation of erectile function after attempted unilateral cavernous nerve-sparing retropubic radical prostatectomy with versus without unilateral sural nerve grafting for clinically localized prostate cancer. *Eur Urol* 2009;55:1135–43
- Doi K. Distal Nerve Transfer: Perspective of Reconstructive Microsurgery. *J Reconstr Microsurg.* 2018 Nov;34(9):675-677
- Fang, T., Shao, Y., Oswald, T., Lineaweaver, W.C., & Zhang, F. (2013) Effect of sildenafil on peripheral nerve regeneration. *Ann. Plast. Surg.*, **70**, 62–65.
- Ferrari, A., Cecchini, M., Serresi, M., Faraci, P., Pisignano, D., & Beltram, F. (2010) Neuronal polarity selection by topography-induced focal adhesion control. *Biomaterials*, **31**, 4682–4694.
- Fueshko, S., and S. Wray. 1994. 'LHRH cells migrate on peripherin fibers in embryonic olfactory explant cultures: an in vitro model for neurophilic neuronal migration', *Dev Biol*, 166: 331-48.
- Gnavi, S., Fornasari, B.E., Tonda-Turo, C., Ciardelli, G., Zanetti, M., Geuna, S., & Perroteau, I. (2015) The influence of electrospun fibre size on Schwann cell behaviour and axonal outgrowth. *Mater. Sci. Eng. C. Mater. Biol. Appl.*, **48**, 620–631.
- Gnavi, S., Fornasari, B.E., Tonda-Turo, C., Laurano, R., Zanetti, M., Ciardelli, G., & Geuna, S. (2018) In vitro evaluation of gelatin and chitosan electrospun fibres as an artificial guide in peripheral nerve repair: a comparative study. *J. Tissue Eng. Regen. Med.*, **12**, e679–e694.
- Gomez-Amaya SM, Barbe MF, Brown JM, Lamarre NS, Braverman AS, Massicotte VS, Ruggieri MR Sr. Bladder reinnervation using a primarily motor donor nerve (femoral nerve branches) is functionally superior to using a primarily sensory donor nerve (genitofemoral nerve). *J Urol.* 2015 Mar;193(3):1042-51.
- Haastert-Talini, K., Geuna, S., Dahlin, L.B., Meyer, C., Stenberg, L., Freier, T., Heimann, C., Barwig, C., Pinto, L.F.V., Raimondo, S., Gambarotta, G., Samy, S.R., Sousa, N., Salgado, A.J., Ratzka, A., Wrobel, S., & Grothe, C. (2013) Chitosan tubes of varying degrees of acetylation for bridging peripheral nerve defects.

Biomaterials, **34**, 9886–9904.

- Hai, M., Muja, N., DeVries, G.H., Quarles, R.H., & Patel, P.I. (2002) Comparative analysis of Schwann cell lines as model systems for myelin gene transcription studies. *J. Neurosci. Res.*, **69**, 497–508.
- Kelly, M.P. & Brandon, N.J. (2009) Differential function of phosphodiesterase families in the brain: gaining insights through the use of genetically modified animals. *Prog. Brain Res.*, **179**, 67–73.
- Korkmaz, M.F., Parlakpınar, H., Ceylan, M.F., Ediz, L., Şamdancı, E., Kekilli, E., & Sağır, M. (2016) The Effect of Sildenafil on Recuperation from Sciatic Nerve Injury in Rats. *Balkan Med. J.*, **33**, 204–211.
- Kovanecz, I., Rambhatla, A., Ferrini, M.G., Vernet, D., Sanchez, S., Rajfer, J., & Gonzalez-Cadavid, N. (2008) Chronic daily tadalafil prevents the corporal fibrosis and veno-occlusive dysfunction that occurs after cavernosal nerve resection. *BJU Int.*, **101**, 203–210.
- Li, G., Zhao, X., Zhang, L., Wang, C., Shi, Y., & Yang, Y. (2014) Regulating Schwann Cells Growth by Chitosan Micropatterning for Peripheral Nerve Regeneration In Vitro. *Macromol. Biosci.*, **14**, 1067–1075.
- Maier, O., Böhm, J., Dahm, M., Brück, S., Beyer, C., & Johann, S. (2013) Differentiated NSC-34 motoneuron-like cells as experimental model for cholinergic neurodegeneration. *Neurochem. Int.*, **62**, 1029–1038.
- Muratori, L., S. Gnani, F. Fregnan, A. Mancardi, S. Raimondo, I. Perroteau, and S. Geuna. 2018. 'Evaluation of Vascular Endothelial Growth Factor (VEGF) and Its Family Member Expression After Peripheral Nerve Regeneration and Denervation', *Anat Rec (Hoboken)*, 301: 1646-56.
- Patel, V.R., Samavedi, S., Bates, A.S., Kumar, A., Coelho, R., Rocco, B., & Palmer, K. (2015) Dehydrated human amnion/chorion membrane allograft nerve wrap around the prostatic neurovascular bundle accelerates early return to continence and potency following robot-assisted radical prostatectomy: Propensity score-matched analysis. *Eur. Urol.*, **67**, 977–980.
- Porpiglia, F., Bertolo, R., Fiori, C., Manfredi, M., De Cillis, S., & Geuna, S. (2018) Chitosan membranes applied on the prostatic neurovascular bundles after nerve-sparing robot-assisted radical prostatectomy: a phase II study. *BJU Int.*, **121**, 472–478.
- Porpiglia, F., Fiori, C., Bertolo, R., Manfredi, M., Mele, F., Checcucci, E., De Luca, S., Passera, R., & Scarpa, R.M. (2018) Five-year Outcomes for a Prospective Randomised Controlled Trial Comparing Laparoscopic and Robot-assisted Radical Prostatectomy. *Eur. Urol. Focus*, **4**, 80–86.
- Porpiglia, F., Manfredi, M., Checcucci, E., Garrou, D., De Cillis, S., Amparore, D., De Luca, S., Fregnan, F., Stura, I., Migliaretti, G., & Fiori, C. (2019) Use of chitosan membranes after nerve-sparing radical prostatectomy improves early recovery of sexual potency: results of a comparative study. *BJU Int.*, **123**, 465–473.
- Reece JC, Dangerfield DC, Coombs CJ. End-to-side Somatic-to-autonomic Nerve Grafting to Restore Erectile Function and Improve Quality of Life After Radical Prostatectomy. *Eur Urol.* 2019 Aug;76(2):189-196.
- Richter, W., Menniti, F.S., Zhang, H.T., & Conti, M. (2013) PDE4 as a target for cognition enhancement. *Expert*

Opin. Ther. Targets, **17**, 1011–1027.

- Salmasi, A., Lee, G.T., Patel, N., Goyal, R., Dinizo, M., Kwon, Y.S., Modi, P.K., Faiena, I., Kim, H.J., Lee, N., Hannan, J.L., Kohn, J., & Kim, I.Y. (2016) Off-Target Effect of Sildenafil on Postsurgical Erectile Dysfunction: Alternate Pathways and Localized Delivery System. *J. Sex. Med.*, **13**, 1834–1843.
- Souza Trindade JC, Viterbo F, Petean Trindade A, Fávaro WJ, Trindade-Filho JCS. Long-term follow-up of treatment of erectile dysfunction after radical prostatectomy using nerve grafts and end-to-side somatic-autonomic neurorraphy: a new technique. *BJU Int.* 2017 Jun;119(6):948-954.
- Wieringa, P., Tonazzini, I., Micera, S., & Cecchini, M. (2012) Nanotopography induced contact guidance of the F11 cell line during neuronal differentiation: a neuronal model cell line for tissue scaffold development. *Nanotechnology*, **23**.
- Wu, W., Lee, S.Y., Wu, X., Tyler, J.Y., Wang, H., Ouyang, Z., Park, K., Xu, X.M., & Cheng, J.X. (2014) Neuroprotective ferulic acid (FA)-glycol chitosan (GC) nanoparticles for functional restoration of traumatically injured spinal cord. *Biomaterials*, **35**, 2355–2364.
- Xiao, C. G., De Groat, W. C., Godec, C. J., Dai, C. and Xiao, Q.: “Skin-CNS-bladder” reflex pathway for micturition after spinal cord injury and its underlying mechanisms. *J Urol*, **162**: 936, 1999
- Youssef, A.M., Abou-Yousef, H., El-Sayed, S.M., & Kamel, S. (2015) Mechanical and antibacterial properties of novel high performance chitosan/nanocomposite films. *Int. J. Biol. Macromol.*, **76**, 25–32.

3.8 Experimental Methods to Simulate and Evaluate Postsurgical Peripheral Nerve Scarring.

Crosio A, Ronchi G, Fornasari BE, Odella S, Raimondo S, Tos P.

J Clin Med. 2021 Apr 10;10(8):1613



Review

Experimental Methods to Simulate and Evaluate Postsurgical Peripheral Nerve Scarring

Alessandro Crosio ^{1,†}, Giulia Ronchi ^{2,†}, Benedetta Elena Fornasari ², Simonetta Odella ¹,
Stefania Raimondo ^{2,*} and Pierluigi Tos ¹

¹ UO Microchirurgia e Chirurgia della Mano, Ospedale Gaetano Pini, Piazza Andrea Ferrari 1, 20122 Milano, Italy; Alessandro.Crosio@asst-pini-cto.it (A.C.); simonettaodella@gmail.com (S.O.); Pierluigi.Tos@asst-pini-cto.it (P.T.)

² Department of Clinical and Biological Sciences & Neuroscience Institute of the “Cavalieri Ottolenghi” Foundation (NICO) University of Turin, Regione Gonzole 10, 10043 Orbassano (TO), Italy; giulia.ronchi@unito.it (G.R.); benedettaelena.fornasari@unito.it (B.E.F.)

* Correspondence: stefania.raimondo@unito.it; Tel.: +39-011-670-5433

† A.C. and G.R. contributed equally to this work.

Abstract: As a consequence of trauma or surgical interventions on peripheral nerves, scar tissue can form, interfering with the capacity of the nerve to regenerate properly. Scar tissue may also lead to traction neuropathies, with functional dysfunction and pain for the patient. The search for effective antiadhesion products to prevent scar tissue formation has, therefore, become an important clinical challenge. In this review, we perform extensive research on the PubMed database, retrieving experimental papers on the prevention of peripheral nerve scarring. Different parameters have been considered and discussed, including the animal and nerve models used and the experimental methods employed to simulate and evaluate scar formation. An overview of the different types of antiadhesion devices and strategies investigated in experimental models is also provided. To successfully evaluate the efficacy of new antiscarring agents, it is necessary to have reliable animal models mimicking the complications of peripheral nerve scarring and also standard and quantitative parameters to evaluate perineural scars. So far, there are no standardized methods used in experimental research, and it is, therefore, difficult to compare the results of the different antiadhesion devices.

Keywords: scar tissue; peripheral nerve regeneration; antiadhesion devices; animal models



Citation: Crosio, A.; Ronchi, G.; Fornasari, B.E.; Odella, S.; Raimondo, S.; Tos, P. Experimental Methods to Simulate and Evaluate Postsurgical Peripheral Nerve Scarring. *J. Clin. Med.* **2021**, *10*, 1613. <https://doi.org/10.3390/jcm10081613>

Academic Editor: Lucas Prantl

Received: 27 January 2021

Accepted: 7 April 2021

Published: 10 April 2021

Publisher's Note: MDPI stays neutral with regard to jurisdictional claims in published maps and institutional affiliations.



Copyright: © 2021 by the authors. Licensee MDPI, Basel, Switzerland. This article is an open access article distributed under the terms and conditions of the Creative Commons Attribution (CC BY) license (<https://creativecommons.org/licenses/by/4.0/>).

1. Introduction

Scar tissue around the nerve can arise as a consequence of traumatic injuries and surgical procedures on peripheral nerves. This condition easily worsens the capacity of the peripheral nerve to regenerate and can give rise to traction neuropathies. Nerve tethering in the surgical scar is still the main cause of symptoms related to perineural scarring [1].

Traction neuropathies can be the consequence of elective procedures, including nerve decompression, primary nerve repair, and so on. For instance, 7–20% of patients subjected to primary median nerve release report pain and symptom recurrence [2,3]. Thus, peripheral nerve injuries compromise the quality of life of affected people, with a consequent important socioeconomic impact [4–6].

This condition is difficult to manage; according to different reports, compression symptoms persist after 40–90% of revision procedures, and 20% of patients actually require a third operation [7]. Moreover, 5% of nerve sutures have been estimated to induce a pain syndrome [8].

A primary role in this pathological condition has been attributed to the formation of scar tissue around the injured nerve. In particular, extrinsic nerve scarring occurs at the periphery of the epineurium, while intrinsic nerve scarring occurs within the nerve and can surround neural structures at all levels (both perineurium and endoneurium) [9]. To

overcome scar tissue formation, a lot of different antiadhesion devices have been tested, developed, and introduced in clinical practice.

Since the late 1990s, researchers have tried to develop experimental models to investigate the efficacy of different antiadhesion devices. Several types of devices have been tested so far, but the methods employed to produce, simulate, and evaluate postsurgical scars are completely inhomogeneous and not reproducible [10]. This makes it difficult to compare the efficacy of the different antiadherence strategies in order to optimize clinical treatment.

The aim of this review is to illustrate the different methods adopted in experimental research to simulate and evaluate postsurgical scars. Finally, an overview of the antiadhesion devices tested so far in preclinical research is also provided.

2. Materials and Methods

An extensive research on PubMed was performed, employing the following search string: “peripheral nerves AND fibrosis OR perineural scar OR scar neuropathy OR traction neuropathy AND prevention”, limited to English, other animals, and between 1 January 1995 and 31 December 2020. Furthermore, the reference list of each article was screened in order to find any additional original articles. Selection by title, abstract, and text was then performed; a total of 60 papers were retrieved. We did our best to include all articles available; nevertheless, inadvertently, we could have missed some papers, and we apologize in advance to their authors.

3. Scar Simulation: Animal and Nerve Choice

The choice of an appropriate animal model for preclinical research depends on different factors, including the aim and duration of the study, the anatomy and physiology of the animal model, the size of the medical device that needs to be tested, and, of course, the similarity with human clinical characteristics of the disease/condition. Finally, the cost and care of the animal model (housing, feeding, and caring) can also be considered.

For the study of peripheral nerve scarring, the most employed animal model is the rat model, followed by mouse and rabbit used in a limited number of studies (see Tables 1–6). This can be due to the lower cost of rats compared to rabbits, the easier caregiving, and the faster scar formation in smaller rather than bigger animals. On the other hand, mice (and their nerves) are very small and, therefore, more difficult to manage. Additionally, different rat/rabbit/mouse strains have been used. No research with other animal species (sheep, pigs, monkeys, cats, or dogs) has been found, in contrast with studies on peripheral nerve regeneration, where sheep as an animal model is often used to test regeneration across long distances [11,12].

Moreover, the choice of nerve model can be guided by several factors, including nerve size and the surrounding tissues. Most researchers use the sciatic nerve because it can be easily dissected, and there are no surrounding vascular and nervous structures that can impair the efficacy of the study. Only a few papers have used other nerve models such as the ulnar [13,14], peroneal [15], and median nerves [16].

4. Scar simulation: Experimental Methods to Induce Scar Formation

The main aim of most of the research dealing with scar formation is to test the efficacy of antiadhesion devices. Only very few papers [17–21] are focused on the standardization of a scarring method without testing any antiadhesion device (Table 1). These papers are very important in this field because a shared, effective, reliable, and reproducible protocol to induce and evaluate the amount of scar tissue is needed to compare the efficacy of different antiadhesion devices; so far, this is not available [18,20–22].

Table 1. No antiscarring agents tested.

Reference	Method to Induce Scar Formation	Animal and Nerve Model	Analyses	Results
Lemke et al., 2017 [21]	Application of “glutaraldehyde glue” on the nerve and surrounding muscle or scratching	Female Sprague–Dawley Rat Sciatic nerve	<ul style="list-style-type: none"> - Functional evaluation (CatWalk, SFI) (once a week) - Gross evaluation (Petersen’s classification) (3 weeks) - Histology on nerve and surrounding tissue (H&E, Masson’s trichrome and Luxol fast blue, chromotrop-aniline-blue) (3 weeks) - IHC (2F11, S100, CD-68, CD-3, CD-8) (3 weeks) - Electrophysiological evaluation (3 weeks) 	Severe intra- and perineural scarring, vigorous nerve inflammation and nerve degeneration and functional deficit.
Crosio et al., 2014 [20]	Burning or scratching	Male Mouse Sciatic nerve	<ul style="list-style-type: none"> - Biomechanical analysis (3 weeks) - Histology on nerve and surrounding tissue (Picosirius staining) (3 weeks) 	Both methods produced fibrotic reactions with no differences in biomechanical results between the two methods; histology showed a different distribution pattern of the scar tissue.
Okuhara Y et al., 2014 [19]	Irradiation of the nerve with X-radiation	Female LEW/CrJCrJ Rat Sciatic nerve	<ul style="list-style-type: none"> - Functional evaluation (SFI) (4, 8, 12, 16, 20, and 24 weeks) - Electrophysiological evaluation (24 weeks) - Gross evaluation (qualitative) (24 weeks) - Histology on nerve and surrounding tissue (Masson’s trichrome and Toluidine Blue for morphometric analysis) (24 weeks) 	Scar formation around the radiated nerve. No differences in SFI between groups, but axonal degeneration in the irradiated nerve.
Zanjani et al., 2013 [18]	Laceration, crush, mince, and burn of the surrounding muscles	Female Wistar Rat Sciatic nerve	<ul style="list-style-type: none"> - Functional evaluation (Toe Out Angle) (weekly up to 4 weeks) - Gross Evaluation (Petersen’s classification) (1, 2, 3, 4 weeks) - Histology on nerve and surrounding tissue (Masson’s trichrome) (1, 2, 3, 4 weeks) 	Scar tissue formation surrounding the sciatic nerve in gross examination and histological analysis; no differences in functional assessment compared to control.

Table 1. Cont.

Reference	Method to Induce Scar Formation	Animal and Nerve Model	Analyses	Results
Abe et al., 2005 [17]	Nerve bed cauterization and suturing the nerve in place	Male Japanese White Rabbit Sciatic nerve	<ul style="list-style-type: none"> - Gross evaluation (classification based on Fontana’s bands and Sakurai’s classification) (6, 14, 22, 30, or 38 weeks) - Electrophysiological evaluation (6, 14, 22, 30, or 38 weeks) - Nerve fascicle blood flow (6, 14, 22, 30, or 38 weeks) - Histology on nerve and surrounding tissue (Toluidine Blue) (6, 14, 22, 30, or 38 weeks) 	Adhesion of peripheral nerve to surrounding tissues results in fibrosis in the nerve. Compound muscle action potentials were reduced in amplitude, and blood flow was significantly decreased at adhesion sites in Group IIb.

SFI (Sciatic functional index), IHC (Immunohistochemistry), 2F11 (antibody labelling neurofilament), S100 (antibody labelling Schwann cells), CD-68 (Cluster of Differentiation 68, antibody labelling macrophages), CD-3 (Cluster of Differentiation 3, antibody labelling T cells), CD-8 (Cluster of Differentiation 8, antibody labelling cytotoxic T cells).

The methods used to induce scar formation are several (Figure 1), but two of these are more frequently used. The first one consists of a direct injury (mechanical, epiperineurectomy, suture and repair, thermal, chemical, or physical) applied to the nerve surface. The second one consists of inducing an injury in the surrounding muscular bed by means of electrocoagulation, triggering the process of fibrosis from the surrounding tissue. Some researchers have induced a global injury to the nerve and surrounding tissues by scratching both nerve and muscles with irradiation or chemical injuries. Furthermore, the envelopment of the nerve in a silastic tube in order to let the scar tissue rise has been proposed.

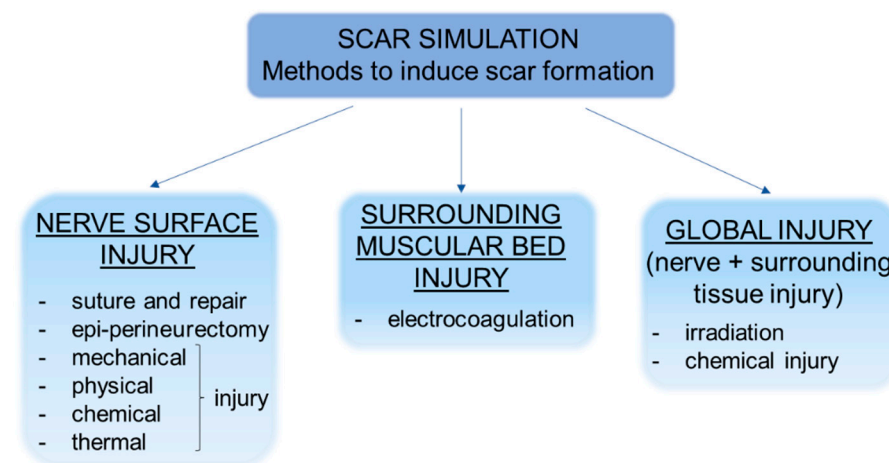


Figure 1. Representative scheme showing the different strategies to simulate scar formation in preclinical models.

Some of the earlier papers [23–25] performed a two-stage procedure (first stage injury, second stage neurolysis and antiadhesion application), which is a more traumatic experience for animals, without evidence of increased efficacy compared to a one-stage procedure. With respect to the 3Rs statement [26], a single-stage experiment can have the same efficacy as a two-stage one.

5. Scar Evaluation: Methods to Evaluate Scar Formation in Experimental Models

Different procedures can be used to evaluate scar formation, including gross examination of the scar tissue, microscopical analysis of the nerve and surrounding tissue, functional tests, and electrophysiological and biomechanical evaluations (Figure 2). All of these evaluation methods are combined differently by authors. It must also be noted that the time points analyzed are very different among the studies, ranging from few days to several months from the induction of scar formation; the research also differs according to the employed animal model.

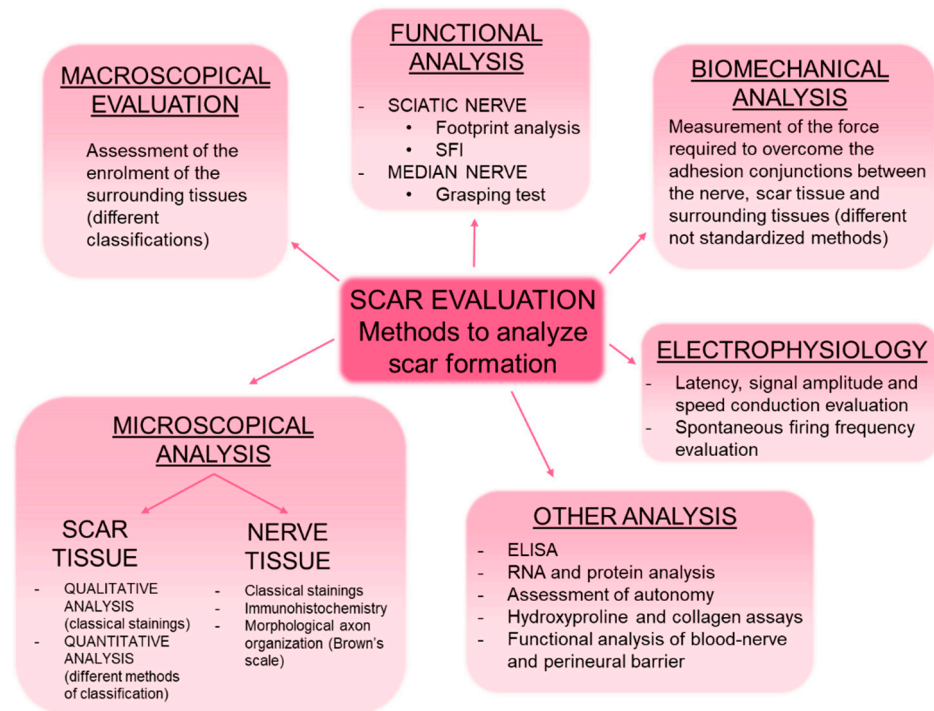


Figure 2. Representative scheme showing the different methods of evaluating scar formation in preclinical models. SFI (sciatic functional index), ELISA (enzyme-linked immunosorbent assay).

5.1. Macroscopical Analysis

Gross evaluation is the first fundamental step to macroscopically grade scar tissue; it aims to assess the enrolment of the surrounding tissues (including skin, muscles, and deep tissues) in the compression of the nerve and the collaboration with the newborn perineural scar tissue.

Different classifications have been proposed by different authors to evaluate the degree of scar formation. The most used and complete classification is the numeric grade scheme defined by Petersen [27]. This classification allows us to evaluate closure of skin and muscle fascia (Grade 1: skin or muscle fascia entirely closed; Grade 2: skin or muscle fascia partially open; Grade 3: skin or muscle fascia completely open) and to evaluate nerve adherence (Grade 1: no dissection or mild blunt dissection; Grade 2: some vigorous blunt dissection required; Grade 3: sharp dissection required). Another adopted grading scheme is the 4-point qualitative scale that evaluates the perineural adhesions and type of dissection required to achieve complete neurolysis, as follows: absent or thin adhesions—delicate blunt (score 0); mild adhesion—vigorous blunt (score 1); moderate adhesion—delicate sharp (score 2); severe adhesion—difficult sharp (score 3) [13,14,23,28].

Abe [17] proposed a classification of nerve adhesion based on Fontana’s band (an optical manifestation of axonal undulations characteristic of peripheral nerves). They classify nerve adhesion as Group I (nonadhesion group) when the bands appear and Group II if they are not visible. Additionally, Group II is divided into Group IIa when a thickening

of the epineurium and perineurium is observed (but not endoneurial fibrosis) and Group IIb when endoneurial fibrosis is observed.

Finally, some authors have reported the presence or absence and qualitative observations of scar tissue around the nerve without grading it.

5.2. Microscopical Analysis: Histological Staining and Immunohistochemistry

Microscopical analysis is employed by most authors and consists mainly of the use of different histological stainings to visualize and describe the different structures involved (not only the scar tissue but also the nerve and surrounding tissues, such as muscle), both qualitatively and quantitatively (see Tables 1–6).

5.2.1. Analysis of the Scar Tissue

The most employed method to highlight scar tissue is Masson's trichrome staining because it specifically marks collagen in green/blue and can be easily distinguished from other structures such as muscle fibers (stained in red), cytoplasm (light red or pink), and cell nuclei (dark brown to black).

Haematoxylin and eosin (H&E) is the most widely used staining for histological purposes because it provides a general overview of the tissue, and it is mainly used to distinguish nerves from surrounding tissues. It is the combination of two histological stains: hematoxylin, which stains cell nuclei in blue/dark-purple, and eosin, which stains cytoplasm in pink, and other structures, including extracellular matrix and collagen, in shades of pink.

Picrosirius red is often used since it selectively highlights collagen fibers [29]; indeed, this dye allows us to visualize collagen fibers in red (specific for collagen types I and III), while the other structures are stained in yellow (nuclei, cytoplasm, muscular fibers, red blood cells). The Gordon and Sweet technique, used to reveal reticulinic acid, a collagenous tissue marker, has also been adopted, as well as chromotrop-aniline-blue, which stains collagen in blue and muscle fibers in red.

Besides a qualitative analysis of scar tissue formation, histological staining allows us to also perform quantitative analyses. One of the most used parameters to measure scar tissue is the scar tissue formation index, calculated by dividing the mean thickness of the scar tissue by the mean thickness of the nerve tissue [18,27,28,30–41]. Sakurai's classification of neural fibrosis [42] allows us to describe the extension of the perineural scar from epineurium to endoneurium (Grade 1: the nerve is normal; Grade 2: extraneural type; Grade 3: intraneural, epineural type; Grade 4: intraneural, perineural type; Grade 5: intraneural, endoneurial type; Grade 6: dispersive type) [17].

The number of fibroblasts/fibrocytes is another parameter that is often used, and it allows us to classify the specimens into Grade 1—less than 100 fibroblasts; Grade 2—100–150 fibroblasts; Grade 3—more than 150 fibroblasts [30,32,34,41,43,44].

The classification of Ornelas [45] has also been adopted [46,47], and it allows us to classify extraneural and intraneural fibrosis; extraneural fibrosis is classified into Grade 1—absent or minimal fibrosis; Grade 2—moderate fibrosis; Grade 3—major fibrosis. Intraneural fibrosis is classified into Grade 1—the presence of fibrous tissue between the nerve fibers; Grade 2—fibrous tissue partially blocking the passage of nerve fibers; Grade 3—fibrous tissue completely interrupting the passage of nerve fibers.

Dam-Hieu [28] calculated the thickness of the dense scar surrounding the nerve. The largest thickness of the scar ring (ST) was measured. This value was then normalized by dividing it by the nerve diameter (ND). The authors call this value the fibrotic index (fibrotic index = $2 \text{ ST} / \text{ND}$).

Other quantitative or semiquantitative analyses have also been proposed, such as the average thickness of collagen in the epineurium [14,48], the count of fibroblasts and inflammatory cells [36,38,46], the thickness of the epifascicular epineurium, the amount of connective tissue in the interfascicular and epifascicular epineurium [49], and the percentage of area of staining (PAS) calculation by outlining the intraneural tissue [50–53].

5.2.2. Analysis of the Nerve Tissue

To investigate the nerve tissue specifically, Luxol fast blue, P-phenylenediamine, silver staining, the Weil method, and toluidine blue were used to describe axon distribution and highlight the myelin sheath. In particular, toluidine blue staining offers the possibility of performing morphoquantitative analyses to estimate the number of myelinated fibers, axon density, fiber and axon diameter, myelin thickness, and g-ratios (axon-diameter/fiber-diameter), which can be correlated with functional recovery [5,54].

Moreover, the longitudinal histomorphological organization of the axon at the nerve repair site can be evaluated according to the scale developed by Brown et al. [55] and adopted by several authors [31,35,36,38,56]: Grade 1—failure, no continuity of the axons from the proximal to the distal ends; Grade 2—poor organization (interlacing or whirling appearance of the nerve fibers); Grade 3—fair organization (focal whirling appearance, focal parallel alignment); Grade 4—good organization, approaching normal (mostly parallel, without a whirling or wavy appearance); Grade 5—excellent organization of the repair site, indistinguishable from the norm.

Finally, some authors have added immunohistochemistry to classical staining methods. This method is efficient in describing nerve regeneration quality with antibodies, which specifically mark Schwann cells (anti-S100, to mark the myelin sheath) [21,36], nerve cones (anti-GAP 43) [37], or antineurofilament [21,57]. Immunohistochemistry has been also adopted to study perineural scars by using antibodies against TGF- β markers of macrophages [58], CD68 for activated macrophages [21,37,57,59], anti-CCR7 for proinflammatory M1 macrophages [57], CD3, CD8 [21], and collagen I [60]. Additionally, antibodies against decorin, aggrecan, laminin 2, collagen IV, and fibronectin have been used [61]. Finally, Murakami [62] performed immunohistochemistry analysis on dorsal root ganglia using the inflammation marker CGRP and tissue stress ATF3 antibodies.

5.3. Functional Analysis

Some studies performed functional analyses, even though these analyses are not precise for scar quantification and we are not sure that they can be directly correlated to the amount of scarring observed around the nerve.

Most of the studies dealing with peripheral scarring use the sciatic nerve model, foot print analysis, and the Sciatic Function Index (SFI) as the most adopted tests [63]. Other parameters evaluated are allodynia by means of von Frey filaments [62] and walking patterns induced by pain with the CatWalk system [21,51,62].

The only study that used the median nerve model tested the function of the nerve by means of the grasping test [16].

5.4. Electrophysiological Study

Electrophysiology is another test that can be used in order to analyze the formation of scars around the nerve. Indeed, compression around a nerve causes pathophysiological changes that can be registered with this assessment.

The electrophysiological analysis is based on compound motor action potential (CMAP). Different aspects of electrical activity can be registered, such as latency, signal amplitude, and speed conduction. These parameters correlate with nerve conduction; the more the scar is present, the more these parameters are altered.

Another assessment that is useful to evaluate is the frequency of spontaneous firing because it has been demonstrated to be related to nerve suffering: the more frequent the firing is, the more the nerve is suffering [64].

Zuijndendorp [22] and its colleagues performed the evaluation by means of magnetoneurography of first peak amplitude, peak–peak amplitude, area, and conduction velocity over the nerve segment between the stimulation and the recording site.

Recently, the combination of electrodiagnostic evaluation, with the commonly used grasping test (reflex-based gross motor function) and the staircase test (skilled forelimb reaching), has been found to produce results with high translatability [65].

5.5. Biomechanical Analysis

Biomechanical analysis gives an objective evaluation of scar tissue formation and consists of measuring the force required to overcome the adhesion conjunctions between the nerve, scar tissue, and surrounding tissues. Different methods have been proposed, but the results obtained represent, with variability according to the precision of the utilized instruments, a quantitative expression of newborn scar tissue.

Dumanian [66] and his colleagues were the first to describe a method and device to measure the strength of nerve adhesion to surrounding muscles. They used a standard alligator clamp placed on the nerve and a force transducer connected, in turn, to a micrometer. The micrometer was distracted in 1 mm increments. The measurement is continued until final failure of the nerve or nerve pullout from the clamp.

Another method is to mount the nerve proximal stump on a digital force gauge using a suture connected to the load cell; then, the nerve is subjected to traction at a rate of 2 cm/min (or 1 cm/s) [24] until its complete detachment from the neural bed; the ultimate strength is recorded [57,67–69].

A different way consists of transecting both the proximal and distal ends of the nerve; the proximal end is then interconnected to a force transducer, which is connected, in turn, to a motorized drive with a constant extension rate of 29 mm/min. The force required to pull the nerve segment out of its tissue bed is recorded [10,22].

In another paper, after nerve and surrounding tissue removal from the animal, the distal end of the nerve was held by a clamp to the cross-head of an Instron machine. The subsequent cross-head movement (at a rate of 10 mm/min) then gradually peeled the nerve away from the adhesion site, and the maximum peeling force was recorded [15].

Finally, some recent papers have described a simple and cheap method that consists of connecting the nerve to a plastic can that is gradually filled with water at a constant flow of 100 mL/min. The adhesion force is obtained from the grams of water at the break moment [20,70,71].

5.6. Other Analysis

Other types of analyses have also been described, such as enzyme-linked immunosorbent assays (ELISAs) to evaluate neurotrophic factor concentration [62], RNA and protein analysis [61], assessment of autotomy [37], functional analysis of the blood–nerve barrier and the perineurial barrier [69], and hydroxyproline and collagen assays [60].

In vitro culture of rat skin fibroblasts to test the efficacy of drug administration has also been described [58].

Histological staining can also be used to describe muscle tissue organization in order to evaluate atrophy and fibrous degeneration of the innervated muscles [13,49,57]. Moreover, atrophy is often investigated by measuring muscle wet weight. Finally, transmission electron microscopy has been adopted to describe the ultrastructure of nerve tissue and surrounding tissues [30,39,48,60,72].

6. How to Prevent Scar Formation? An Overview on Different Antiadhesion Devices

Every surgical practice on peripheral nerves is followed by postsurgical scar tissue formation. In order to limit this event, surgeons apply different procedures such as local or free tissue transfer and antiadherent items of different origins. There are many different kinds of antiadhesion devices, composed of different materials with different ways of application, but there is no evidence of their efficacies. Below is an overview of the different antiadhesion devices tested so far in experimental models.

6.1. Polysaccharide-Based Devices

Different polysaccharides were used as antiscarring agents, and the available preclinical studies on the polysaccharides-based devices are reported in Table 2.

Table 2. Polysaccharide-based antiscarring agents.

Reference	Method to Induce Scar Formation	Agent	Animal and Nerve Model	Analyses	Results
Hachinota et al., 2020 [73]	Section of transvers carpal ligament, excision of median nerve bed, suture of carpal ligament	Alginic acid-based gel formulation	Japanese White Rabbit Median nerve	<ul style="list-style-type: none"> - Electrophysiological evaluation (1, 2, 3, 6 weeks) - Macroscopic evaluation (adhesion scoring system modified from Palatinsky ones) - Histology on tissues excised after electrophysiological evaluation (H&E staining) 	Longer latency, not significant, in the control group. Lower adhesion score values in the treatment group at 2–3–6 weeks, more scar tissue in the control group. More severe perineural fibrosis in the control group.
Li et al., 2018 [48]	Crush injury	Chitosan conduit (CC); hyaluronic acid (HA); CC + HA	Sprague–Dawley RatSciatic nerve	<ul style="list-style-type: none"> - Functional evaluation (SFI) (4, 8, 12 weeks) - Gross Evaluation (Petersen’s classification) (4, 8, 12 weeks) - Electrophysiological evaluation (12 weeks) - Histology on nerve and surrounding tissue (H&E, Masson’s trichrome and Toluidine Blue) (4, 8, 12 weeks) - Ultrastructural evaluation (TEM) (4, 8, 12 weeks) 	Both chitosan and HA inhibited extraneural scarring, promoted nerve regeneration, increased nerve conduction velocity, and improved the recovery of nerve function.
Mekaj et al., 2017 [36]	Section + suture	HA	Male European Rabbit Sciatic nerve	<ul style="list-style-type: none"> - Gross evaluation (Petersen’s classification) (12 weeks) - Muscle wet weight (12 weeks) - Histology on nerve and surrounding tissue (H&E, Masson’s trichrome) (12 weeks) - Nerve IHC (S100) (12 weeks) 	Reduction scar around the nerve, both macroscopically and microscopically. Increased nerve diameter. Higher gastrocnemius mass. Improved microstructural organization. Higher expression of S100.

Table 2. Cont.

Reference	Method to Induce Scar Formation	Agent	Animal and Nerve Model	Analyses	Results
Tos et al., 2016 [71]	Burning	Carboxymethylcellulose (CMC)-polyethylene oxide (PEO) gel	CD1 Mouse Sciatic nerve	<ul style="list-style-type: none"> - Biomechanical analysis (3 weeks) - Histology on nerve and surrounding tissue (Picrosirius staining) (3 weeks) 	Reduction in scar tissue after CMC-PEO gel application. The qualitative histological analysis supported the biomechanical findings depicting the pattern of scar tissue.
Urano et al., 2016 [68]	Enwrapping with silicon tube (nerve compression)	CMC-phosphatidyl-ethanolamine (PE)	Male Lewis Rat Sciatic nerve	<ul style="list-style-type: none"> - Electrophysiological evaluation (1, 2, 3 months) - Biomechanical analysis (1, 2, 3 months) - Muscle wet weight (1, 2, 3 months) - Histology on nerve and morphometric analysis (Toluidine Blue) (1, 2, 3 months) 	Electrophysiology showed significantly quicker recovery; mean wet muscle weight was constantly higher; the axon area at one month was twice as large as control.
Marcol et al., 2011 [37]	Section + suture	Chitosan	Male Wistar Rat Sciatic nerve	<ul style="list-style-type: none"> - Autotomy assessment (daily, until 20th week) - Histology on nerve and surrounding tissue (H&E, Masson's trichrome and Toluidine Blue) (20 weeks) - Nerve IHC (CD-68, GAP43) (20 weeks) 	High incidence of amputations (about 100%, no sig. diff.). Reduction in microscopical analysis of neuroma in chitosan; significant reduction of scar around nerve; increased mast cells and macrophages in chitosan. Application of the microcrystalline chitosan gel is easy and requires no special equipment but does not influence the features of neuropathic pain.
Park et al., 2011 [38]	Section + suture	HA-CMC	Sprague-Dawley Rat Sciatic nerve	<ul style="list-style-type: none"> - Gross evaluation (Petersen's classification) (3, 6, 9, 12 weeks) - Histology on nerve and surrounding tissue (H&E, Masson's trichrome) (3, 6, 9, 12 weeks) 	Macroscopical scar reduction. Reduction of inflammation cells and fibroblasts. Reduction of scar formation index. Better axonal organization.

Table 2. Cont.

Reference	Method to Induce Scar Formation	Agent	Animal and Nerve Model	Analyses	Results
Hernández-Cortés et al., 2010 [74]	Tissue aggression (cauterization of muscle bed)	Oxidized regenerated cellulose	Male Sprague-Dawley RatSciatic nerve	- Histology on nerve and surrounding tissue (H&E, Masson’s trichrome, PAS, or Sirius red) (3 and 6 weeks)	No statistical differences in intra- and perineural scars, which demonstrate no antifibrogenic effect of oxidized regenerated cellulose. Inflammatory phenomena and foreign body granulomatous reactions were more frequently detected in oxidized regenerated cellulose-treated samples.
Yamamoto et al., 2010 [67]	Burning muscle + epi- and perineurium removal	CMC-PE	Lewis Rat Sciatic nerve	- Gross evaluation (evaluation of healing of skin and fascia—Grade 1–3) (6 weeks)	CMC-PE hydrogel offered superior efficacy to 1% HA and caused no delay in wound healing. Reduction of macroscopical scar, reduction of scar in biomechanical testing. Electrophysiological and muscle weight analyses demonstrated the effectiveness of CMC-PE treatment after extensive internal neurolysis.
		HA		- Biomechanical analysis (6 weeks) - Histology on nerve and surrounding tissue (H&E Masson’s trichrome) (1, 2, 3, 4, 5, 6 weeks) - Electrophysiology (2,7, 20, and 42 days) - Muscle wet weight (2,7, 20, and 42 days)	
Magill et al., 2009 [72]	Section + suture	HA-CMC (Septrafilm)	Male Lewis Rat Sciatic nerve	- Functional evaluation (SFI) (biweekly until day 32) - Histology on nerve and surrounding tissue and morphometric analysis (Toluidine Blue) (18, 32, 42 days) - Ultrastructural evaluation (TEM) (18, 32, 42 days)	Qualitatively less perineural scar tissue was observed using Septrafilm. No functional or histological deleterious effects were detected with Septrafilm placed on intact nerves or cut and repaired nerves.
Zuijendorp et al., 2008 [22]	Crush injury	Regenerating agents (sulfated glycosaminoglycan)	Female Wistar RatSciatic nerve	- Biomechanical analysis (6 weeks) - Magnetoneurography (5 weeks) - Footprint analysis (1, 7, 14, 17, 21, 24, 28, 35 and 42 days)	Reduction of biomechanical resistance. No differences in magnetoneurography and functional analysis were detected.

Table 2. Cont.

Reference	Method to Induce Scar Formation	Agent	Animal and Nerve Model	Analyses	Results
Dam-Hieu et al., 2005 [28]	Abrasive injury/section + suture	Auto cross-linked polysaccharide (ACP) with different viscosity	Male Sprague–Dawley Rat Sciatic nerve	<ul style="list-style-type: none"> - Gross evaluation (4-point qualitative Scale) (4 weeks) - Histology on nerve and surrounding tissue (H&E, Masson’s trichrome, Gordon and Sweets stain and Toluidine Blue) (4 weeks) 	Significant reduction of scar tissue formation was observed through macro and micro analyses.
Ohsumi et al., 2005 [69]	Burning	Alginate sol	Lewis Rat Sciatic nerve	<ul style="list-style-type: none"> - Histology on nerve and surrounding tissue (H&E Masson’s trichrome) (1, 2, 3, 4, 5, 6 weeks) - Functional analysis of the blood–nerve barrier and the perineurial barrier (6 weeks) - Biomechanical analysis (6 weeks) 	Strong inhibition of perineurial granulation, recovering of the perineurial barrier function, antiadhesive effect.
Smit et al., 2004 [10]	Section + suture	HA	Female Wistar Rat Sciatic nerve	<ul style="list-style-type: none"> - Biomechanical analysis (6 weeks) 	Significant biomechanical reduction of adhesion after HA application.
Ikeda et al., 2003 [24]	Burning muscular bed + suture	HA (after 6 weeks)	White Japanese Rabbit Sciatic nerve	<ul style="list-style-type: none"> - Electrophysiological evaluation (6 weeks) - Histology on nerve and surrounding tissue (Masson’s trichrome) (6 weeks) - Biomechanical analysis (6 weeks) 	Significant latency reduction. Qualitative reduction of scar in microscopical analysis. No significant reduction in biomechanical analysis.

Table 2. Cont.

Reference	Method to Induce Scar Formation	Agent	Animal and Nerve Model	Analyses	Results
Ozgenel et al., 2003 [35]	Section + suture	HA	Male Sprague–Dawley Rat Sciatic nerve	<ul style="list-style-type: none"> - Functional evaluation (SFI) (every two weeks until week 12) - Gross evaluation (Petersen’s classification) (4, 12 weeks) - Electrophysiological evaluation (12 weeks) - Wet muscle weight (12 weeks) - Histology on nerve and surrounding tissue (Masson’s trichrome 4, 12 weeks, H&E, Weil method for morphometric analysis) (12 weeks) 	Significant reduction in scarring, better conduction velocities, increased axon and fiber diameter, and faster functional recovery.
Adanali et al., 2003 [49]	Section + suture	HA–CMC	White New Zealand Rabbit Sciatic nerve	<ul style="list-style-type: none"> - Gross evaluation (qualitative) (3 months) - Electrophysiological evaluation (3 months) - Histology on muscle (H&E, Masson’s trichrome) (3 months) - Histology on nerve and surrounding tissue (H&E, Masson’s trichrome, Toluidine Blue) (3 months) 	Macroscopically reduction of scar tissue around the nerve. Increased quality of myelin sheets and the number of axons.

SFI (Sciatic functional index), TEM (Transmission Electron Microscope), IHC (Immunohistochemistry).

6.1.1. Hyaluronic acid

Hyaluronic acid is a glycosaminoglycan that is widely found in the body of all living organisms as it is an important extracellular matrix component. Since it does not exhibit species or tissue specificity and is biodegradable in vivo, it is often used as an ideal biomaterial. It has been demonstrated that hyaluronic acid reduces epineural and extraneural scar formation [36,38,67]. Additionally, biomechanical reduction of scar tissue has been documented [10], together with an improvement of latency [24].

6.1.2. Carboxymethylcellulose

Carboxymethylcellulose is another biocompatible polysaccharide that acts as a physical barrier and can reduce scar formation in the central nervous system; it has been demonstrated that carboxymethylcellulose, in association with phosphatidylethanolamine, reduces peripheral nerve scarring and biomechanical resistance [67,71]. It has also been used in association with hyaluronic acid; additionally, in this case, it reduces scar formation, reduces inflammation cells and fibroblasts, and leads to better axonal organization [38,72], together with an increase in the quality of myelin sheets and the number of axons [49].

6.1.3. Chitosan

Chitosan is a polysaccharide obtained by partial deacetylation of chitin. It has well-known advantageous properties, such as lack of toxicity and biocompatibility, biodegradability, and antimicrobial properties. Various forms of chitosan can be produced and microcrystalline chitosan gel applied to the proximal stump of a transected sciatic nerve has been shown to reduce the incidence and size of the neuroma and the formation of extraneural fibrosis [37]. It has also been used in the form of conduit in association with hyaluronic acid, and it has been demonstrated to reduce nerve scarring and promote nerve regeneration and recovery [48].

6.1.4. Other polysaccharides

Few papers have tested other polysaccharides, such as oxidized regenerated cellulose [74], regenerating agent OTR4120 [22], cross-linked polysaccharides [28], or alginate [69,74].

Oxidized regenerated cellulose is a chemically altered form of cellulose used mainly as a hemostatic agent. It has been shown to not give an advantage to the prevention of nerve fibrosis; on the contrary, it interferes with healing by increasing inflammatory phenomena and granulomatous reactions [74]. Other polysaccharides have demonstrated their efficacy in the reduction of scarring through biomechanical and macro- and microscopical testing [22,28,69,74].

6.2. Collagen-Based Devices

The available preclinical studies on collagen-based devices are reported in Table 3.

Table 3. Collagen-based antiscarring agents.

Reference	Method to Induce Scar Formation	Agent	Animal and Nerve Model	Analyses	Results
Colonna et al., 2019 [16]	Section + suture	Collagen sheath derived from an acellular hypoallergenic dermal matrix (OrACELL)	Female Wistar Rat Median nerve	<ul style="list-style-type: none"> - Functional evaluation (grasping test) (every two months) - Histology on nerve and surrounding tissue and morphometric analysis (Toluidine Blue) (7 months) 	Axon diameter was higher in the treated group. No significant differences in the functional test were observed.
Lee et al., 2014 [76]	Section + suture	Collagen-based film (NeuraGen)	Male Wistar Rat Sciatic nerve	<ul style="list-style-type: none"> - Electrophysiological evaluation (12 weeks) - Wet muscle weight (12 weeks) - Histology on nerve and surrounding tissue and morphometric analysis (Toluidine Blue) (12 weeks) 	Reduction of scar in microscopical analysis, although the scar-decreasing effect of bioabsorbable nerve wrap did not translate into a better motor nerve recovery.
Mathieu et al., 2012 [47]	Section + suture	Collagen membrane and vein wrapping	Female Wistar Rat Sciatic nerve	<ul style="list-style-type: none"> - Gross evaluation (Petersen’s classification) (12 weeks) - Histology on nerve and surrounding tissue (Masson’s trichrome—extraneural and intraneural fibrosis, foreign body reaction) 	The collagen membrane was effective in reducing neural scar formation. Autologous vein wrapping also showed a favorable effect in this indication despite less successful histological outcomes.
Kim et al., 2010 [75]	Section + suture	Collagen wrap	Sprague–Dawley Rat Sciatic nerve	<ul style="list-style-type: none"> - Gross evaluation (Petersen’s classification) (3 months) - Histology on nerve and surrounding tissue and morphometric analysis (Toluidine Blue) (3 months) 	Significant reduction of inner epineurium thickness in the treated group.

Table 3. Cont.

Reference	Method to Induce Scar Formation	Agent	Animal and Nerve Model	Analyses	Results
Isla et al., 2003 [13]	Section + suture or repair with silastic tube	ADCON/TN	Male Wistar Rat Ulnar nerve	<ul style="list-style-type: none"> - Gross evaluation (4-point qualitative Scale) (3 months) - Histology on nerve, surrounding tissue and muscle (H&E, Masson's trichrome) (3 months) 	Significant reduction of fibrosis. No differences in terms of fiber density.
Palatinsky et al., 1997 [23]	Scratch; a second neurolysis performed 4 weeks later	ADCON/TN (applied after the second neurolysis)	Sprague Dawley Rat Sciatic nerve	<ul style="list-style-type: none"> - Gross evaluation (4-point qualitative Scale) (4 and 8 weeks) - Histology on nerve and surrounding tissue (H&E, Masson's trichrome, phenylenediamine staining) (4 and 8 weeks) 	Significant reduction of composite score (macroscopical evaluation). No statistical difference in axons diameter.
Petersen et al., 1996 [27]	External neurolysis, abrasive injury on muscle and nerve, section + suture	ADCON/TN	Lewis's Albino Rat Sciatic nerve	<ul style="list-style-type: none"> - Gross Evaluation (Petersen's classification) (4 and 6 weeks) - Electrophysiological evaluation (4 and 6 weeks) - Histology on nerve and surrounding tissue (H&E, silver stain, van Gieson's stain, Toluidine blue for morphometric analysis) (4 and 6 weeks) 	Significant reduction of scar tissue; no differences in morphometrical analysis.

The use of ADCON-T/N, a bioabsorbable gel composed of a polyglycan ester in a phosphate-buffered saline solution, showed a significant reduction of scar formation with no residual implant material [13,23,27]. Additionally, the use of collagen-based film wrapped around the suture stitches showed a reduction in epineural and perineural scar tissue formation [47,75,76]. Finally, a recent study showed that a collagen sheath derived from an acellular hypoallergenic dermal matrix wrapped around the suture leads to better nerve regeneration in terms of axon diameter [16].

6.3. Autologous Devices

Different autologous devices were used as antiadhesion devices, and the results of the preclinical studies are reported in Table 4.

Table 4. Autologous tissues used as antiscarring agents.

Reference	Method to Induce Scar Formation	Agent	Animal and Nerve Model	Analyses	Results
Cherubino et al., 2017 [70]	Burning	Fat Graft	CD1 nude Mouse Sciatic nerve	<ul style="list-style-type: none"> - Biomechanical analysis (4 weeks) - Histology on nerve and surrounding tissue (Picrosyrius red) (4 weeks) 	No significant difference in biomechanical analysis. Reduction of scar observed through microscopical analysis
Baltu et al., 2017 [46]	Epineurectomy	Buccal mucosa graft	Female Sprague-Dawley Rat Sciatic nerve	<ul style="list-style-type: none"> - Gross evaluation (Petersen’s classification) (4, 8 weeks) - Histology on nerve and surrounding tissue (H&E, Masson’s trichrome—extraneural scar tissue and inflammation) (4, 8 weeks) 	Buccal mucosa graft decreases postoperative adhesion and scar tissue formation. Higher inflammation at 4 weeks.
Murakami et al., 2014 [62]	Ligature on sciatic nerve	Vein Wrapping	Male Wistar Rat Sciatic nerve	<ul style="list-style-type: none"> - Gross evaluation (qualitative evaluation) (14 days and 5 months) - Functional evaluation (von Frey filaments at 1, 4, 7, 14, 21, 28 days; CatWalk system, first 2 weeks) - IHC on L4-L5 DRG (CGRP, ATF3) (14 days) - Histology on nerve and surrounding tissue (H&E, Toluidine Blue) (14 days and 5 months) - ELISA assay on nerve tissue (NGF, VEGF, and HGF) (1, 3, 7, 14, 28 days). 	Significant allodynia reduction. Significant increase in VEGF and HGF. Reduction of immunoreactive cells in dorsal root ganglia.
Meng et al., 2011 [39]	Section + suture	Amniotic membrane	Male Sprague-Dawley Rat Sciatic nerve	<ul style="list-style-type: none"> - Functional evaluation (SFI) (weekly) - Gross evaluation (Petersen’s classification) - Electrophysiological tests (every 4 weeks until Week 12) - Histology on nerve and surrounding tissue (Picrosyrius red, toluidine blue for morphometrical analysis) (4, 8, 12 weeks) - Ultrastructural evaluation (TEM) (4, 8, 12 weeks) 	Significant reduction of scar index. No functional and morphological differences were observed.

Table 4. Cont.

Reference	Method to Induce Scar Formation	Agent	Animal and Nerve Model	Analyses	Results
Kim et al., 2010 [14]	Section + suture	Amniotic membrane	White New Zealand Rabbit Ulnar nerve	- Gross evaluation (4-point qualitative Scale) (3 months) - Histology on nerve and surrounding tissue (Masson's trichrome—morphometrical analysis) (3 months)	Four-point evaluation system was significant in the treatment group. Significant reduction of scar thickness.
Ozgenel et al., 2004 [40]	Epineurectomy	Amniotic membrane + HA	Male Sprague–Dawley Rat Sciatic nerve	- Gross evaluation (Petersen's classification) (4 and 12 weeks) - Histology on nerve and surrounding tissue (H&E) (4 and 12 weeks)	Significant reduction in scarring was observed through microscopical analysis.
Xu et al., 2000 [25]	Silastic tube around the nerve	Vein wrapping (after 8 months from nerve compression)	Sprague–Dawley Rat Sciatic nerve	- Functional evaluation (SFI) (4, 8, 12, 24, and 48 weeks) - Gross Evaluation (qualitative evaluation) (4, 8, 12, 24, and 48 weeks) - Electrophysiological tests (4, 8, 12, 24, and 48 weeks) - Histology on nerve and surrounding tissue (H&E, Masson's trichrome, silver staining, toluidine blue) (4, 8, 12, 24, and 48 weeks)	Significant improvement in functional analysis. Electromyography and microscopical analysis showed no significant scar reduction.
Dumanian et al., 1999 [66]	Epineurectomy	Fat graft	Sprague–Dawley Rat Sciatic nerve	- Biomechanical analysis (2 months) - Histology on nerve and surrounding tissue (Masson's trichrome) (2 months)	Significant reduction of nerve stiffness in biomechanical analysis. Insignificant reduction of scar thickness in microscopical analysis. Higher but not significant incidence of neuropathy in fat-graft group.

SFI (Sciatic functional index), TEM (Transmission Electron Microscope), IHC (Immunohistochemistry), H&E (Hematoxylin Eosin staining), CGRP (Calcitonin gene related peptide), ATF3 (Activating transcription factor 3), VEGF (vascular endothelial growth factor), HGF (Hepatocyte growth factor), NGF (Nerve growth factor).

6.3.1. Amniotic Membrane

The amniotic membrane is the inner layer of fetal membranes; it is composed of an inner layer of epithelial cells on a thick basement membrane. It is nonimmunogenic, and it has been demonstrated to reduce inflammation, inhibit vascularization, combat infection, and reduce scarring. It is widely used in multiple fields of surgery and medicine, including skin substitute, wound care, urethral reconstruction, and repair of corneal and other tissues [77]. Its use in reducing peripheral nerve scarring has been demonstrated in different papers [14,39,40].

6.3.2. Fat Grafting

In the last decade, adipose tissue has been widely studied in the field of regenerative medicine due to the presence of adipose-tissue-derived mesenchymal stem cells (which can differentiate into different cellular lineages) and its endocrine activity (release of adipocytokines, cytokines, transcriptional and growth factors). It is easy to access and harvest with painless procedures. The use of fat grafting in the prevention of peripheral scar tissue formation has had different results: it produces nerve stiffness reduction in biomechanical testing [66], but no significant differences were reported when compared to

other antiadhesion devices. Moreover, in microscopical analysis, it appears to be able to reduce scar thickness [70].

6.3.3. Vein Wrapping and Buccal Mucosa Graft

Another autologous tissue that has been tested for scar formation prevention is vein tissue, which is harvested from the same animal (femoral vein) and wrapped in a spiral pattern around the nerve [25] or harvested from the abdominal portion of the donor animal vena cava and wrapped around the ligated nerve [62]. In both cases, it has been demonstrated to reduce scar formation and improve nerve function recovery.

Finally, the use of a buccal mucosa graft has also been proposed as an antiadherent device since it is composed of nonkeratinized epithelium with underlying connective tissue and includes type I and III collagen. It has been shown that when wrapped around the nerve, it decreases adhesion and scar tissue formation but leads to higher inflammation in the early postoperative period [46].

6.4. Drugs

Several drugs have been tested; the preclinical results are reported in Table 5. Most of them (aprotinin, tacrolimus, mannose-6-phosphate, doxorubicin, mitomycin C, citicoline, cytidine-59-diphosphocholine-choline) were locally placed around the nerve [30–33,36,41,51,56]; others were intraepineurially injected (chondroitinase ABC) [61], intraperitoneally injected (citicoline and verapamil) [60,78], or intragastrically injected (tacrolimus) [58]. It has been shown that tacrolimus, an immunosuppressive drug used mainly after allogenic organ transplant, promotes nerve regeneration [79,80] and scar tissue reduction [36,58]. Moreover, the application of other drugs is correlated with scar formation reduction either in macro- or microscopical analysis. In addition, the improvement of axon quality has been reported in some papers, together with enhanced functional results.

Table 5. Drugs used as antiscarring agents.

Reference	Method to Induce Scar Formation	Agent	Animal and Nerve model	Analyses	Results
Mekaj et al., 2017 [36]	Section + suture	Tacrolimus (FK506)	Male European Rabbit Sciatic nerve	<ul style="list-style-type: none"> - Gross evaluation (Petersen’s classification) (12 weeks) - Muscle wet weight (12 weeks) - Histology on nerve and surrounding tissue (H&E, Masson’s trichrome) - Fibroblast and inflammatory cell counts (12 weeks) - Nerve IHC (S100) (12 weeks) 	Scar reduction around the nerve, both macroscopically and microscopically. Increased nerve diameter. Higher gastrocnemius mass. Improved microstructural organization. Higher expression of S100.
Zhu et al., 2017 [61]	Silicone tube around the nerve	Decompression and chondroitinase ABC (6 weeks after compression injury)	Male Sprague–Dawley Rat and Male C57BL/6 Mouse Sciatic nerve	<ul style="list-style-type: none"> - Electrophysiology (1 month) - RNA (neuron–glial antigen 2, phosphacan, brevican, versican, aggrecan, and decorin) and protein expression (decorin, aggrecan, laminina 2, collagen IV, and fibronectin) (1 month) - Nerve IHC (decorin, aggrecan, laminina 2, collagen IV, and fibronectin) (1 month) 	Surgical decompression alone does not reverse the functional changes to the nerve, whereas the administration of chondroitinase-ABC, in addition to decompression, resulted in functional improvement.

Table 5. Cont.

Reference	Method to Induce Scar Formation	Agent	Animal and Nerve model	Analyses	Results
Vural et al., 2016 [41]	Abrasion	Mitomycin C/ Daunorubicin	Male Wistar Rat Sciatic nerve	<ul style="list-style-type: none"> - Gross evaluation (Petersen's classification) (8 weeks) - Histology on nerve and surrounding tissue (H&E and Masson's trichrome—fibroblast count) (8 weeks) 	Macroscopically, mitomycin C, and daunorubicin decreased adhesion. Scar tissue thickness and fibroblast/fibrocyte cell number were reduced.
Xue et al., 2016 [60]	Section + suture	Verapamil (calcium channel blockers)	Sprague–Dawley Rat Sciatic nerve	<ul style="list-style-type: none"> - Gross evaluation (qualitative evaluation) (4 and 12 weeks) - Nerve IHC (collagen I) (4 and 12 weeks) - Ultrastructural evaluation (TEM) (4 and 12 weeks) - Hydroxyproline and collagen assay (4 and 12 weeks) 	The collagen content of nerve scar was apparently less than that of the control group; more cytoplasmic vesicles in the fibroblasts of the treated group were observed.
Kaplan et al., 2014 [78]	Section + suture	Citicoline	Female Wistar Albino Rat Sciatic nerve	<ul style="list-style-type: none"> - Functional evaluation (SFI) (4, 8, 12 weeks) - Electromyography (12 weeks) - Gross evaluation (Petersen's classification) (12 weeks) - Histology on nerve and surrounding tissue (Masson's trichrome and Toluidine Blue for morphometrical analysis) (12 weeks) 	Improvement of SFI. Significant reduction in scarring. Significant increase in myelinated axons in C900 and reduction of scar in the treated group.
Que et al., 2013 [58]	Section + suture	Tacrolimus (FK506)	Male Sprague–Dawley Rat Sciatic nerve	<ul style="list-style-type: none"> - Nerve IHC (TGF-β) (4 weeks) - Histology on nerve and surrounding tissue (Masson's trichrome) (4 weeks) - In vitro analysis 	FK506 has a valid effect on scar formation reduction in sciatic nerve-injured rat by inducing fibroblast apoptosis.
Ngeow et al., 2011 [50]	Section + suture	Triamcinolone acetone, Interleukin-10 (IL 10), mannose-6-phosphate (M6P)	C57 Black-6 Mouse Sciatic nerve	<ul style="list-style-type: none"> - Electrophysiological evaluation (6 and 12 weeks) - Functional evaluation (CatWalk) (1, 3, 6, 9, and 12 weeks) - Histology on nerve and surrounding tissue (Picrosirius staining) (6 and 12 weeks) 	The percentage of scarring was not significantly different between methods in microscopical analysis. Reduction of compound action potential in triamcinolone and M6P 200 was observed through EMG.
Ngeow et al., 2011 [51]	Section + suture	Mannose-6-phosphate	C57 Black-6 mice Sciatic nerve	<ul style="list-style-type: none"> - Electrophysiological evaluation (6 and 12 weeks) - Histology on nerve and surrounding tissue (Picrosirius staining) (6 and 12 weeks) - Functional evaluation (CatWalk) (1, 3, 6, 9 and 12 weeks) 	Larger compound action potential and better functional recovery in early evaluation. Reduction in collagen staining.

Table 5. Cont.

Reference	Method to Induce Scar Formation	Agent	Animal and Nerve model	Analyses	Results
Aslan et al., 2011 [56]	Section + suture (immediate or 3 days later)	CDP-choline, cytidine, choline, or cytidine–choline (during nerve repair)	Female Sprague–Dawley Rat Sciatic nerve	<ul style="list-style-type: none"> - Functional evaluation (SFI) (4, 8, 12 weeks) - Gross evaluation (Petersen’s classification) (12 weeks) - Histology on nerve and surrounding tissue (H&E, Weil method for morphometrical analysis) (12 weeks) 	Treatment with CDP-choline or cytidine–choline reduced scar formation and decreased nerve adherence.
Albayrak et al., 2010 [30]	Abrasion	Doxorubicin	Male Wistar Albino Rat Sciatic nerve	<ul style="list-style-type: none"> - Gross evaluation (Petersen’s classification) (12 weeks) - Histology on nerve and surrounding tissue (Toluidine Blue) (12 weeks) - Ultrastructural evaluation (TEM) (12 weeks) 	Topical application of doxorubicin effectively reduced epineural scar formation.
Atkins et al., 2007 [53]	Section + suture	IL-10	C57 Black-6 Mouse Sciatic nerve	<ul style="list-style-type: none"> - Electrophysiological analysis (6 weeks) - Histology on nerve and surrounding tissue (Picrosirius staining and Toluidine Blue for morphometrical analysis) (6 weeks) 	Compound action potential and area of staining for collagen not significantly different compared to controls. Higher number of myelinated fibers compared to control but no difference with the other groups.
Ozay et al., 2007 [31]	Section + suture	Citicoline	Female Sprague-Dawley Rat Sciatic nerve	<ul style="list-style-type: none"> - Functional evaluation (SFI) (4, 8, 12 weeks) - Electrophysiological analysis (4, 12 weeks) - Gross evaluation (Petersen’s classification) (4 weeks) - Histology on nerve and surrounding tissue (Masson’s trichrome, H&E, Weil method for morphometrical analysis) (4, 12 weeks) 	Rats treated with citicoline showed significantly better SFI and improvement at 12 weeks of electromyography. Nerves were surrounded by only a very thin, lucent membrane and showed thin dark bands of connective tissue surrounding the nerve.
Ilbay et al., 2005 [32]	Scratch	Mitomycin C	Male Wistar Rat Sciatic nerve	<ul style="list-style-type: none"> - Gross evaluation (Petersen’s classification) (4 weeks) - Histology on nerve and surrounding tissue (H&E, Masson’s trichrome—fibroblasts/fibrocytes count) (4 weeks) 	Macroscopical and microscopical reduction of perineural adhesions in the treated groups; lower number of fibroblast/fibrocytes.
Gorgulu et al., 1998 [33]	External neurolysis, abrasive injury, anastomosis	Aprotinin	Male Sprague-Dawley Rat Sciatic nerve	<ul style="list-style-type: none"> - Functional analysis (sciatic nerve function) (weekly) - Gross evaluation (Petersen’s classification) (4, 6 weeks) - Histology on nerve and surrounding tissue (Masson’s trichrome) (4, 6 weeks) 	Scar reduction after aprotinin application. No differences in neurological tests were observed.

6.5. Others

Many other devices/techniques have been investigated as antiscarring agents, and the preclinical results of these devices are reported in Table 6. A very recent study compared the efficacy of two novel biodegradable wraps made of synthetic 1% oxidized polyvinyl alcohol (OxPVA) and a leukocyte-fibrin-platelet membrane (LFPm) with the commercial product NeuroWrap, demonstrating their effectiveness in sustaining nerve regeneration, together with an absence of scar tissue/neuroma formation and significant inflammatory infiltrate [81].

Table 6. Other antiscarring agents.

Reference	Method to induce scar formation	Agent	Animal and Nerve model	Analyses	Results
Kikuchi et al., 2020 [82]	Burning	Polylactic acid (PLA)-based biodegradable three-layered membrane (E8002) with or without L-ascorbic acid (AA)	Male Sprague–Dawley Rat Sciatic nerve	<ul style="list-style-type: none"> - Motor functional (rotarod) and mechanical sensitivity (von Frey) evaluation (before surgery and 2, 4, 6 weeks after). - Gross evaluation (Petersen’s classification) (6 weeks) - Histology on nerve and surrounding tissue (aldehyde fuchsin Masson–Goldner staining) (6 weeks) 	AA in E8002 has an antiadhesional effect by enhancing fibrinolysis. Adhesion formation was lower in the group containing AA. Motor function and mechanical sensitivity were not impaired after surgery, and no differences were detected among groups.
Stocco et al., 2019 [81]	Section + suture	Wraps made of a synthetic 1% oxidized polyvinyl alcohol (OxPVA) and a leukocyte-fibrin-platelet membrane (LFPm) compared to NeuroWrap	Sprague–Dawley rats Sciatic nerve	<ul style="list-style-type: none"> - Functional analysis (sciatic function index assessment) (2 and 12 weeks) - Gross evaluation (12 weeks) - Histology on nerve and surrounding tissue (H&E, IHC and Toluidine blue) (12 weeks) - Ultrastructural analysis (TEM) (12 weeks) - Neural collagen deposition evaluation (12 weeks) 	LFPm wraps were completely resorbed, while residues of OxPVA and NeuroWrap were observed. Functional recovery was achieved in all groups. Additionally, at the morphological level, scar tissue formation and inflammatory infiltrate were not observed. Both myelinic and unmyelinic axons were observed.
Shintani et al., 2018 [57]	Burning	Poly lactide (PLA)-poly(e-caprolactone) PCL conduit and HA	Lewis Rat Sciatic nerve	<ul style="list-style-type: none"> - Gross evaluation (Petersen’s classification) (6 weeks) - Biomechanical examination (6 weeks) - Electrophysiological evaluation (6 weeks) - Muscle wet weight and histology (6 weeks) - Nerve IHC (antineurofilament, anti-CD68, and anti-CCR7) (6 weeks) 	Morphological properties of axons were preserved with PLA-PCL conduit. HA was less effective for nerve protection from adhesion.
Servet et al., 2016 [59]	Section + suture	Ankaferd blood stopper (ABS) hemostatic agent	Male Sprague–Dawley Rat Sciatic nerve	<ul style="list-style-type: none"> - Electrophysiology (12 weeks) - Histology on nerve and surrounding tissue (H&E, Masson’s trichrome, and Luxol fast blue) (24 weeks) - Nerve IHC (CD68) (24 weeks) 	Significant improvement of latency and speed in the ABS group. Other results were not statistically different.

Table 6. Cont.

Reference	Method to induce scar formation	Agent	Animal and Nerve model	Analyses	Results
Okui et al., 2010 [83]	Neurolysis and burning	PLA	Male Lewis Rat Sciatic nerve	<ul style="list-style-type: none"> - Electrophysiological evaluation (6 weeks) - Histology on nerve and surrounding tissue (H&E, Masson's trichrome) (1, 2, 4, 6 weeks) - Muscle wet weight (2, 4, 6 weeks) - Analysis of the blood–nerve barrier (2 days) 	PLA film has the potential to prevent adhesion even after internal neurolysis, and it is a useful substitute for perineurium.
Atkins et al., 2006 [52]	Section + suture	TGF- β 1 and TGF- β 2	Male Sprague–Dawley Rat Sciatic nerve	<ul style="list-style-type: none"> - Electrophysiological evaluation (7 weeks) - Histology on nerve and surrounding tissue (Picrosirius staining and Toluidine Blue for morphometrical analysis) (7 weeks) 	No differences in the percentage of collagen staining area were observed. Compound action potential ratios significantly smaller; increased number of myelinated fibers distally (no differences between TGF- β 1 and TGF- β 2)
Gorgulu et al., 2003 [34]	Neurolysis vs. scratching vs. suture vs. radiation treatment	Low-dose radiation therapy (24 h after surgery)	Male Sprague–Dawley Rat Sciatic nerve	<ul style="list-style-type: none"> - Functional analysis (sciatic nerve function) (weekly) - Gross evaluation (Petersen's classification) (6 weeks) - Histology on nerve and surrounding tissue (Masson's trichrome—fibroblast/fibrocytes count) (6 weeks) 	Significant reduction of scar tissue in radiation + surgery groups. No increase in scar tissue formation after radiation in normal nerves was observed.
Ikedo et al., 2002 [84]	Burning	Absorbable oxidized regenerated cellulose sheet	White Japanese Rabbit Sciatic nerve	<ul style="list-style-type: none"> - Electrophysiological evaluation (6 weeks) - Gross evaluation (qualitative evaluation—observation of Fontana's bands) (6 weeks) - Histology on nerve and surrounding tissue (Masson's trichrome) (6 weeks) 	No significant differences between groups in electrophysiological evaluation. High adhesion between nerve and surrounding tissue in the damage group.
Ip et al., 2000 [15]	Section + suture	Early mobilization	Albino Rabbit Peroneal nerve	<ul style="list-style-type: none"> - Biomechanical examination (stretch test and peel test) (3 weeks) 	No difference in the biomechanical features of the adhesions

A biodegradable polylactide (PLA) honeycomb film [83] and a nerve conduit composed of PLA and poly(ϵ -caprolactone) (PCL) and enriched with hyaluronic acid [57] have been shown to prevent nerve adhesion. Additionally, a novel multilayer membrane made of PLA-based biodegradable polymer (E8002) containing L-ascorbic acid has been demonstrating to reduce scar formation compared to the same membrane without ascorbic acid [82]. Atkins et al. [52] proposed the local administration of neutralizing antibodies to TGF- β 1 and TGF- β 2, showing a significant reduction in intraneural scar formation. The use of Ankaferd blood stopper resulted in better healing and better results in the histopathological evaluations [59], and the use of an absorbable oxidized regenerated cellulose sheet showed the prevention of adhesion in a histological study [84]. Finally, low-dose radiation therapy [34] and early mobilization [15] have also been proposed.

7. Discussion

Traction neuropathies are diffused and frequent consequences of injuries or surgical procedures on peripheral nerves [2,7]. Surgeons and researchers have been trying to prevent scar tissue formation, especially by applying antiadhesion devices on the surgical site. Before human implantation, preclinical studies are of crucial importance for assessing the effectiveness of antiadhesion strategies; however, the results reported in the literature are not easily comparable due to the many different methods to induced scar formation as well as quantitatively evaluate the amount of scar tissue and its impact on peripheral nerve regeneration and function. The reason is connected to the absence of a shared, effective, reliable, reproducible, and standardized protocol to induce and test the scar tissue around the peripheral nerves [18,20–22].

The purpose of this review was, therefore, to resume and show the different strategies adopted in the last few years to simulate and evaluate scar tissue formation.

Different kinds of injuries have been proposed by researchers to simulate perineural scar tissue formation: nerve injury, injury to surrounding tissues, global injury by means of chemical or physical agents, and so on. Some authors have designed studies to simulate and evaluate perineural scars [17–22], but these works are incomplete because they have not considered all the aspects of induction and the evaluation methods available. Our review reveals that the widest protocol used to induce scar tissue is represented by section and suture of the nerve. This partially represents what really happens in clinical settings and results in a partial injury. In our opinion, an injury to the perineural tissue should always be associated in clinical settings by means of burning or chemical injury to the nerve. None of the papers have combined this kind of injury. It would, therefore, be very interesting and useful to test the combination of these methods in an experimental model that better mimics the clinic. Furthermore, researchers should consider that a different pattern of scar tissue arises if the nerve is transected or not. Without a nerve section and suture or without a crush injury, no internal scar will form, especially when there has been only a short period between the surgery and the analysis. In this way, no or only minimal impairment of nerve function will be present.

This aspect links to the other main aspect of this review: so many different types of analysis were performed to quantitatively or qualitatively assess the perineural scar and its reduction. We strongly encourage the use of quantitative analysis. Gross evaluation is certainly a fundamental step to macroscopically grading the scar, and the adoption of a numerical grading scheme is necessary to quantify (or semiquantify) the amount of scar tissue. Different grading schemes have been adopted [13,14,17,23,27,28] and most of the authors have used these schemes to score scar tissue during macroscopical inspection. Nevertheless, other authors have described only the presence or absence of scar tissue, and, sometimes, they qualitatively describe the scar tissue by relying on subjective observations.

Microscopical evaluation is usually conducted both on the nerve and scar tissue. Beyond the type of staining used, the quantitative evaluation of the perineural scar is very important. First of all, a staining solution that is able to visualize collagen fibers specifically (such as Masson's Trichrome, Sirius Red) is preferred to the classical H&E and methylene blue stainings. Quantification of scar tissue is proposed in different ways, but the most adopted is the calculation of the scar tissue formation index (by dividing the mean thickness of the scar tissue by the mean thickness of the nerve tissue) [18,28,30–34,36–41]. Moreover, in these cases, some other authors have used different parameters to quantify (or semiquantify) the scar tissue histologically; sometimes, the structure of scar tissue is only qualitatively described. Some authors have added immunohistochemistry to conventional staining. Very interesting are the attempts to detect scar tissue using antibodies against macrophages and lymphocytes, but it is difficult to obtain a quantification of these findings [21,37,59].

Biomechanical analysis provides another quantitative parameter and consists of measuring the peak force required to pull the nerve from the muscular bed. Different tools have been adopted, and, in general, they consist of applying a continuous force to the nerve until

the complete detachment of the nerve from the surrounding tissue. This should be the other main method that is useful to demonstrate the strength of the scar tissue in preclinical analysis. In addition, the structure and function of the nerve must be assessed. Quantification of different parameters (number of fibers, axon and fiber diameter, myelin thickness) are important to assess the degree of nerve regeneration and can be related to electrophysiological parameters and functional evaluations, often assessed in studies dealing with peripheral nerve scarring. In our thoughts, morphological and functional impairments correlate more to a direct nerve injury than an experimental perineural scar. Hence, morphometry and electrophysiology should be associated, especially when nerve injury and repair have been performed or when scar neuropathy has lasted for several months.

Different animal models have been proposed, each one with pros and cons. Mice are easy to house and allow quick and easy surgery. The sciatic nerve allows the performance of all the main analyses described above. Otherwise, in this model of nerve repair, functional and electrophysiological tests are more difficult to perform due to the smallness of the animal itself. Conversely, rats allow the testing of both the sciatic nerve and the median nerve; the size of these nerves is feasible for nerve repair and electrodiagnostic tests. Furthermore, functional evaluation on the median nerve can be carried out, especially when a direct nerve injury is performed.

Due to the limitations of the present models, no definitive conclusion can be derived about the efficacy of antiadhesion devices. In most of the experiments, every treated group showed scar reduction according to the evaluation methods. The most employed antiadhesion devices were polysaccharide-based and collagen-based ones. Their effectiveness was, in most cases, well known in spine surgery, tendon surgery, or abdominal surgery. It is similar for biological barriers: vein wrapping has been described to protect nerve sutures in the past [25,85], with good clinical outcomes. Fat grafts were previously adopted in spine surgery with controversial results; in peripheral nerves, it seems to be effective, and promising results were obtained with Coleman's lipoaspirate [70]. From our review, it has emerged that the application of amniotic membrane can be promising, considering the increased chance of tissue storage [14,39,40]. This requirement can also be considered a limit for this technique. Drugs and other devices can also be promising, but currently, no clinical experience exists.

This preclinical literature review suggests that we reconsider the whole argument of traction neuropathies. This pathology was classified by Millesi [86] in intra- and extraneural scar, but more extensive classification would be effective to better understand the correct treatment. Perineural scarring arises after closed trauma and nerve decompression or can be associated with a repaired nerve. The intraneural involvement is different in each case, and different approaches should be considered. When an intraneural scar is present, it should be treated as a neuroma in continuity. In contrast, when the perineural scar is the main concern, other procedures should be performed. According to our clinical practice and the results obtained in these experimental models, vein wrapping can be a feasible procedure to prevent intraneural and epineural adhesion after nerve suture. Otherwise, in a secondary peripheral nerve decompression, the application of an antiadhesion device, either in the form of gel or film composed of polysaccharide or collagen, could be adequate as well as autologous lipoaspirate, local adipose flap, synovial flap, or amniotic membrane wrapping. The choice, at state of the art, is up to the individual surgeon's experience and availability since no clear evidence exists.

To better understand traction neuropathies, a more extensive classification should be designed by considering the extension of the scar, the amount of fibrous tissue (both pre- and intraoperative by means of a quantitative scale, as proposed by Petersen [27]), and previous surgery on the nerve (suture, traction injury, nerve decompression). On these, prognostic criteria would be found and a more fitted treatment protocol developed.

In our experience and considering the literature, to completely evaluate scar tissue formation around a nerve, we require a scored macroscopical analysis, a quantitative microscopical analysis conducted with a staining solution that is able to collagen fibers

visualize specifically (such as Masson's Trichrome, Sirius Red) in order to clearly measure the thickness and extension of scar tissue, and a computed biomechanical analysis with the appropriate microinstruments. The structure, organization, and function of the nerve should also accompany scar tissue data, but these are not always mandatory since they depend on the type of nerve injury induced.

Finally, this review reports on the different antiadhesion devices that have been experimentally tested so far. Due to the high variability of scar induction and evaluation methods described, it is not possible to compare the results obtained in terms of scar reduction and efficacy of the antiadhesion devices employed.

Author Contributions: A.C., G.R. and P.T. organized the manuscript. A.C., G.R., B.E.F., S.O. and S.R. wrote different sections of the manuscript. All authors contributed to manuscript revision and approved the submitted version of the manuscript.

Funding: This research received no external funding.

Informed Consent Statement: Not applicable.

Conflicts of Interest: The authors declare no conflict of interest.

References

1. Tos, P.; Crosio, A.; Pugliese, P.; Adani, R.; Toia, F.; Artiaco, S. Topic: Peripheral Nerve Repair and Regeneration Painful scar neuropathy: Principles of diagnosis and treatment. *Plast. Aesthet. Res.* **2015**, *2*. Available online: www.parjournal.net (accessed on 18 May 2020). [[CrossRef](#)]
2. Jones, N.F.; Ahn, H.C.; Eo, S. Revision surgery for persistent and recurrent carpal tunnel syndrome and for failed carpal tunnel release. *Plast. Reconstr. Surg.* **2012**, *129*, 683–692. [[CrossRef](#)]
3. Siemionow, M.; Brzezicki, G. Chapter 8 Current Techniques and Concepts in Peripheral Nerve Repair. *Int. Rev. Neurobiol.* **2009**, *87*, 141–172. [[CrossRef](#)] [[PubMed](#)]
4. Wiberg, M.; Terenghi, G. Will it be possible to produce peripheral nerves? *Surg. Technol. Int.* **2003**, *11*, 303–310.
5. Geuna, S. Appreciating the difference between design-based and model-based sampling strategies in quantitative morphology of the nervous system. *J. Comp. Neurol.* **2000**, *427*, 333–339. [[CrossRef](#)]
6. Siemionow, M.; Mendiola, A. Methods of assessment of cortical plasticity in patients following amputation, replantation, and composite tissue allograft transplantation. *Ann. Plast. Surg.* **2010**, *65*, 344–348. [[CrossRef](#)] [[PubMed](#)]
7. Amadio, P.C. Interventions for recurrent/persistent carpal tunnel syndrome after carpal tunnel release. *J. Hand Surg.* **2009**, *34*, 1320–1322. [[CrossRef](#)] [[PubMed](#)]
8. Sunderland, S. *Nerves and Nerve Injuries*, 2nd ed.; Churchill Livingstone: Edinburgh, UK, 1978.
9. Wang, M.L.; Rivlin, M.; Graham, J.G.; Beredjikian, P.K. Peripheral nerve injury, scarring, and recovery. *Connect. Tissue Res.* **2019**, *60*, 3–9. [[CrossRef](#)]
10. Smit, X.; van Neck, J.W.; Afoke, A.; Hovius, S.E.R. Reduction of neural adhesions by biodegradable autocrosslinked hyaluronic acid gel after injury of peripheral nerves: An experimental study. *J. Neurosurg.* **2004**, *101*, 648–652. [[CrossRef](#)] [[PubMed](#)]
11. Ronchi, G.; Morano, M.; Fregnan, F.; Pugliese, P.; Crosio, A.; Tos, P.; Geuna, S.; Haastert-Talini, K.; Gambarotta, G. The median nerve injury model in pre-clinical research—A critical review on benefits and limitations. *Front. Cell. Neurosci.* **2019**, *13*. [[CrossRef](#)]
12. Diogo, C.C.; Camassa, J.A.; Pereira, J.E.; da Costa, L.M.; Filipe, V.; Couto, P.A.; Geuna, S.; Mauricio, A.C.; Varejão, A.S. The use of sheep as a model for studying peripheral nerve regeneration following nerve injury: Review of the literature. *Neurol. Res.* **2017**, *39*, 926–939. [[CrossRef](#)]
13. Isla, A.; Martinez, J.; Perez-Lopez, C.; Conde, C.P.; Morales, C.; Budke, M. A reservable antiadhesion barrier gel reduces the perineural adhesions in rats after anastomosis/Comment. *J. Neurosurg. Sci.* **2003**, *47*, 195–199. Available online: <http://search.proquest.com/openview/298ef0c6b31f2fb391e0685f5ab5c636/1?pq-origsite=gscholar&cbl=49236> (accessed on 19 May 2020). [[PubMed](#)]
14. Kim, S.S.; Sohn, S.K.; Lee, K.Y.; Lee, M.J.; Roh, M.S.; Kim, C.H. Use of human amniotic membrane wrap in reducing perineural adhesions in a rabbit model of ulnar nerve neurotomy. *J. Hand Surg. Eur. Vol.* **2010**, *35*, 214–219. [[CrossRef](#)]
15. Ip, W.Y.; Shibata, T.; Tang, F.H.; Mak, A.F.T.; Chow, S.P. Adhesion formation after nerve repair: An experimental study of early protected mobilization in the rabbit. *J. Hand Surg.* **2000**, *25*, 582–584. [[CrossRef](#)] [[PubMed](#)]
16. Colonna, M.R.; Fazio, A.; Costa, A.L.; Galletti, F.; lo Giudice, R.; Galletti, B.; Galletti, C.; lo Giudice, G.; Orabona, G.D.; Papalia, I.; et al. The Use of a Hypoallergenic Dermal Matrix for Wrapping in Peripheral Nerve Lesions Regeneration: Functional and Quantitative Morphological Analysis in an Experimental Animal Model. *BioMed Res. Int.* **2019**, *2019*. [[CrossRef](#)] [[PubMed](#)]
17. Abe, Y.; Doi, K.; Kawai, S. An experimental model of peripheral nerve adhesion in rabbits. *Br. J. Plast. Surg.* **2005**, *58*, 533–540. [[CrossRef](#)] [[PubMed](#)]
18. Zanjani, L.O.; Firouzi, M.; Nabian, M.-H.; Nategh, M.; Rahimi-Movaghar, V.; Kamrani, R.S. Comparison and Evaluation of Current Animal Models for Perineural Scar Formation in Rat. *Iran. J. Basic Med. Sci.* **2013**, *16*, 890.

19. Okuhara, Y.; Shinomiya, R.; Peng, F.; Kamei, N.; Kurashige, T.; Yokota, K.; Ochi, M. Direct effect of radiation on the peripheral nerve in a rat model. *J. Plast. Surg. Hand Surg.* **2014**, *48*, 276–280. [CrossRef] [PubMed]
20. Crosio, A.; Valdatta, L.; Cherubino, M.; Izzo, M.; Pellegatta, I.; Pascal, D.; Geuna, S.; Tos, P. A simple and reliable method to perform biomechanical evaluation of postoperative nerve adhesions. *J. Neurosci. Methods* **2014**, *233*, 73–77. [CrossRef]
21. Lemke, A.; Penzenstadler, C.; Ferguson, J.; Lidinsky, D.; Hopf, R.; Bradl, M.; Redl, H.; Wolbank, S.; Hausner, T. A novel experimental rat model of peripheral nerve scarring that reliably mimics post-surgical complications and recurring adhesions. *Dis. Models Mech.* **2017**, *10*, 1015–1025. [CrossRef]
22. Zuijendorp, H.; Smit, X.; Blok, J.; Caruelle, J.; Barritault, D.; Hovius, S.; van Neck, J. Significant reduction in neural adhesions after administration of the regenerating agent OTR4120, a synthetic glycosaminoglycan mimetic, after peripheral nerve injury. *J. Neurosurg.* **2008**, *109*, 967–973. Available online: <https://thejns.org/view/journals/j-neurosurg/109/5/article-p967.xml> (accessed on 19 May 2020). [CrossRef] [PubMed]
23. Palatinsky, E.A.; Maier, K.H.; Touhalisky, D.K.; Mock, J.L.; Hingson, M.T.; Coker, G.T. ADCON[®]-T/N reduces in vivo perineural adhesions in a rat sciatic nerve reoperation model. *J. Hand Surg. Eur. Vol.* **1997**, *22*, 331–335. [CrossRef]
24. Ikeda, K.; Yamauchi, D.; Osamura, N.; Hagiwara, N.; Tomita, K. Hyaluronic acid prevents peripheral nerve adhesion. *Br. J. Plast. Surg.* **2003**, *56*, 342–347. [CrossRef]
25. Xu, J.; Varitimidis, S.E.; Fisher, K.J.; Tomaino, M.M.; Sotereanos, D.G. The effect of wrapping scarred nerves with autogenous vein graft to treat recurrent chronic nerve compression. *J. Hand Surg.* **2000**, *25*, 93–103. [CrossRef] [PubMed]
26. Animals NRC (US). *C on R and A of P in L. Recognition and Alleviation of Pain in Laboratory Animals*; National Academies Press: Washington, DC, USA, 2010. [CrossRef]
27. Petersen, J.; Russell, L.; Andrus, K.; MacKinnon, M.; Silver, J.; Klot, M. Reduction of extraneural scarring by ADCON-T/N after surgical intervention. *Neurosurgery* **1996**, *38*, 976–984. [CrossRef] [PubMed]
28. Dam-Hieu, P.; Lacroix, C.; Said, G.; Devanz, P.; Liu, S.; Tadie, M. Reduction of postoperative perineural adhesions by hyaloglidle gel: An experimental study in the rat sciatic nerve. *Neurosurgery* **2005**, *56* (Suppl. S4). [CrossRef] [PubMed]
29. Junqueira, L.C.U.; Bignolas, G.; Brentani, R.R. Picrosirius staining plus polarization microscopy, a specific method for collagen detection in tissue sections. *Histochem. J.* **1979**, *11*, 447–455. [CrossRef]
30. Albayrak, B.S.; Ismailoglu, O.; Ilbay, K.; Yaka, U.; Tanriover, G.; Gorgulu, A.; Demir, N. Doxorubicin for prevention of epineurial fibrosis in a rat sciatic nerve model: Outcome based on gross postsurgical, histopathological, and ultrastructural findings—Laboratory investigation. *J. Neurosurg. Spine* **2010**, *12*, 327–333. [CrossRef]
31. Özay, R.; Bekar, A.; Kocaeli, H.; Karli, N.; Filiz, G.; Ulus, I.H. Citicoline improves functional recovery, promotes nerve regeneration, and reduces postoperative scarring after peripheral nerve surgery in rats. *Surg. Neurol.* **2007**, *68*, 615–622. [CrossRef]
32. Ilbay, K.; Etus, V.; Yildiz, K.; Ilbay, G.; Ceylan, S. Topical application of mitomycin C prevents epineurial scar formation in rats. *Neurosurg. Rev.* **2005**, *28*, 148–153. [CrossRef]
33. Görgülü, A.; Imer, M.; Şimşek, O.; Sencer, A.; Kutlu, K.; Çobanoğlu, S. The effect of aprotinin on extraneural scarring in peripheral nerve surgery: An experimental study. *Acta Neurochir.* **1998**, *140*, 1303–1307. [CrossRef] [PubMed]
34. Görgülü, A.; Uzal, C.; Doğanay, L.; Imer, M.; Eliuz, K.; Çobanoğlu, S.; Loeffler, J.S.; Gerszten, P.C.; Kondziolka, D.; Kline, D.G. The effect of low-dose external beam radiation on extraneural scarring after peripheral nerve surgery in rats. *Neurosurgery* **2003**, *53*, 1389–1396. [CrossRef] [PubMed]
35. Özgenel, G.Y. Effects of hyaluronic acid on peripheral nerve scarring and regeneration in rats. *Microsurgery* **2003**, *23*, 575–581. [CrossRef] [PubMed]
36. Mekaj, A.Y.; Manxhuka-Kerliu, S.; Morina, A.A.; Duci, S.B.; Shahini, L.; Mekaj, Y.H. Effects of hyaluronic acid and tacrolimus on the prevention of perineural scar formation and on nerve regeneration after sciatic nerve repair in a rabbit model. *Eur. J. Trauma Emerg. Surg.* **2017**, *43*, 497–504. [CrossRef]
37. Marcol, W.; Larysz-Brysz, M.; Kucharska, M.; Niekraszewicz, A.; Slusarczyk, W.; Kotulska, K.; Wlasczczuk, P.; Wlasczczuk, A.; Jedrzejowska-Szypulka, H.; Lewin-Kowalik, J. Reduction of post-traumatic neuroma and epineurial scar formation in rat sciatic nerve by application of microcrystalline chitosan. *Microsurgery* **2011**, *31*, 642–649. [CrossRef]
38. Park, J.S.; Lee, J.H.; Han, C.S.; Chung, D.W.; Kim, G.Y. Effect of hyaluronic acid-carboxymethylcellulose solution on perineurial scar formation after sciatic nerve repair in rats. *Clin. Orthop. Surg.* **2011**, *3*, 315–324. [CrossRef]
39. Meng, H.; Li, M.; You, F.; Du, J.; Luo, Z. Assessment of processed human amniotic membrane as a protective barrier in rat model of sciatic nerve injury. *Neurosci. Lett.* **2011**, *496*, 48–53. [CrossRef]
40. Özgenel, G.Y.; Filiz, G. Combined application of human amniotic membrane wrapping and hyaluronic acid injection in epineurectomized rat sciatic nerve. *J. Reconstr. Microsurg.* **2004**, *20*, 153–157. [CrossRef]
41. Vural, E.; Yilmaz, M.; Ilbay, K.; Ilbay, G. Prevention of epineurial fibrosis in rats by local administration of mitomycin C or daunorubicin. *Turk. Neurosurg.* **2016**, *26*, 291–296. [CrossRef]
42. Sakurai, M.; Miyasaka, Y. Neural fibrosis and the effect of neurolysis. *J. Bone Joint Surg. Ser. B* **1986**, *68*, 483–488. [CrossRef]
43. He, Y.; Revel, M.; Loty, B. A quantitative model of post-laminectomy scar formation: Effects of a nonsteroidal anti-inflammatory drug. *Spine* **1995**, *20*, 557–563. [CrossRef]
44. Hinton, J.L.; Warejcka, D.J.; Mei, Y.; McLendon, R.E.; Laurencin, C.; Lucas, P.A.; Robinson, J.S. Inhibition of epidural scar formation after lumbar laminectomy in the rat. *Spine* **1995**, *20*, 564–570. [CrossRef]

45. Ornelas, L.; Padilla, L.; di Silvio, M.; Schalch, P.; Esperante, S.; Infante, R.L.; Bustamante, J.C.; Avalos, P.; Varela, D.; López, M. Fibrin glue: An alternative technique for nerve coaptation—Part II. Nerve regeneration and histomorphometric assessment. *J. Reconstr. Microsurg.* **2006**, *22*, 123–128. [[CrossRef](#)]
46. Baltu, Y.; Uzun, H.; Özgenel, G.Y. The reduction of extraneural scarring with buccal mucosa graft wrapping around the sciatic nerve: An experimental study in a rat model. *J. Plast. Surg. Hand Surg.* **2017**, *51*, 259–263. [[CrossRef](#)]
47. Mathieu, L.; Adam, C.; Legagneux, J.; Bruneval, P.; Masmejean, E. Reduction of neural scarring after peripheral nerve suture: An experimental study about collagen membrane and autologous vein wrapping. *Chir. Main* **2012**, *31*, 311–317. [[CrossRef](#)] [[PubMed](#)]
48. Li, R.; Liu, H.; Huang, H.; Bi, W.; Yan, R.; Tan, X.; Wen, W.; Wang, C.; Song, W.; Zhang, Y.; et al. Chitosan conduit combined with hyaluronic acid prevent sciatic nerve scar in a rat model of peripheral nerve crush injury. *Mol. Med. Rep.* **2018**, *17*, 4360–4368. [[CrossRef](#)] [[PubMed](#)]
49. Adanali, G.; Verdi, M.; Tuncel, A.; Erdogan, B.; Kargi, E. Effects of hyaluronic acid-carboxymethylcellulose membrane on extraneural adhesion formation and peripheral nerve regeneration. *J. Reconstr. Microsurg.* **2003**, *19*, 29–35. [[CrossRef](#)] [[PubMed](#)]
50. Ngeow, W.C.; Atkins, S.; Morgan, C.R.; Metcalfe, A.D.; Boissonade, F.M.; Loescher, A.R.; Robinson, P.P. A comparison between the effects of three potential scar-reducing agents applied at a site of sciatic nerve repair. *Neuroscience* **2011**, *181*, 271–277. [[CrossRef](#)]
51. Ngeow, W.C.; Atkins, S.; Morgan, C.R.; Metcalfe, A.D.; Boissonade, F.M.; Loescher, A.R.; Robinson, P.P. The effect of Mannose-6-Phosphate on recovery after sciatic nerve repair. *Brain Res.* **2011**, *1394*, 40–48. [[CrossRef](#)]
52. Atkins, S.; Smith, K.G.; Loescher, A.R.; Boissonade, F.M.; Ferguson, M.W.J.; Robinson, P.P. The effect of antibodies to TGF- β 1 and TGF- β 2 at a site of sciatic nerve repair. *J. Peripher. Nerv. Syst.* **2006**, *11*, 286–293. [[CrossRef](#)]
53. Atkins, S.; Loescher, A.R.; Boissonade, F.M.; Smith, K.G.; Occleston, N.; O’Kane, S.; Ferguson, M.W.J.; Robinson, P.P. Interleukin-10 reduces scarring and enhances regeneration at a site of sciatic nerve repair. *J. Peripher. Nerv. Syst.* **2007**, *12*, 269–276. [[CrossRef](#)]
54. Geuna, S. The revolution of counting “tops”: Two decades of the disector principle in morphological research. *Microsc. Res. Tech.* **2005**, *66*, 270–274. [[CrossRef](#)]
55. Brown, R.E.; Erdmann, D.; Lyons, S.F.; Suchy, H. The use of cultured Schwann cells in nerve repair in a rabbit hind-limb model. *J. Reconstr. Microsurg.* **1996**, *12*, 149–152. [[CrossRef](#)]
56. Aslan, E.; Kocaeli, H.; Bekar, A.; Tolunay, Ş.; Ulus, I.H. CDP-choline and its endogenous metabolites, cytidine and choline, promote the nerve regeneration and improve the functional recovery of injured rat sciatic nerves. *Neurol. Res.* **2011**, *33*, 766–773. [[CrossRef](#)]
57. Shintani, K.; Uemura, T.; Takamatsu, K.; Yokoi, T.; Onode, E.; Okada, M.; Nakamura, H. Protective effect of biodegradable nerve conduit against peripheral nerve adhesion after neurolysis. *J. Neurosurg.* **2018**, *129*, 815–824. [[CrossRef](#)]
58. Que, J.; Cao, Q.; Sui, T.; Du, S.; Kong, D.; Cao, X. Effect of FK506 in reducing scar formation by inducing fibroblast apoptosis after sciatic nerve injury in rats. *Cell Death Dis.* **2013**, *4*. [[CrossRef](#)]
59. Servet, E.; Bekler, H.; Kiliçoğlu, V.; Özler, T.; Özkut, A. Effect of bleeding on nerve regeneration and epineural scar formation in rat sciatic nerves: An experimental study. *Acta Orthop. Traumatol. Turc.* **2016**, *50*, 234–241. [[CrossRef](#)] [[PubMed](#)]
60. Xue, J.W.; Jiao, J.B.; Liu, X.F.; Jiang, Y.T.; Yang, G.; Li, C.Y.; Yin, W.T.; Ling, L. Inhibition of peripheral nerve scarring by calcium antagonists, also known as calcium channel blockers. *Artif. Organs* **2016**, *40*, 514–520. [[CrossRef](#)] [[PubMed](#)]
61. Zhu, D.; Tapadia, M.D.; Palispis, W.; Luu, M.; Wang, W.; Gupta, R. Attenuation of robust glial scar formation facilitates functional recovery in animal models of chronic nerve compression injury. *J. Bone Joint Surg. Am. Vol.* **2017**, *99*, e132. [[CrossRef](#)] [[PubMed](#)]
62. Murakami, K.; Kuniyoshi, K.; Iwakura, N.; Matsuura, Y.; Suzuki, T.; Takahashi, K.; Ohtori, S. Vein wrapping for chronic nerve constriction injury in a rat model: Study showing increases in VEGF and HGF production and prevention of pain-associated behaviors and nerve damage. *J. Bone Joint Surg. Am. Vol.* **2014**, *96*, 859–867. [[CrossRef](#)]
63. Bain, J.R.; Mackinnon, S.E.; Hunter, D.A. Functional evaluation of complete sciatic, peroneal, and posterior tibial nerve lesions in the rat. *Plast. Reconstr. Surg.* **1989**, *83*, 129–136. [[CrossRef](#)] [[PubMed](#)]
64. Nakamura, S.; Atsuta, Y. The effects of experimental neurolysis on ectopic firing in a rat chronic constriction nerve injury model. *J. Hand Surg.* **2006**, *31*, 35–39. [[CrossRef](#)] [[PubMed](#)]
65. Stöbel, M.; Rehra, L.; Haastert-Talini, K. Reflex-based grasping, skilled forelimb reaching, and electrodiagnostic evaluation for comprehensive analysis of functional recovery—The 7-mm rat median nerve gap repair model revisited. *Brain Behav.* **2017**, *7*. [[CrossRef](#)]
66. Dumanian, G.A.; McClinton, M.; Brushart, T.M. The effects of free fat grafts on the stiffness of the rat sciatic nerve and perineural scar. *J. Hand Surg.* **1999**, *24*, 30–36. [[CrossRef](#)] [[PubMed](#)]
67. Yamamoto, M.; Endo, N.; Ito, M.; Okui, N.; Koh, S.; Kaneko, H.; Hirata, H. Novel polysaccharide-derived hydrogel prevents perineural adhesions in a rat model of sciatic nerve adhesion. *J. Orthop. Res.* **2010**, *28*, 284–288. [[CrossRef](#)] [[PubMed](#)]
68. Urano, H.; Iwatsuki, K.; Yamamoto, M.; Ohnisi, T.; Kurimoto, S.; Endo, N.; Hirata, H. Novel anti-adhesive CMC-PE hydrogel significantly enhanced morphological and physiological recovery after surgical decompression in an animal model of entrapment neuropathy. *PLoS ONE* **2016**, *11*, e0164572. [[CrossRef](#)] [[PubMed](#)]
69. Ohsumi, H.; Hirata, H.; Nagakura, T.; Tsujii, M.; Sugimoto, T.; Miyamoto, K.; Horiuchi, T.; Nagao, M.; Nakashima, T.; Uchida, A. Enhancement of perineurial repair and inhibition of nerve adhesion by viscous injectable pure alginate sol. *Plast. Reconstr. Surg.* **2005**, *116*, 823–830. [[CrossRef](#)]
70. Cherubino, M.; Pellegatta, I.; Crosio, A.; Valdatta, L.; Geuna, S.; Gornati, R.; Tos, P. Use of human fat grafting in the prevention of perineural adherence: Experimental study in athymic mouse. *PLoS ONE* **2017**, *12*, e0176393. [[CrossRef](#)]

71. Tos, P.; Crosio, A.; Pellegatta, I.; Valdatta, L.; Pascal, D.; Geuna, S.; Cherubino, M. Efficacy of anti-adhesion gel of carboxymethyl-cellulose with polyethylene oxide on peripheral nerve: Experimental results on a mouse model. *Muscle Nerve* **2016**, *53*, 304–309. [CrossRef]
72. Magill, C.K.; Tuffaha, S.H.; Yee, A.; Luciano, J.P.; Hunter, D.A.; Mackinnon, S.E.; Borschel, G.H. The short- and long-term effects of Seprafilm® on peripheral nerves: A histological and functional study. *J. Reconstr. Microsurg.* **2009**, *25*, 345–354. [CrossRef]
73. Hachinota, A.; Tada, K.; Yamamoto, D.; Nakajima, T.; Nakada, M.; Tsuchiya, H. Preventive effect of alginate gel formulation on perineural adhesion. *J. Hand Surg. Asian Pac. Vol.* **2020**, *25*, 164–171. Available online: <https://pubmed-ncbi-nlm-nih-gov.bibliopass.unito.it/32312202/> (accessed on 14 December 2020). [CrossRef] [PubMed]
74. Hernández-Cortés, P.; Peregrina, M.; Aneiros-Fernández, J.; Tassi, M.; Pajares-López, M.; Toledo, M.; O’Valle, F. Oxidized regenerated cellulose does not prevent the formation of experimental postoperative perineural fibrosis assessed by digital analysis. *Histol. Histopathol.* **2010**, *25*, 741–747. [CrossRef] [PubMed]
75. Kim, P.D.; Hayes, A.; Amin, F.; Akelina, Y.; Hays, A.P.; Rosenwasser, M.P. Collagen nerve protector in rat sciatic nerve repair: A morphometric and histological analysis. *Microsurgery* **2010**, *30*, 392–396. [CrossRef] [PubMed]
76. Lee, J.Y.; Parisi, T.J.; Friedrich, P.F.; Bishop, A.T.; Shin, A.Y. Does the addition of a nerve wrap to a motor nerve repair affect motor outcomes? *Microsurgery* **2014**, *34*, 562–567. [CrossRef]
77. Jay, R.M.; Huish, J.P.; Wray, J.H. Amniotic membrane in clinical medicine: History, current status, and future use. In *Extracellular Matrix-Derived Implants in Clinical Medicine*; Elsevier Inc.: Amsterdam, The Netherlands, 2016; pp. 151–176. [CrossRef]
78. Kaplan, T.; Kafa, I.M.; Cansev, M.; Bekar, A.; Karli, N.; Taskapiloglu, M.O.; Kanar, F. Investigation of the dose-dependency of citicoline effects on nerve regeneration and functional recovery in a rat model of sciatic nerve injury. *Turk. Neurosurg.* **2014**, *24*, 54–62. [CrossRef] [PubMed]
79. Shahraki, M.; Mohammadi, R.; Najafpour, A. Influence of tacrolimus (FK506) on nerve regeneration using allografts: A rat sciatic nerve model. *J. Oral Maxillofac. Surg.* **2015**, *73*, 1438.e1–1438.e9. [CrossRef]
80. Davis, B.; Hilgart, D.; Erickson, S.; Labroo, P.; Burton, J.; Sant, H.; Shea, J.; Gale, B.; Agarwal, J. Local FK506 delivery at the direct nerve repair site improves nerve regeneration. *Muscle Nerve* **2019**, *60*, 613–620. [CrossRef]
81. Stocco, E.; Barbon, S.; Macchi, V.; Tiengo, C.; Petrelli, L.; Rambaldo, A.; Borean, A.; Capelli, S.; Filippi, A.; Romanato, F.; et al. New bioresorbable wraps based on oxidized polyvinyl alcohol and leukocyte-fibrin-platelet membrane to support peripheral nerve neurorrhaphy: Preclinical comparison versus NeuraWrap. *Sci. Rep.* **2019**, *9*. Available online: <https://pubmed-ncbi-nlm-nih-gov.bibliopass.unito.it/31748615/> (accessed on 14 December 2020). [CrossRef]
82. Kikuchi, K.; Setoyama, K.; Takada, S.; Otsuka, S.; Nakanishi, K.; Norimatsu, K.; Tani, A.; Sakakima, H.; Kawahara, K.I.; Hosokawa, K.; et al. E8002 inhibits peripheral nerve adhesion by enhancing fibrinolysis of l-ascorbic acid in a rat sciatic nerve model. *Int. J. Mol. Sci.* **2020**, *21*, 3972. Available online: <https://pubmed-ncbi-nlm-nih-gov.bibliopass.unito.it/32492845/> (accessed on 14 December 2020). [CrossRef]
83. Okui, N.; Yamamoto, M.; Fukuhira, Y.; Kaneko, H.; Hirata, H. Artificial perineurium to enhance nerve recovery from damage after neurolysis. *Muscle Nerve* **2010**, *42*, 570–575. [CrossRef]
84. Ikeda, K.; Yamauchi, D.; Tomita, K. Preliminary study for prevention of neural adhesion using an absorbable oxidised regenerated cellulose sheet. *Hand Surg.* **2002**, *7*, 11–14. [CrossRef] [PubMed]
85. Masear, V.R.; Tullos, J.; St Mary, E.; Mayer, R. Venous wrapping of nerves to prevent to prevent scarring. *J. Hand Surg.* **1990**, *15*, 817–818. Available online: <https://ci.nii.ac.jp/naid/10026286269/> (accessed on 23 March 2021).
86. Millesi, H.; Zoch, G.; Reihnsner, R. Mechanical properties of peripheral nerves. *Clin. Orthop. Relat. Res.* **1995**, *314*, 76–83. Available online: <https://europepmc.org/article/med/7634654> (accessed on 23 March 2021). [CrossRef]

4. DISCUSSION AND CONCLUSION

Successful treatment of peripheral nerve injuries is, up to now, uncertain and numerous complications can arise even if an appropriate treatment is planned and executed. It means debilitating consequences for patients who may suffer from incomplete sensory or motor recovery to unbearable pain.

Over years novel procedures have been introduced and expanded in clinical practice. For example, nerve transfers have become even more employed both in primary and secondary reconstruction, processed nerve allografts showed promising results for sensory and mixed nerve reconstruction and new procedures have been introduced for the treatment of painful neuromas. Moreover, nerve conduits found their place in nerve reconstruction, limiting their employment in sensory nerve gaps up to 3 cm.

Following these premises, the evolution of knowledges in basic research and in clinical practice moved us to further investigate aspects to ameliorate nerve reconstruction. Objective of this research program has been to investigate biological mechanisms and new techniques to improve all steps of nerve repair. Both clinical and experimental studies have been presented.

Biological processes of nerve regeneration.

The basis of treatment is to understand, as much as possible, the pathophysiological mechanism underlying axons elongation and nerve repair. Through the experiments presented in chapter 3.1, a new role of fibroblasts in nerve regeneration has been described. Since then, NRG1 was thought to be released only by SCs during nerve regeneration. Our researches clarify that fibroblasts are the main actors responsible for NRG1 release. Our study was focused on a short nerve gap model, but it is reasonable to imagine the same in primary nerve repair. Furthermore, endothelial cells also have been analyzed, reporting their important role for SCs migration into the nerve gap to reach the distal stump. Our findings add one more brick in the undisclosed puzzle of nerve repair, suggesting to use fibroblasts as novel enrichment in nerve gap. On the other hand, it is required to understand which is the limit over that fibroblasts induce pathological scar leading to neuroma in continuity. Following our findings some authors experimented a fibrin-collagen hydrogel to promote nerve regeneration. They registered, in short term analysis, an upregulation of NRG1 release, confirming what we described (El Soury 2023). Further investigations could be useful to understand if filling conduits with fibroblast may be helpful to bridge long nerve gaps.

Strategies of somatic and autonomic nerve repair: conduits, allografts and membranes

Nerve conduits in peripheral nerve repair have been extensively studied. As stated by Rbia in 2017 (Rbia 2017) the role of tubes is clearly defined. What is under research now are technologies to go beyond their own limits. As anticipated in chapter 1, conduits can be synthesized through biocompatible molecules.

Our group took part to the development of a chitosan conduit, named commercially Reaxon® (Haastert-Talini 2013, Shapira 2016). This device presents the intrinsic limit reported in literature so that, over years, attempts of amelioration of its efficacy have been done. For example, micro conduits have been created into chitosan conduit using nanotechnologies to implement SCs migration. This implementation showed a recovery comparable to autograft in vivo and amazing support for neurite elongation in vitro (Jiang 2023, Zhou 2023). Previously, the same tube was filled by muscle fibers showing comparable results to autograft either in acute and delayed nerve gap reconstruction on animal model (Ronchi 2018, Crosio 2019). Despite good results obtained in pre-clinical papers, recently more than one clinical report showed drawbacks about chitosan and collagen conduits. Usually it was noted that tubes did not degrade, they were associated to perineural scar and were responsible of partial joint stiffness due to their intrinsic rigidity (Rein 2023). Moreover, a recent Cochrane review about the use of nerve conduits highlighted that patients may experience adverse events with use of currently available tubes more than with standard repair techniques, and the need for revision surgery may also be greater when a nerve guide was used (Thomson 2022). These results should not demonize nerve conduits, but should be a suggestion for basic researchers to improve material properties such as biodegradation time or elasticity. In chapter 3.6 of this thesis a novel nerve conduit was presented. The biocompatibility and biomechanical properties of silk fibroin-based conduit were tested in vitro revealing proliferation of motor neurons and neurites lengthening compared to control substrate (Alessandrino 2019). Those preliminary results were further confirmed by the paper presented in this thesis. As for most of nerve conduits, functional results have been comparable to autograft at each time point. But one of the most interesting aspect, more fascinating from a surgical point of view, was the capacity of the tube not to collapse and its smoothness: these two characteristics are not common in commercially available nerve conduits and of great interest in clinical application, especially when the tube has to bridge a finger joint, where motion is fundamental to prevent complications. The results obtained in the animal model should be confirmed in human clinical trial.

Decellularized nerve allografts are a special type of nerve conduits. Their role in nerve reconstruction is still debated (Frostadottir 2023). Numerous papers showed very good results in nerve recovery with the use of decellularized nerve allograft both in sensory and mixed nerves (Isaacs 2017, Safa 2019). Despite these reports, in which frequently the company who produces graft is involved, recent negative results on its efficacy in the treatment of large mixed nerve gaps have been published (Huddleston 2021). Pre-clinical papers reported results of rat nerve reconstruction using human allograft (Giusti 2019), that is namely a xenograft. Considering so, in chapter 3.2 is presented our experience with decellularized nerve xenograft, with pig nerves as donor. As stated above, the employed chemical decellularization method is affordable also in pig nerve. Very few immunogenic components were present in morphological analysis. In vivo study demonstrated that four weeks after injury, regenerating fibers have colonized the graft suggesting a promising use for repairing severe nerve lesions. Morphological analyses were able to identify both myelinic

and amyelinc fibers in all xenograft samples and all along the graft. The main advantage induced by processed xenograft regards the source of the nerve, that can be easily obtained from food industry. The main drawback still consists in the creation of an appropriate cycle of sterilization and conservation of the graft.

Not only tubes have been proposed to reconstruct nerve gap. Most of the early papers about nerve bridging tested membranes, especially to investigate the efficacy of the material to sustain and induce nerve regeneration (Amado 2008, Simoes 2010). Our research group conducted an experiment using a modified crosslinked chitosan-based membrane to repair a median nerve gap. Chitosan (CS) was crosslinked with dibasic sodium phosphate (DSP) alone (CS/DSP) or in association with the γ -glycidoxypropyltrimethoxysilane (CS/GPTMS_ DSP). These two substances were selected to improve the regeneration capacity of the device, based on the in vitro results previously obtained. This is the example of device engineering in which the flat membrane was functionalized through other molecules (Fregnan 2016).

In the following years, attempt to repair motor nerves were then diverted on the use of conduits instead of membranes because of the tube is a better guide for the nerve to grow having a closed environment in which growth factors have the possibility to drive the axons distally, limiting un-useful collateral sprouting. Membranes were then proposed to reinnervate plexual nerve structures, where a not unique proximal and distal nerve stumps are available. Flat chitosan membranes were in fact applied on prostatic plexus after nerve sparing radical prostatectomy in order to promote axons regeneration (Porpiglia 2019). Despite the promising results obtained in humans, was not clear the exact regenerative potential of membrane in this field. This is why part of this thesis was focused on this. The study presented in chapter 3.7 includes a section in which flat membranes were used to bridge a gap of cavernous nerve. Moreover, the actual knowledges in nanotechnologies allow scientists to create micro and nano-patterns on scaffold. This was done in our study in which the chitosan membranes have been modified with different micro pathways. Our results demonstrate the effectiveness of scaffold modification in which axons elongation both in vitro and in vivo followed the membrane pattern. Confirmation of our findings in long term pre-clinical study are required, merging morphological and functional evidences. However, our results further confirm the effectiveness of scaffold improvement through nanotechnologies as tested elsewhere (de Ruitter 2009, Thomson 2022).

Strategies of nerve repair: Nerve transfer

With the last research all the group have been introduced on a novel aspect of peripheral nerve repair: autonomic nerve system reconstruction. Criticisms are related to the plexual anatomy of the nerves that driven autonomic organs, furthermore the function of targets are frequently associated to a balance between two systems that is dissimilar to what happens in muscle control, so that is more difficult to simulate and evaluate in animal models the efficacy of nerve reconstruction. About autonomic nerve system injuries, two types of lesion can be identified: spinal cord injuries and pelvic nerve injuries. As described in chapter

3.3, proximal root transfer (L4 to L6) failed to reanimate bladder control despite the positive morpho-functional results obtained in animal models (Wang 2007, Tuite 2016, Peters 2014). In pre-clinical studies, very interesting results were obtained by distal nerve transfer using motor and mixed nerve in pelvic area to reinnervate bladder (Ruggieri 2008, Ruggieri 2011). This novel approach follows, more than root transfers, nerve transfer principles, moving the donor nerve closer to the target organ. Considering the un-successful experience reported in literature with cavernous nerve reconstruction with autograft or vein graft (Davis 2009, Kung 2015), a nerve transfer for corpora cavernosa has been proposed to treat erectile dysfunction secondary to cavernous nerve injury. What we described in chapter 3.7 is a double motor nerve transfer to neurotize directly corpora cavernosa, basing the project on the case series from Souza Trindade 2017 and Reece 2019, as discussed previously. The motor nerve transfer seemed to be feasible in rat without breakdown of the suture after 4 months. The efficacy of this procedure is studied up to now through genes expression of target organ, but will be interesting in future associate functional evaluation to compare this procedure to results obtained through chitosan membranes and, moreover, to understand what happens morpho-functionally inside the corpora cavernosa. It is unknown yet what happens when somatic fibers encounter an autonomic organ. The only papers who investigated plasticity following somatic to autonomic transfer revealed changing in cholinergic receptor expression in detrusor muscles moving from muscarinic to nicotinic ones (Gomez-Amaya SM 2015). The analysis of gene expression, actually on going, could show changing in BDNF, GDNF, VEGF, NOS and GAP 43 expression that could be associated to organ and nerve plasticity. If experimental results would be positive, showing reinnervation of corpora cavernosa, translation on humans will be quite easy, considering the case series already published. In humans, possible donors could be the obturator nerve with its branches to gracilis muscle or others muscles of the medial thigh: these nerves can be easily dissected and muscles are expandable with low functional impairment.

Complications after nerve repair: scar and neuroma

Complications following nerve repair are frequent and it is not clear how to prevent and treat them. First, adhesions after trauma or surgical procedures may cause traction neuropathies. In this thesis an extensive literature review with the aim to identify a way to simulate scar neuropathies was presented. In fact a shared pre-clinical model is essential to compare different strategies to solve this problem. What emerged from our research is a great heterogeneity of way to induce and evaluate perineural scar. What emerged is the requirement of a macroscopical and microscopical analysis to better express the amount of scar tissue around the injured nerve. The combination of these two evaluation methods allows to quantitatively compare the efficacy of anti-adhesion devices that will be tested on animal models. Up to now, none of the papers included in the review are able to combine these types of evaluation. Furthermore, it is impossible to compare the efficacy of the devices that have been tested for the reason expressed above. Most of them are effective on animal models, but comparison between them is not possible. Translating

this research in human is difficult, no guidelines have been published in treatment of scar neuropathy and there is no a device that one works better than other nowadays. Our feeling and our clinical approach is to use a device associated with a local flap when a nerve is freed from scar tissue due to a recurrence and the nerve is left in site. Recently, we introduced vein wrapping of the scarred segment after neurolysis to interpose a biological barrier between epineurium and soft tissue bed as proposed by Murakami (Murakami 2014). This procedure uses a cheap biological barrier that can be easily found in the operating field without donor site morbidity. Moreover, is an autologous barrier, reducing the requirement to put an external device. On the other site, the use of nerve barrier is increasing and associated to good functional results (Hones 2023).

Painful neuroma is the other devastating complication that affects nerve injuries. Considering the disability that may cause painful neuromas, we conducted two clinical researches on this topic. It is unknown, so far, how to prevent and treat with success such pathology. As reported in chapter 3.4 different techniques have been described in order to prevent painful neuroma formation after a nerve injury. Specifically, in that paper it has been asked to expert hand surgeons which technique they prefer to prevent terminal painful neuromas in finger amputation. Emerged that none of the cited techniques is superior to the others and none of them is able to prevent, for sure, symptoms onset. The most significant message that arise is the importance of soft tissue debridement to reduce pro inflammatory environment around nerve stumps. Whereas, execution of the proposed procedure on nerve stumps seems not to be able to prevent this devastating complication at all. This paper is focused only on prevention of terminal neuromas of the finger in primary amputation. Painful neuromas are prone to recurrences and their treatment is even more complex, especially when a mixed nerve is affected. In the last 15 years targeted muscle reinnervation (TMR) and peripheral nerve regenerative interface (RPNI) have been proposed with success (Kurlander 2020, Senger 2023). Criticism still persists, especially treating patients with long lasting pain. In these patients, neural plasticity in spinal cord and cerebral cortex induces molecular changes that make pain independent from peripheral nerves activation (Smith 2023). When this occurs, surgical procedures are un-successful and sometimes is impossible to predict positive or negative response, even with pain reduction following local anesthetic block. In our clinical practice unpredictable results were obtained with TMR in patients affected by painful neuromas lasting more than 6 months, but we believe that type of trauma, patients' characteristics and other non-clarified and understood conditions may influence the result.

Chapter 3.5 discuss in part this problem. The main intent of the research was to improve nerve debridement to maximize nerve recovery. In the case series presented, through intraoperative ultrasound usually nerve resection was extend by 1 cm more than macroscopical guided resection. Unfortunately, greater resection did not correspond always to better results. The most interesting aspect is relapsing of painful neuroma in those patients who were treated for this problem. Time from trauma, as stated above, may interfere also with recovery due to central plasticity, but seems to be not the only factor involved. In

fact, in our series, patients who had pain from the beginning, relapsed painful neuromas despite the great nerve resection. This could be a sign that painful neuromas are independent by quality of nerve stumps, as we can assess nowadays. Maybe patients' characteristics, not only nerve characteristics, type of trauma and local tissues could be more responsible for this complex condition. When neuroma relapses after graft reconstruction, TMR and RPNI should be consider as further treatment.

As emerged from the last two discussed papers, one of the main problems in nerve reconstruction is painful neuromas. Here some biological and psychological aspects not yet identified are involved and responsible for symptoms other than molecular mechanism strictly related to the neuroma. In this field the animal models used to simulate neuromas are not adequate and can't simulate what happens in humans.

Conclusions

In conclusion, researches presented in this thesis showed novel aspects about pathophysiological mechanisms involved in nerve regeneration, enhancing the role of NRG1, that could be used in future to improve nerve regeneration. For nerve gap, xenograft, as presented, is a potential device that could be able to change approach in nerve reconstruction. What is still a problem, to assess efficacy of novel nerve conduits, is to have a model for long nerve gap, that is lacking actually. Autonomic organ reinnervation, less studied field, has been also explored in this thesis. Using actual techniques for nerve repair, such as nerve transfer, it is possible to imagine new strategies to restore bladder, cavernous body and bowel function. Moreover, discover how somatic nerves can reinnervate autonomic organs is extremely fascinating, considering also cerebral plasticity associated to this process. That said, we are far from a complete understanding of mechanism that drive nerve repair and more knowledges are required to improve treatment strategies, especially in complications such as scar neuropathies and painful neuromas.

5. REFERENCES

- Adani R, Tarallo L, Battiston B, Marcoccio I. Management of neuromas in continuity of the median nerve with the pronator quadratus muscle flap. *Ann Plast Surg.* 2002 Jan;48(1):35-40
- Alessandrino A, Fregnan F, Biagiotti M, Muratori L, Bassani GA, Ronchi G, Vincoli V, Pierimarchi P, Geuna S, Freddi G. SilkBridge™: a novel biomimetic and biocompatible silk-based nerve conduit. *Biomater Sci.* 2019 Oct 1;7(10):4112-4130
- Amadio PC. Interventions for recurrent/persistent carpal tunnel syndrome after carpal tunnel release. *J Hand Surg Am.* 2009 Sep;34(7):1320-2
- Amado S, Simões MJ, Armada da Silva PA, Luís AL, Shirosaki Y, Lopes MA, Santos JD, Fregnan F, Gambarotta G, Raimondo S, Fornaro M, Veloso AP, Varejão AS, Maurício AC, Geuna S. Use of hybrid chitosan membranes and N1E-115 cells for promoting nerve regeneration in an axonotmesis rat model. *Biomaterials.* 2008 Nov;29(33):4409-19
- Atkins S, Smith KG, Loescher AR, Boissonade FM, O’Kane S, Ferguson MWJ, Robinson PP, Scarring impedes regeneration at sites of peripheral nerve repair. *Neuroreport* 2006;17:1245–1249
- Bates D, Schultheis BC, Hanes MC, Jolly SM, Chakravarthy KV, Deer TR, Levy RM, Hunter CW. A Comprehensive Algorithm for Management of Neuropathic Pain. *Pain Med.* 2019 Jun 1;20(Suppl 1):S2-S12
- Battiston B, Tos P., Conforti L, Geuna S (2007). Alternative techniques for peripheral nerve repair: conduits and end-to-side neurorrhaphy. *How to Improve the Results of Peripheral Nerve Surgery.* Springer: 43-50
- Battiston B, Raimondo S, Tos P, Gaidano V, Audisio C, Scevola A, Perroteau I, Geuna S (2009). "Chapter 11: Tissue engineering of peripheral nerves." *Int Rev Neurobiol* 87: 227-249
- Becker C, Gilbert A. Le lambeau cubital [The cubital flap]. *Ann Chir Main.* 1988;7(2):136-42. French
- Belanger K, Dinis TM, Taourirt S, Vidal G, Kaplan DL, Egles C. Recent Strategies in Tissue Engineering for Guided Peripheral Nerve Regeneration. *Macromol Biosci.* 2016 Apr;16(4):472-81
- Belcher HJ, Pandya AN. Centro-central union for the prevention of neuroma formation after finger amputation. *J Hand Surg Br* 2000;25:154-159
- Bertelli JA, dos Santos AR, Taleb M, Calixto JB, Mira JC, Ghizoni MF. Long interpositional nerve graft consistently induces incomplete motor and sensory recovery in the rat. An experimental model to test nerve repair. *J Neurosci Methods.* 2004 Mar 15;134(1):75-80
- Bertelli JA, Taleb M, Saadi A, Mira JC, Pecot-Dechavassine M. The rat brachial plexus and its terminal branches: an experimental model for the study of peripheral nerve regeneration. *Microsurgery.* 1995;16(2):77-85

- Brooks DN, W. R., Chao JD (2012). "Processed nerve allografts for peripheral nerve reconstruction: a multicenter study of utilization and outcomes in sensory, mixed, and motor nerve reconstructions." *Microsurgery* 32: 1–14
- Brown JM, M. S. (2008). "Nerve transfers in the forearm and hand." *Hand Clin* 24: 319–340
- Brunelli G. Direct neurotization of severely damaged muscles. *J Hand Surg Am.* 1982 Nov;7(6):572-9.
- Burnett MG, Z. E. (2004). "Pathophysiology of peripheral nerve injury: A brief review." *Neurosurgical Focus* 16: E1
- Calcagni M, Zimmermann S, Scaglioni MF, Giesen T, Giovanoli P, Fakin RM. The novel treatment of SVF-enriched fat grafting for painful end-neuromas of superficial radial nerve. *Microsurgery.* 2018 Mar;38(3):264-269.
- Carriel V, A. M., Garzón I, Campos A, Cornelissen M (2014). "Tissue engineering of the peripheral nervous system." *Expert review of neurotherapeutics* 14: 301-318
- M. S. Cartwright, H. W. Shin, L. V Passmore, and F. O. Walker, "Ultrasonographic findings of the normal ulnar nerve in adults.," *Arch. Phys. Med. Rehabil.*, vol. 88, no. 3, pp. 394–6, Mar. 2007
- Chen P, P. X., Bonaldo P (2015). "Role of macrophages in Wallerian degeneration and axonal regeneration after peripheral nerve injury." *Acta neuropathologica* 130: 605- 618
- Cherubino M, Pellegatta I, Crosio A, Valdatta L, Geuna S, Gornati R, Tos P. Use of human fat grafting in the prevention of perineural adherence: Experimental study in athymic mouse. *PLoS One.* 2017 Apr 26;12(4):e0176393.
- Chong ZZ, S. Y., Wang S, Maiese K (2012). "Shedding new light on neurodegenerative diseases through the mammalian target of rapamycin." *Prog Neurobiol* 99: 128–148
- Chuang DC. Distal Nerve Transfers: A Perspective on the Future of Reconstructive Microsurgery. *J Reconstr Microsurg.* 2018 Nov;34(9):669-671
- Chu CT (2006). "Autophagic stress in neuronal injury and disease." *J Neuropathol Exp Neurol* 65(5): 423-432
- Clark WL, T. T., Swiontkowski MF, Tencer AF (1992). "Nerve tension and blood flow in a rat model of immediate and delayed repairs." *J Hand Surg [Br]* 17A: 677–687
- Cramer LM (1985). Local fat coverage for the median nerve. *ASSH. L. LL. Correspondence Newsletter for Hand Surgery:* 35
- Crompton KE, G. J., Bellamkonda RV (2007). "Polylysine-function- alised thermoresponsive chitosan hydrogel for neural tissue engineering." *Biomaterials* 28: 441–449

Crosio A, Valdatta L, Cherubino M, Izzo M, Pellegatta I, Pascal D, Geuna S, Tos P. A simple and reliable method to perform biomechanical evaluation of postoperative nerve adhesions. *J Neurosci Methods*. 2014 Aug 15;233:73-7.

Crosio A, Fornasari BE, Gambarotta G, Geuna S, Raimondo S, Battiston B, Tos P, Ronchi G. Chitosan tubes enriched with fresh skeletal muscle fibers for delayed repair of peripheral nerve defects. *Neural Regen Res*. 2019 Jun;14(6):1079-1084.

Dahlin L, B. J., Nilsson A, Lundborg G, Kanje M (2007). Schwann cells, acutely dissociated from a predegenerated nerve trunk, can be applied into a matrix used to bridge nerve defects in rats. *How to Improve the Results of Peripheral Nerve Surgery*. Springer: 57-59

Davis JW, Chang DW, Chevray P, et al. Randomized phase II trial evaluation of erectile function after attempted unilateral cavernous nerve-sparing retropubic radical prostatectomy with versus without unilateral sural nerve grafting for clinically localized prostate cancer. *Eur Urol* 2009;55:1135–43

de Lange JWD, Hundepool CA, Power DM, et al. Prevention is better than cure: Surgical methods for neuropathic pain prevention following amputation - A systematic review. *J Plast Reconstr Aesthet Surg* 2022;75:948-959

De Jongh F, Pouwels S, Tan LT. Autologous Fat Grafting for the Treatment of a Painful Neuroma of the Hand: A Case Report and Review of Literature. *Cureus*. 2020 Sep 11;12(9):e10381.

Deumens R, B. A., Meek MF, Marcus MA, Joosten EA, Weis J, Brook GA (2010). "Repairing injured peripheral nerves: Bridging the gap." *Prog Neurobiol* 92: 245-276

de Putter CE, S. R., Polinder S, Panneman MJ, Hovius SE, van Beeck EF (2012). "Economic impact of hand and wrist injuries: health-care costs and productivity costs in a population-based study." *J Bone Joint Surg Am* 2(94(9)): e56

de Ruyter GC, M. M., Yaszemski MJ, Windebank AJ, Spinner RJ (2009). "Designing ideal conduits for peripheral nerve repair." *Neurosurg Focus* 26: E5

Deumens R, B. A., Meek MF, Marcus MA, Joosten EA, Weis J, Brook GA (2010). "Repairing injured peripheral nerves: Bridging the gap." *Prog Neurobiol* 92: 245-276

di Summa PG, K. P., Raffoul W, Wiberg M, Terenghi G, Kalbermatten DF (2010). "Adipose-derived stem cells enhance peripheral nerve regeneration." *Jour Plast Rec Aest Sur* 63: 1544-1552

Doi K. Distal Nerve Transfer: Perspective of Reconstructive Microsurgery. *J Reconstr Microsurg* 2018;34:675–677

Dornseifer U, F. A., Leichtle S, Wilson A, Rupp A, Rodenacker K, Ninkovic M, Biemer E, Machens HG, Matiasek K (2011). "Peripheral nerve reconstruction with collagen tubes filled with denatured autologous muscle tissue in the rat model." *Microsurgery* 31: 632-641

Ducic I, Mesbahi AN, Attinger CE, Graw K. The role of peripheral nerve surgery in the treatment of chronic pain associated with amputation stumps. *Plast Reconstr Surg* 2008;121:908

Dumanian GA, M. M., Brushart TM (1999). "The effects of free fat grafts on the stiffness of the rat sciatic nerve and perineural scar." *J Hand Surg Am* 24(1): 30–36

Ederer IA, Mayer JA, Heinzl J, Kolbenschlag J, Daigeler A, Wahler T. Outcome After Reconstruction of 43 Digital Nerve Defects With Muscle-in-Vein Conduits. *J Hand Surg Am*. 2023 Sep;48(9):948.e1-948.e9. doi: 10.1016/j.jhsa.2022.02.002. Epub 2022 Apr 7. PMID: 35400539.

Elliot D (2014). "Surgical management of painful peripheral nerves." *Clin Plast Surg* 41(3): 589-613

El Soury M, García-García ÓD, Tarulli I, Chato-Astrain J, Perroteau I, Geuna S, Raimondo S, Gambarotta G, Carriel V. Chitosan conduits enriched with fibrin-collagen hydrogel with or without adipose-derived mesenchymal stem cells for the repair of 15-mm-long sciatic nerve defect. *Neural Regen Res*. 2023 Jun;18(6):1378-1385.

Faroni A, T. G., Reid AJ (2013). "Adipose-derived stem cells and nerve regeneration: promises and pitfalls." *Int Rev Neurobiol* 108: 121–136

Fornaro M, L. J., Raimondo S, Nicolino S, Geuna S, Giacobini-Robecchi M ((2008). "Neuronal intermediate filament expression in rat dorsal root ganglia sensory neurons: an in vivo and in vitro study." *Neuroscience* 153: 1153-1163

Fornasari BE, G. G. (2016). Neuregulin1 expression following peripheral nerve injury and new tools to improve nerve regeneration. DEPARTMENT OF CLINICAL AND BIOLOGICAL SCIENCES, UNIVERSITÀ DEGLI STUDI DI TORINO. PhD program in NEUROSCIENCE

Fregnan F, Ciglieri E, Tos P, Crosio A, Ciardelli G, Ruini F, Tonda-Turo C, Geuna S, Raimondo S. Chitosan crosslinked flat scaffolds for peripheral nerve regeneration. *Biomed Mater*. 2016 Aug 10;11(4):045010.

Freier T, M. R., Shan Koh H, Shoichet MS (2005). "Chitin-based tubes for tissue engineering in the nervous system." *Biomaterials* 26: 4624–4632

Frostadottir D, Chemnitz A, Johansson Ot LJ, Holst J, Dahlin LB. Evaluation of Processed Nerve Allograft in Peripheral Nerve Surgery: A Systematic Review and Critical Appraisal. *Plast Reconstr Surg Glob Open*. 2023 Jun 27;11(6):e5088.

Gaudet AD, P. P., Ramer MS (2011). "Wallerian degeneration: gaining perspective on inflammatory events after peripheral nerve injury." *Journal of neuroinflammation* 8: 110

Geuna S, R. S., Ronchi G, Di Scipio F, Tos P, Czaja K, Fornaro M (2009). "Histology of the peripheral nerve and changes occurring during nerve regeneration." *Int Rev Neurobiol* 87: 27-46

Geuna S, T. P., Titolo P, Ciclamini D, Beningo T, Battiston B (2014). "Update on nerve repair by biological tubulization." *J Brachial PlexPeripher Nerve Inj* 9: 3

Giusti G, Willems WF, Kremer T, Friedrich PF, Bishop AT, Shin AY. Return of motor function after segmental nerve loss in a rat model: comparison of autogenous nerve graft, collagen conduit, and processed allograft (AxoGen). *J Bone Joint Surg Am*. 2012 Mar 7;94(5):410-7.

Gnavi S, B. C., Freier T, Haastert-Talini K, Grothe C, Geuna S (2013). "The use of chitosan-based scaffolds to enhance regeneration in the nervous system." *Int Rev Neurobiol* 109: 1-62

Goitz RJ, S. J. (2005). "Microvascular omental transfer for the treatment of severe recurrent median neuritis of the wrist: a long-term follow-up." *Plast Reconstr Surg* 115: 163-171

Gomez-Amaya SM, Barbe MF, Lamarre NS, Brown JM, Braverman AS, Ruggieri MR Sr. Neuromuscular nicotinic receptors mediate bladder contractions following bladder reinnervation with somatic to autonomic nerve transfer after decentralization by spinal root transection. *J Urol*. 2015 Jun;193(6):2138-45.

Gosset J, Andre P, Levame M. [The prevention of amputation neuromas of the fingers and of amputation neuromas in general]. *Mem Acad Chir (Paris)* 1962;88:548-550

Hadlock TA, S. C., Hunter DA, Vacanti JP, Cheney ML (2001). "A new artificial nerve graft containing rolled Schwann cell monolayers." *Microsurgery* 21: 96-101

Haastert-Talini K, G. S., Dahlin LB, Meyer C, Stenberg L, Freier T, Heimann C, Barwig C, Pinto LF, Raimondo S, Gambarotta G, Samy SR, Sousa N, Salgado AJ, Ratzka A, Wrobel S, Grothe C (2013). "Chitosan tubes of varying degrees of acetylation for bridging peripheral nerve defects." *Biomaterials* 34: 9886-9904

Hones KM, Nichols DS, Barker H, Cox E, Hones JA, Chim H. Outcomes following use of VersaWrap nerve protector in treatment of patients with recurrent compressive neuropathies. *Front Surg*. 2023 Mar 21;10:1123375.

Höpker VH, S. D., Tessier-Lavigne M, Poo M-m, Holt C (1999). "Growth-cone attraction to netrin-1 is converted to repulsion by laminin-1." *Nature* 401: 69-73

Huang DX, Yang MX, Jiang ZM, Chen M, Chang K, Zhan YX, Gong X. Nerve trunk healing and neuroma formation after nerve transection injury. *Front Neurol*. 2023 Jun 12;14:1184246.

Huddleston HP, Kurtzman JS, Connors KM, Koehler SM. A Retrospective Case Series of Peripheral Mixed Nerve Reconstruction Failures Using Processed Nerve Allografts. *Plast Reconstr Surg Glob Open*. 2021 Dec 7;9(12):e3983.

Huelsenbeck SC, R. A., Handreck A, Hellmich G, Kiaei E, Roettinger I, Grothe C, Just I, Haastert-Talini K (2012). "C3 peptide promotes axonal regeneration and functional motor recovery after peripheral nerve injury." *Neurotherapeutics* 9: 185-198

Hunter JM (1991). "Recurrent carpal tunnel syndrome, epineural fibrous fixation, and traction neuropathy." *Hand Clin* 7: 491-504

Jones NF, A. H., Eo S (2012). "Revision surgery for persistent and recurrent carpal tunnel syndrome and for failed carpal tunnel release." *Plast Reconstr Surg* 129: 683-692

Kung TA, Waljee JF, Curtin CM, Wei JT, Montie JE, Cederna PS. Interpositional nerve grafting of the prostatic plexus after radical prostatectomy. *Plast Reconstr Surg Glob Open* 2015;3:e452

Kurlander DE, Wee C, Chepla KJ, Lineberry KD, Long TC, Gillis JA, Valerio IL, Khouri JS. TMRpni: Combining Two Peripheral Nerve Management Techniques. *Plast Reconstr Surg Glob Open*. 2020 Oct 27;8(10):e3132.

Isaacs J, Safa B. A Preliminary Assessment of the Utility of Large-Caliber Processed Nerve Allografts for the Repair of Upper Extremity Nerve Injuries. *Hand (N Y)*. 2017 Jan;12(1):55-59.

Jiang Z, Zhang Y, Wang Y, Wang S, Chang J, Liu W, Han B. Multichannel nerve conduit based on chitosan derivatives for peripheral nerve regeneration and Schwann cell survival. *Carbohydr Polym*. 2023 Feb 1;301(Pt B):120327.

Kehoe S, Z. X., Boyd D (2012). "FDA approved guidance conduits and wraps for peripheral nerve injury: a review of materials and efficacy." *Injury* 43: 553-572)

Klein D, M. R. (2016). "Myelin and macrophages in the PNS: An intimate relationship in trauma and disease." *Brain research* 1641: 130-138

Ko PY, Y. C., Kuo YL, Su FC, Hsu TI, Tu YK, Jou IM (2018). "Schwann-Cell Autophagy, Functional Recovery, and Scar Reduction After Peripheral Nerve Repair." *J Mol Neuroscience* 64(4): 601-610

Konofaos P, V. H. J. (2013). "Nerve repair by means of tubulization: past, present, future." *J Reconstr Microsurg* 29: 149-164

Lang J (1962). "On connective tissue and blood vessels of the nerves." *Z Anat Entwicklungsgesch* 123: 61-79

Lipinski LJ, S. R. (2014). "Neurolysis, neurectomy, and nerve repair/ reconstruction for chronic pain." *Neurosurg Clin N Am* 25: 777-787

Liu GB, C. Y., Feng YK, Pang CJ, Li Q, Wang Y (2011). "Adipose-derived stem cells promote peripheral nerve repair." *Arch Med Sci* 7(4): 592–596

Luís A, A. S., Geuna S, Rodrigues J, Simões M, Santos J, Fregnan F, Raimondo S, Veloso AP, Ferreira A (2007). "Long-term functional and morphological assessment of a standardized rat sciatic nerve crush injury with a non-serrated clamp." *Journal of neuroscience methods* 163: 92-104

Lundborg G (2005). *Nerve Injury and Repair: Regeneration, Reconstruction, and Cortical Remodeling*

Mackinnon SE (1989). "New directions in peripheral nerve surgery." *Ann Plast Surg* 22: 257- 273.

M. J. Malessy, S. G. van Duinen, H. K. Feirabend, and R. T. Thomeer, "Correlation between histopathological findings in C-5 and C-6 nerve stumps and motor recovery following nerve grafting for repair of brachial plexus injury.," *J. Neurosurg.*, vol. 91, no. 4, pp. 636–44, Oct. 1999

Manoli T, Schulz L, Stahl S, Jaminet P, Schaller HE. Evaluation of sensory recovery after reconstruction of digital nerves of the hand using muscle-in-vein conduits in comparison to nerve suture or nerve autografting. *Microsurgery*. 2014 Nov;34(8):608-15. doi: 10.1002/micr.22302. Epub 2014 Aug 2. PMID: 25088084.

Mantovani C, M. D., Kingham PJ, Terenghi G, Shawcross SG, Wiberg M (2010). "Bone marrow-and adipose-derived stem cells show expression of myelin mRNAs and proteins." *Regenerative medicine* 5: 403-410

Martinez-Pineiro, L. *et al.* Rat model for the study of penile erection: pharmacologic and electrical-stimulation parameters. *Eur Urol*. 25 (1), 62-70 (1994)

Mathur A, M. J., Russell RC, Zook EG (1983). "A scanning electron microscopy evaluation of peripheral nerve regeneration." *Scan Electron Microsc* 1983(Pt 2): 975–998

Midha R, M. C., Dalton PD, Tator CH, Shoichet MS (2003). "Growth factor enhancement of peripheral nerve regeneration through a novel synthetic hydrogel tube." *Journal of neurosurgery* 99: 555-565

Millesi H, M. G., Berger A (1976). "Further experience with interfascicular grafting of the median, ulnar, and radial nerves." *J Bone Joint Surg Am* 58(2): 209-218

Millesi H. Peripheral nerve injuries. Nerve sutures and nerve grafting. *Scand J Plast Reconstr Surg* 1982; Suppl. 19:25-37.

Moore AM, Kasukurthi R, Magill CK, et al. Limitations of conduits in peripheral nerve repairs. *Hand (N Y)* 2009;4:180-186

Muratori L, Fregnan F, Ronchi G, Haastert-Talini K, Metzen J, Bertolo R, Porpiglia F, Geuna S. New basic insights on the potential of a chitosan-based medical device for improving functional recovery after radical prostatectomy. *BJU Int*. 2019 Dec;124(6):1063-1076.

Navarro, X. (2016). Functional evaluation of peripheral nerve regeneration and target reinnervation in animal models: a critical overview. *Eur. J. Neurosci*. 43, 271–286

Neubrech F, Heider S, Harhaus L, Bickert B, Kneser U, Kremer T. Chitosan nerve tube for primary repair of traumatic sensory nerve lesions of the hand without a gap: study protocol for a randomized controlled trial. Trials. 2016;17:48

M. W. Neumeister and J. N. Winters, "Neuroma," *Clin. Plast. Surg.*, vol. 47, no. 2, pp. 279–283, 2020

Pace LA, P. J., Mannava S, Barnwell JC, Koman LA, Li Z, Smith TL, Van Dyke M (2013). "A human hair keratin hydrogel scaffold enhances median nerve regeneration in nonhuman primates: an electrophysiological and histological study." Tissue Engineering Part A 20: 507-517

Peters KM, Gilmer H, Feber K, Girdler BJ, Nantau W, Trock G, Killinger KA, Boura JA. *US Pilot Study of Lumbar to Sacral Nerve Rerouting to Restore Voiding and Bowel Function in Spina Bifida: 3-Year Experience.* *Adv Urol.* 2014;2014:863209.

Pitarokoili K, Gold R, Fisse AL. *Nerve ultrasound for the diagnosis and follow-up of peripheral neuropathies.* *Curr Opin Neurol.* 2023 Oct 1;36(5):373-381

Porpiglia F, Manfredi M, Checcucci E, Garrou D, De Cillis S, Amparore D, De Luca S, Fregnan F, Stura I, Migliaretti G, Fiori C. *Use of chitosan membranes after nerve-sparing radical prostatectomy improves early recovery of sexual potency: results of a comparative study.* *BJU Int.* 2019 Mar;123(3):465-473. doi: 10.1111/bju.14583. Epub 2018 Nov 1. PMID: 30303604.

Radtke C (2016). *"Natural Occurring Silks and Their Analogues as Materials for Nerve Conduits."* *Int J Mol Sci* 17

Rbia N, Shin AY. *The Role of Nerve Graft Substitutes in Motor and Mixed Motor/Sensory Peripheral Nerve Injuries.* *J Hand Surg Am* 2017;42:367-377

Reece JC, Dangerfield DC, Coombs CJ. *End-to-side Somatic-to-autonomic Nerve Grafting to Restore Erectile Function and Improve Quality of Life After Radical Prostatectomy.* *Eur Urol.* 2019 Aug;76(2):189-196

Regas I, Loisel F, Haight H, Menu G, Obert L, Pluvy I. *Functionalized nerve conduits for peripheral nerve regeneration: A literature review.* *Hand Surg Rehabil.* 2020 Oct;39(5):343-351. doi: 10.1016/j.hansur.2020.05.007. Epub 2020 May 30. PMID: 32485240.

Rein S, Schober R, Poetschke J, Kremer T. *Non degradation of chitosan and initial degradation of collagen nerve conduits used for protection of nerve coaptations.* *Microsurgery.* 2023 Jul 21.

Ronchi G, Morano M, Fregnan F, Pugliese P, Crosio A, Tos P, Geuna S, Haastert-Talini K and Gambarotta G (2019) *The Median Nerve Injury Model in Pre-clinical Research – A Critical Review on Benefits and Limitations.* *Front. Cell. Neurosci.*

Ronchi G, Fornasari BE, Crosio A, Budau CA, Tos P, Perroteau I, Battiston B, Geuna S, Raimondo S, Gambarotta G. *Chitosan Tubes Enriched with Fresh Skeletal Muscle Fibers for Primary Nerve Repair.* *Biomed Res Int.* 2018 Jun 13;2018:9175248.

Rose EH, N. M., Kowalski TA, Lucas A, Flegler EJ (1991). *"Palmaris brevis turnover flap as an adjunct to internal neurolysis of the chronically scarred median nerve in recurrent carpal tunnel syndrome."* *J Hand Surg Am* 16: 191-201

Riccio M, Pangrazi PP, Parodi PC, Vaienti L, Marchesini A, Neuendorf AD, Bottegoni C, Tos P, Geuna S. *The amnion muscle combined graft (AMCG) conduits: a new alternative in the repair of wide substance loss of peripheral nerves.* *Microsurgery.* 2014 Nov;34(8):616-22.

Rinker B, V. K. (2014). *"Clinical Applications of Autografts, Conduits, and Allografts in Repair of Nerve Defects in the Hand Current Guidelines."* *Clin Plastic Surg* 41: 533–550

- Rivlin M, M. A., Tulipan J, Beredjikian PK, Wang ML, Fertala J, Steplewski A, Fertala KA (2017). "Patterns of production of collagen-rich deposits in peripheral nerves in response to injury: A pilot study in a rabbit model." *Brain and Behavior* 7: e00659
- Ronchi, G., Nicolino, S., Raimondo, S., Tos, P., Battiston, B., Papalia, I., et al. (2009). Functional and morphological assessment of a standardized crush injury of the rat median nerve. *J. Neurosci. Methods* 179, 51–57
- Ruggieri MR, Braverman AS, D'Andrea L, McCarthy J, Barbe MF. Functional reinnervation of the canine bladder after spinal root transection and immediate somatic nerve transfer. *J Neurotrauma*. 2008 Mar;25(3):214-24.
- Ruggieri MR Sr, Braverman AS, Bernal RM, Lamarre NS, Brown JM, Barbe MF. Reinnervation of urethral and anal sphincters with femoral motor nerve to pudendal nerve transfer. *Neurourol Urodyn*. 2011 Nov;30(8):1695-704.
- Sabongi RG, F. M., dos Santos JBG (2015). "Peripheral nerve regeneration with conduits: use of vein tubes." *Neural regeneration research* 10: 529
- Safa B, Buncke G. Autograft Substitutes: Conduits and Processed Nerve Allografts. *Hand Clin*. 2016 May;32(2):127-40. doi: 10.1016/j.hcl.2015.12.012. PMID: 27094886.
- Safa B, Shores JT, Ingari JV, Weber RV, Cho M, Zoldos J, Niaccaras TR, Nesti LJ, Thayer WP, Buncke GM. Recovery of Motor Function after Mixed and Motor Nerve Repair with Processed Nerve Allograft. *Plast Reconstr Surg Glob Open*. 2019 Mar 13;7(3):e2163
- Saffari TM, Saffari S, Vyas KS, Mardini S, Shin AY. Role of adipose tissue grafting and adipose-derived stem cells in peripheral nerve surgery. *Neural Regen Res*. 2022 Oct;17(10):2179-2184. doi: 10.4103/1673-5374.336870. PMID: 35259826; PMCID: PMC9083182.
- Schmidt CE, L. J. (2003). "Neural tissue engineering: strategies for repair and regeneration." *Annu Rev Biomed Eng* 5: 293-347
- Senger JB, Hardy P, Thorkelsson A, Duia S, Hsiao R, Kemp SWP, Tenorio G, Rajshekar M, Kerr BJ, Chan KM, Rabey KN, Webber CA. A Direct Comparison of Targeted Muscle Reinnervation and Regenerative Peripheral Nerve Interfaces to Prevent Neuroma Pain. *Neurosurgery*. 2023 Jun 2.
- Shapira Y, T. M., Nissan M, Reider E, Koren A, Biron T, Bitan Y, Livnat M, Ronchi G, Geuna S, Rochkind S (2016). "Comparison of results between chitosan hollow tube and autologous nerve graft in reconstruction of peripheral nerve defect: An experimental study." *Microsurgery* 36: 664-671
- Siemionow M, B. G. (2009). "Chapter 8: Current techniques and concepts in peripheral nerve repair." *Int Rev Neurobiol* 87: 141-172
- Simões MJ, Amado S, Gärtner A, Armada-Da-Silva PA, Raimondo S, Vieira M, Luís AL, Shirosaki Y, Veloso AP, Santos JD, Varejão AS, Geuna S, Maurício AC. Use of chitosan scaffolds for repairing rat sciatic nerve defects. *Ital J Anat Embryol*. 2010;115(3):190-210.

Simoes MJ, G. A., Shiroasaki Y, Gil da Costa RM, Cortez PP, Gartner F (2011). "In vitro and in vivo chitosan membranes testing for peripheral nerve reconstruction." *Acta Med Port* 24: 43e52

Sinis, N., Schaller, H. E., Becker, S. T., Lanaras, T., Schulte-Eversum, C., Muller, H. W., et al. (2006). Cross-chest median nerve transfer: a new model for the evaluation of nerve regeneration across a 40 mm gap in the rat. *J. Neurosci. Methods* 156, 166–172

Smith PA. Neuropathic pain; what we know and what we should do about it. *Front Pain Res (Lausanne)*. 2023 Sep 22;4:1220034.

Souza Trindade JC, Viterbo F, Petean Trindade A, Fávoro WJ, Trindade-Filho JCS. Long-term follow-up of treatment of erectile dysfunction after radical prostatectomy using nerve grafts and end-to-side somatic-autonomic neurorrhaphy: a new technique. *BJU Int*. 2017 Jun;119(6):948-954.

Squintani G, B. B., Paolin A, Vici D, Cogliati E, Murer B, Stevanato G (2013). "Nerve regeneration across cryopreserved allografts from cadaveric donors: a novel approach for peripheral nerve reconstruction." *Journal of neurosurgery* 119: 907-913

Taylor CA, B. D., Rice JB, Dillingham T. (2008). "The incidence of peripheral nerve injury in extremity trauma." *Am J Phys Med Rehabil*. 87(5): 381 - 385.

Thakker A, Sharma SC, Hussain NM, et al. Nerve wrapping for recurrent compression neuropathy: A systematic review. *J Plast Reconstr Aesthet Surg* 2021;74:549-559

Thomson SE, Ng NY, Riehle MO, Kingham PJ, Dahlin LB, Wiberg M, Hart AM. Bioengineered nerve conduits and wraps for peripheral nerve repair of the upper limb. *Cochrane Database Syst Rev*. 2022 Dec 7;12(12):CD012574.

Tos P, Battiston B., Ciclamini D, Geuna S, Artiaco S (2012). "Primary repair of crush nerve injuries by means of biological tubulization with muscle-vein-combined grafts." *Microsurgery* 32: 358-363

Tos P, Conforti G, Ciclamini D, Titolo P, Pugliese P, Artiaco S (2014). "Clinical applications of end-to-side neurorrhaphy: an update." *Biomed Res Int* 2014: 646128

Tos P, Crosio A, Pugliese P, Adani R, Toia F, Artiaco S (2015). "Painful scar neuropathy: principles of diagnosis and treatment." *Plastic and Aesthetic Research* 2(4): 156-164

Tos P, Crosio A, Pellegatta I, Valdatta L, Pascal D, Geuna S, Cherubino M. Efficacy of anti-adhesion gel of carboxymethylcellulose with polyethylene oxide on peripheral nerve: Experimental results on a mouse model. *Muscle Nerve*. 2016 Feb;53(2):304-9

Tuite GF, Polsky EG, Homsy Y, Reilly MA, Carey CM, Parrish Winesett S, Rodriguez LF, Storrs BB, Gaskill SJ, Tetreault LL, Martinez DG, Amankwah EK. Lack of efficacy of an intradural somatic-to-autonomic nerve anastomosis (Xiao procedure) for bladder control in children with myelomeningocele and lipomyelomeningocele: results of a prospective, randomized, double-blind study. *J Neurosurg Pediatr*. 2016 Aug;18(2):150-63.

- Vaianti L, Gazzola R, Villani F, Parodi PC. Perineural fat grafting in the treatment of painful neuromas. *Tech Hand Up Extrem Surg.* 2012 Mar;16(1):52-5.
- Vijayavenkataraman S. Nerve guide conduits for peripheral nerve injury repair: A review on design, materials and fabrication methods. *Acta Biomater.* 2020 Apr 1;106:54-69.
- Vögelin E, B. D., Constantinescu M, Büchler U (2008). "Revision surgery after carpal tunnel release using a posterior interosseous artery Island flap." *Handchir Mikrochir Plast Chir* 40: 122-127
- Wang W, I. S., Matsuda A (2008). "Influences of mechanical properties and permeability on chitosan nano/microfiber mesh tubes as a scaffold for nerve regeneration." *J Biomed Mater Res A* 84: 557–566
- M. Willsey, T. J. Wilson, P. T. Henning, and L. J.-S. Yang, "Intraoperative Ultrasound for Peripheral Nerve Applications.," *Neurosurg. Clin. N. Am.*, vol. 28, no. 4, pp. 623–632, Oct. 2017
- Whishaw, I. Q., Pellis, S. M., and Gorny, B. P. (1992). Skilled reaching in rats and humans: evidence for parallel development or homology. *Behav. Brain Res.* 47, 59–70
- Whitlock EL, T. S., Luciano JP, Yan Y, Hunter DA, Magill CK, Moore AM, Tong AY, Mackinnon SE, Borschel GH (2009). "Processed allografts and type I collagen conduits for repair of peripheral nerve gaps." *Muscle & nerve* 39: 787-799)
- Wimalawansa SM, Lygrisse D, Anderson SR, et al. Targeted Muscle Reinnervation in Partial Hand Amputations. *Plast Reconstr Surg Glob Open* 2021;9:e3542
- Xiao, C. G., De Groat, W. C., Godec, C. J., Dai, C. and Xiao, Q.: "Skin-CNS-bladder" reflex pathway for micturition after spinal cord injury and its underlying mechanisms. *J Urol*, 162: 936, 1999
- Yasui G, Y. Y., Shichinohe R, Funayama E, Oyama A, Hayashi T, Furukawa H (2016). "Neuregulin-1 released by biodegradable gelatin hydrogels can accelerate facial nerve regeneration and functional recovery of traumatic facial nerve palsy." *Journal of Plastic Reconstructive & Aesthetic Surgery* 69: 328-334
- Zhou G, Chen Y, Dai F, Yu X. Chitosan-based nerve guidance conduit with microchannels and nanofibers promotes schwann cells migration and neurite growth. *Colloids Surf B Biointerfaces.* 2023 Jan;221:112929.

ACKNOWLEDGMENTS

My PhD program is the last brick of a long journey started in the 2007 when, for the first time I met the Human Anatomy team of the department of clinical and biological sciences during my master degree in Medicine. Since then, I have been fascinated by their work and, through this, my passion for peripheral nerve repair and regeneration was switched on. I will be forever grateful to **Stefania Raimondo, Giulia Ronchi, Federica Fregnan and Luisa Muratori** who followed me since the very first years, they were active part for the realization of my master degree and specialization theses; a long journey ended in 2018. The collaboration continued during the PhD program and, I think and hope, will continue as well. **Stefania** has been my accurate, wisdom and placid tutor. A lighthouse in the ocean. **Giulia** and, especially, **Federica and Luisa** have been very good sometimes fellows and sometimes guides with whom joys and sorrows were shared.

Moreover, I have the pleasure to collaborate also with **Giovanna Gambarotta** and their present and past PhD students, especially **Benedetta Fornasari** and **Federica Zen**, with whom part of the papers presented and still ongoing have been realized.

All this was possible thanks to **Stefano Geuna** who transmitted its passion for human anatomy through lectures during master degrees and let me meet **Pierluigi Tos**. He is the person who, without any doubts, changed my life and I always be debtors and grateful to him. He was able to merge my raising passion for peripheral nerve regeneration to limbs reconstruction, giving me the possibility to discover the world of medicine that I like most. He taught me how to cure patients, how to do and to be a surgeon, what to be a physician means. Something that it can't be taught and wrote down on a book. **Pierluigi**, as my first chief in the hospital, has been part of the PhD program either directly and indirectly. He gave me time to accomplish my PhD student duties even the heavy work shifts in the hospital, knowing how this journey was important. Of course, I want to thank all my colleagues of the **Hand Surgery and Reconstructive Microsurgery department of Gaetano Pini hospital**. They supported me during my work as a PhD student, without any regrets and complaints when I could not be in the ward.

A special thanks is directed to my parents, **Rita and Mario**, who always support me with loving and firm suggestions, putting my comfort in front of everything and understanding all the choices I made in these years, nevertheless the great time spent in working and studying.

Finally, a great loving mention to **Chiara**. She is the person who endured the heavier moments occurred during the years of the PhD program. She always sustained me, even if meant to sacrifice time for us, understanding, in her heart, how important was this journey for me.